The University of Nottingham

UNITED KINGDOM • CHINA • MALAYSIA

A FUNDAMENTAL STUDY OF BIOMASS OXY-FUEL COMBUSTION AND CO-COMBUSTION

TIMIPERE SALOME FARROW, MRes, BTech

THESIS SUBMITTED TO THE UNIVERSITY OF NOTTINGHAM FOR THE DEGREE OF DOCTOR OF PHILOSOPHY, JULY 2013

ABSTRACT

While oxy-fuel combustion research is developing and large scale projects are proceeding, little information is available on oxy-biomass combustion and co-combustion with coal. To address this knowledge gap, this research conducted has involved comprehensive laboratory based fundamental investigation of biomass firing and co-firing under oxy-fuel conditions and compared it to conventional air firing conditions. First, TGA was employed to understand the fundamental behaviour of biomass devolatilisation, char combustion and nitrogen partitioning between volatiles and residual char. The results revealed that CO_2 did not have effect on the devolatilisation of sawdust at temperatures below 1100°C due to higher mass transfer resistance of primary volatiles in CO_2 than in N_2 at low temperatures. Secondly, by optimising the devolatilisation procedure in a combustion system that simulates closely to an industrial scale such as drop tube furnace (DTF), the devolatilisation/char combustion characteristics of sawdust was investigated. The effect of CO_2 on volatile yields, nitrogen partitioning and char burnout were all significant in relation to N_2. While coal combustion additives are being used to enhance coal burnout, this study observed improved coal char burnout when biomass char was co-fired with coal char, again a faster burnout was observed in oxy-firing condition compared to air firing. This was due to the catalytic effect of biomass inherent alkali and alkaline earth metals. Similarly, improved volatile yields were observed during co-devolatilisation. These fundamental results have provided insight into oxy-biomass firing and co-firing and the data can be used in appropriate CFD modelling to aid the design of oxy-biomass co-firing burners.

PUBLICATIONS

Poster Presentations

Farrow, Timipere S.; Snape, C. (2010), Oxy-fuel biomass combustion for a sustainable clean environment, Social Sciences Research for Low Carbon Future, 29th April, 2010, Nottingham, UK (Poster)

Farrow, Timipere S.; Snape, C. (2010), Oxy-fuel biomass combustion: an energy choice for near zero emission control in the power sector, Midlands Energy Graduate School 1st Annual Conference, May 2010, Loughborough, UK (Poster).

Farrow, Timipere S.; Snape, C. (2010), Devolatilisation behaviour and Combustion Reactivity of Biomass fuel under oxy-fuel conditions, Third International Symposium on Energy from Biomass and Waste, November, 2010, Venice, Italy (Poster).

Conference Proceedings

Farrow, Timipere S.; Snape, C. (2010), Fundamental study of biomass and coal oxy-fuel combustion, Young Researchers Forum on Oxy-fuel combustion, October 2010, Stuttgart, Germany.

Farrow, Timipere S.; Snape, C. (2010), Fundamental Aspects of combustion reactivity of Biomass in Relation to Oxy-fuel Combustion, Engineering Response

to Climate Change: Energy Options for Sustainable Development in Nigeria, December 2010, Abuja, Nigeria.

Farrow, Timipere S.; Snape, C. (2010), A Fundamental Study of Biomass Oxy-fuel Combustion and Co-combustion, Midlands Energy Gradual School Christmas Event, December 2010, Birmingham, UK.

Farrow, Timipere S.; Zhao D.; Sun, C.; Snape, C. (2011), Impact of biomass on char burn-out under air and oxy-fuel conditions, Fifth International Conference on Clean Coal technology (CCT), May 2011, Zaragoza, Spain.

Farrow, Timipere S.; Sun, C.; Snape, C Impact of biomass on char burn-out under air and oxy-fuel conditions, International Conference on Coal Science and Technology (ICCS&T), October 2011, Oviedo, Spain

Journal Publications

Farrow, Timipere S.; Sun, C.; Snape, C 'Impact of Biomass Char on Coal Char Burn-out under Air and Oxy-fuel Conditions' Fuel 2012, available online September 2012

Proposed Journal Publications

Farrow, Timipere S.; Sun, C.; Snape, C, 'Comparative Study of the TGA Combustion Reactivity of Sawdust Chars produced by a TGA and DTF' to be submitted to Energy and Fuels.

Farrow, Timipere S.; Sun, C.; Snape, C, 'Impact of CO_2 on Biomass Devolatilisation, Nitrogen Partitioning and Char Combustion: a Drop Tube Furnace study' to be submitted to Energy and Fuels.

Farrow, Timipere S.; Sun, C.; Snape, C, 'Synergetic effects of biomass on coal devolatilisation' to be submitted to Fuel.

Farrow, Timipere S.; Sun, C.; Snape, C, 'developing a method to determine biomass volatile yields in the drop tube furnace' to be submitted to Fuel.

ACKNOWLEDGEMENTS

I am ever grateful to God for the enabling grace to do this study.

I also appreciate my sponsors, the Petroleum Development Trust Fund, Nigeria for the financial support. Also, this study would not have been completed without the financial support from Engineering and Physical Sciences Research Council (EPSRC), Oxy-CAP UK Project (Ref: EP/G062153/1)

I sincerely appreciate the effort of my supervisor, Professor Colin E. Snape for his advice, guidance and systematic supervision of this work.

My profound gratitude also goes to Dr Chenggong Sun who has made tremendous input into various aspect of this work.

I also appreciate Dave Clift, the workshop and the technical staff of the department of Chemical and Environmental Engineering for their assistance during my laboratory work.

Finally, I want to thank members of my family, the pastorate and members of God's vineyards ministries for their prayers. I sincerely appreciate my colleagues such as Chidi Ogbuka, Marco Dri, Chijioke Nwankwor and Sylvia Kokonya for their support during this study.

TABLE OF CONTENTS

LIST OF FIGURES

LIST OF TABLES

1 INTRODUCTION

1.1 GENERAL BACKGROUND

The alarming increase in CO_2 emissions from fossil fuel consumption has greatly shifted attention to renewable energy sources and clean sustainable fossil fuels combustion technologies to reduce such emissions. Energy production from fossil fuel combustion has resulted in greenhouse gas emissions with CO_2 as the major contributor to climate change. Increase in population growth and the subsequent demand for electricity has contributed to the continuous use of fossil fuel globally. In the UK, population is projected to increase to 27% by 2050 from 6% in 1990 (POSTnote, 2008). Energy use and carbon emissions have risen with population and economic growth. The increase in population growth has translated into greater demand in energy consumption. This increased utilisation of coal could be as a result of the abundance of coal available worldwide. Currently proven reserves of coal are estimated to be 861 billion tonnes of oil equivalent (BP, June 2012). Coal is therefore expected to be in the energy mix for a long time. Moreover, the increasing concern about nuclear radiation released from nuclear plants, or waste from the plants has reinforced the continuous use of coal in the electricity industry. This will lead to further increases in CO_2 and other emissions if mitigation measures are not in place. One of the ways that is been used to tackle this problem is to switch from carbon intensive fossil fuels to low carbon renewable fuels. However, to meet UK's target to reduce CO_2 emissions, high level of co-firing biomass with coal is necessary.

Among the three major fossil fuels; oil, natural gas and coal, coal is known to produce the highest amount of CO_2 per KWh of power generated. As such CO_2 emissions are expected to rise above 39% if new mitigation technologies are not

put in place and subsequently, future global warming is eminent (IPCC, 2007). Therefore, a sustainable future requires an efficient use of coal with mitigation strategies including CO_2 capture. Furthermore, the CO_2 emissions are particularly high in the case of power generation from coal (Scheffknecht et al., 2011) because coal generates about 2 times the CO_2 emitted by gas due to the high carbon content (Sun et al., 2011). Table 1.1 shows the share of world energy in CO_2 emissions by coal utilisation (IEO, 2011). Unfortunately, the target to increase carbon price which is an administrative cost imposed on greenhouse gas emissions is being planned and this will increase cost of electricity production. However, to meet the UK's 2050 targets to cut greenhouse gas emissions by 80%, the electricity sector will largely depend on renewable energy resources of which biomass is a major resource.

Table 1.1 Share of world energy in CO_2 emissions by coal (IEO, 2011)

Year	1990	2008	2035
CO_2 Emissions	39%	43%	45%

1.2 WHY BIOMASS?

With the EU's energy policy target to increase renewable energy in the final energy consumption by 20% in 2020 (Tous et al., 2011), 45 % by 2030 (EREC, 2011) and the transition to full scale by 2050 (EREC, 2010), increasing research is being carried out in this sector. Biomass has received significant attention in the power sector as a combustion fuel (Bain et al., 1998, Demirbas, 2005, Domenichini et al., 2011, Menghini et al., 2008, Tarelho et al., 2011, van den Broek et al., 1996) to achieve this target. This is because the power industry is faced with continuous demand to reduce CO_2 emissions from their operation and

this has resulted in the use of alternative fuels to produce heat and electricity in order to cut greenhouse gases.

Bio-energy is attractive at all stages of development due to its potential integration in the energy sector. Among the renewable energy resources, biomass has played a significant role in energy production. Historically, biomass, especially woody biomass was used as a source of energy for cooking and heating in the home. It is common and widespread across the world compared to other renewable resources and can be utilized on a sustainable basis. Biomass firing is progressing with the introduction of renewable heat incentive (RHI) by the UK Government in 2011 (DECC, 2012a) to meet the UK's target of 15% renewable energy sources. Also, UK Government considers that biomass electricity has a key role in providing secure, clean and affordable electricity to 2020 and beyond (DECC, 2012b). It is reported that for every 10% by energy content of biomass used, a greenhouse gas emission saving of just over 60 gCO_2eq/kWh can be realised and converting a coal plant to run on 100% biomass will have roughly the same emissions as a combined cycle gas turbine (CCGT) plant (DECC, 2012b).

The use of biomass fuel for sustainable and environmentally friendly fuel goes beyond energy provision. It is the important renewable energy option at present and can be used to produce different forms of energy carriers such as activated carbon.

Sugar cane bagasses have been used to produce electricity in India and Brazil. In Brazil alone, about 570 million tons of sugar cane was harvested in 2009 and the bagasses generated about 3% of the country's electricity supply. Biomass fuel includes wood, short rotation crops, woody crops, agricultural wastes, short rotation herbaceous species, wood wastes, bagasses, industrial residues, waste

papers, municipal solid wastes, sawdust, bio solids, grass, wastes from food processing, aquatic plants and algae animals. This unlimited list of biomass fuels removes the concept of seasonal availability of biomass fuel (Demirbas, 2004) and supplies energy needed without affecting food supply. Again, the fact that many regions do not have enough solar and wind energy resources has made biomass an energy source for the power sector (Holtmeyer et al., 2012).

There have also been many studies performed in recent years to estimate the potential demand and supply of biomass fuel for electricity production. Although there is a projected renewable energy growth as shown in Figure 1.1, coal still dominates and is expected to maintain a major share of the energy use in the world (Demirbas, 2003) despite the environmental consequences (Hahn et al., 2003, Hu et al., 2000). Moreover, transportation, storage, milling and feeding of biomass are still challenges in the biomass utilisation (Hughes and Tillman, 1998, Wang and Baxter, 2007). It therefore means that co-firing will be a better option to utilise biomass fuels as well as reducing the percentage of coal utilisation.

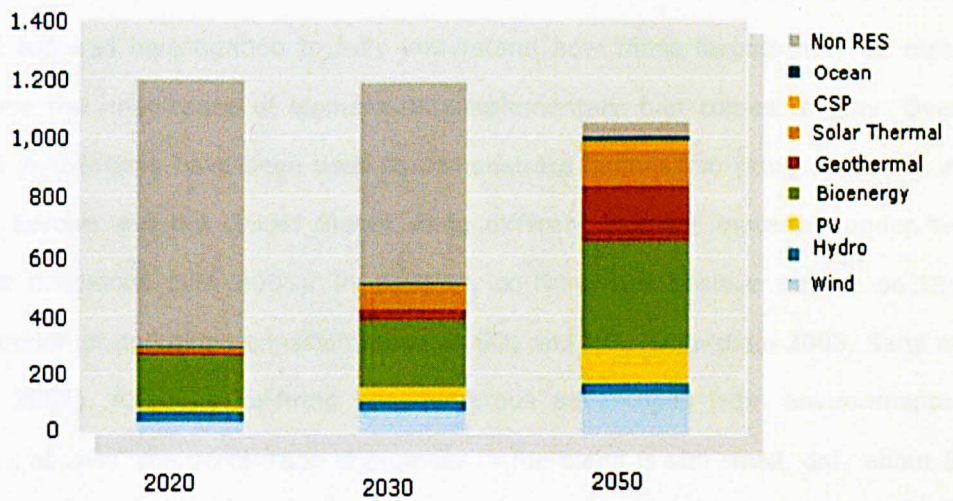

Figure 1.1 Projected contributions of renewable energy technologies to final energy consumption (Mtoe) source: EREC 2010

1.3 WHY CO-FIRING?

Since most of the environmental problems associated with coal combustion are the release of greenhouse gases, there should be a balance between CO_2 build up and sink. It is therefore necessary to source for alternative but sustainable energy sources to supplement fossil for the power industry. Also, most of the coal-fired stations (20 GW) are already 40 years old and several natural gas-fired combined cycle gas turbine (CCGT) stations have operated for 20 years. More importantly, the Large Combustion Plant Directive (LCPD) requirement is to close coal-fired plants without flue gas desulphurisation and low NOx technology before January 2016. Some loss of electricity is anticipated. Therefore, a number of PF plants that will not sign up to the LCPD will operate on either dedicated biomass or high levels of biomass co-firing beyond 2016.

Most importantly, one of the main advantages of co-firing biomass and coal is the fact that it is relatively easy to retrofit in existing pulverised coal power plants without making major modifications in plants compared to building new biomass-only fired power plants (Syed et al., 2011). On the other hand, legislation in the UK is strong on CO_2 reduction to meet Kyoto target and EU's target to reduce CO_2 emissions by 80% by 2050. This is a challenging target and requires investigation to fully understand how these targets may be met. Hence the importance of biomass as supplementary fuel comes to play. Over 150 installations have been used to demonstrate biomass co-firing especially in the Europe and the United States using different biomass materials under air fired conditions (IEA 2005). In addition, co-firing has positive impact on the reduction of pollutants emissions such as SO_x and NO_x (Demirbas, 2003, Sami et al., 2001). Although co-firing has numerous advantages from environmental point of view, the percentage of biomass in the blend is still small, only about 5 – 20% on thermal basis, For example, the 4000 MWe Drax plant in the UK has

the capability to generate 500 MWe from co-firing biomass which corresponds to a co firing ratio of 12.5% while two of the four 500 MWe units at Fiddler's Ferry power is co-firing about 20% on thermal basis (Fernando, 2012). The need for high blending ratios is being proposed (Fernando, 2012). Since the contribution of coal is still high in the energy mix, a technology is required to efficiently reduce CO_2.

1.4 CATALYTIC EFFECT OF BIOMASS ON COAL

Previously, in pulverised coal combustion systems, catalysts have used as additives to enhance complete burnout of coal char and reduce emissions (Kakaras and Vourliotis, 1998, Zhang et al., 1997) However, the cost of purchasing chemical catalysts is expensive (Zhu et al., 2008). It is therefore necessary to identify inexpensive biomass as a catalyst that will improve coal devolatilisation and char burnout.

Apart from reducing net CO_2 emissions, the addition of biomass to coal for co-firing has resulted in improving the combustion and gasification of coal as earlier discussed (Haykiri-Acma and Yaman, 2007, Sutcu, 2007, Vamvuka et al., 2003b, Zhang et al., 2007). This improved behaviour is attributed to the presence of alkali metals such as potassium (K) and sodium (Na), alkaline earth metals such as calcium (Ca) and magnesium (Mg) contained in biomass fuel that catalysis the reaction. Some studies have identified the catalytic role played by alkali metals during biomass combustion (Jones et al., 2007). Jones et al (2007) demineralised biomass (willow) with hydrochloric acid and impregnated it with potassium.

Mineral matter in the ash of biomass fuel has been found to influence co-gasification reactions. Ren et al (2011) observed that the gasification rate of the coal char mixed with bone meal ash was found to be 1.5 time higher than the pure coal. Zhu et al (2008) did a similar experiment testing the catalytic effects of wheat straw and coal in co-pyrolysis. Interestingly they found that with the increased wheat straw/coal blending ratio, the reactivity of char gasification increased, with possible explanations coming from the high potassium content (25%) of wheat straw. These studies have focused on the catalytic effect of biomass containing alkali and alkaline metals as a source of catalysts for coal combustion and gasification under air fired condition.

1.5 LEADING TECHNOLOGIES FOR CO_2 CAPTURE

There are three leading technologies for carbon capture, namely pre-combustion capture, post combustion capture and oxy-fuel combustion technology. However, there are emerging technologies such as chemical-looping combustion. This technology involves the use of a metal oxide as an oxygen carrier which transfers oxygen from the combustion air to the fuel under atmospheric or pressurised conditions. In this case, the basic competitive advantage is the omission of an air separation process. Also the CO_2 and H_2O are inherently separated from the other components of the flue gas (Fang et al., 2009). Figure 1.2 present the major leading techniques in CO_2 capture.

1.5.1 *Post combustion capture*

This technology involves the scrubbing of dilute CO_2 from flue gas stream using amine solvents as the leading technique (Adams et al., 2009). There are current state of the art technologies for post-combustion capture which uses aqueous solutions of alkanolamines to achieve CO_2 separation from flue gas. However,

some drawbacks of this technology are that the CO_2 levels are also relatively small which leads to the use of very large column equipment for the capture section. Also, the use of such solvents could lead to corrosion of metal piping as well as high energy-intensive regeneration of the solvents (Leci, 1996). This has led to the proposal of a range of potentially more efficient and less energy intensive capture technologies. One of such technique is the development of solid adsorbents which have high CO_2 selectivity and adsorption capacity and at the same time can be thermally stable during regeneration (Drage et al., 2009).

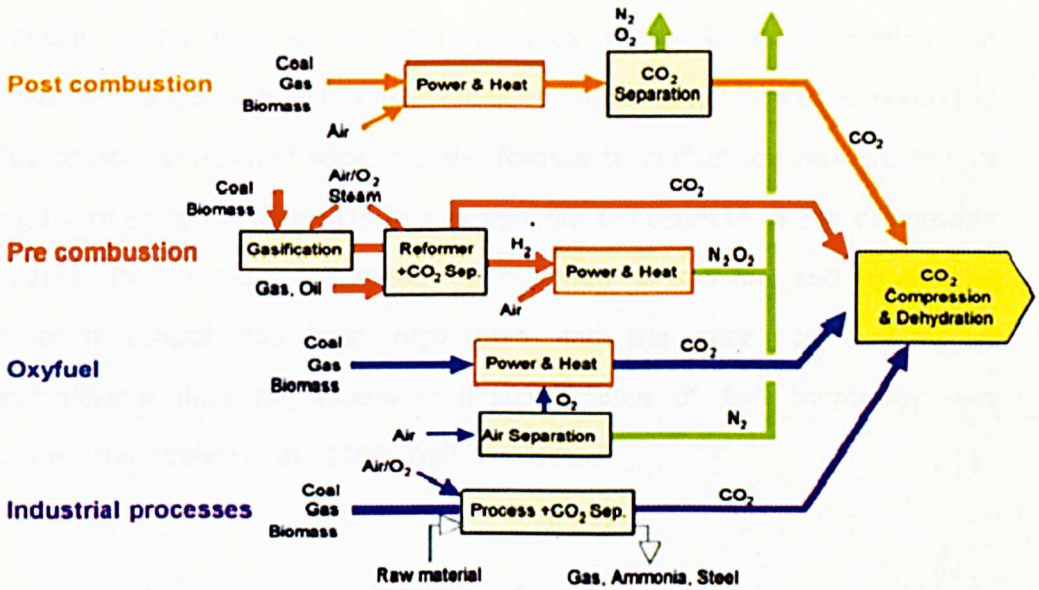

Figure 1.2 Leading Technologies for CO_2 capture (IPCC, 2005)

1.5.2 *Pre-combustion capture*

In this technology, CO_2 is removed from the process stream prior to combustion. Here, the fuel is gasified to H_2 and CO to form synthesis gas. Then the CO is converted to CO_2 through shift reaction. The CO_2 is captured while the H_2 gas is sent to the combustion chamber. This system requires an additional unit called gasifier. The Integrated Gasification Combined Cycle (IGCC) is being used to

achieve this process. However, loss in electric efficiency during carbon capture is a major challenge associated with pre-combustion IGCC process (Carbo et al., 2009). This necessitates the implementation of other technologies that will capture CO_2.

1.5.3 *Oxy-fuel combustion technology*

Oxy-fuel combustion involves the burning of fuel in oxygen rich environment to generate CO_2-rich flue gas that requires minimal treatment prior to compression, transport and storage. Hence, Oxy-fuel combustion technology is one of the main methods being considered for carbon capture from large coal fired power plants in order to reduce CO_2 to a bearable level. This technology eliminates nitrogen supply from air to the combustion system by air separation and produces flue gas with high concentration of CO_2 for easy capture. However, the flue gases are recycled back into the furnace to control temperature and to ensure there is sufficient gas to maintain the temperature in the combustion system. In the past, a comprehensive review of oxy-fuel technology and emission control has been highlighted and the need for fundamental experimental data for successful implementation of this technology was documented (Buhre et al., 2005, Wall, 2007).

More recently, the economic feasibility of oxy-fuel combustion technology has been studied and the results indicated that the technique is effective for reduction of CO_2 emissions in laboratory and pilot scale to provide design criterion for retrofitting (Wall et al., 2009, Xiong et al., 2009). Furthermore, increasing research is being carried out on coal oxy-fuel combustion using varying O_2/CO_2 concentrations and has provided useful information (Arias et al., 2008, Borrego and Alvarez, 2007, Croiset and Thambimuthu, 2001, Hjärtstam et al., 2009, Normann et al., 2009, Sturgeon et al., 2009, Wall et al., 2009, Wall, 2007). Studies so far have demonstrated that oxygen concentrations in the

range 30-40% produce temperature profiles matching those of conventional air firing (Arias et al., 2008, Kim and Lee, 2010, Liu et al., 2005a, Liu et al., 2005b, Molina and Shaddix, 2007, Tan et al., 2006). The higher oxygen concentration required is due to the fact that diffusivity of O_2 in CO_2 is lower than in N_2 and CO_2 has higher specific heat capacity than N_2 (Borrego and Alvarez, 2007, Shaddix and Molina, 2009, Wall et al., 2009). Other fundamental issues that affect pulverised combustion systems such as gas recycling ratio, heat transfer, ignition, flame stability, combustion performance and the participation of CO_2 in the chemical reaction at high temperatures have been investigated (Kutne et al., 2011).

Subsequently, devolatilisation and char burnout have also occurred at more pronounced levels under higher oxygen concentration, (Arias et al., 2008, Borrego and Alvarez, 2007, Rathnam et al., 2009) although significant differences have been found in the devolatilisation behaviour of lower and higher rank coals. Also, higher temperatures have resulted in higher volatile yield and higher char burnout under oxy-fuel conditions than air fired conditions. The higher char combustion rate has been attributed to CO_2-char gasification reaction which increases the combustion reactivity of the char (Arias et al., 2008, Rathnam et al., 2009, Wall et al., 2009).

Oxy-fuel technology is currently undergoing rapid development towards commercialisation with a number of demonstration projects commencing. Wall et al (2009) provided a comprehensive overview on the most recent developments in pilot plants and demonstration projects for the coal oxy-fuel technology . In recent years, there have been number of pilot-scale facilities, ranging in size from about 0.3–3.0 MWth that have been used to characterise the combustion performance of coals under oxy-fuel combustion conditions. A number of demonstration projects ranging in size from 30 to 40 MWth have been

implemented such as the pilot plant operated by Vatterfall in Schwarze Pumpe (Rehfeldt et al., 2011). These results showed high flame stability. The 40 MWth state of the art oxy-fuel combustion systems at Doosan Power system is a proven and commercially available plant (Sturgeon et al., 2011).

Fundamentally, due to the variation in the furnace gas environment as compared to conventional air-fired combustion, oxy-fuel combustion affects the combustion process of pulverised coal as well as the related processes such as heat transfer. Numerous studies and research projects have been performed that covered many scientific and engineering fundamental issues, including: coal ignition and burnout (Man and Gibbins, 2011, Riaza et al., 2011), flame stability (Kutne et al., 2011), heat transfer (Smart et al., 2010a, Smart et al., 2010b, Haykiri-Acma et al., 2010b) and combustion characteristics (Becher et al., 2011). While oxy-fuel demonstration is fast growing worldwide, the cleaning of the CO_2 from the flue is receiving attention. Gas cleaning systems such as electrostatic precipitators, desulfurization units are investigated to clean the CO_2 in order to obtain high quality flue gas (Wall et al., 2011, Hu and Yan, 2012).

1.6 MOTIVATION FOR THIS STUDY

As a result of the increasing use of biomass for co-firing in pulverised fuel systems for power generation (Basu et al., 2011, Berggren et al., 2008) and the subsequent movement towards complete biomass fired boilers (Bain et al., 1998, Demirbas, 2005, van den Broek et al., 1996), further research is needed to improve our understanding of biomass combustion. The reason is that biomass firing is considered as an environmentally safe way of providing energy (Narodoslawsky and Obernberger, 1996) and thereby contribute to decarbonising the UK energy sector by 2050 (CCC, 2009), while co-firing is

aimed at reducing greenhouse gas emissions (Domenichini et al., 2011, Huang et al., 2006, McIlveen-Wright et al., 2011).

Subsequently, energy conversion technologies that will promote clean coal energy usage are important tools in achieving a sustainable future. Oxy-coal combustion has been recognised as a promising technology for carbon capture in pulverised coal combustion systems. Until now, only few experiments have been reported on biomass oxy-combustion especially in system that simulates closely to industrial pf boilers. Due to the presence of high levels of inertinite in a number of internationally traded coals, complete carbon burnout has become inherently more difficult to achieve during pf combustion (Le Manquais et al., 2011b). This has resulted in the use of combustion catalysts such as alkali and alkaline earth metals to enhance coal burnout. However, such catalysts are too expensive for industrial application (Zhu et al., 2008). Biomass contains high level of alkali and alkaline earth metal which will serve as natural and inexpensive source of catalysts to enhance coal char burnout during co-firing. It is therefore important to investigate the potential catalytic characteristics of such metals on coal char burnout.

1.7 AIMS AND OBJECTIVES

The aim of this study is to investigate some fundamental aspects of biomass combustion in relation to oxy-fuel combustion. The specific objectives are to study:

- The effect of CO_2 on the devolatilisation of biomass in terms of volatile yield and to understand how nitrogen partitioning and potential NOx emissions are influenced by biomass in co-firing under oxy-fuel conditions compared to conventional air firing.

- Char burnout reactivity in oxy-fuel conditions compared to normal air firing.

- The char carbon burnout improvement by the addition of biomass to coal with particular interest on the potential catalytic effect of biomass contained alkali and alkali earth metals.

- Compatibility of the two fuels by evaluating the synergetic effect occurring during devolatilisation as well as in combustion.

1.8 THESIS STRUCTURE

This thesis is divided into 12 chapters and they are organised as follows:

- Chapter 2 presents the literature review on biomass fuel, properties and conversion characteristics. It also covers coal properties, combustion and co-firing.

- Chapter 3 presents description of experimental techniques and methodology employed in this research.

- Chapter 4 discusses the fundamental results from TGA. They include the devolatilisation and char combustion reactivity of sawdust under air and oxy-fuel conditions.

- Chapter 5 discusses the results of the DTF tests, mainly on the developing a methodology for measuring biomass volatile yields during DTF experiments.

- Chapter 6 compares sawdust char reactivity in TGA and DTF.

- Chapter 7 presents the impact of CO_2 on sawdust devolatilisation, nitrogen partitioning and combustion, highlighting the significance of sawdust oxy-fuel combustion compared to conventional air fired conditions.

- Chapter 8 discusses the impact of biomass char on coal char burnout, with particular emphasis on the potential catalytic effect of the alkali and alkaline metals inherent in biomass fuels

- Chapter 9 correlates the synergetic effect of sawdust on coal volatile yield.

- Chapter 10 presents the effect of particle size and moisture content on devolatilisation and combustion performance of sawdust.

- Chapter 11 presents a general discussion on the relevance of the data in the power sector and the application of this data in relevant CFD codes to design dedicated biomass firing or co-firing plants.

- Chapter 12 presents the overall conclusions from the study and the future work.

2 LITERATURE REVIEW

2.1 ORIGIN AND PROPERTIES OF BIOMASS

Biomass is a general term for materials derived from growing plants or animal manure (Demirbas, 2005). It is also categorised as waste such as sewage sludge, refuse; woody products such as hard and softwoods and agricultural residues such grasses, stalks and straws (Williams et al., 2001). All lignocelluloses (woody and herbaceous) biomasses are composed of three components: cellulose, hemicellulose and lignin.

2.1.1 *Cellulose*

Cellulose is a linear crystalline polysaccharide polymer which is strong and resistant to hydrolysis. It constitutes major part of the combustibles in biomass. About 50 wt% of biomass is made up of cellulose. A typical structure of cellulose is presented in Figure 2.1

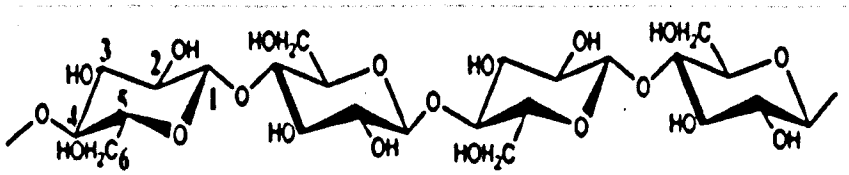

Figure 2.1 Structure of cellulose (Zhang et al., 2011))

2.1.2 *Hemicellulose*

Hemicelluloses are branched chain polysaccharides which have random and amorphous structure with shorter and weaker chains than cellulose. They

constitute usually 25-35% of the mass in the dry wood, 28% in softwoods and 35% in hardwoods. A typical structure of hemicellulose is shown in Figure 2.2.

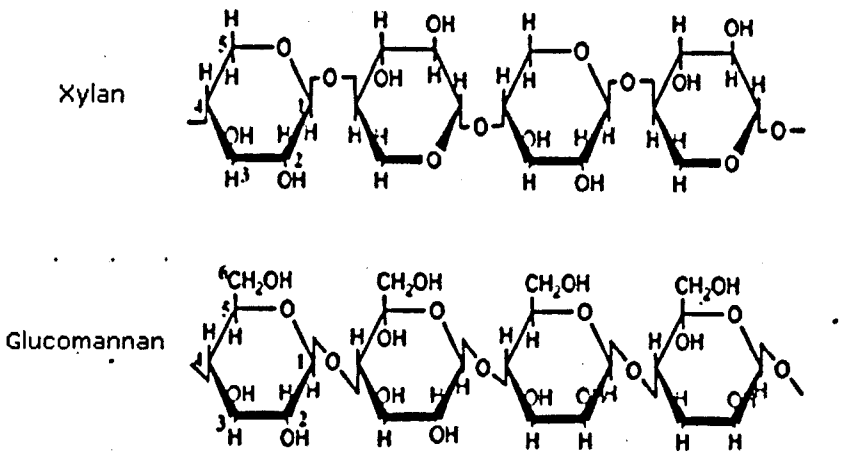

Figure 2.2 A typical structure of hemicellulose (Zhang et al., 2011)

2.1.3 *Lignin*

Lignin is a cross linked macromolecular polymer and constitutes about 30% of lignocellulose biomass. It is formed by de-hydrogenation of p-hydroxy-cinnamyl alcohols. Lignin is made up of different units which differ in different plant groups. For example, gymnosperm lignin is formed from coniferyl alcohols; angiosperm lignin is formed from the mixture of coniferyl and cinapyl alcohols, and grass lignin from mixtures of coniferyl, sinapyl and coumaryl alcohols. Lignin is also phenolic in nature; it is very stable and difficult to isolate. It occurs between the cell walls and this gives the plants their excellent strength and rigidity. During combustion, it burns more slowly and yields more energy than cellulose so that it is recognised as the main component responsible for char formation and the fixed carbon in biomass chars (Gani and Naruse, 2007, Manya

et al., 2003, Orfão et al., 1999, Skodras et al., 2006). Figure 2.3 presents a typical structure of lignin.

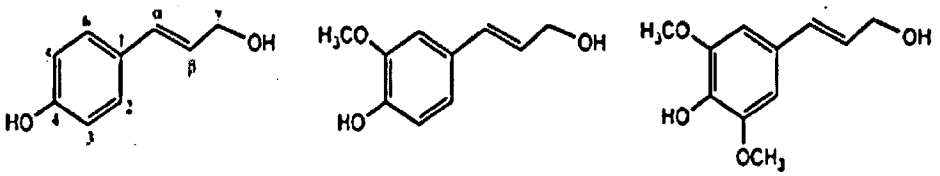

Paracoumaryl alcohol (H-unit) Coniferyl alcohol (G-unit) Sinapyl alcohol (S-unit)

Figure 2.3 A typical structure of lignin (Zhang et al., 2011)

2.1.4 *Moisture content of biomass fuel*

The moisture content of biomass fuel varies from one type of biomass to another depending on the season of harvest and storage conditions. During combustion, moisture will evaporate at low temperature and since evaporation uses energy released from combustion process, it lowers the temperature in the combustion system which slows down the combustion process (Van Loo and Koppejan, 2008).

2.1.5 *Volatile Matter*

Volatile matter in solids fuel is the main factor for its ignition process. Biomass loses up to 70-85% of its mass as volatiles during devolatilisation (Baxter, 2005) compared to coal which loses usually less than 50 % of its mass. The release of volatile matter is as a result of depolymerisation reactions which decompose the macromolecular structure (Moghtaderi et al., 2004) and depends on the devolatilisation temperature, residence time and heating rate.

Shuangning et al (2006) studied the devolatilisation of biomass at flash heating rate of 10^4K/s between 750-900°C and residence time between 0.115-0.24s. They observed that the yield of volatiles from the rapid decomposition was higher. During thermal decomposition, biomass releases its volatiles at lower temperatures than coal. The volatile yield in biomass starts about 160-200°C compared to coal which starts between 350-400°C depending on the coal type (Werther et al., 2000).

2.1.6 *Mineral matter in biomass*

Biomass contains inorganic mineral matters which are bound to the fuel as salts in the carbon structure or added to the fuel during harvesting, processing, transportation and storage (Van Loo and Koppejan, 2008). These include sodium, magnesium, calcium, potassium, phosphorus, iron, aluminium and other heavy metals. These are the major ash forming elements in biomass fuel and undergo different transformations during biomass combustion. A fraction of the mineral material particularly the alkali and alkaline earth metals compounds in the fuel are volatilised depending on the fuel characteristics, gas atmosphere and combustion technology used (Van Loo and Koppejan, 2008).

During combustion, the ash formed may form a protective layer around the burning char particles and this may inhibit combustion. In general, herbaceous materials potentially produce high ash deposition rates while many forms of wood waste produce relatively small ash deposit rates (Baxter, 2005). However, the low melting point of biomass ash is associated with agglomeration, fouling and scaling of furnace walls during conversion. Nevertheless, the catalytic effect of biomass containing alkali and alkaline metal can compensate for the negative effects during biomass co-firing.

2.2 BIOMASS CONVERSION

Biomass can be converted into carbonaceous solids, liquids and gases using thermo chemical or biological methods (Demirbas, 2004). Thermal conversion involves the breaking down of biomass using heat while in the biological technique enzymes of bacterial and other micro-organisms are used to break down the biomass. The thermochemical conversion processes include pyrolysis, combustion, gasification and most recently, torrefaction. The main direct application of the thermochemical conversion techniques is in the heat and power industry. Here, the biomass is burned in a boiler to produce high-pressure steam. The steam is then introduced into a steam turbine and flows over a series of turbine blades, causing the turbine to rotate. The rotating turbine causes the electric generator to rotate thereby producing electricity. The heat from the turbine is also converted and used for other energy purposes and the process is known as the combined heat and power (CHP).

2.2.1 *Biomass Combustion*

Combustion is the oxidation of fuel accompanied by the production of heat. It generally entails several stages including the devolatilisation of organic material, the combustion of volatile matter and the combustion of residual char, during which ash is formed. Once devolatilisation is completed, a flame is formed through the combustion of volatile compounds. This consumes oxygen and increases the temperature of the chamber (Biagini et al., 2006). Once the volatile combustion is completed, oxygen will react with the char and char combustion would take place. The speed of this reaction step is generally determined by the slow diffusion rate of oxygen in the char prior to the reattachment; which, in turn, is determined by the distribution of pores in the solid (Yu et al., 2007). As a result, this reaction phase is often considered the rate-limiting step of the char oxidation. For biomass fuels, devolatilisation is

complex due to differences in chemical composition of components; cellulose, hemicellulose and lignin within the biomass materials (Kruse and Gawlik, 2003). The different steps which entailed the complete combustion process are discussed in detail.

2.2.1.1 Biomass devolatilisation/Pyrolysis

Devolatilisation is the thermal degradation of the biomass into gases, tar and char in the absence of an oxidising agent. Devolatilisation and pyrolysis are usually interchangeably used because they produce the same products (Senneca et al., 2004a, Senneca et al., 2004b). The products are gases, tars and solids though these depend on the type of biomass fuel and the operating conditions. Biomass contains about 70-85% volatiles compared to usually less than 50% for coal (Baxter, 2005, Biagini et al., 2006). During devolatilisation, there is a rapid mass loss as a result of there is evolution of the volatiles. Though this process appear to be simple, it involves the breaking down of different components at different temperature ranges and the subsequent release of inherent volatiles leading to structural changes (Yu et al., 2007). The amount of volatiles in biomass fuel strongly influences the thermal decomposition and combustion behaviour of the fuel.

The three components of biomass fuel behave differently during thermal heating. Hemicellulose which has relatively weaker bonds decomposes at lower temperatures (160-260°C) to release CO and CO_2. Cellulose is the next to decompose at about 200-350°C while lignin decomposes for a long range of temperature. A typical example of the thermal decomposition behaviour of the three components of biomass fuel is shown in Figure 2.4.

Several investigations on the devolatilisation behaviour of biomass have been carried out at different heating rates and temperature. In a laboratory investigation using thermo gravimetric analysers, biomass samples were heated from ambient temperature to desired temperatures either at constant heating rates (isothermal) or different heating rates (non-isothermal).

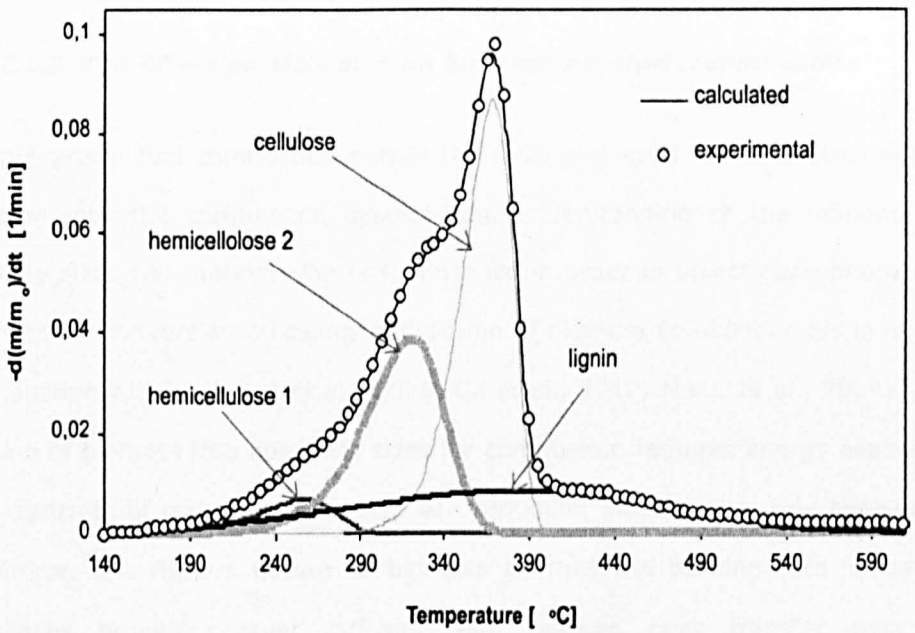

Figure 2.4 Typical example of Pyrolysis of biomass fuel (Vamvuka et al., 2003a)

Heating rates of 5,10, up to 100°C/min were used for pyrolysis by Biagini et al (2006) and Skodras et al (2006) . The results revealed that at higher heating rate, faster conversion of biomass to volatiles matters were achieved resulting in high quality chars for subsequent combustion. The rate of biomass devolatilisation has also been widely studied in inert atmosphere (Saddawi et al., 2010, Shen et al., 2009, Várhegyi et al., 1997) and in oxidative atmosphere (Amutio et al., 2011a, Cetinkaya and Yu¨ru¨m, 2000, Cordero et al., 1991, Senneca et al., 2004a). The rate of devolatilisation focuses on how fast thermal decomposition takes place.

In modelling the reaction kinetics of biomass devolatilisation, first order reactions have been used to describe the thermal decomposition (Conesa et al., 2001, Gronli et al., 2002) or parallel first order reaction describing the different components of biomass (Cordero et al., 1991, Cordero et al., 1990, Di Blasi and Branca, 2001, Gronli et al., 2002). The knowledge of the kinetics is important for the design of the combustion process (Saddawi et al., 2010).

2.2.1.2 The Effect particle size on biomass pyrolysis/combustion

As pulverised fuel combustion entails the milling of solid fuel into sizes before feeding into the combustion system, the understanding of the influence of particle sizes will therefore be of importance in order to select appropriate size fraction for conversion efficiency and design of biomass combustion alone or co-combustion with coal (Cai et al., 2008, Gil et al., 2010, Munir et al., 2009). The milling of biomass into adequate sizes for combustion requires energy especially the agricultural residues. However, size reduction plays a vital role because it minimises the fibrous nature of biomass so that the burning rate is faster, enhances boundary layer diffusion and reduces heat transfer resistant (Damartzis et al., 2009, Le Manquais et al., 2009, Ryu et al., 2006, Yang et al., 2005).

To date, many studies have been carried out on the effect of particle size on biomass conversion. Most of the studies have considered biomass pyrolysis using one particle size fractions putting into account the devolatilisation behaviour of the different components and their kinetic parameters (Manya et al., 2003, Park et al., 2009, Skodras et al., 2006). The influence of fuel particle sizes on the chemical properties of biomass fuel has been studied (Cloke et al., 1997, Di Blasi et al., 1999a, Encinar et al., 2000, González et al., 2003, González et al., 2009, Levenspiel, 1999, Sricharoenchaikul et al., 2001). These properties significantly influence combustion behaviour of solid fuels. For example, larger particle size

will release limited amount of volatiles due to mass transfer resistance compared to smaller particle size. Limited release of volatiles leads to secondary reaction.

The effect of fuel particle size has also been considered in fluidised bed pyrolysis by Shen et al (2009). It was reported that the yield of bio-oil decreases with increasing particle size. They attributed the high yield of bio-oil in the smaller particle size to the partial destruction of the cellulose structure during milling so that the cell content is easily released during pyrolysis. While in the case of large particle size ranges, diffusion of pyrolysis product to the external surface could pose problem due to the cellulose fibrous structure hence char formation is preferentially favoured. However, char yield was reported to increase with increasing particle size fraction but the quality of char in terms of fixed carbon decreased with increasing particle size fraction (Encinar et al., 2000, González et al., 2003). This variability could be due to the devolatilisation behaviour of the different particle size fractions. The fibrous nature of biomass fuel is more evident during combustion especially when agricultural residues are used (Damartzis et al., 2009).

For coal devolatilisation, the effect of particle size has also been observed. This was attributed to the maceral enrichment in different size fractions during sample preparation (Yu et al., 2005). The presence of unburnt carbon in fly ash is also associated with the combustion of larger particle size fractions.

2.3 BIOMASS GASIFICATION

Gasification is the partial oxidation or incomplete combustion of biomass fuel using air, CO_2 or steam or a mixture of them as a gasifying agent resulting in the production of producer gas. It is a mixture of carbon monoxide, hydrogen, methane and carbon dioxide. Gasification is being used to improve the energy

conversion efficiency in power generation industries through the use of gas turbines. The steam from the waste gases is recovered to generate electricity. Many studies have investigated the gasification of biomass fuel. Like combustion process, it also entails drying, pyrolysis before proceeding to gasification of the resultant char. Biomass gasification has been used to produce gaseous mixtures as feedstocks for heat and electricity industry (Wang et al., 2008).

2.3.1 *Types of gasifier*

2.3.1.1 Fixed bed gasifiers

Fixed bed gasifiers are named according to the way air or oxygen is introduced into the system; downdraft, updraft and cross draft. In the updraft gasifier, air is passed into the system from the bottom and the combustible gases are collected from the top. In the downdraft one, the air passes through the top downward while in the case of the cross draft, the air is passed across and the gases are collected on the other side. The choice of these gasifiers depends on the fuel physical and chemical composition. It means that gasifiers may be fuel specific.

2.3.1.2 Fluidized bed gasifiers

Fluidized bed gasifiers are mostly used to convert biomass waste products into a combustible gas. The major advantages of fluidized bed gasifiers are their feedstock flexibility resulting from easy control of temperature. The feed can be kept below the melting or fusion point of the ash and they have the ability to deal with fluffy and fine grained materials such as sawdust without the need of pre-processing. Problems with feeding, instability of the bed and fly-ash sintering in the gas channels can occur with some biomass fuels. The primary benefit of biomass gasification compared to direct combustion is that gases can be used in a variety of power plant configurations.

2.3.1.3 Entrained flow gasifiers

In entrained-flow gasifiers, fuel particles (coal or biomass) and the oxidant are fed into the top of the gasifier. The oxidant entrains the fuel particles as they flow through the gasifier. Gasifiers of this type operate at very high temperatures. The fine coal feed and high operating temperature allow the gasification reaction to occur at a very high rate and at very short residence times with high carbon conversion efficiencies. Entrained-flow gasifiers have the ability to handle practically any feedstock and produce a clean, tar-free, syngas.

2.4 ORIGIN AND COMPOSITION OF COAL

Coal is heterogeneous substance because it was formed from dissimilar kinds of debris and contains various entities which contains inorganic minerals that are called macerals (Berkowitz, 1994). The organic materials are derived mainly from plant remains and have undergone various decomposition processes in peat swamp resulting in physical and chemical alteration after burial (Ting, 1982). It is also known to be a complex heterogeneous mixture of organic and inorganic matter containing solid, liquid and gaseous phases with different origin (Liu et al., 2005). Physical or petrographic structure of coal depends on the dominant features present during formation or metamorphosis. A typical structure of coal is shown in Figure 2.6. Coal exists as a large macromolecule network polymer structure. This structure consists of aromatic clusters that are cross linked to other aromatic structures by bridges. A typical coal is made up of carbon, hydrogen, oxygen, sulphur and some minerals. It is classified into ranks by different characterisation properties.

Coal is either termed high or low rank depending on the carbon content and heating rate during combustion. High rank coal exhibits high carbon content and high heating value, low hydrogen and low oxygen contents. They are harder and

stronger and often have a black vitreous lustre. Increasing rank is accompanied by an increase in the carbon and energy contents and a decrease in the inherent moisture content (Berkowitz, 1994). Low rank coals have low carbon and low heating value but high hydrogen, oxygen and sulphur contents. Low-rank coals, such as lignite and sub-bituminous coals, are softer, friable materials with a dull appearance, and are characterised by high moisture levels and low carbon content, exhibiting lower energy value. There are two analyses to characterise coal namely proximate and ultimate analysis. Proximate analysis determines the moisture content, volatile matters, fixed carbon and the ash content. The ultimate analysis is used to determine the main elements contained in the sample such as nitrogen, hydrogen, sulphur etc (Berkowitz, 1994).

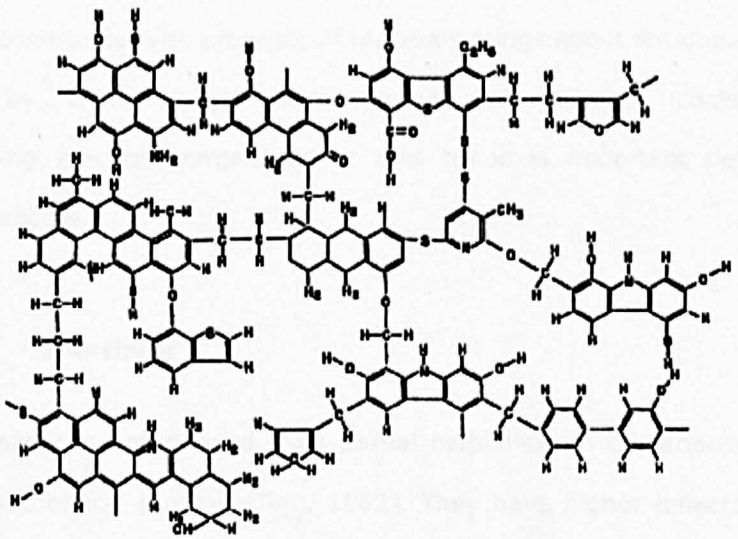

Figure 2.5 A typical structure of coal (LOISON et al., 1989, Levine et al., 1982)

2.4.1 *Mineral Matter in coal*

Like biomass, coal also contains inorganic mineral matters. Some minerals enter the coal substance as a constituent of parent vegetation during metamorphosis (Berkowitz, 1994). Mineral matter found in coal at a particular deposit depends

on the geography of the deposit. The different mineral matter in coal may undergo different physical and chemical transformations (Liu et al., 2005). It has also been found that the presence of inorganic matter in coal chars only marginally affects the evolution of the average char microstructure (Sheng, 2007). Additionally, most of these minerals also undergo transformation during devolatilisation depending on the temperature (Tomeczek and Palugniok, 2002, Vassilev et al., 1995). Like biomass, the transformation of these minerals causes ash deposits in boilers and other combustion systems.

2.4.2 *Maceral composition*

Macerals are microscopic distinct components of the organic matter of coal (Joseph et al., 1991). Macerals are derived from plant tissues commonly preserved in peat swamps. There are three groups of macerals namely liptinite, vitrinite and inertinite. The presence of macerals brings about structural different exhibited by chars during devolatilisation of different coals. Hence, understanding maceral composition of coal becomes important before coals utilisation process.

2.4.2.1 **Inertinite**

Inertinite macerals are derived from partial carbonisation of various plants or intensive biochemical process (Ting, 1982). They have higher reflectance, high carbon and oxygen contents. They are further re-grouped into reactive and unreactive components on the basis of their reflectance values.

2.4.2.2 Liptinite

Liptinites macerals are derived from cuticle, resin and waxy materials of plants (dark yellow or dark grey). The liptinite group of macerals, which has the highest hydrogen content, volatile yield, and heating value, is regarded as the most reactive maceral group in coals of the same rank.

2.4.2.3 *Vitrinite*

Vitrinites form major discrete constituents of coal. Vitrinite is derived from decomposed wood tissue and the most abundant, more than 70-80% of most coal beds. Of the three maceral groups, vitrinites exhibit greater thermal alteration during combustion. The degree of oxidation or pyrolisation of a coal is related to the rank of the vitrinite content. Additionally, vitrinite reflection has been used to determine the rank of coal. Pyrolysis of high vitrinite coals may produce vesiculated and swollen chars depending on the fluidity development and rate of volatile release.

2.5 COAL CONVERSION

Coal combustion is a complex and heterogeneous process involving different steps producing volatile and solid products. The characteristics exhibited during combustion such as swelling, fluidity and heating values are affected by the rank of coal utilised. This implies that coal rank has significant role to play in the overall utilisation of coal. Moreover, not only coal rank has been found to influence the combustion characteristics of coal, its petrographic composition also has an influence on the combustion behaviour of coal. For example, macerals have been identified as having distinct and unique physical properties and chemical composition and these have been reported to influence the burning characteristics of different coals (Choudhury et al., 2008).

The mechanism of coal combustion for power generation entails different stages including devolatilisation, combustion of volatile and the char formed and finally the formation of ash. Coal is utilised in pulverised fuel combustion systems and fluidised bed combustion or gasification systems. Figure 2.6 presents a pulverised coal combustion unit for power generation.

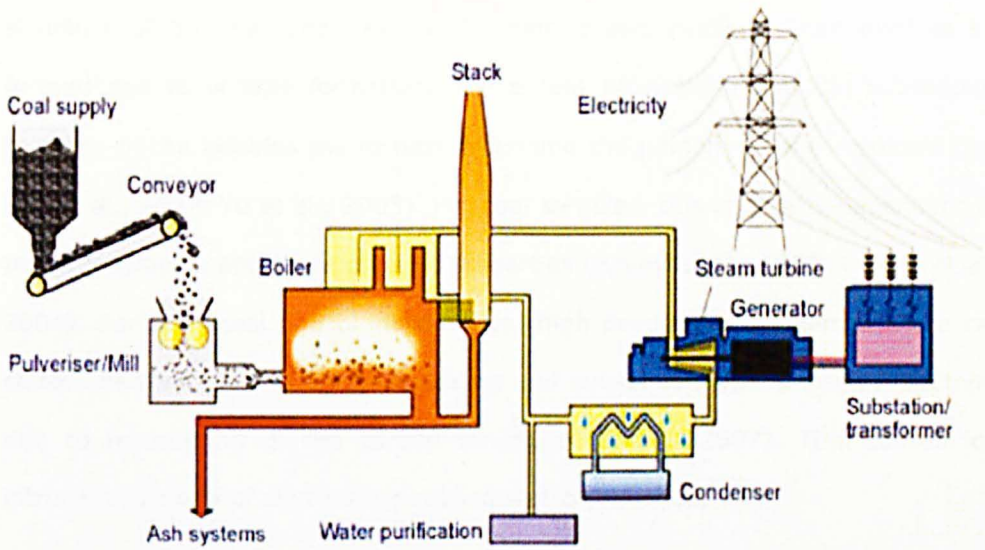

Figure 2.6 Pulverised coal combustion units for power generation ((WCA, 2011)

2.5.1 ***Coal devolatilisation/Pyrolysis***

Devolatilisation/Pyrolysis refers to the thermal decomposition of coal and it occurs usually in an inert atmosphere leading to the release of volatile compounds (Biagini et al., 2006). It involves the breaking of aliphatic and aromatic bonds to release gases such as carbon dioxide and methane and continues until the solid char remains. However, oxidative pyrolysis has also been carried out by researchers where the fuel combustion takes place in air. Unlike biomass, coal devolatilisation takes place at much higher temperatures. However, devolatilisation behaviour varies with coal ranks. For example, low rank coals in general, generate a high volatile yield like biomass and a low yield of tar. High volatile bituminous coals generate a high yield of tar and a moderate volatile matter yield while high-rank coals generate a low yield of tar and a low volatile matter yield.

2.5.2 *Effect of devolatilisation temperature on char structure*

Devolatilisation temperature plays an important role in the structural formation of the coal and biomass chars. After the release of volatiles, the physical structure of the char changes due to melting and swelling. Then bubbles are formed due to volatile formation. The extent of swelling and the subsequent bursting of the bubbles will in turn determine the porosity of the resultant char (Yu et al., 2007, Yu et al., 2003). For coal samples, this is greatly dependent on the petrographic and thermoplastic properties (Bailey et al., 1990, Kidena et al., 2004). For both coal and biomass chars, high devolatilisation temperature can cause deactivation or thermal annealing and subsequently, the loss of reactivity due to re-ordering of the carbon structure (Sheng, 2007). This causes low intrinsic reactivity of char during subsequent combustion.

2.5.3 *Heating rate*

Heating rate has some influence on the devolatilisation behaviour and char reactivity of solid fuels. At high heating rate, a faster pyrolytic conversion to volatile matters occurs (Fushimi et al., 2003). This is mainly because a high heating rate may shift the reaction to a much higher temperature range, therefore causing the devolatilisation to take place at a much higher rate. High heating rate during pyrolysis has produced more reactive char for combustion and greater percentage of fixed carbon content (Encinar et al., 2000, Di Blasi, 2009).

2.5.4 *Effect of structural variations on char combustion*

Combustion reactivity is determined by how quickly conversion takes place with time and during char combustion. It is a function of how easily gaseous reactants diffuse into the surface and pore of char for combustion process to take place. The morphology, structure and texture of chars affect the behaviour

of char during combustion. This is because the porous char will allow the diffusion of reactant gas into the active sites of the char for reaction to take place. It also allows the diffusion of gas products out of the particle.

Precious works have demonstrated that char morphology plays an important role in char combustion reactivity (Biagini et al., 2008a, Biagini et al., 2009, Cetin et al., 2004, Hu et al., 2008, Sharma et al., 2001). During pyrolysis/devolatilisation, depending on the heating rate and final pyrolysis temperature, volatiles are rapidly released from the fuel sample leading to structural variations. Fast heating rates produce chars with mesopores and macropores and these are indicators of reactive surfaces that reduce mass transfer limitations (Di Blasi, 2009). Such macroporous chars usually have irregular indented surfaces and large openings due to escape of volatiles for easy accessibility of gaseous reactants during char combustion. Softening, swelling surfaces and formation of bubbles are some physical features of chars that affect combustion reactivity. These features are related to the effect of different pyrolysis temperatures and heating rates (Biagini et al., 2009, Cetin et al., 2004) and subsequently affect the intrinsic reactivity of the char.

2.5.5 *Intrinsic Reactivity and chemical kinetic parameters*

The intrinsic reactivity of char can be defined as the rate of reaction between the oxidising gas and internal surface areas of the char, in the absence of any mass transfer or pore diffusion limitation. This involves the study of the chemical kinetic parameters that are free from heat and mass transfer limitations. In the determination of intrinsic kinetic reactivity parameters, it is essential that the reaction is purely kinetic controlled (Guo and Lua, 2001) and combustion temperature should be low (Biagini et al., 2009). Experimentally, it is determined by recording the time taken for a sample to lose a reasonable

proportion of its weight with a range of temperatures under isothermal or non-isothermal conditions. Activation energy and pre-exponential factor are used to predict the time-conversion profile for the pyrolysis and combustion process.

Different global kinetic models with different reaction orders have been used to determine the intrinsic kinetics of combustion processes at both low and high heating rates (Backreedy et al., 2003, Everson et al., 2006, Hurt and Calo, 2001, Senneca, 2008, Vamvuka et al., 2003a). The first order one step kinetic model is widely used among other models to determine the devolatilisation/char reactivity (Shuangning et al., 2006, Sima-Ella et al., 2005b) because of its simplicity. Though, (Biagini et al., 2008b) of the opinion that the first order reaction model gives only a representation of the main devolatilisation but not the earliest and the final tail of the process. Various studies have obtained activation energy of the different pseudo-components of biomass pyrolysis and biomass/coal blends resulting in relatively different values. These are largely due to the fact that different particle sizes or size ranges of the samples are used though operating conditions and the reaction rate controlling step can (Dong et al., 2010a, Molcan et al., 2009) affect kinetic parameters.

2.5.6 *Heterogeneous Reaction Mechanism*

The mechanism of heterogeneous reaction needs proper understanding in order to effectively describe the rate controlling steps in a chemical reaction. During solid combustion, the reactant gas diffuses into the particle and reaction takes place. This has led to the assumption that char combustion occurs at different rates and with different orders of magnitude in three specified regimes (Backreedy et al., 1999). There is a chemical control regime (low temperature, zone I) where the oxygen concentration within the pores is equivalent to that in the bulk phase and consequently the reaction rate is controlled by adsorption, desorption or the truly inherent chemical kinetics between the solid carbon and

some adsorbed oxygen containing species. Though small particle sizes enhance boundary layer diffusion and char deactivation can cause low intrinsic reactivity at relatively short heat treatment (SMITH, 1982), a combination of chemical kinetics and diffusion controls can dominate during the combustion process (regime II combustion). However, the transition between regimes I and II is fuel specific (Nowak et al., 2013). Thirdly, an external diffusion control regime (high temperature, zone III) where the oxygen concentration is zero at the particle surface and the reaction is controlled by the diffusion of oxygen and oxides of carbon in the bulk. Then at high temperature and with large particle size, combustion process is dominated by the diffusion of the reacting gas through the boundary layer to the surface (regime III combustion). This means that combustion rate is controlled by the intrinsic reaction rate of the internal surface of the char particles, the size of the surface and the extent to which oxygen diffuses through the pores (SMITH, 1982).

2.6 BIOMASS/COAL CO-FIRING

Biomass fuel can be used alone as a combustion fuel to produce heat and power. However, the cost of building new power plants for biomass combustion would be capital intensive. Therefore, co-firing biomass with coal in the existing coal fired systems became the most attractive technology. Co-firing biomass with coal entails substituting a certain percentage of coal with biomass fuel and carrying out combustion in a coal fired systems. Though remarkable differences exist in the two fuels, blending them together has recorded improved product yield and char reactivity depending on the blending ratio (Haykiri-Acma and Yaman, 2007, Sutcu, 2007, Vamvuka et al., 2003b, Zhang et al., 2007).

The high carbon content of coal and high volatile content of biomass can compensate each other during co-firing and provide a better combustion process

than the individual fuels. As a result of these foreseeable benefits, efforts are made to explore the possibility of supplementing fossil fuels through the use of biomass renewable and CO_2-neutral fuel in order to reduce fossil fuel generated CO_2 emissions and to reduce fuel cost (Annamalai et al., 2003).

Biomass co-firing can be carried out in most coal fired systems including pf fired systems and fluidized beds (Dare et al., 2001, Pronobis, 2006). The combustion of biomass with coal in coal fired plants have been widely investigated in different laboratory and field demonstration (Biagini et al., 2002a, Chao et al., 2008, Gani et al., 2005a, Jr et al., 2000, Senneca, 2008, Vamvuka et al., 2003b, Wang et al., 2007a) in order to fully understand the impact of co-firing in the reduction of the emissions of greenhouse gases. Over 100 field demonstrations have been carried out in 16 countries and one of such plants making use of pulverized biomass fuel is Gelderland power station in Holland (Baxter, 2005). In the UK, Drax power limited has the World's largest co-firing facility commissioned and fully operational in 2010 (IEA, 2011).

There are different options available for co-firing biomass in coal-fired boilers. One option is to install new, dedicated biomass burners (Fernando, 2012). For this feeding method, large supply of biomass fuel is possible and feed rate can be easily controlled to avoid agglomeration. However, it is relatively expensive to install new equipment (Fernando, 2012) and requires paying attention to biomass fuel particle sizes (Tillman, 2000). In the second feeding method, biomass is pre-milled and injected separately into the coal burner. This is also relatively expensive because extra injector is needed. However, high blending ratios and good combustion performance can be achieved (Sami et al., 2001). In the third category, biomass fuel is premixed with coal before injecting into the burner through one injector point. This is the cheapest method (Boylan et al., 2000) because no extra cost is required since the existing coal fired system is

being used and premixing could lead to high combustion efficiency. This approach is possible for co-firing up to 10% biomass on a thermal basis (Fernando, 2012).

Apart from the mitigation of greenhouse gases, co-firing biomass with coal has been found to reduce other emissions such as NOx and SOx. The calcium and magnesium oxides present in the ash formed during the combustion absorbs sulphur dioxide which would have been emitted (Spliethoff and Hein, 1998). Also, the ignition temperature is enhanced by co-firing biomass with high rank coal (Gani et al., 2005a). Poor fly ash deposition and formation of chlorine can also be minimized. However, the right proportion of biomass fuel to supplement coal is an important factor to consider during co-firing.

2.6.1 *Biomass/Coal Blend Ratio*

Blending fuels to stay within emission level or to create boiler ready blend fuel is an important aspect of co-firing. In simple terms, blending ratios play vital roles in promoting the efficiency of the combustion system. Additionally, the information on devolatilisation behaviour of biomass/coal blends during co-firing is necessary in order to understand the combustion chemistry and the kinetics involved (Biagini et al., 2002a). Most of the studies have provided useful information to aid the understanding of the impact of biomass/coal blending ratios on combustion performance. Different blend ratios of biomass/coal fuels have been considered in co-firing experiments ranging from 5, 10, and 25 to 50 wt% of biomass in coal (Annamalai et al., 2003, Folgueras et al., 2003, Robinson et al., 2002, Spliethoff and Hein, 1998, Wang et al., 2007a). In the industrial pulverised systems, blending about 10% biomass on thermal basis with coal will not require much alteration in the combustion system though 20% mix has been used (Demirbas, 2003).

Recently, due to the growing concerns over carbon emissions from coal-fired power plants co-firing biomass at high ratios drawn greater focus (Fernando, 2012). Furthermore, the latest Government response to proposals under the Renewable Obligation (DECC, 2012a) recognises the incentives needed to encourage high levels of co-firing in coal-fired plants. This is due the Large Combustion Plant Directive (LCPD) requirement to close coal-fired plants without flue gas desulphurisation and low NOx technology before January 2016.

2.7 SYNERGETIC BEHAVIOUR DURING BIOMASS/COAL CO-FIRING

2.7.1 *Synergy during co-pyrolysis*

For effective utilisation of the biomass and coal as pulverised fuel (PF), compatibility of the fuels during combustion which is synergetic effect is preferable. This is because chemical interactions between the two fuels during co-firing will consequently increase co-pyrolysis products and the carbon burnout efficiency of coal char, allowing the fly ash to meet up specification for other uses. Such interactions between biomass and coal have been investigated extensively during co-pyrolysis. For example, Haykiri-Acma and Yaman (Haykiri-Acma and Yaman, 2007, Haykiri-Acma and Yaman, 2008a) reported that synergetic interaction occurred during combustion of biomass and coal in air using TGA from ambient to 900°C. Synergetic effect which indicates the compatibility of the two fuels (Haykiri-Acma and Yaman, 2009) resulted in higher yield of volatiles than the individual fuels (Park et al., 2010, Sonobe et al., 2008). Other studies have also shown interactive behaviour between biomass and coal during co-gasification in a fluidised bed gasifier (Sjöström et al., 1999). Presumably, synergetic behaviour during devolatilisation may be dependent upon the contact time of the fuel particles, and the relative rates of pyrolysis of the different fuels. However, coal rank has played a significant role in the synergetic behaviour of the two fuels (Haykiri-Acma and Yaman, 2010).

Blending ratio, pyrolysis temperature and high hydrogen content of biomass fuel have been found to influence interaction taking place during co-pyrolysis. The co-pyrolysis investigation carried out by Zhang et al (2007) showed that above 50:50 wt% blends, significant synergetic effect was observed suggesting that there is an optimum blending ratio for biomass/coal co-firing. Also, temperatures between 400-600°C have been documented to favour synergy during co-pyrolysis (Haykiri-Acma and Yaman, 2007, Park et al., 2010, Sonobe et al., 2008, Zhang et al., 2007). In most of the studies carried out, the enhanced devolatilisation processes have been attributed to hydrogen donor potential of biomass fuel (Haykiri-Acma and Yaman, 2007, Park et al., 2010, Sharypov et al., 2007, Straka et al., 2004, Zhang et al., 2007).

On the contrary, no synergetic effects have also observed by some workers during co-pyrolysis. The absence of synergy during reaction simply implies that the addition of biomass to coal did not influence coal behaviour. For instance, wood waste and wheat straw were co-pyrolysed differently with a sub bituminous coal using TGA in argon atmosphere heated from ambient to 1250°C (Vuthaluru, 2004). The predicted mass loss behaviour perfected matched the expected results highlighting that there was no chemical interaction between the two fuels during pyrolysis. The activation energy obtained for the blends at 50:50wt% ratio was higher than for other blend indicating that chemical interaction was observed in the kinetic parameters.

Also, similar results have been obtained for wood waste and lignite coal co-pyrolysis using TGA in nitrogen gas (Sadhukhan et al., 2008). More recent works of co-pyrolysis of biomass/coal in nitrogen atmosphere using TGA has also concluded that synergetic effect was absent in all blends during the co-pyrolysis (Di Nola et al., 2010, Gil et al., 2010, Idris et al., 2010). There are contradictions reported regarding interaction taking place between biomass and coal fuels

during co-pyrolysis. This diversity of results might be due to properties of the individual fuels such as differences in volatile matter produced or as a result of limited contact time for both fuels during pyrolysis. Nevertheless, for both scenarios, the addition of biomass fuel in coal has enhanced devolatilisation processes.

The chars produced from co-pyrolysis have also been examined to have different structural features from the individual fuels. Also, the addition of biomass to coal has been reported to have a sulphur fixing ability (Haykiri-Acma and Yaman, 2007). The synergetic interaction between biomass and coal in co-pyrolysis has also been extensively studied.

2.7.2 *Synergy between biomass and coal char in co-firing*

Biomass/coal char co-firing has also been investigated by physically mixing biomass and coal chars for co-firing. The advantage of this is that it makes grinding easy since bulk density of biomass is not involved (Sahu et al., 2010). Kastanaki and Vamvuka (2006) assessed the combustion of biomass-coal char blend using non isothermal TGA with two coal types and different biomass fuels over a temperature range of 20-850°C and heating rate of 10°C in air until complete burnout. Biomass/coal chars were blended in the ratios of 5:95; 10:90; 20:80 wt%. The impact of biomass char on coal char burnout was evaluated in terms of initial and final combustion temperatures, maximum reaction rate, kinetic rate constants and burnout times. The burnout times of the coal char was only slightly reduced with the addition of biomass char indicating that there were interactions between the fuels though this depended on coal rank, biomass type and the proportion of biomass char in the blend. Initial and burnout (final) temperatures were lowered by 26-32°C and 22-45°C, respectively for a lignite-biomass char blend containing 20 wt% biomass.

However, the small amount of biomass char used in this study may not be enough to substantially evaluate the impact of such chars on the reactivity of coal char. Sahu et al. (2010) used DSC-TGA to investigate the compatibility and blending ratio of biomass (sawdust & rice husk) and coal chars. Biomass chars were produced at 300°C and 450°C. Chars were blended in the ratios of biomass/coal char: 10:90; 20:80; 30:70; 50:50 and 70:30 wt% and particle size of <75 μm. Parameters used to investigate combustion reactivity were DTG peak temperature where weight loss is maximum, ignition index and burnout times. The results from the combustion behaviour showed that blends with <50 wt% biomass and prepared at 300°C performed better. Peak temperature was lower and burnout times were faster than predicted value and activation energy decreasing with increasing biomass char in the blend. Biomass (chestnut & olive stones) and bituminous coal blend char gasification was carried out using non isothermal TGA. Chars were prepared in a fluidised bed at 1100°C for 30min. There was no interaction observed for chestnut-coal char blend though some interaction was observed for olive stone and coal. Chars of particle size <150μm and biomass/coal char blend ratio was 30:70 wt%. This also confirms that the type of biomass used can influence coal char combustion performance because the concentration of alkali and alkaline minerals differ in different biomass samples. Subsequently, this will affect the catalytic effect. However, char morphology can affect combustion behaviour, intrinsic reactivity of char and char combustion mechanism.

2.8 NO_X EMISSIONS DURING OXY-COAL COMBUSTION

In combustion processes nitrogen oxides (collectively called NO_x) can be formed from fixation of molecular nitrogen in the combustion air or from nitrogen chemically bound in the fuel (fuel-N). In pulverized coal combustion fuel-N conversion to NO typically accounts for more than 80% of the NO emission

(Glarborg et al., 2003). The release of NO_x into the atmosphere can contribute to smog, ground level ozone, and acid rain. The concern about NO_x emissions and the need to comply with increasingly stringent regulations resulted in the use of some techniques to reduce these emissions. One of such techniques is the use of low NO_x burners which reduces volatile-N up to 80%. The conversion of fuel-N to NO and then to molecular nitrogen is a complex gas phase reaction chemistry (Kazanc et al., 2011). Figure 2.7 shows a schematic diagram of the nitrogen partitioning and possible NOx formation and reduction during fuel combustion process. For low rank coals and biomass, the pathway is: fuel-N to HCN and then to NH which is later oxidised to NO or N_2 depending on the reaction mechanism (Glarborg et al., 2003). On the other hand, char-N is reported to be the major contributor to NO formation (Glarborg et al., 2003) and NO_x reduction from char-N is more difficult to achieve (Liu et al., 2011).

Oxy-fuel combustion technology has been observed to reduce NO_x emissions. This is also partly because of the suppression of thermal NO_x (Koornneef et al., 2010) due to the absence of atmospheric N_2 and the reduction of NO to N_2 by recycling the NO. For example, from previous studies, lower NO_x emissions have been observed during oxy-fuel coal firing compared to conventional air fired conditions (Liu et al., 2005b, Sturgeon et al., 2009, Tan et al., 2006), up to 50-75% NO_x reduction was achieved (Croiset and Thambimuthu, 2001, Sturgeon et al., 2009, Wall, 2007). Liu et al (2005b) investigated NO_x reduction under oxy-fuel condition using a pulverised fuel burner and observed that recycling the flue gas could lead to high percentage reduction of NO_x to N_2. High NO_x reduction efficiency has also been achieved when NO_x was recycled into the primary air stream (zhou et al., 1996). More recently, NO_x reduction in O_2/CO_2 combustion have been found to be much higher than in O_2/N_2 (Ikeda et al., 2012, Liu et al., 2011) and during biomass co-firing (Kazanc et al., 2011). A mathematical

modelling investigation has also predicted that NO_x reduction is feasible when N_2 is replaced with CO_2 (Cao et al., 2010).

Nimmo et al (2010) studied the effect of O_2 concentration on NO_x formation during biomass co-firing. Their results revealed that NO_x emission can decrease or increase during co-firing depending on the operating temperature. However, the reduction of NO_x could be associated with char reactivity since combustion reactivity can affect the conversion of fuel nitrogen to Nitrogen oxides. This was observed when NO reduction over biomass char was investigated by (Dong et al., 2010b).

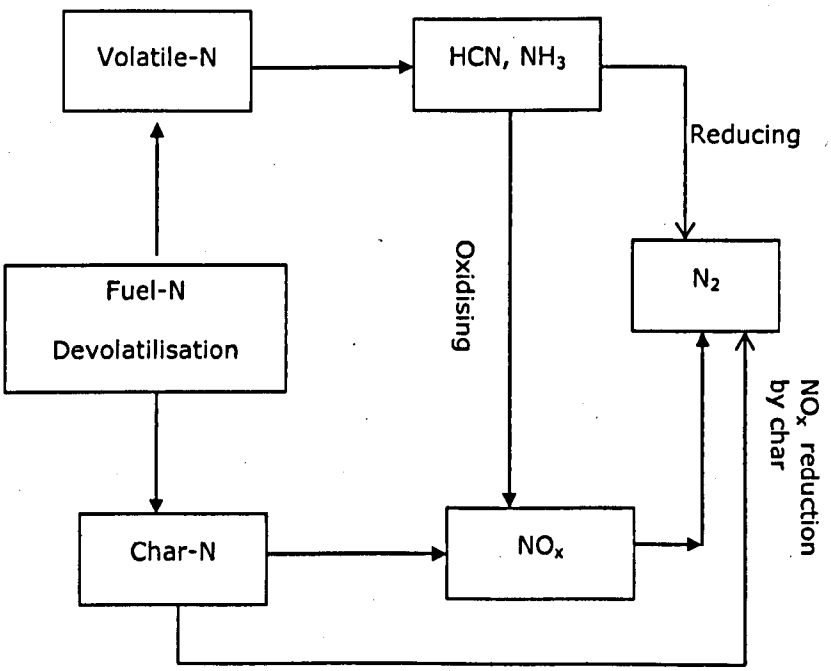

Figure 2.7 Schematic diagram of the fate of nitrogen during solid fuel combustion

Sulphur in coal originates from the parent plant materials or water in the coal forming environment (Chou, 2001). It occurs as sulphides, mainly as pyrites

(FeS_2), organic sulphur, elemental sulphur and sulphates. The level of sulphur in the coal (low or high sulphur coal) depends on the sulphur content in the coal forming environment. During combustion, the fuel bound sulphur is oxidised into oxides of sulphur i.e SO_2 and SO_3 (collectively called SO_x). The emission of these oxides is associated with a number of health effects and therefore requires reduction. In oxy-fuel combustion with recycle systems, higher concentration of SO_x are found, up to about three times higher in the flue gas than with conventional air firing (Croiset and Thambimuthu, 2001, Wall et al., 2009). However, SO_x emissions per unit energy are found to be low due to higher conversion of SO_2 to elemental sulphur. An investigation carried out previously revealed on a heat input basis (mg/MJ) oxy-fuel firing furnace exit SO_2 was reduced by approximately 25% compared to air firing (Sturgeon et al., 2009).

Biomass as an alternative fuel has negligible sulphur content hence, the combination of oxy-fuel combustion with biomass fuel becomes not just a sink for CO_2 emissions but also reduce SOx emissions (Arias et al., 2008). However, the characteristic behaviour of biomass fuel combustion under oxy-fuel condition is yet to be fully understood. Few studies so far have considered the co-combustion of biomass and coal under oxy-fuel conditions (Haykiri-Acma et al., 2010a, Normann et al., 2009). These studies considered the co-production of syngas by using biomass as a carbon neutral fuel to co-fire with coal (Normann et al., 2009) and the excess heat flow arising from biomass/coal co-combustion.

2.10 SUMMARY OF THE FINDINGS

From the findings of previous studies, the addition of biomass to coal has greatly influenced the pyrolysis and it can contribute to the combustion characteristics of coal. However, most of the investigations were carried out under air fired conditions so that the behaviour of biomass/coal combustion under oxy-fuel conditions is not yet understood. This has led to some knowledge gap in the on-going oxy-coal combustion technology in terms of the contribution of CO_2-char gasification reaction during oxy-biomass co-firing. Moreover, the potential ability of the alkali and alkaline metals in biomass to catalyse coal burnout has not been fully demonstrated.

3 MATERIALS AND METHODOLOGY

This chapter describes in detail the experimental techniques employed in this research.

3.1 BIOMASS SAMPLES AND PREPARATION

Two sawdust samples were used in this study. The first sawdust sample (pulverised woodchips) was supplied by E-on. The sawdust bulk particle size was greater than 500 μm. Therefore, the required particle sizes were obtained by milling and sieving. The properties of the sample are presented in Tables 3.1 and 3.2. Secondly, wet pelletized softwood sample of different size fractions with different moisture conditions (10, 20, 30, 40 and 50%) was supplied by Doosan Babcock. The properties of the bulk and different sized samples are presented in Tables 3.3 and 3.4 respectively. The devolatilisation and burnout behaviour of the Doosan Babcock samples are presented in chapter 10. Additionally, pinewood used was supplied by British Petroleum (BP). The properties of pinewood are also presented in Table 3.5.

Table 3.1 TGA proximate analysis of sawdust (as received basis)

Parameters	Particle Sizes (μm)					
	45	45-63	63-75	75-90	90-106	125-250
Moisture	7.5	6.7	6.8	6.8	6.0	6.4
Volatiles (wt%)	83.2	83.1	83.4	82.7	83.0	83.9
Fixed carbon (wt%)	16.8	16.9	16.6	17.3	17.0	16.1
Ash (wt%)	1.4	1.4	1.3	1.0	1.3	1.2
N (%)	0.5	0.4	0.4	0.4	0.4	0.4
C (%)	49.3	50.3	50.6	50.8	50.4	50.4
H (%)	5.0	5.6	5.6	5.7	5.9	5.7

Table 3.2 Bulk fuel analysis of the pelletized softwood sawdust before introduction of moisture

Proximate Analysis (as received)	
Moisture	8.8
Volatile mater	77
Fixed carbon	13.8
Ash	0.2
Fuel Ratio	0.18
Ultimate Analysis	
C	46.04
H	5.52
N	0.07

Table 3.3 The proximate analysis the wet sawdust size fractions analysed using the TGA.

Sample particle size	Proximate analysis, wt % (as received)			
	Moisture	Ash	Volatile matter	Fixed carbon
< 0.6 mm	3.69	0.53	83.45	12.33
<1.18 mm	3.13	0.45	82.82	13.60
<2.0 mm	2.00	0.47	84.32	13.21
<3.15 mm	3.17	0.44	83.92	12.47
< 5.0 mm	2.14	0.42	84.36	13.08

Table 3.4 TGA Proximate analysis of pinewood (as received)

Properties (Wt %)	125-250 μm
Moisture	8.1
Volatiles	69.7
Fixed carbon	19.2
Ash	3.1
Volatiles (% daf)	21.6
Fixed carbon (% daf)	78.4
Ash (% db)	3.3

3.2 Coal sample preparation

The coal sample used for co-firing in the study is South African coal (Kleinkojpe). This was supplied by E-on as pulverised coal. It was sieved into two particle sizes, 53-75 and 106-150 μm using the methods described in section 3.1.2 and 3.1.3. The properties of the coal are presented in Table 3.3.

Table 3.5 TGA proximate analysis of Kleinkojpe (as received)

Properties (Wt %)	53-75 μm	106-150 μm
Moisture	3.1	2.5
Volatiles	24.7	25.6
Fixed carbon	56.6	56.6
Ash	15.6	15.3
Volatiles (% daf)	30	31
Fixed carbon (% daf)	69.6	68.8
Ash (% db)	16.1	15.7

3.2.1 *Milling*

Since pulverised fuel combustion entails the milling of solid fuel into sizes before feeding into the combustion system, the understanding of the influence of particle sizes is therefore important to select the appropriate size fraction for conversion and design of biomass combustion alone or co-combustion with coal (Cai et al., 2008, Gil et al., 2010, Munir et al., 2009). Biomass samples were milled into particle sizes using a laboratory bench-top planetary ball mill Pulverisette 6. The pulveriser has 12 tungsten grinding balls that are inside the sample holder. About 10 g of the sawdust sample was placed in the sample holder and milled at a rotational speed of 250 revolutions per minute for about 5 minutes. Milled samples were stored in sample bags for sieving. Picture of the ball mill pulveriser is shown in Figure 3.1.

3.2.2 *Sieving into different size fractions*

Sieving was carried out using different size sieve pans. The required size was placed on each other in ascending size range from the smallest to the largest size and the sample was placed on the top sieve pan. It was then shaken for 15 minutes. Afterwards, the sieves were removed and the different size fractions placed into sample bottles. The sample sizes are as follow: < 45μm, 45- 63, 63-75, 75-90, 90-106, and 125-250 μm. This was done for all samples to obtain the above size ranges. Subsequently, entrained fine particles were removed from the each particle size range using Alpine A200 LS air Jet sieve (Figure 3.2).

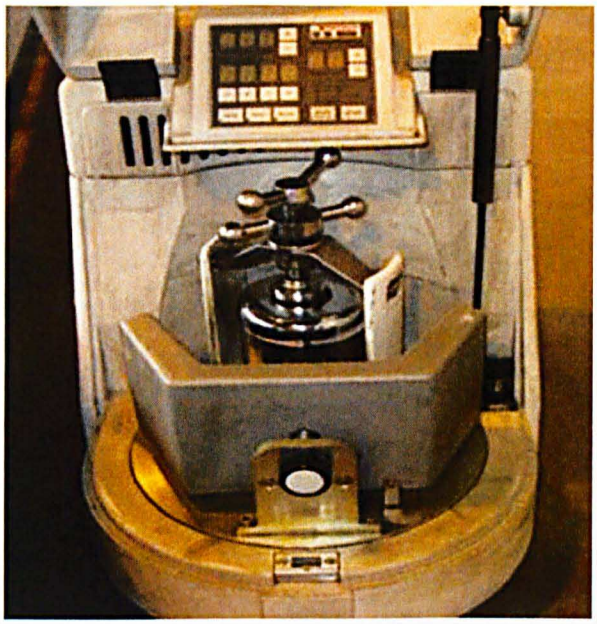

Figure 3.1 Ball mill pulverisette 6 used for crushing biomass

3.2.3 ***Alpine jet sieve***

This equipment allows suction to be maintained on the underside of modified Endecott sieves while allowing a rotating finger to blow a thin jet air back through the sieve. The thin jet air releases biomass particles stuck on the surface of the sieve when the sieves are been agitated. At the end of the process, representative sample were obtained for each size fractions and kept in sample bottles for analysis. A photograph of the Alpine Air Jet sieve is shown in Figure 3.2.

Figure 3.2 Alpine A200 LS Air Jet Sieve

3.3 THERMOGRAVIMETRIC ANALYSIS (TGA)

3.3.1 *Introduction*

Thermal analysis of solid fuels has gained wide acceptance as researchers have found the technique acceptable for investigating pyrolysis and combustion. It provides one of the most convenient and widely used methods or analysing the kinetics of gas–solid reactions, and distinguishing between competing models. The method gives measures of temporal variation of sample mass and of the rate of change of mass, as reactions occur. The resulting curve of variation of sample mass with time, and of its derivative is usually represented in terms of a rate-conversion curve and is interpreted by means of a suitable model (Feng and Bhatia, 2002).

There are two types of TGA analysers; a vertical and a horizontal balance analyser which was used in this work. The horizontal balance instruments have a

reference and a sample pan. It performs differential thermal analysis (DTA) and Differential Scanning Calorimetry (DSC) measurements. The DTA measures the temperature difference between the specimen pan and a reference pan. DSC measures the change of the difference in the heat flow rate to the sample and to a reference pan. The analysis is usually performed in an oxidising atmosphere or in an inert atmosphere. The picture of the TA SDT Q600 instrument and the data processing unit is presented in Figure 3.3.

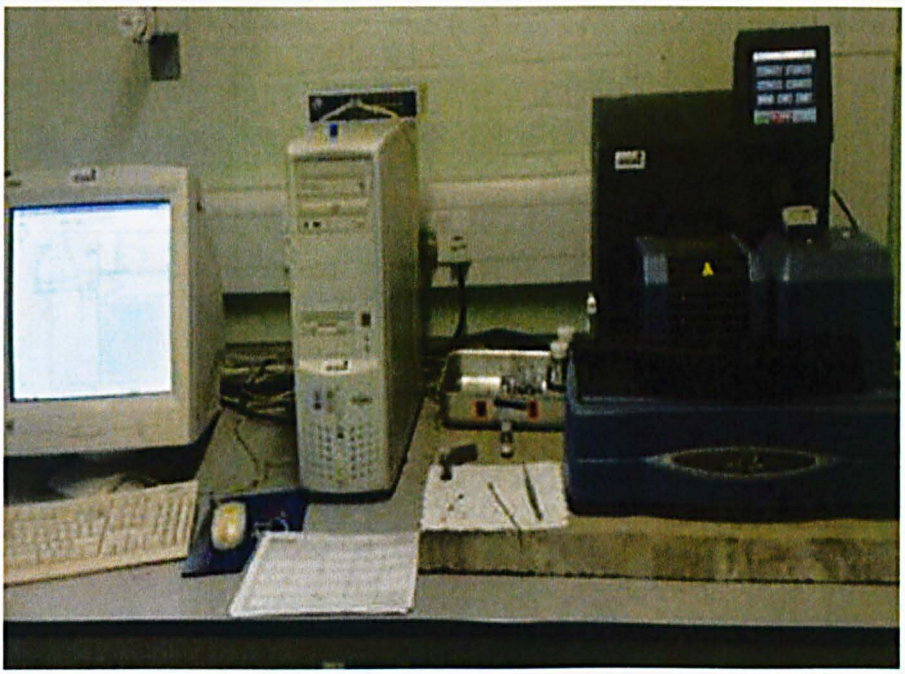

Figure 3.3 TA instrument SDT Q600

3.3.2 *Experimental Procedure*

3.3.2.1 **TGA Proximate Analysis**

TGA was employed to assess the composition of the fuels used by measuring the moisture, volatile matter, fixed carbon and ash contents. About 7-10 mg of sample was heated to 110°C at the heating rate of 50°C/min in nitrogen atmosphere flowing at 100 ml/min and kept isothermal for 5 minutes to ensure

complete removal of moisture. The biomass samples were then heated to 700°C at the same heating rate and then kept isothermal for 15 minutes to remove volatile matter until no further mass loss occurred. They were then heated to 850°C and then the gas was switched from nitrogen to air and kept isothermal for 30 minutes to combust the char. Figure 3.5 shows an example of the mass loss profile of sawdust in the TGA proximate analysis. For coal samples, about 7-10 mg of sample was heated to 110°C at the heating rate of 50°C/min in nitrogen atmosphere flowing at 100 ml/min and kept isothermal for 5 minutes to ensure complete removal of moisture. It then heated to 850°C at the same heating rate and then kept isothermal for 15 minutes to remove volatile matter until no further mass loss occurred. The gas was switched from nitrogen to air and kept isothermal for 30 minutes to combust the char.

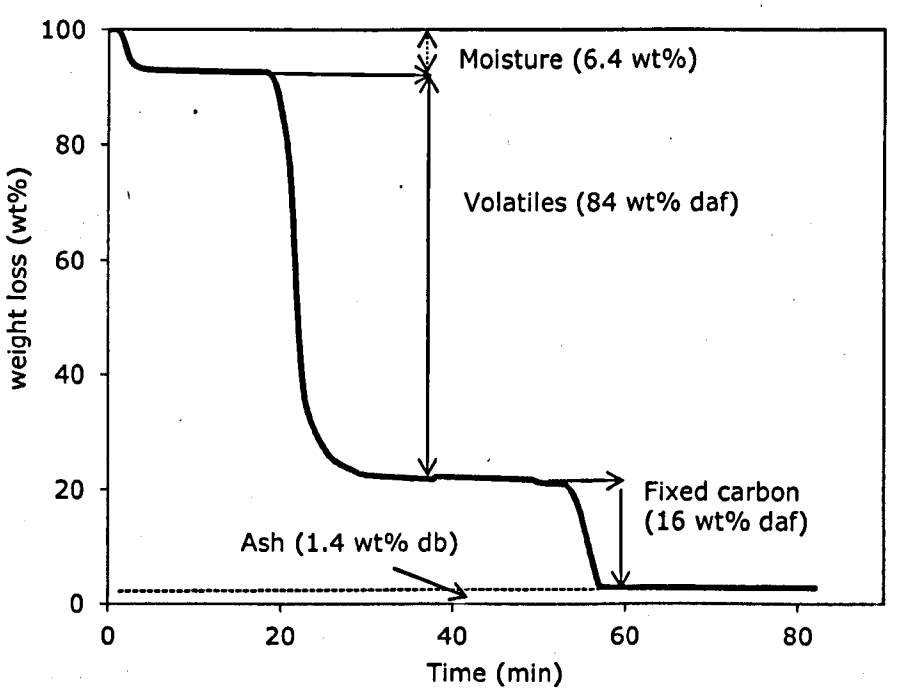

Figure 3.4 TGA proximate analysis of <45 μm sample

3.3.2.2 Determination of the maximum devolatilisation temperature for burnout

In this study, sawdust sample was subjected to different devolatilisation peak temperatures (700-1100°C) to investigate the effect on char burnout. For these experiments, the sample size used was <45 μm. The sample was heated from ambient to 110°C at 50°C/min in nitrogen flowing at 100 ml min^{-1} and kept at that temperature for 5 minutes. The sample was then heated to 700°C at a heating rate of 150°C/min for devolatilisation/char formation. The temperature was brought to thermal equilibrium at 525°C for char combustion. The gas flow was switched to air and the char was combusted isothermally for 10 minutes. This was repeated for pyrolysis temperatures of 800°C, 900°C, 1000°C and 1100°C.

3.3.2.3 TGA data analysis

The TGA data was then opened in TA universal analysis software and was exported to Excel spread sheet. By removing the volatiles and ash contents, the carbon burnout rate of char was normalised with respect to the initial mass of char produced. Also, the char burnout time was normalised to the start of combustion of char. This was achieved by making the start point of combustion as 0 minutes and 100 % char, where the oxidising gas was introduced into the system and to the end of set burnout time.

Basically, from the char burnout profile, two quantities were used to measure the reactivity parameters; the time to obtain 90 % char burnout and the first order rate constant which was derived between 5-95 % char conversion. This limit was chosen to eliminate the points where the burnout graph deviated from the linear first order due to the diffusion time lag at the beginning.

From the derivative weight loss curve of the combustion of char produced from the different devolatilisation temperatures it was observed that at 700°C, the char produced has the highest burnout peak and it was taken as the devolatilisation temperature because peak height is directly proportional to reactivity (Vamvuka, 2006). Although chars obtained from higher temperatures showed relatively high reactivity, to avoid intra-particle mass transfer limitations and thermal annealing which can lead to the formation of chars with less macro-porosity (Cai et al., 1996, Zolin et al., 2002). Therefore, 700°C was selected as the devolatilisation temperature for char generation. Similar observations were made by Encinar et al (2000) who studied the devolatilisation of biomass fuel at different temperatures and observed that the char produced between 600 and 700°C had a higher heating value than char produced at 800°C.

3.3.2.4 **Determination of isothermal char combustion regime**

Due to high variability and the general low repeatability of the char combustion characteristics at 525°C, and low kinetic parameters obtained at 475-575°C due to mass transfer limitation, a lower char burnout temperature at 350°C was investigated. A high repeatability of the burnout profiles was obtained and hence isothermal char combustion of the biomass samples were carried out between 325-425°C.

3.3.2.5 **Sample variability and reproducibility study for sawdust samples**

In order to verify the reproducibility and repeatability of results and to establish the source and magnitude of possible errors, the experimental procedure was repeated 5 times using the above procedure for the six particle size ranges of the sawdust samples. The carbon burnout vs time was plotted for <45 μm size to determine the closeness of the plots to each other as an indication of reproducibility. The standard deviations of rate constants and burnout times

were also calculated. The reproducibility and repeatability results are presented in chapter 4

3.3.2.6 **Determination of reactivity parameters**

The reactivity of char in terms of the rate of carbon burnout was determined by carrying out char combustion at different temperatures at 25°C intervals (475°C, 500°C, 525°C, 550°C and 575°C) for all the samples and held at each isothermal temperature for 10 minutes. The intrinsic kinetic parameters and first order reaction rate constants were obtained from 5-95% carbon burnout. The above isothermal experiment was also carried out for lower temperatures (325-425°C) for 80 minutes at 25°C intervals. The reactivity is expressed as the extent of reaction (equation 3.1) and is defined as the mass fraction of biomass char reacted (White et al., 2011).

$$\alpha = \frac{m_o - m_t}{m_o - m_f} \qquad (3.1)$$

Where M_o, is the initial mass of char; m_t is the mass of char at time, t and m_f is the fraction of char combusted at the end of burnout time. The mass was normalised with respect to the initial mass of char. The rate in terms of conversion is given by:

$$\frac{\partial \alpha}{\partial t} = k(1 - \alpha) \qquad (3.2)$$

Here α = (1-C/C_0) is the fractional weight conversion, with C as the remaining carbon mass and C_0 as the original carbon mass (Le Manquais et al., 2009). The solution of equation (3.2) by integration, subject to the initial condition α =0 at t=0, yields:

$$-\ln(1 - \alpha) = kt \qquad (3.3)$$

The rate constant, k can be determined graphically from the gradient of a plot of -ln(1- α) versus t with respect to oxygen. Subsequently, the values of the activation energy (E) and the pre-exponential factor (A) can be estimated from the slope and intercept of an Arrhenius plot:

$$\ln k = \ln A - {}^{E}/_{RT_{isothermal}} \qquad (3.4)$$

Therefore, the activation energy of the sawdust char combustion can be determined by completing isothermal TGA runs at a range of temperatures.

3.4 CHAR PRODUCTION IN THE HORIZONTAL TUBE FURNACE (HTF)

In order to produce sufficient amount of TGA devolatilised chars for characterisation, these chars were produced using a horizontal tube furnace (HTF) at 700, 900 and 1100°C to mimic the conditions in the TGA. Figure 3.5 shows the horizontal furnace used. The furnace was heated to desired temperature; the extraction system was switched on to remove volatiles produced by samples during devolatilisation/char formation. Nitrogen was allowed to flow at 5 l min^{-1} through the furnace to create an inert atmosphere. Each sample (3g) was weighed into a pre-weighed ceramic combustion boat.

The boat was placed on a refractory brick block and put into the furnace gradually towards the centre of the furnace using a rod and a thermocouple at 150°C/min to the desired temperature. The sample was kept for 5 minutes to achieve complete devolatilisation. Then the boat and brick block was pushed through to the other end of the furnace tube. The sample was allowed to cool under nitrogen atmosphere before removing it in a desiccator for further cooling down so that char combustion did not take place when exposed to air. Chars

were produced 3 batches to assess the reproducibility of the production. Subsequently, the combustion reactivity of HTF chars was assessed to ensure that they are similar to the TGA equivalent chars. The confirmation of the reproducibility of HTF char production process and the comparison of the combustion reactivity between the HTF and TGA chars are presented in chapter 4.

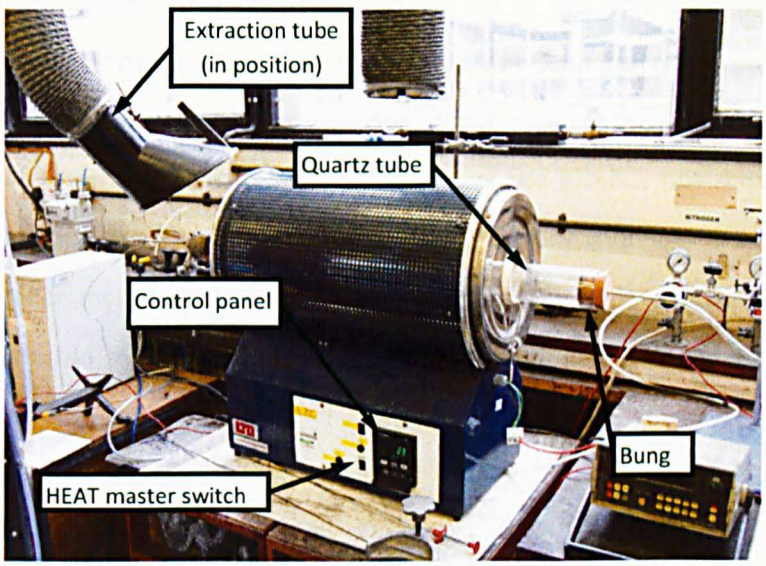

Figure 3.5 Horizontal tube furnace used to mimic the TGA devolatilisation procedure

3.5 DROP TUBE FURNACE (DTF)

3.5.1 *Description of equipment*

The DTF is an effective means of generating combustion data under conditions that relates closely to pulverised fuel (pf) combustion conditions. It is an electrically preheated vertical tube furnace with the ability to devolatilise and combust fuel samples to produce char and ash respectively under well controlled

conditions. The furnace consists of a high temperature ceramic work tube with an internal diameter of 50 mm and a length of 1550 mm. The main heater comprises four vertically mounted silicon carbide elements situated around the work tube. This particular DTF apparatus is able to achieve heating rates 10^4 to 10^{5o}C/s and maximum temperature of 1300°C (Le Manquais et al., 2009). Oxygen levels can be regulated to simulate the atmosphere found during full-scale combustion. Two smaller U-shaped trim heaters are located near the base of the work tube to compensate for any heat loss due to the presence of the water-cooled collector probe. At the top of the work tube is mounted a water-cooled feeder probe which has an internal diameter of 3 mm. Around this is a spirally wound silicon carbide pre-heater element which pre-heats the incoming gas to temperatures approaching that of the furnace hot zone. Coal or biomass particles are introduced into the furnace from a hopper via a horizontal screw feeder mounted above the feeder probe. Burnt/devolatilised char samples are collected by a water-cooled collector probe linked to a cyclone fitted with a dust collector pot.

Pulverised coal or biomass samples are carried into the furnace in a gentle stream of gas through a water cooled feeder probe into the a pre-heated stream of similar gas flowing downwards at a Reynolds Number low enough to ensure laminar flow. The laminar flow conditions ensure that the fuel particles travel in a narrow stream along the axis of the furnace and can be aspirated into a water-cooled collector probe.

The average operating temperature is determined by changing the temperature setting of the oven. The residence time of the particles in the high temperature region of the DTF is estimated by considering the separation between the feeder and collector probes, the temperature and flow rate of the gas. The composition of the carrier gas can be predetermined using air and nitrogen cylinders. A

cyclone device at the end of the collector probe allows the char material to be separated from any gaseous volatiles that may still remain in the carrier gas. The cooling to the DTF was supplied from the cooling water system in the laboratory. The water flow in and out of the DTF was regulated by flow meters. A photograph of the DTF is presented in Figure 3.9

3.5.1.1 **Gas atmosphere and gas supply**

The control of gas is essential in DTF experimental work. Nitrogen and CO_2 gases are supplied by means of gas cylinders and are regulated depending on the flow rate required. Nitrogen or CO_2 gas can be used in the DTF experiments depending on the experiment condition. Nitrogen gas was used for conventional air fired conditions while CO_2 was used under oxy-fuel conditions. A carrier gas (2 litre min^{-1}) was introduced from the top of the furnace during the sample feeding to ensure laminar flow of feed into the furnace. In each experiment, the carrier gas was the same with the gas flowing into the furnace. For example, for devolatilisation in CO_2, the carrier gas was also CO_2.

In each case, 1% concentration of oxygen (mol mol^{-1}) was maintained in the carrier gas during devolatilisation, rather than true pyrolysis conditions, to allow for the combustion of any tars formed. The inlet stream of O_2 to the furnace is monitored by using a digital oxygen analyser to enable the desired inlet concentration of oxygen to be achieved. The control of the inlet gases was achieved by using different flow meters for each gas. All the gases and fuel particles entering the furnace in an entrained manner were further straightened towards the centre of the furnace by a flow straighteners situated at the end of the feed probe.

Subsequently, experiments were carried out without using 1% oxygen in order to investigate the effect of oxygen reactivity during devolatilisation. In this case, 100% nitrogen or CO_2 was used as the feed gas.

The possible artificial activating effect of 1% oxygen on sawdust devolatilisation was investigated by carrying out devolatilisation in 100% nitrogen or CO_2. However, this led to build up of tar in the DTF. Therefore, after about 35-40 g (5-10 runs), the system was kept at 1300°C for 1 hour to burn off any tars sticking to the walls of the furnace.

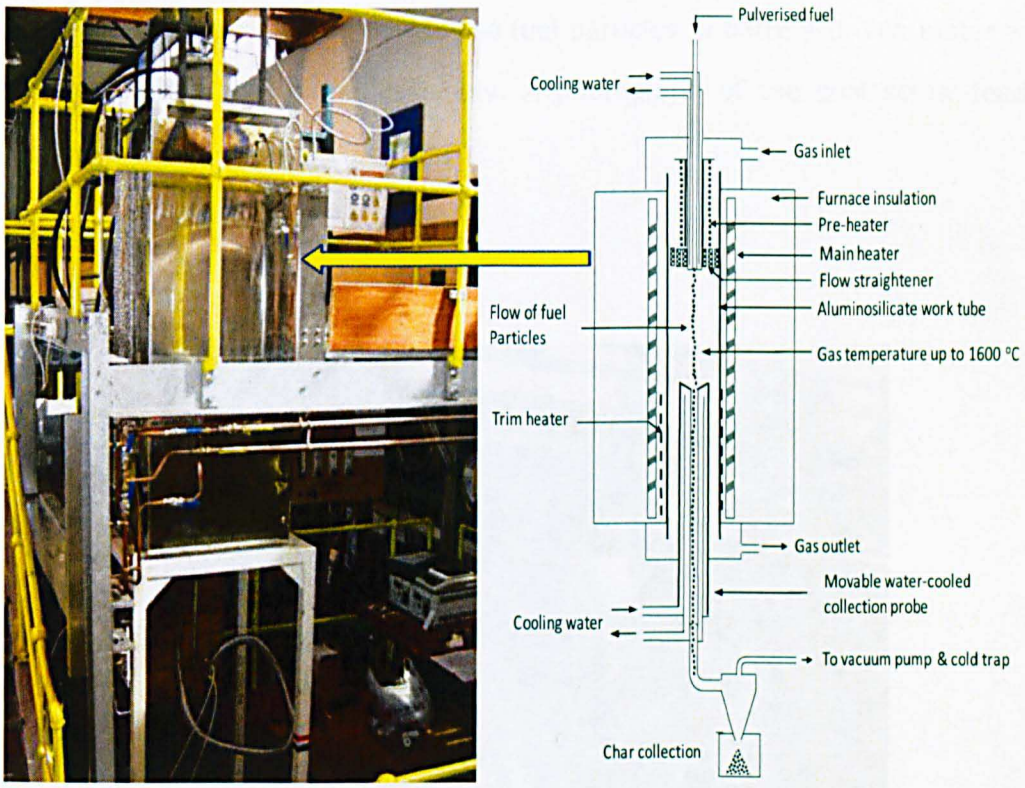

Figure 3.6 Drop tube furnace and a schematic diagram of the experimental set up

3.5.1.2 **Feeder system**

Two screw feeders were used during this study. A specially designed feeder at the University of Nottingham for coal samples and used by previous researchers (Barranco, 2001, Le Manquais, 2011a, Lester, 1994). This feeder is 60 x 80 x 40 mm in dimension (Figure 3.7). When using this feeder, the samples are placed in a 20 x 60 x 6 mm hopper. The coal samples gradually fell into a rotating 100 mm long screw where it was conveyed into a 4 mm (id) vertical tube and then fell into the work tube by gravity. The gentle stream of gas flow is connected to this 4 mm (id) vertical tube from the top to ensure the laminar flow of the fuel particles. To ensure steady flow of the fuel particles, a battery-driven motor was used to vibrate the feeder assembly. A photograph of the coal screw feeder assembly is presented in Figure 3.7

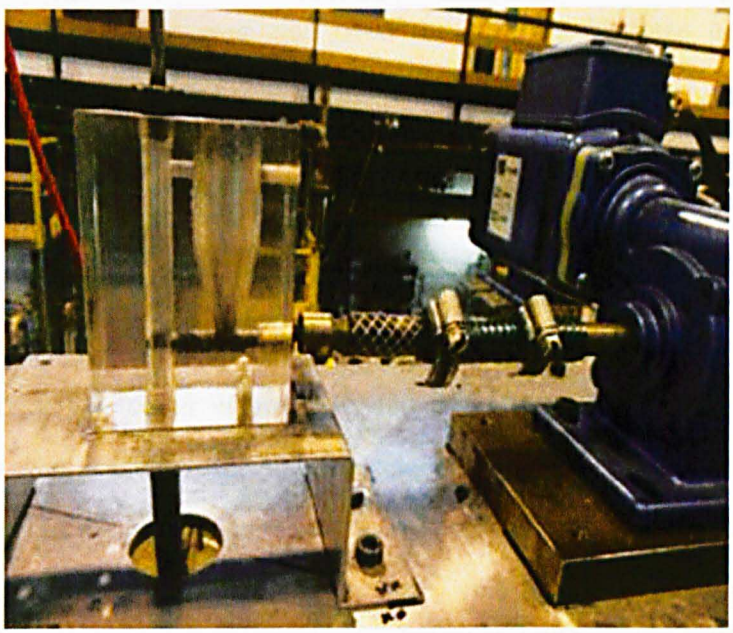

Figure 3.7 DTF screw feeder for coal samples

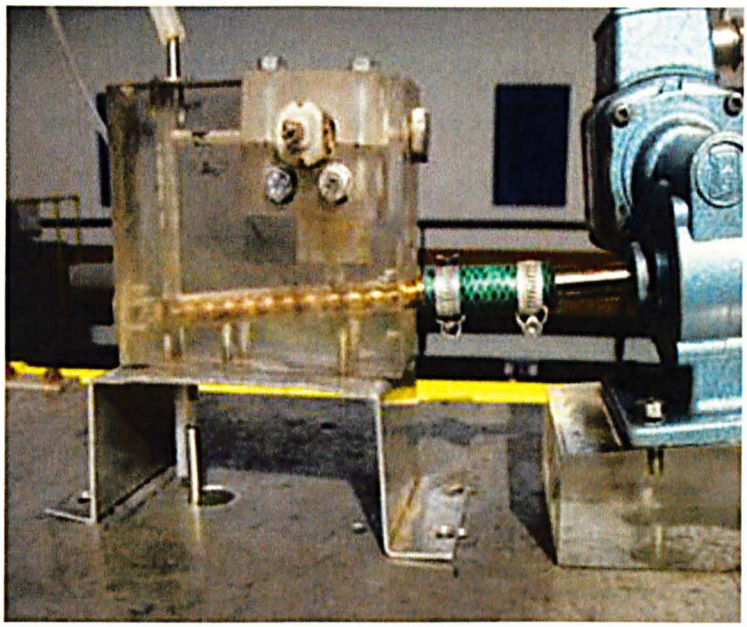

Figure 3.8 DTF screw feeder for biomass samples

On the other hand, a much bigger screw feeder assembly also designed at the University of Nottingham was used for biomass samples due to their fibrous nature. The same feeder was also used for co-firing biomass and coal. The dimensions of this particular screw feeder are 120 x 102 x 48 mm. The hopper is 30 x 83 x 7 mm. The length of the rotating screw is 113 mm where the sawdust was conveyed into a 6 mm (id) vertical tube. The bigger diameter of this screw feeder made the free flow the feed into the reactor easily so that a vibrating device was not needed to assist the flow of sawdust particles into the work tube. Although this screw feeder was wider than the one used for feeding coal, the feeding rate was reduced to avoid blocking of the furnace tube. This was controlled by regulating the speed of the electric motor that drives the screw feeder. To this end, a feed rate of 7-10 g hr^{-1} was used and this was calculated from the mass of biomass fed into the furnace at the end of each run. A photograph of the biomass feeder is presented in Figure 3.8.

In order to protect the feed probe from furnace high temperature, the feeder probe was insulated with detachable insulators, 28 mm o/d x 20 mm i/d x 100 mm long, made from ceramic bricks graded to withstand 1600°C.

3.5.1.3 Heating system and controls

The heating system consists of three separate heaters: a pre-heater, main heater and a trim heater. The pre-heater consists of a coiled carbon graphite plate wrapped round the feeder probe and heats the incoming gas and the fuel as they enter at the top of the apparatus to temperatures approaching that of the furnace hot zone. The main heater comprises four vertically mounted silicon carbide elements situated around the work tube. It provides the major source of heating for the DTF. The trim heater is located near the base of the work tube to compensate for any heat loss due to the presence of the water-cooled collector probe. The heaters are controlled by three 2404 Eurotherm digital controllers and they responded to thermocouples positioned along the work tube. Usually, during experiments, depending on the residence times, the furnace temperature was heated to 25°C or 100°C above the target temperature (Le Manquais, 2011a) in order to provide accurate temperature profile within the furnace. The DTF heating system and control unit is presented in Figure 3.9.

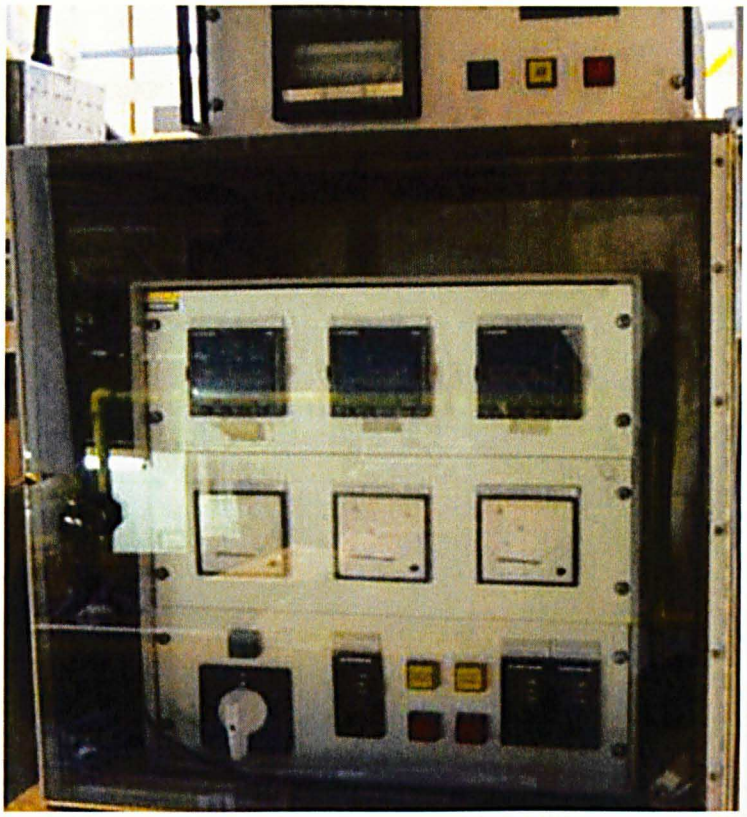

Figure 3.9 DTF heating systems and control panel

3.5.1.4 **Sample collection and filter system**

At the base of the work tube is mounted a moveable, water cooled collector probe to which is attached a cyclone fitted with dust collector pot. The collector probe was insulated with 42 mm o/d x 28 mm i/d x 100 mm long ceramic brick detachable insulators of 1600°C grade (Figure 3.10). These insulators protected the feeder probe from the furnace high temperature during the experiment. The collector probe required regular maintenance due to deposition of tar and incomplete collection of char. Therefore, the feeder probe was cleaned after about 5-10 runs, corresponding 20 or more grams of coal fed. However, cleaning depends on the type of fuel used and the operating conditions, although less often during re-firing (Le Manquais, 2011a). For biomass, due to low char content, the probe was cleaned after feeding about 40 g of biomass (8-10 runs).

Figure 3.10 DTF collector probe

Usually, there is a vacuum pump connected to the collector probe which provides the suction that enables the entrained, cooled char or ash particles to be deposited into the char collector. Two gas filter systems are connected to the vacuum pump for effective removal of tar and entrained char or ash particles from the exit gases before they are passed into the fume cupboard. The filters were connected before and after the vacuum pump. The gas filter systems contain glass tube and a pad of fibreglass. The fibreglass from the filters was changed when they become saturated with waste tar and soot and they were replaced by removing them and putting clean ones. The frequency of changing the filter paper for devolatilisation tests depended upon the type of fuel being used (Le Manquais, 2011a). For effective extraction of gases, the gas outlet flow rate was regulated to approximately 1 litre min^{-1} above the total inlet gas flow and this depended on the furnace temperature and residence time. This was

achieved by manually adjusting the vacuum pump. A photograph of the filters is presented in Figure 3.11.

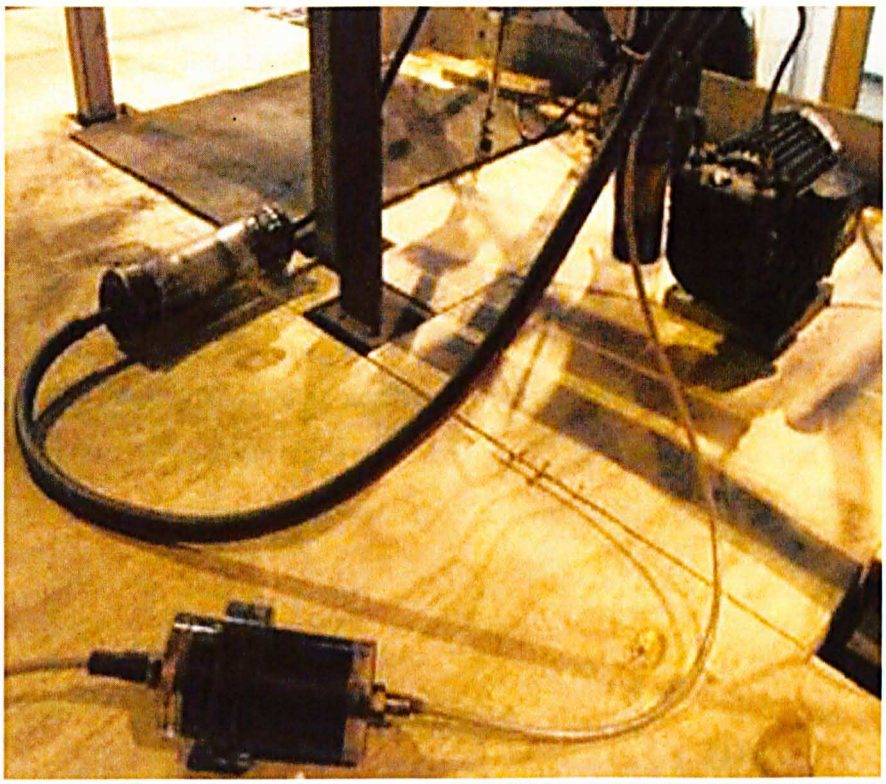

Figure 3.11 DTF gas filters and vacuum pump

3.6 DTF EXPERIMENTAL PROCEDURE

3.6.1 *Residence time calculation*

DTF residence time is defined as the time taken for a sample particle to travel through the furnace. Different residence times were provided by adjusting the separation between the feeder and the collection probes using specially designed rods. However, to determine the probe separation that was required to provide specific residence time, certain assumptions are made. It is assumed that the particle inside the DTF travel in a laminar flow regime and that the gas velocity

at any point is a function of its radial position, hence the laminar flow velocity profile was applied using the following equations (Le Manquais, 2011a).

$$\frac{V_r}{V} = 2(1 - \frac{r^2}{R^2}) \qquad (3.5)$$

Where V_r is the gas velocity at any radius (r) from the centre of the work tube and V is the average velocity across the entire radius of the work tube (R). At the centre of the tube, where r=0 and $V_r=V_0$:

$$V = \frac{1}{2}V_0 \qquad (3.6)$$

Therefore, the velocity of sawdust particle travelling down the centre of the work tube (V_0) can be derived from the residence time (t) of the particle in the furnace and the separation between the feed and the collector probes (L):

$$V = \frac{1L}{2t} \qquad (3.7)$$

$$V = \frac{Q}{A} = \frac{Q}{\pi R^2} \qquad (3.8)$$

Where Q, is the volumetric flow rate of the gas flowing through the DTF and (A) the cross sectional area of the work tube.

Combining 3.7 and 3.8,

$$t = \frac{L\pi R^2}{2Q} \qquad (3.9)$$

Inside the DTF, the volumetric flow rate (Q) is not recorded. Therefore, the volumetric flow rate inside the furnace is calculated by applying the ideal gas equation.

$$\frac{Q_1}{Q_2} = \frac{T_1}{T_2} \qquad (3.10)$$

Where 1 denotes the temperature and gas flow rate of the incoming gas at standard temperature and pressure and 2 is gas flow rate and temperature inside the DTF.

For example, a probe separation of 22 cm, DTF internal diameter of 50 mm, and the inlet gas flow rate of 12.3 l/min operating at temperature of 1300°C, the flow rate inside the furnace can be calculated:

$$Q_2 = \frac{12.3}{1000 \times 60} \times \frac{1300 + 273}{25 + 273} = 1.08 \times 10^{-3}\ m^3/_s \quad (3.11)$$

Subsequently, the residence time of the particle in the furnace can be calculated using equation 3.9:

$$t = \frac{22}{100} \times \frac{\pi(25 \times 10^{-3})^2}{2 \times 1.08 \times 10^{-3}} = 0.200s = 200\ ms \quad (3.12)$$

3.6.2 *Devolatilisation*

For the initial experiments, five particle size fractions of sawdust, 45-63, 63-75, 75-90, 90-106 and 125-250 μm of sawdust used in the DTF operating at 900°C on a residence times of 200, 400 and 600 ms with 1% oxygen present in the gas. The feed rate was between 7-10 g hr^{-1}. This initial study was undertaken to investigate possible particle size variability and the effects of particle size and residence time on char yield. Further experiments were carried out using only the 125-250 μm particle size because its reproducibility was much higher and collection efficiency was higher than other size fractions. The repeatability of char production was investigated at 1100°C and a residence time of 200 ms and the repeatability of the TGA char burnout was assessed. The results are presented in chapter 5. Also, the overall systematic errors associated with

biomass conversion during devolatilisation in DTF were assessed and discussed extensively in chapter 5.

Devolatilisation was then carried out at 1100 and 1300°C in order to assess the effect of operation temperature on volatile and char yields and char characteristics. After establishing the experimental conditions for sawdust, DTF experiments were then carried out at 900°C, 1100°C and 1300°C at 200, 400 or 600 ms. For each experiment, the DTF temperature was set slightly above the target temperature as earlier mentioned. For example, for devolatilisation of 1100°C at 200 ms residence time, the furnace temperature was set at 1150°C while at longer residence time of 600 ms, the set temperature was 1125°C. The corresponding gas inlet flow and exhaust gas out flows were adjusted accordingly. For coal, about 2 g was fed into the furnace for each experiment while in the case of sawdust, 8 g of sample was fed. The corresponding chars were collected from the bottom of the cyclone in a clearly labelled collection pot.

3.6.2.1 **DTF volatile yield calculation using silica as ash tracer**

DTF volatile yield were calculated using the conventional ash tracer method. This method calculates the volatile yield on dry and ash free basis from the ash content of the char and the parent sample as shown in Equation 3.13

$$V_{DTF} = \frac{10^4 \times (Ash_{char} - Ash_{biomass})}{Ash_{char} \times (100 - Ash_{biomass})} \quad (\%daf) \qquad 3.13$$

Due to the low ash content of sawdust, and the high temperature DTF experiments, there was uncertainty in the ash measurements. This could lead to possible errors in the measured volatile yields when using the conventional ash tracer method. Therefore, silica was used as a tracer. The particle size of the

silica was the same as the sawdust. 10 wt% of the oven dried silica was added to the sawdust in a sample bottle and mixed thoroughly together using spatula before feeding into the DTF. The ash content of the char was determined and the volatile matter was determined using equation 3.13. The results are presented in chapter 5.

3.6.3 *DTF Re-firing experiments*

The chars devolatilised at different resident times and temperatures were re-fired into the DTF in nitrogen and CO_2 both containing 5% oxygen. The extent of burnout (B_{DTF}) was calculated using the normal ash tracer method in equation 3.14 and the results are presented in chapter 7.

$$B_{\mathrm{DTF}} = \frac{10^4 \times (\mathrm{Ash}_R - \mathrm{Ash}_P)}{\mathrm{Ash}_R \times (100 - \mathrm{Ash}_P)} \quad (\%\mathrm{daf}) \qquad 3.14$$

Where Ash_P and Ash_R are the ash content of the pyrolysed and the re-fired chars respectively, on a dry basis.

3.7 CO-FIRING EXPERIMENTS ON COAL AND SAWDUST DTF DEVOLATILISED: TGA BURNOUT EXPERIMENTS

3.7.1 *Post mixing (char-char blends) of DTF devolatilised chars: TGA burnout experiment*

DTF or HTF devolatilised chars and TGA replicated HTF chars for both biomass and coal were physically mixed in 50:50 wt% ratios in sample bottles. About 5-10 mg of the mixture was placed in the TGA for char burnout analysis. The results of the impact of biomass char on coal char burnout are presented in chapter 8.

3.7.2 *DTF devolatilisation: Pre mixing*

This refers to mixing the sawdust and coal samples before devolatilisation. These were physically mixed together in 50:50 wt% ratios and kept in sample bottles before feeding into the DTF. Devolatilisation of pre-mixed blends was carried out in the DTF devolatilisation procedures already explained in section 3.5.2 at different temperatures and residence times in N_2 and CO_2 atmospheres. The combustion reactivity tests of the blend chars were assessed by TGA and the results are presented in chapter 9.

3.8 Char characterisation techniques

Both TGA/HTF and DTF devolatilised chars were assessed. One of the extensively used techniques to evaluate the structural variations in fuel particles after thermal treatment is scanning electron microscope (SEM). For porosity studies, BET analysis was used while for elemental compositions; a flash EA 1112 elemental analyser was used.

3.8.1 *Elemental analysis*

Both biomass raw samples, HTF and the DTF chars were analysed using flash EA 1112 elemental analyser (Figure 3.12) to determine the percentage by weight of nitrogen, organic carbon and hydrogen contained in the samples. The Flash EA 1112 system works by completely oxidizing samples with a catalyst through dynamic flash combustion and reducing them to produce CO_2, N_2 and H_2O under high temperature reactor chambers. Analysis in the Flash EA begins with burning a tin capsule containing the sample in a pure oxygen environment (99.996%). The left reactor, a steel column, is surrounded with a furnace operated at 900°C and the combustion convert carbon to carbon dioxide, nitrogen to free gas or some oxides and hydrogen to water.

A stream of helium gas carries those gases into a quartz column filled with copper that reduces the nitrogen oxides to nitrogen and removes the excess oxygen at 680°C. The gas stream then flows through a magnesium perchlorate trap, (absorption filter). The magnesium perchlorate removes water before CO_2 and N_2 gases go into a gas chromatograph (GC) column at room temperature.

3.8.1.1 **Procedure**

About 2.5 mg of the sample was packed tightly into a cylindrical tin foil and weighed using a precision weighing balance. At the start of the run, an empty compressed tin foil was injected into the auto sampler followed by another containing a combustion standard called BBOT, 2, 5-bis (5-tert-butyl-benzoxazol-2-yl) thiophene. The empty sample packet was used to standardise the results against signals from the combustion of the tin foil, while the BBOT standard was to produce baseline standard peaks to calibrate the sample peaks. The weighed samples were then fed into the each auto sampler feed packet. The instrument was heated to 900°C and the instrument check for gas leakage. At the start of the run, each auto sampler injects the sample into the oven, starting from the blank and it was burnt in oxygen and helium atmospheres. The gaseous product from the combustion of the sample flowed into a packed chromatographic column and the relative compounds are measured quantitatively in a thermal conductivity detector. All samples were conducted in duplicate to assess repeatability.

Subsequently, the data collected from the EA was then processed by Eager 300 software. The software integrated the areas under each peak and provides the relative quantities of carbon, hydrogen and nitrogen contents in the sample.

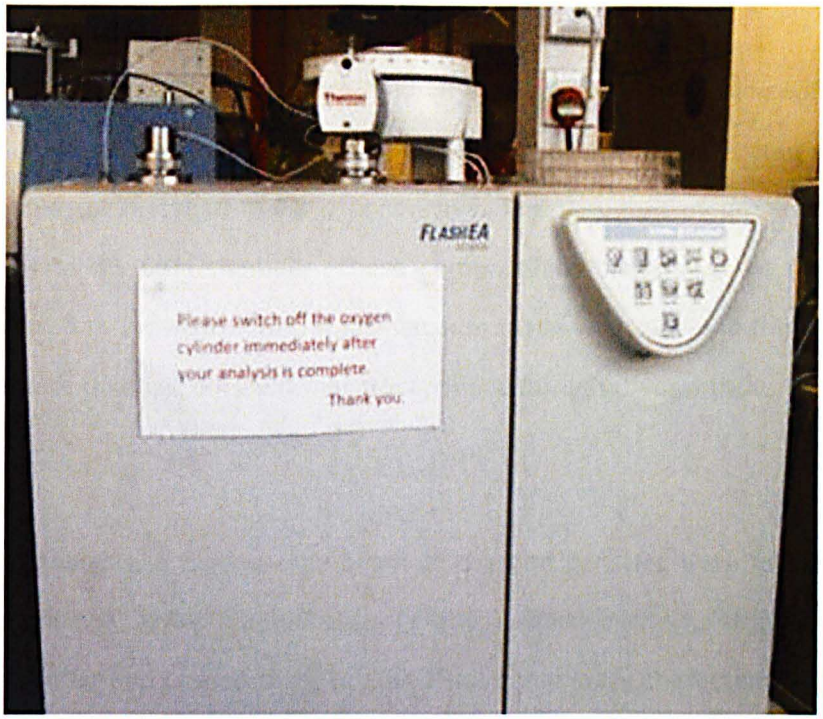

Figure 3.12 Elemental analyser, flash EA 211

3.8.2 ***Scanning electron microscope (SEM)/ energy dispersive X-ray spectrometer (EDX)***

The SEM can be used in conjunction with an Energy Dispersive X-ray spectrometer (EDX) to obtain information about the elements present within the sample. The Quanta 600 SEM (Figure 3.13) instrument produces enlarged images of a wide variety of specimens, using magnifications usually from 100 x to about 100,000x. Digital format images can be collected in 3 operating modes:-

1. High vacuum mode for electrically conducting materials
2. Low vacuum mode for non-conducting materials
3. Environmental mode (ESEM) for observation of beam sensitive materials

3.8.2.1 **Procedure**

In SEM image analysis, samples were held on an aluminium stub using adhesive or double sided sticky carbon tape. The surface of the mount was coated with a very thin layer of metal to make it conductive. The resultant mount was then introduced into the SEM chamber. These carbon tapes containing the samples were then fixed in the instrument. A low vacuum mode was used and the images of sample were taken at different magnifications x100, x800 and x1400.

In the EDX analysis, a high energy beam of charged particles were focused on the char sample at lower magnification (x 160) which excite or stimulate the atoms in the char and caused them to emit X-rays that were characteristic of the element's atomic structure to be identified. The emitted X-rays were sent to a detector which converted the X-rays into voltage signals. These signals were received by a processor and the output was analysed by EDAX Genesis software. This software then displayed a spectrum of peaks corresponding to the different elements or oxides of such elements present in the sample. From the different peaks corresponding to the different element, the quantities of such elements were calculated. Typical examples of SEM image and EDAX spectrum are presented in Figures 3.14 and 3.15.

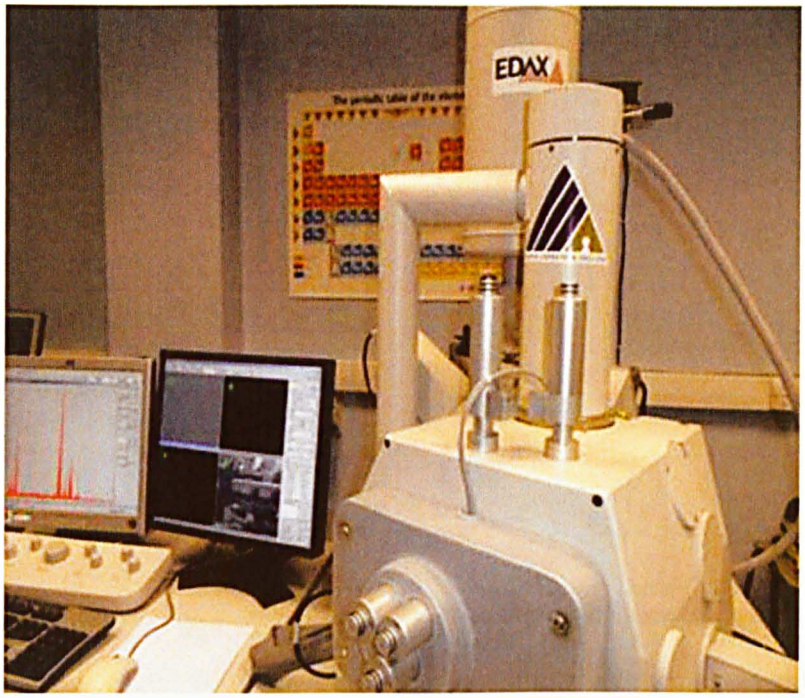

Figure 3.13 Quanta 600 scanning electron microscope with EDX facility by FEI company

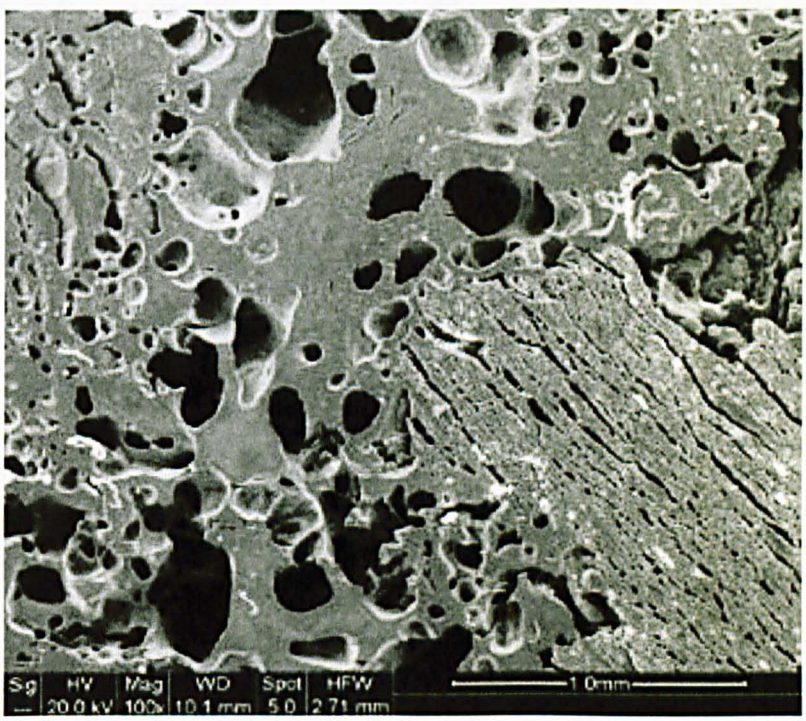

Figure 3.14 Typical example of SEM image showing an internal structure

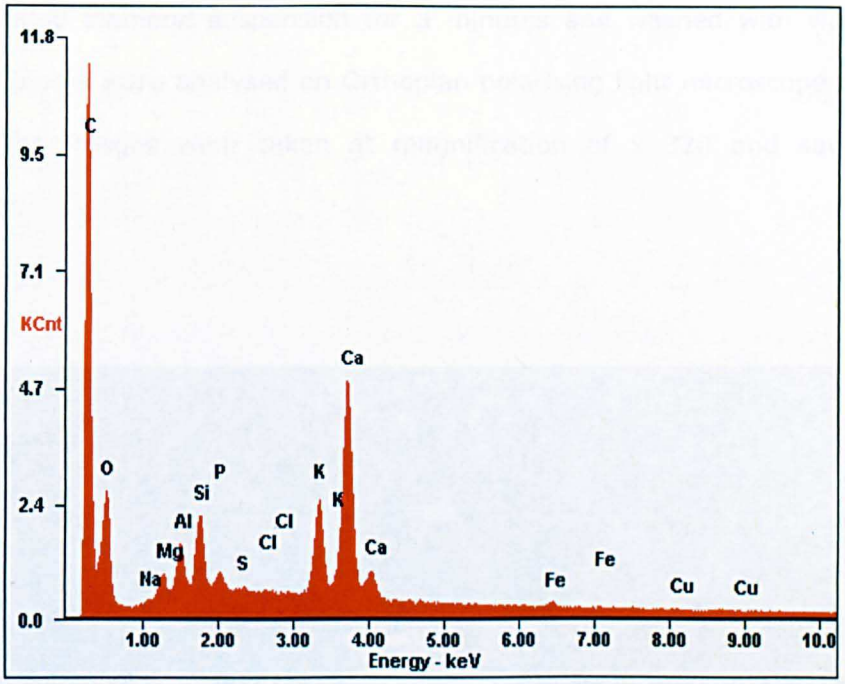

Figure 3.15 A typical example of a spectrum from the EDAX Genesis software showing the different elements contained in a sample

In the order to identify the internal structure of the HTF and DTF chars, they were analysed using an optical imaging system (Figure 3.16). The chars were placed on epofix resin mounts which were in plastic tabs. Epofix resin and hardener were mixed thoroughly and poured on the surfaces of each resin mount containing the chars and kept for few minutes and then evacuated in Epovac to remove air bubbles. It was then pressed firmly by a struers labopress instrument to remove the sample blocks from their plastic tabs. The surfaces of the blocks were ground and polished using streuers Pedemat Raptapo-1 machine. First, the surfaces of the blocks were ground for 60 seconds with 500 grit silicon carbide paper till surface was flat. It was then changed to 1200 grit silicon carbide for another 60 seconds to ensure all scratches were removed. Finally, 2400 grit was used for 30 second to get the scratches as fine as possible ready for polishing. The polishing of the surfaces was carried out with 6 μm Diaduo diamond suspension for 2 minutes and wash in water to remove suspension. Finally, with

3 µm diaduo diamond suspension for 3 minutes and washed with water. The polished blocks were analysed on Orthoplan polarising light microscope made by LEICA. The images were taken at magnification of x 320 and saved in a computer.

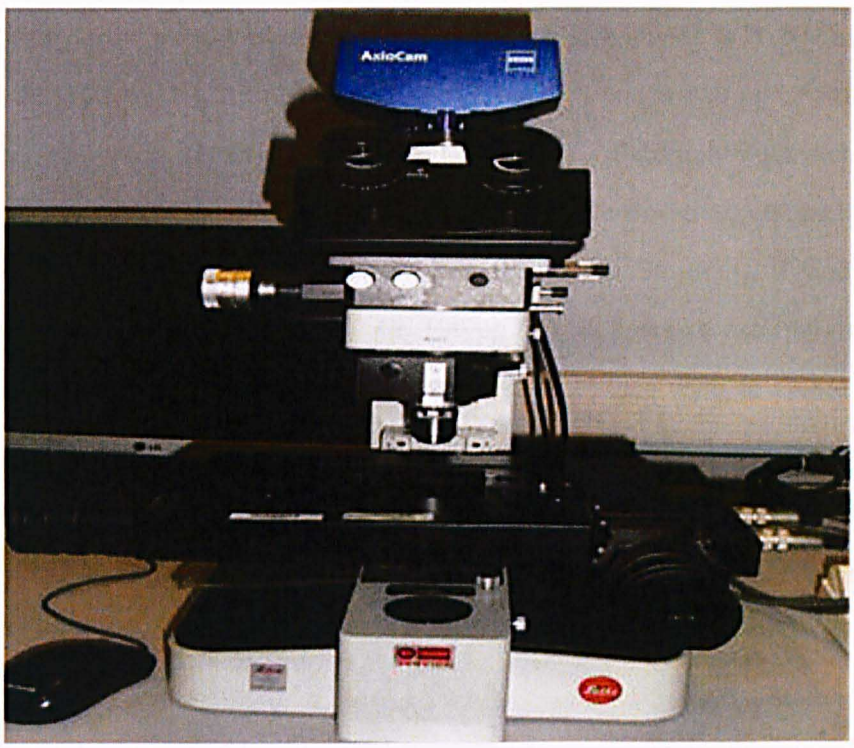

Figure 3.16 Orthoplan polarising light microscope

3.8.3 *Trace elemental analysis by inductively coupled plasma mass spectrometer (ICP-MS)*

In order to determine the mineral composition especially the alkali/alkaline metals inherent in the biomass samples used and the degree of volatilisation of these metals during DTF devolatilisation, (ICP-MS) analysis was carried out in the School of Biology, University of Nottingham. This was important so that the amount of alkali and alkaline metals volatilised during DTF experiments could be quantified.

3.8.3.1 **Description of analysis by ICP-MS**

Multi-element analysis of diluted digestions was undertaken by ICP-MS (Thermo-Fisher Scientific X-Series^{II}) employing a 'hexapole collision cell' (7 % hydrogen in helium) to remove polyatomic interferences. Samples were introduced from an auto sampler (Cetac ASX-520 with 4 x 60-place sample racks) through a concentric glass venturi nebuliser (Thermo-Fisher Scientific; 1 mL min^{-1}). Internal standards were introduced to the sample stream via a T-piece and included Sc (100 µg L^{-1}), Rh (20 µg L^{-1}), Ge (20 µg L^{-1}) and Ir (10 µg L^{-1}) in 2% trace analysis grade (Fisher Scientific, TAG) HNO_3. External multi-element calibration standards (Claritas-PPT grade CLMS-2 from *Certiprep/Fisher*) included Al, As, Ba, Bi, Cd, Co, Cr, Cs, Cu, Fe, Mn, Mo, Ni, Pb, Rb, Se, Sr, U, V, and Zn, all in the range 0 – 100 µg L^{-1} (0, 20, 40, 100 µg L^{-1}). A bespoke external multi-element calibration solution (Plasma CAL, SCP Science) was used to create Ca, Mg, Na and K standards in the range 0-30 mg L^{-1}. Sample processing was undertaken using Plasma laboratory software (version 2.5.4; Thermo-Fisher Scientific) set to separate calibration blocks and internal cross-calibration where required. Figure 3.17 presents a picture of ICP-MS; model X Series^{II} used in this study.

3.8.3.1.1 ***Procedure***

Sawdust ash and DTF chars produced at different temperatures and residence times under N_2 and CO_2 were analysed. Sawdust ash samples from the raw material were produced in a furnace at 350°C in air. The sample was placed in a combustion boat and inserted in a horizontal tube furnace in an air stream for 6 hours to form ash. 1 g of the ash was dissolved 50 ml of 20% nitric acid. The mixture was heated to 60°C for 12 hours and allowed to cool. The solution was filtered to remove undissolved ash particles. The solution was diluted with deionised water to 2% concentration using a dilution factor of 1 ml of sample: 10 ml of water and it was used for the analyses. Demineralised sawdust ash was

also produce and prepared for analysis using this method. Also, DTF chars were prepared for the analysis using the same method.

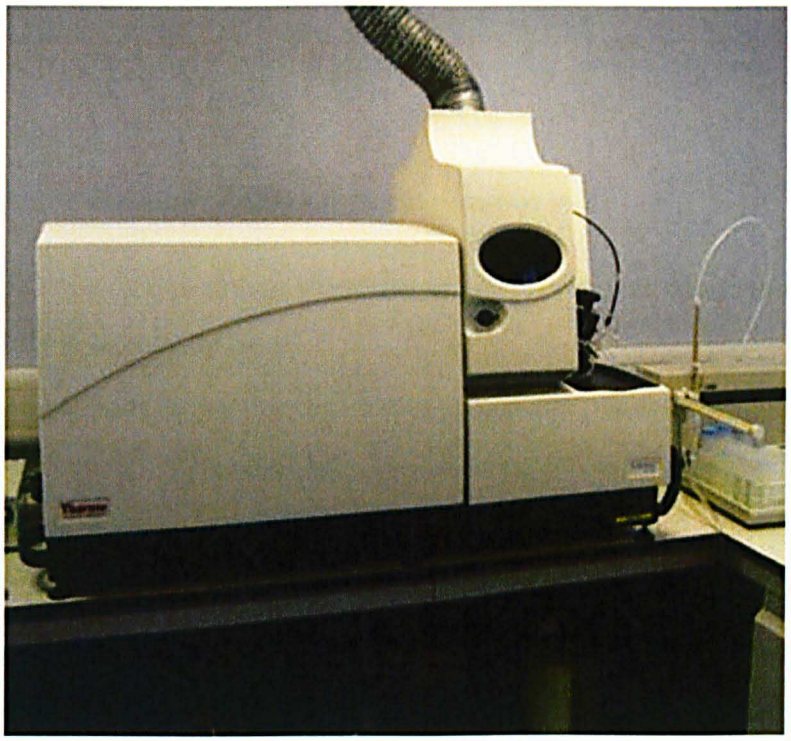

Figure 3.17 Inductively coupled plasma mass spectrometer (ICP-MS); model X Series[II] produced by Thermo-Fisher, Bremen, Germany.

3.8.4 ***Brunauer-Emmett-Teller (BET) surface area and porosity analysis***

3.8.4.1 **BET surface area measurement**

BET adsorption isotherm models have been applied to calculate surface areas in this study. Adsorption models are usually developed using the Langmuir model. The pressure of the system (P), the number of moles adsorbed (n) and the monolayer capacity of the adsorbent (n_m) are connected in the relationship:

$$\frac{n}{n_m} = \frac{bp}{1+bp} \qquad (3.13)$$

The surface area of the adsorbent can be calculated using the Avogadro's constant (L) and the surface area of one molecule of the adsorbate (a_m)

$$A = n_m Lam \qquad (3.14)$$

To relate the two equations, Langmuir model assumed that

- The surface areas of the adsorbent is uniformed and contains a fixed number of equivalent sites
- Only one molecule may be adsorbed onto one site (monolayer capacity).
- The adsorbed molecules have no interaction with other adsorbed molecules on adjacent sites

The restriction of this model is that it does not consider the multiple layers of adsorbate that can be formed and this can lead to over-estimation of the calculated surface area.

Therefore, the BET adsorption model considered multilayer adsorption and made the following assumptions:

- Pressure of the system is equal to the saturated pressure of the adsorbate
- Layer adsorption takes place on top of the other. The first layer of adsorbed molecules acts as a base for the adsorption of the second layer of molecules, which in turn acts as a base for the adsorption of the third layer, and so on.
- At equilibrium, the rates of condensation and adsorption are equal for each layer and the corresponding enthalpy of adsorption (ΔH^0_{AD}) and vaporisation (ΔH^0_{VAP}) are equal

The summation of the amount adsorbed in all the layers yields the BET equation

$$\frac{P}{n(P_0-P)} = \frac{1}{n_m C} + \frac{(C-1)}{n_m C}\left(\frac{P}{P_0}\right) \qquad (3.15)$$

Where C is the BET parameter ($C \approx e^{-}(\Delta H^{o}_{AD} + \Delta H^{o}_{VAP})/RT$), R is the universal gas constant and T is the temperature in Kelvin.

3.8.4.2 **Equipment description**

The BET adsorption models this study for the surface area calculations using Micrometrics ASAP® 2420 Accelerated Surface Area and Porosimetry equipment (Figure 3.18). The Micrometrics ASAP® 2420 Accelerated Surface Area and Porosimetry system includes twelve automatically controlled sample preparation ports that operate independently. Samples are added or removed from degas ports without disturbing the treatment of other samples undergoing preparation or analysis. The sample preparation system is fully automated with controlled heating time profiles. The temperature and ramp rate can be set and monitored individually and controlled from a few degrees above ambient to 450°C. The temperature hold period may extend past the point when evacuation is completed.

A programmable pressure threshold can suspend the temperature ramp if the outlet gassing pressure exceeds the limit specified, preventing destructive steaming or other undesired reactions with residual gases and vapours.

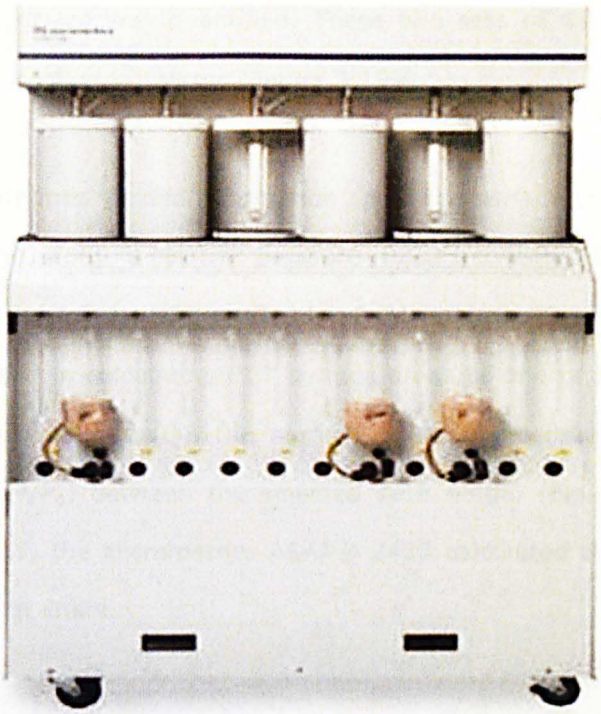

Figure 3.18 Micrometrics ASAP® 2420 accelerated surface area and porosimetry

3.8.4.3 **Procedure**

Here sawdust samples, HTF and DTF chars were first weighed and degassed respectively by heating to 120°C at the heating rate of 5°C min^{-1} and kept isothermal at that temperature for 6 hrs. Then the weights of each sample were taken. The BET analysis was carried out in nitrogen gas at -196°C. The nitrogen was injected into the pores within the sample for a range of relative pressures. The volume of nitrogen absorbed at each relative pressure was measured. As adsorption proceeded, the thickness of the adsorbed film increased. Any micropores in the surface are quickly filled, then the free surface becomes completely covered, and finally larger pores were filled. Then, desorption process began in which pressure systematically was reduced resulting in liberation of the

adsorbed molecules. As with the adsorption process, the changing quantity of gas on the solid surface was quantified. These two sets of data describe the adsorption and desorption isotherms (Figure 3.19a).

Analysis of the isotherms yielded information about the surface characteristics of the material. In this study, a relative pressure (P/P_o) between 0.04-0.1 with six data points was used for the BET surface area calculations. Figure 3.19b shows the data points used in calculating BET surface areas of one of the DTF chars. From the quantity adsorbed (Q), the number of moles adsorbed (n) and the relative pressure (P/P_o) between the selected data range, (Figure 3.19b) and using equation 3.15, the Micrometrics ASAP® 2420 calculated the BET surface areas of the sawdust chars.

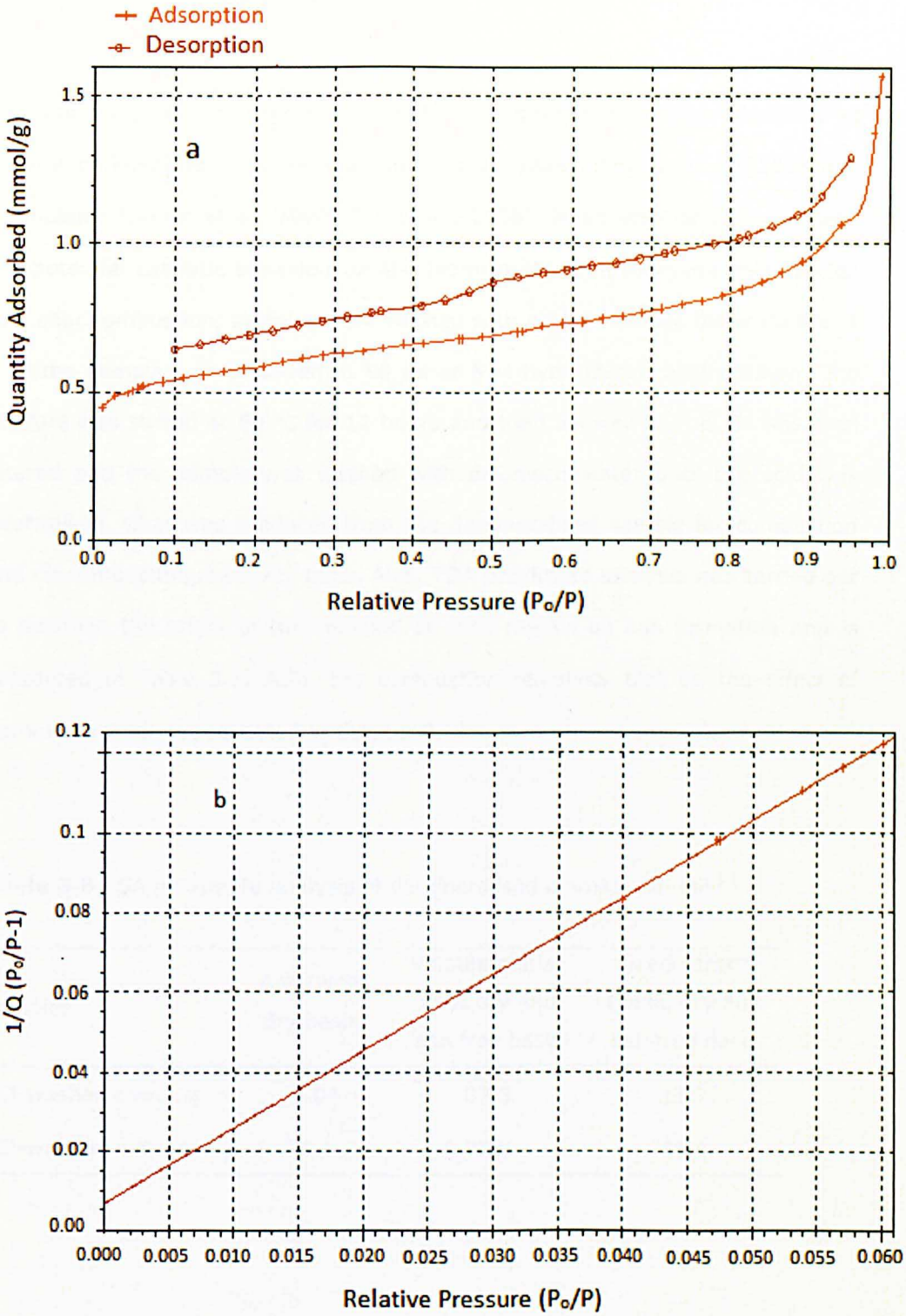

Figure 3.19 Typical examples of (a) nitrogen adsorption/desorption isotherms (b) Data points used for calculating BET surface area

3.9 Demineralisation of sawdust

Biomass contains alkali and alkaline earth metals which have been identified as natural catalysts to enhance coal combustion (Asadullah et al., 2010b) and gasification (Brown et al., 2000, Zhu et al., 2008). In an attempt to understand the potential catalytic behaviour of the biomass inherent inorganic minerals on coal char combustion, samples were washed with acid to remove these metals. 1 g of the sample was dissolved in 50 ml of 5 M hydrochloric acid solution. The mixture was stirred at 60 °C for 12 hours and then allowed to cool. It was then filtered and the sample was washed with deionised water until the acid was neutralised. Char was produced from the demineralised sample for combustion and co-combustion reactivity tests. Also, TGA proximate analysis was carried out to examine the effect of the removal of such metals on ash formation and is presented in Table 3.1. Also, the combustion reactivity test on the effect of demineralisation is presented in chapter 8.

Table 3.6 TGA proximate analysis of demineralised biomass samples

Samples	Ash (wt%, dry basis)	Volatile matter wt% dry and ash free basis	Fixed carbon (wt%, dry and ash free basis
HCl-washed sawdust	0.04	87.3	12.7
HCl-washed pinewood	1.4	77.0	23.4

4 TGA INVESTIGATION OF BIOMASS DEVOLATILISATION AND CHAR COMBUSTION UNDER AIR AND OXY-FUEL CONDITIONS

4.1 SUMMARY

This chapter discusses the initial investigation carried out to establish the standard TGA experimental procedures for devolatilisation temperature and char burnout. The implication of devolatilisation temperatures on volatile yield, nitrogen partitioning between volatiles and char and the residual char burnout were considered under air and oxy-fuel conditions. The burnout characteristics of the chars were studied to understand the role fuel particle size played in char combustion. From the resultant carbon burnout profiles two quantities were used to measure the combustion reactivity. Firstly 90% carbon conversion and, secondly, pseudo-first order kinetics were applied between 5 and 95% carbon burnout to allow for the calculation of a composite rate constant. Therefore, the activation energies of the combustion were determined by completing isothermal TGA runs at a range of temperatures and using the equations described in section 3.2.2.3.

Finally, a detailed investigation of the morphological changes in the chars produced at the different operating conditions and their influence on the combustion reactivity has been explained in the light of scanning electron microscopy (SEM) images and BET surface areas.

4.2 DEVOLATILISATION CHARACTERISTICS UNDER NITROGEN

Figure 4.1 presents the TGA volatile yields for the different temperatures and the different particle sizes used in this work. There was no significant particle size effect on the yield of volatile matter. Also, increasing the devolatilisation temperature to 1100°C did not seem to have much significant influence on volatile yields for all the particle sizes. This was because at 700°C, devolatilisation was completed so that further increase in temperature did not produce significant extra volatile matter. Hence, 700°C was used as the optimum devolatilisation temperature.

Next, the nitrogen partitioning behaviour during devolatilisation, which is the split of fuel-N between volatiles and the residual char, was calculated by material balance from the nitrogen content of the fuel and that of the char. The results are presented in Figure 4.2. From Figure 4.2, it was observed that nitrogen transformation into the volatile phase increased with increase in temperature. This was in contrast to what was observed with volatile yields in Figure 4.1. The possible reason could be that fuel-N partitioning into the volatile phase was slower than the volatile yields. Additionally, less nitrogen was transformed into the volatile phase for particle sizes less than 75μm.

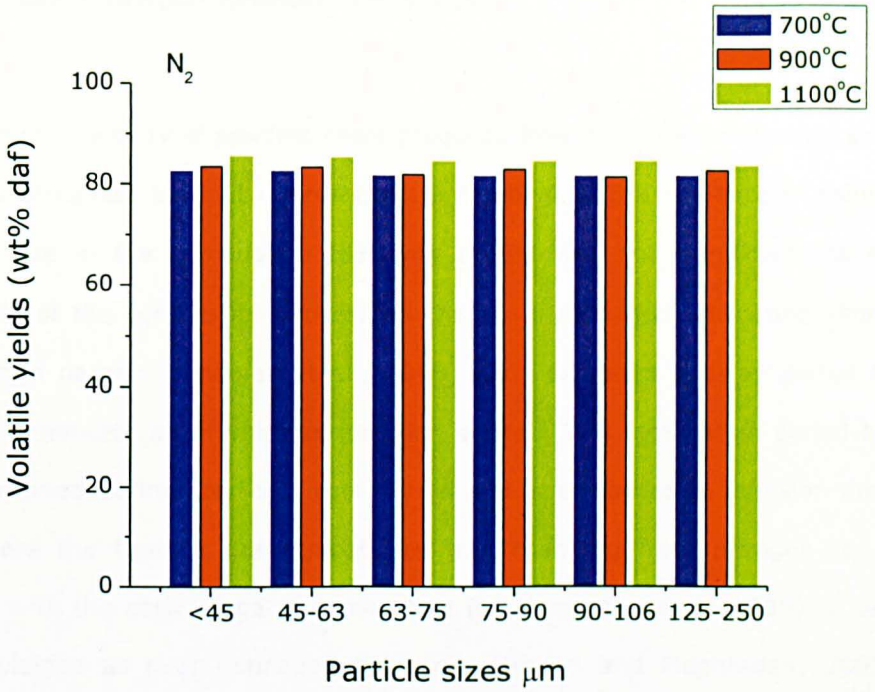

Figure 4.1 Sawdust TGA volatile yields demonstrating the influence of temperature and particle size effects

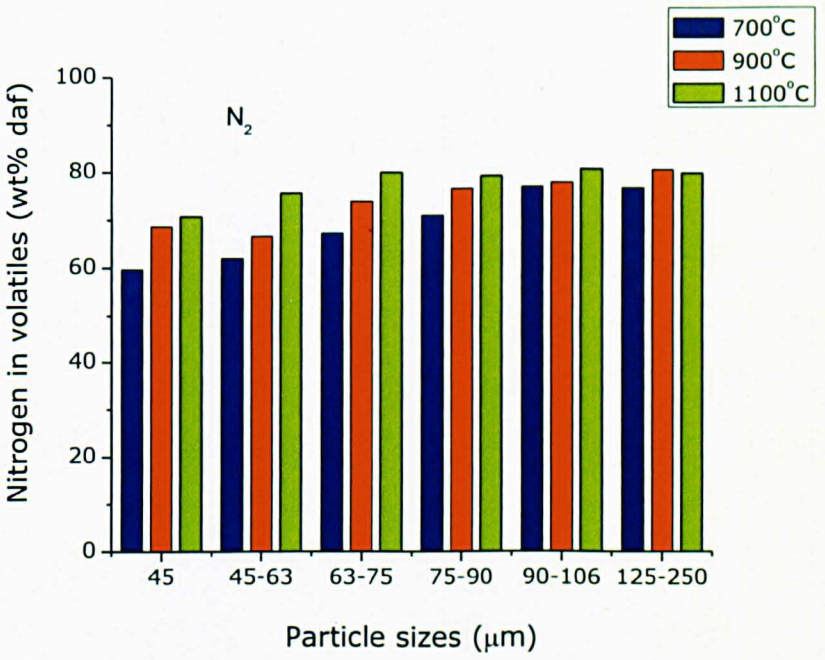

Figure 4.2 Nitrogen partitioning behaviour of sawdust between volatiles and chars during devolatilisation of 700°C, 900°C and 1100°C for the particle sizes under N_2

4.3 CHAR BURNOUT CHARACTERISTICS

Combustion reactivity of sawdust chars produced from the different particle sizes in terms of carbon burnout is presented in Figure 4.3. The influence of sample particle size in the combustion reactivity profile was not significant. At the beginning of the combustion process all the chars coincided, indicating similar combustion pattern (Ambalae et al., 2006) and exhibited a delay period for about 3-6 minutes after which combustion started. This retardation period has been observed during coal char combustion and is attributed to diffusion time-lag, where the furnace gas atmosphere was changing from nitrogen to air coupled with the early stage of combustion (Le Manquais et al., 2009). It was also explained as near extinction behaviour (Meesri and Moghtaderi, 2003), opening of previously closed pores (Naredi and Pisupati, 2008) or the time taken to build up partial gas pressure (Naredi et al., 2011b). Due to the presence of the diffusion time-lag, the intrinsic reaction kinetic calculations were taken from 5% of carbon burnout which corresponded to about 5 minutes period for the air filling of the furnace and the early stages of char combustion.

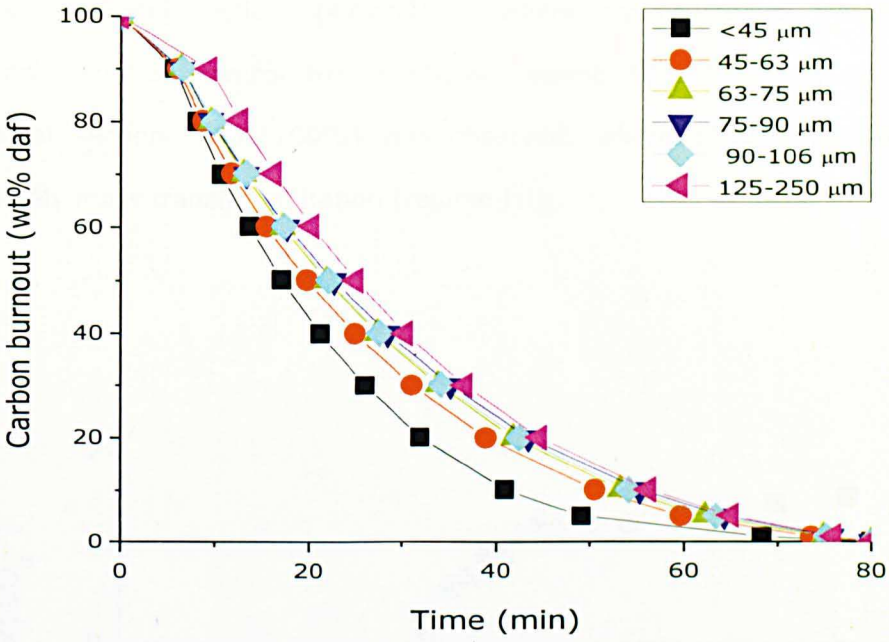

Figure 4.3 TGA burnout profiles of the chars at 375°C showing relationship with particle size.

4.4 COMBUSTION REACTIVITY AND REGIME MEASUREMENT

In order to adequately describe the combustion regime of the sawdust chars used in this work, Arrhenius plot of the burnout profile of the smallest particle size (<45 μm) at different isothermal temperatures is shown in Figure 4.4. For easy understanding of the graph, the actual temperatures were used for the x-axis. The burnout profile can be divided into distinct regimes. First, a linear ascending region (325-425°C) where some level of kinetic control was assumed (regime I). In this study, char combustion was carried out in this regime because 425°C was found to be the upper limit for establishing intrinsic chemical kinetically controlled combustion. Figure 4.5 shows the burnout profiles of the <45 μm char at the operating isothermal temperatures to highlight the upper

boundary temperature where reduced burnout was exhibited. Secondly, a slightly horizontal section, (475-575°C) where both chemical kinetics and diffusion limitation control the reactions (regime II). Thirdly, a completely horizontal section (600-1100°C) was observed, where combustion rate was completely mass transfer limitation (regime III).

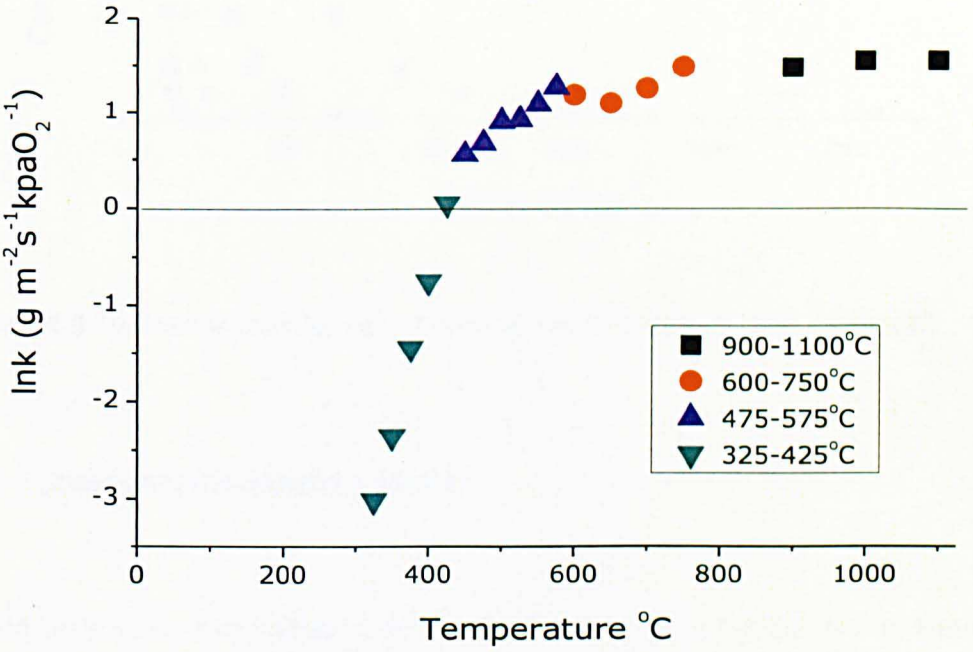

Figure 4.4 The effect of TGA burnout temperature on the reaction kinetic control regimes sawdust (125-250 μm)

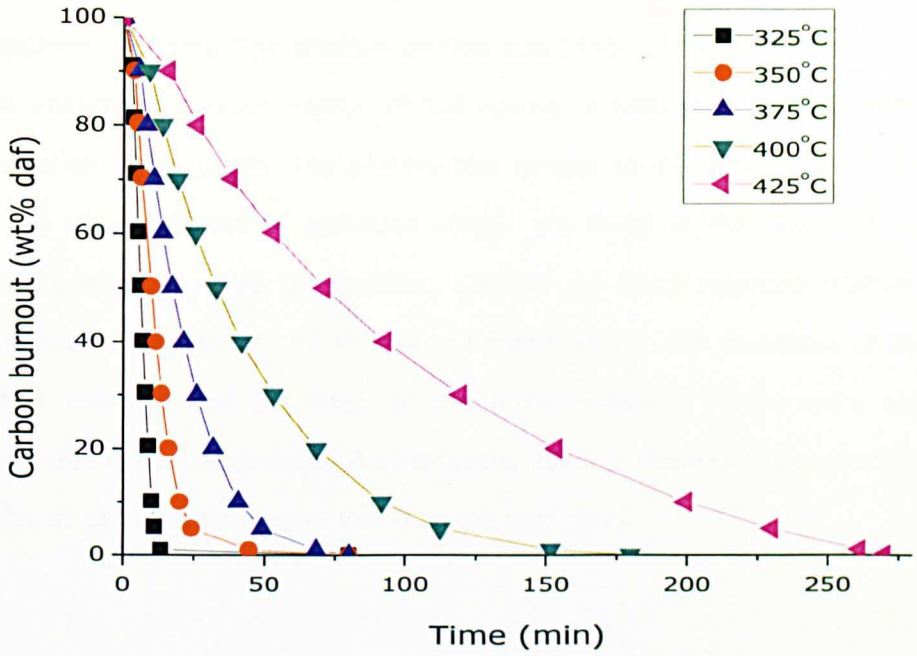

Figure 4.5 Isothermal combustion temperatures for sawdust char (<45 μm)

4.5 COMBUSTION KINETIC STUDY

Having understood the reaction boundaries from the experimental data in Figure 4.4, the kinetic parameters were calculated from the gradient of the first section of the Arrhenius plot. From the results, it was observed that there is slight decrease in activation energy between the smallest and the biggest particle size. The smallest particle size (<45 μm) exhibited an apparent activation energy of 116 KJ/mol. The largest particle size exhibited apparent activation energy of 107 KJ/mol. This suggested that there could be a correlation between particle size and apparent activation energy but not well defined (Le Manquais et al., 2009) though the underlying fact remains that mineral composition could play a role in reactivity of the different particle sizes.

Furthermore, Figure 4.6 shows a compensation effect of the TGA data which displayed systematic variation of the activation energies and the Log of their pre-exponential factors. The smallest particle size (<45 μm) which recorded the highest apparent activation energy of 116 KJ/mol is located at the top of the compensation effect graph. The particle size ranges 45-63, 63-75, 75-90 μm which are closely related in activation energy are found at the centre of the graph. The largest particle size fraction, 125-250 μm which recorded relatively small activation energy of 107 KJ/mol is located below. The variations of the activation energies and the Log_{10} of the pre-exponential factors were also observed during coal combustion (Le Manquais, 2011a). However, the variations exhibited by sawdust chars were less than the coal chars.

Table 4.1 Kinetic Parameters obtained from isothermal char combustion

Particle size (μm)	TGA char Burnout		
	E (KJ/mol)	A (min^{-1})	R^2
< 45	116	7.09×10^8	1.00
45-63	111	2.42×10^8	0.99
63-75	111	2.23×10^8	0.99
75-90	110	1.76×10^8	0.99
90-106	108	1.19×10^8	0.99
125-250	107	1.04×10^8	1.00

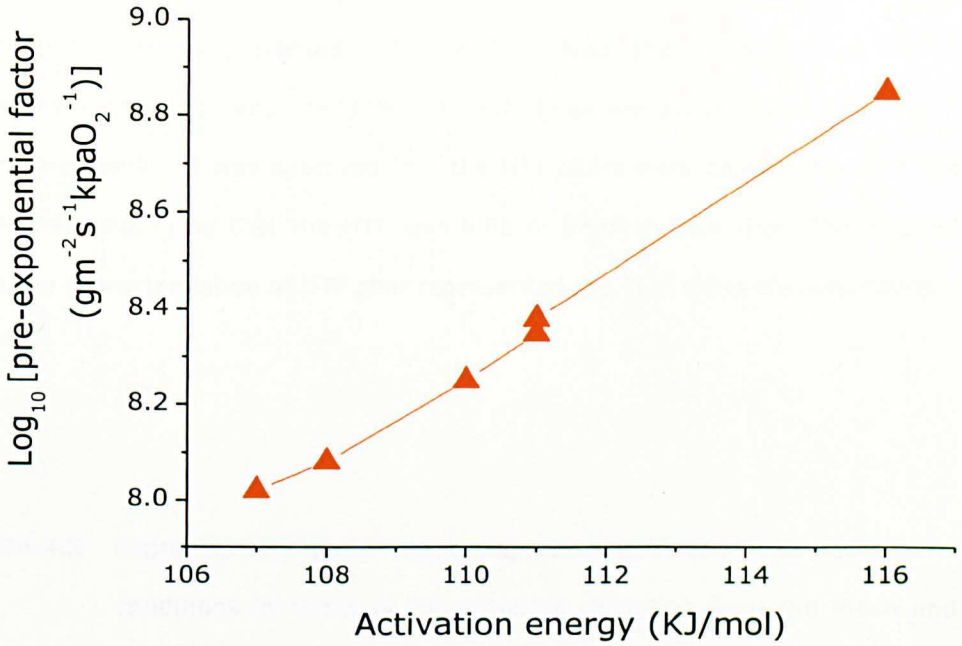

Figure 4.6 Compensation effect graph for sawdust TGA 700°C char showing relationship between activation and pre-exponential factor for the different particle sizes.

4.6 HORIZONTAL TUBE FURNACE (HTF) AND TGA CHAR ASSESSMENT

Before carrying out the TGA char characterisation, sufficient chars were produced in the HTF at 700°C as described in section 3.3.1 imitating TGA devolatilisation behaviour. The char production process was first assessed and the results are presented in Table 4.3. From the results, it can be seen that the reproducibility of the HTF char production process was quite reasonable. The standard deviation from the mean of chars produced at three different times were significantly small yielding an error of between 1-3 % for the rate constants and between 1-2 % for the 90% burnout time.

Next, the consistency of HTF devolatilised chars with their TGA counterpart was assessed using carbon burnout profile, 1st order rate constants and the 90%

burnout times. The burnout profile of the smallest particle size (<45 μm) of the HTF devolatilised char was assessed and it was found to be consistent with its TGA counterpart as presented in Figure 4.7. Also, the comparison of the 1st order rate constants and the 90% burnout times are presented in Table 4.4. From the results, it was observed that the HTF chars were comparable with the TGA chars signifying that the HTF was able to produce TGA char. This implied that the characterisation of HTF char represented the TGA chars characteristics.

Table 4.2 Reproducibility of HTF chars prepared at different times under same conditions in terms of the standard deviation from the mean and the % error

Particle size (μm)	Rate constants (min^{-1})		Burnout times (min)	
	Standv	% Error	Standv	% Error
<45	0.0008	1.25	0.83	1.98
45-63	0.0008	1.65	0.55	1.04
63-75	0.0012	2.54	0.68	1.28
75-90	0.0011	2.23	0.80	1.45
90-106	0.0003	0.62	0.61	1.09
125-250	0.0007	1.47	0.62	1.11

* % error= standard deviation divided by the mean x 100.

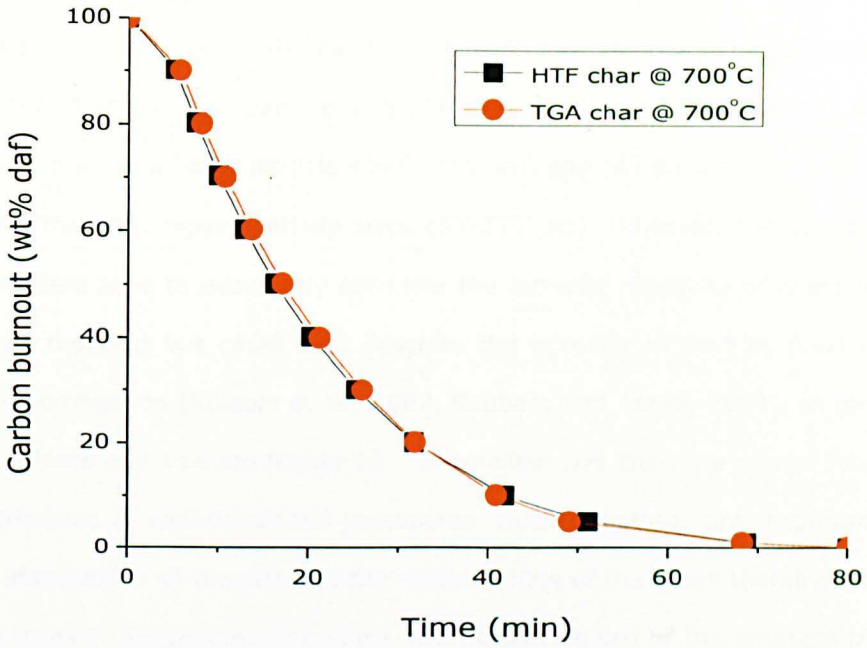

Figure 4.7 Comparison of the burnout profiles for the smallest particle size (<45 μm) HTF and TGA chars at 375°C

Table 4.3 Comparison of HTF and TGA devolatilised char burnout at 375°C

	TGA char burnout		HTF char burnout	
Particle size (μm)	Rate Constant (min^{-1})	90% burnout time (min)	Rate Constant (min^{-1})	90% burnout time (min)
<45	0.0656	40.80	0.0623	41.80
45-63	0.0515	50.50	0.0501	52.60
63-75	0.0494	53.20	0.0503	52.40
75-90	0.0471	55.30	0.0480	64.70
90-106	0.0485	54.20	0.0472	55.00
125-250	0.0476	56.40	0.0492	56.20

Subsequently, char porosity was investigated to understand surface area, pore volume and pore sizes. The porosity study of the chars shows that surface areas of the chars increase with increasing particle size while pore sizes decrease from smallest to the largest particle size (Table 4.5). Surprisingly, the BET surface areas of the two smaller particle sizes (<45 μm) and (45-63 μm) are found to be smaller than the bigger particle sizes (63-250 μm). However, the suitability of BET surface area to accurately correlate the intrinsic reactivity of chars is still not yet resolved but could best describe the porosity of char to reactive gas during combustion (Külaots et al., 2007, Suuberg and Aarna, 2009). In contrast, pore volume and size are higher for the smallest size than the others indicating the presence of well-developed mesopores. Such structures are responsible for easy accessibility of oxygen into the reactive sites of the chars thereby reducing mass transfer limitations. Therefore, the porous nature of the smallest particle size could be responsible for the higher apparent activation energy exhibited by the smallest size (<45μm) followed by particle size 45-63 μm.

Table 4.4 Porosity characterization of HTF chars produced at 700°C

Sawdust Particle Sizes (μm)	BET surface area (m^2/g)	Pore Volume (cm^3/g)	Pore Size (nm)
<45	149	0.096	5.3
45-63	210	0.111	4.3
63-75	229	0.109	4.7
75-90	245	0.1235	3.6
90-106	217	0.098	4.7
125-250	303	0.119	4.5

4.7 THE EFFECT OF TGA DEVOLATILISATION TEMPERATURES ON CHAR COMBUSTION PERFORMANCE

Although devolatilisation temperature used was 700°C, the effect of higher devolatilisation temperatures on sawdust char combustion reactivity in terms of carbon burnout and activation energy was investigated using the biggest particle size (125-250 μm). From Figure 4.8 and Table 4.6, it was observed that the burnout decreased with increasing devolatilisation temperature. The reduced reactivity with devolatilisation temperature can be explained in relation to thermal annealing which is the reorganisation of the char surface area and a reduction in the amount of hydrogen molecules retained during devolatilisation as a result of complete devolatilisation (Le Manquais et al., 2009, Lu et al., 2002, Senneca et al., 2004b, Senneca et al., 2005, Senneca et al., 2007b, Zolin et al., 2001a, Zolin et al., 2002). Coal pyrolysis at different temperatures has also shown decreasing char reactivity with increasing pyrolysis temperature (Cetin et al., 2005, Zolin et al., 2001a, Zolin et al., 2002).

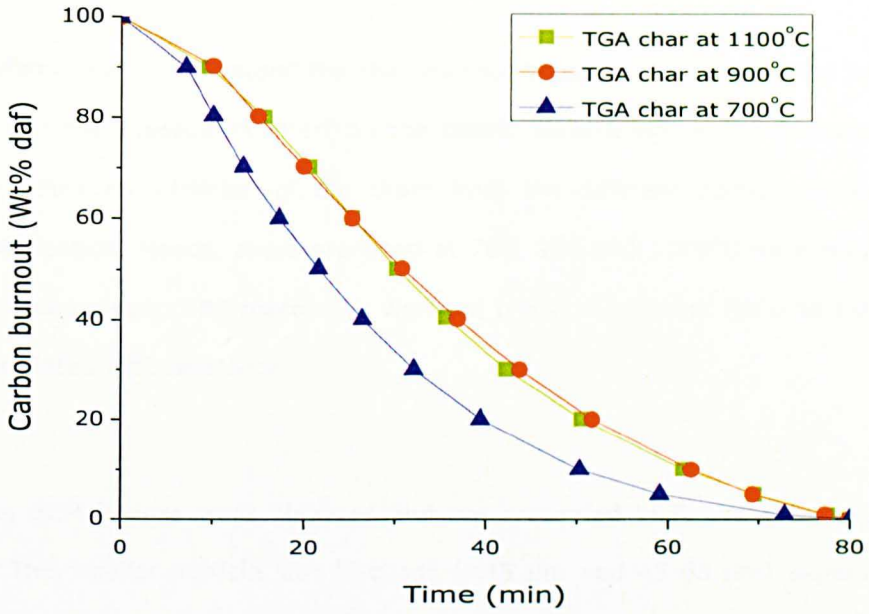

Figure 4.8 Carbon burnout profile of sawdust char at 375°C (125-250 μm) showing decrease in reactivity with increase in devolatilisation temperature

Table 4.5 Influence of devolatilisation temperature on combustion reactivity expressed as rates constants and time to achieve 90% carbon burnout at burnout temperature 375°C (125-250 μm).

Devolatilisation temperature (°C)	1st order rate constants at 5-95% carbon burnout (min^{-1})	90% carbon burnout time (min)
700	0.054	28.5
900	0.044	62.6
1100	0.044	61.7

4.8 CHAR CHARACTERISATION

Therefore, having understood the char burnout behaviour of the different particle sizes and the subsequent effect on the kinetic parameters, it was necessary to study structural variation of the chars from the different particle sizes after devolatilisation. Hence, chars produced at 700, 900 and 1100°C were subjected to scanning electron microscope to view the physical apparent features that can be correlated with reactivity.

Hence, SEM images were obtained and are presented in Figure 4.9, 4.10 and 4.11. The smaller particle size fractions (<45 μm and 45-63 μm) experienced some swelling due to the softening and melting of the original cellulosic cell matrix during devolatilisation leading to formation of bubbles for 700°C chars. However, as particle size ranges increase, the lignocellulose oblong structure becomes visible. For the largest particle size range examined (90-106 μm and 125-250 μm), the lignocellulose fibre was clearly seen with evidence of some large macropores for the chars obtained at 700 and 900°C. However, as temperature increased to 1100°C, the chars experienced swelling. The fibrous cellulose cell structure had completely melted even for the largest particle size.

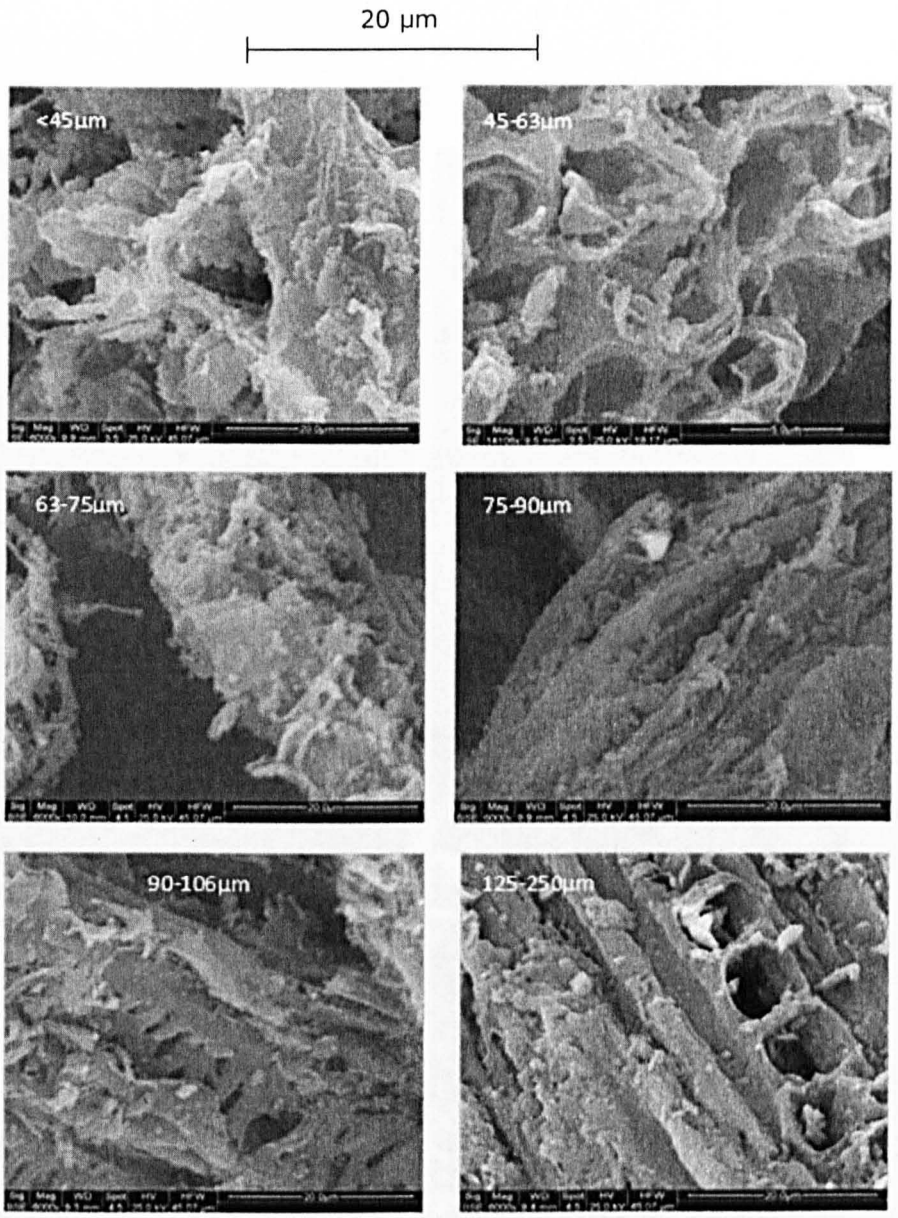

Figure 4.9 SEM images of chars produced at a devolatilisation temperature of 700°C in nitrogen

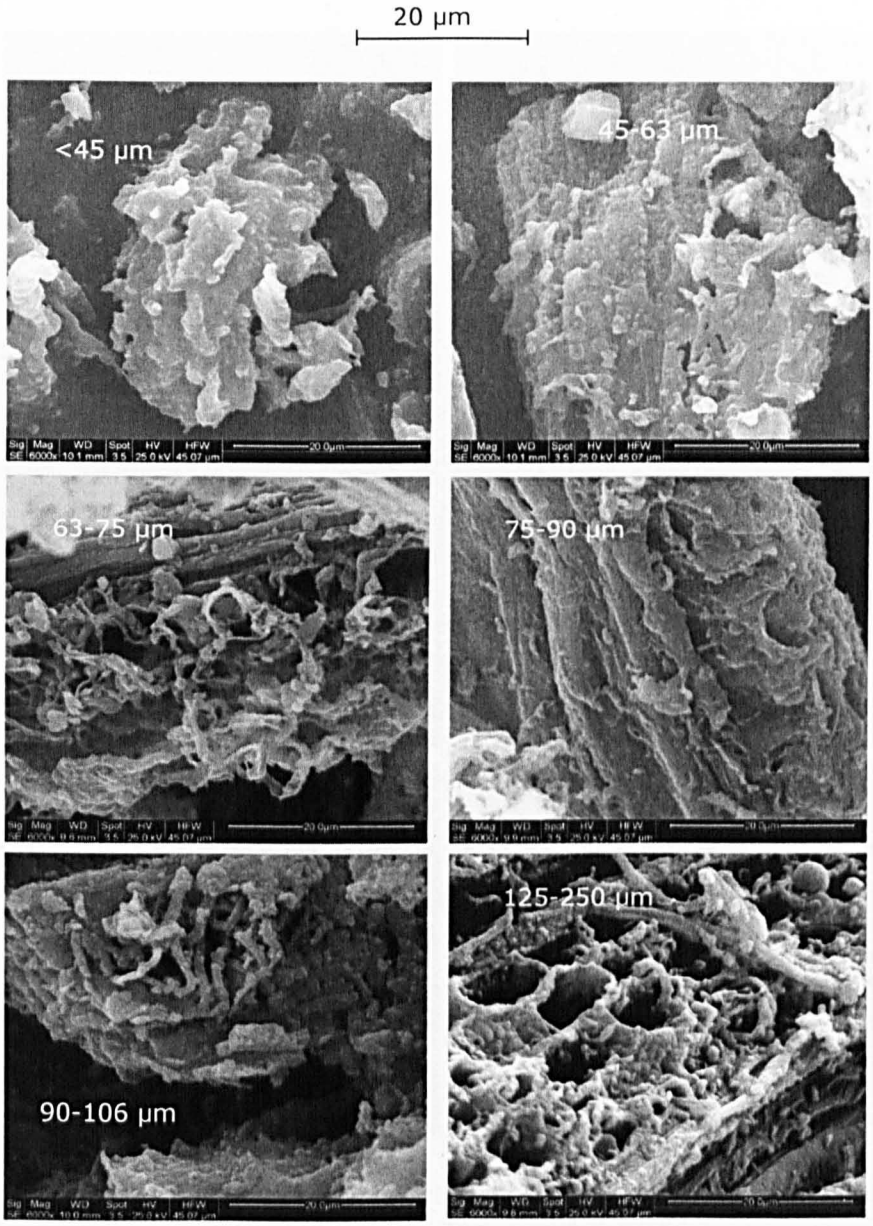

Figure 4.10 SEM images of chars produced at a devolatilisation temperature of 900°C in nitrogen

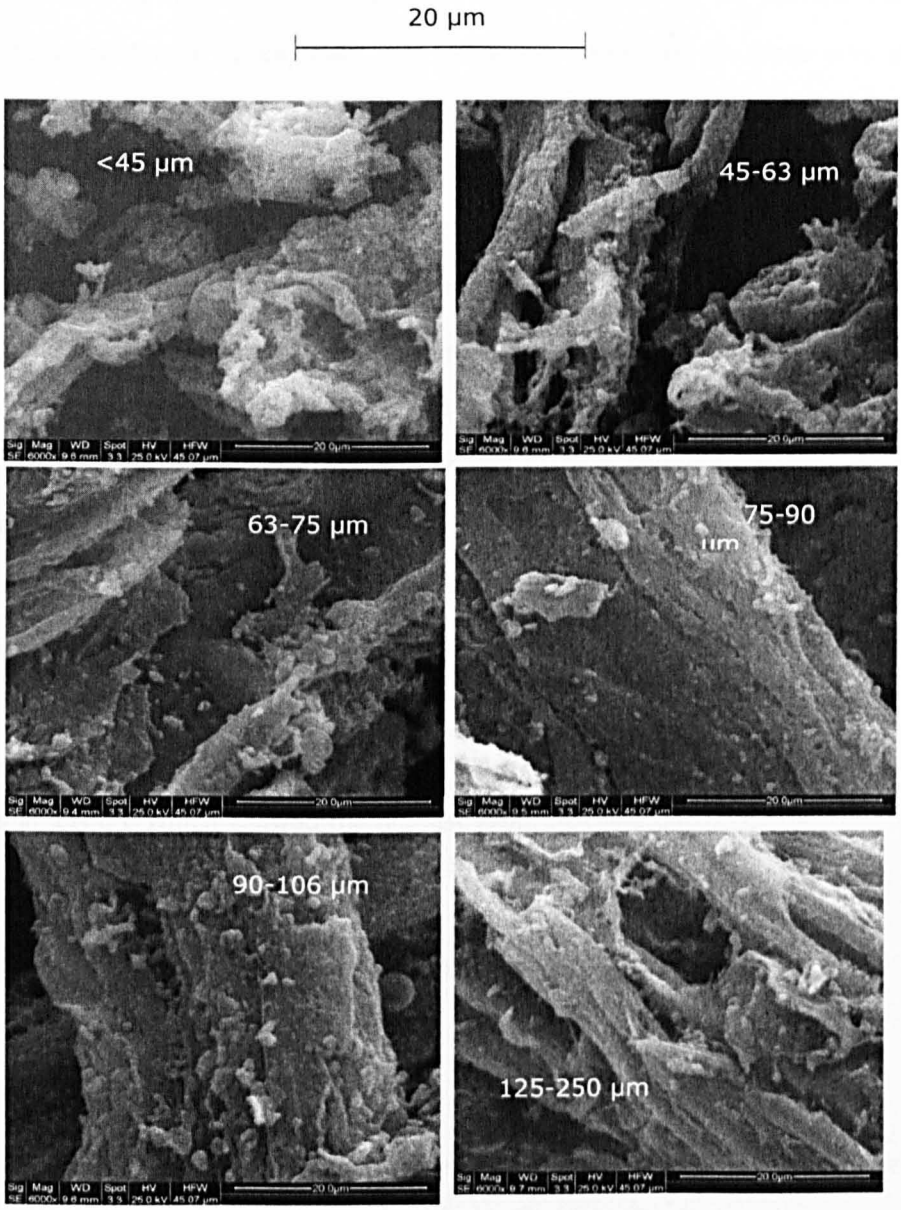

Figure 4.11 SEM images of chars produced at a devolatilisation temperature of 1100°C in nitrogen

4.9 TGA VOLATILE YIELDS AT DIFFERENT TEMPERATURES IN CO_2

Figure 4.12 presents volatile yields for the particle sizes was carried out in a laboratory horizontal furnace by imitating the heating rate of the TGA in CO_2

atmosphere at different temperatures. Volatile yields for all particle sizes at 700°C were found to be lower (76-78 wt%) compared to what was earlier observed at 700°C in Nitrogen atmosphere (82-84 wt%). The lower yield of volatiles at 700°C was indicative of the higher mass transfer resistance of primary volatiles in CO_2 than in nitrogen because of the low reactivity of CO_2 at such low temperature. At 900°C, volatile yields increased to about 80-82 wt% but is still slightly lower than the yields in nitrogen conditions in Figure 4.1 However, at 1100°C, about 90-97 wt% volatile yield was achieved with the smallest particle size (<45 μm) having the highest yield of 97 wt%. This was significantly higher than what was observed in nitrogen conditions in Figure 4.1. The reason for the high yield of volatile at 1100°C in CO_2 atmosphere was attributed to CO_2-char gasification reaction as was observed in coal devolatilisation (Wall et al., 2009). Additionally, the devolatilisation characteristics did not show strong particle size variability except for the smallest size at 1100°C which showed the highest yield.

4.10 NITROGEN PARTITIONING IN CO_2

In Figure 4.13, the nitrogen partitioning behaviour of sawdust in CO_2 was examined at TGA devolatilisation temperatures (700, 900 and 1100°C) for all the particle sizes considered in this work. As was observed in Figure 4.12, fuel-N released into the volatile phase increased with in increasing in temperature for all the particle sizes. However, more nitrogen was retained in char at 700°C and 900°C for particle sizes less than 75 μm. This was much lower than what was observed in Figure 4.2 for nitrogen conditions. However, at 1100°C, significant amount of fuel-N was released into the volatile phase. This was much higher than what was observed in Figure 4.2 in nitrogen condition. This behaviour suggested that potentially less NO_x will be formed under oxy-biomass firing at high temperatures.

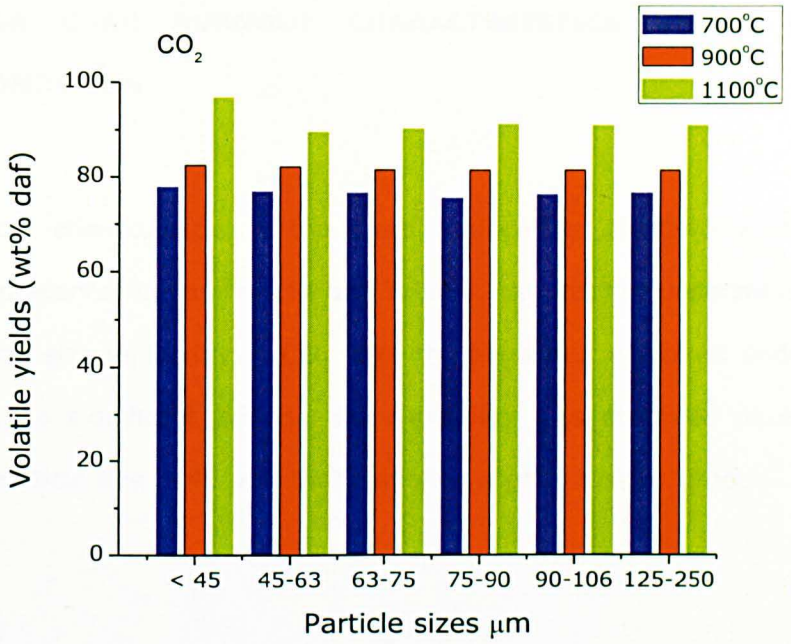

Figure 4.12 Volatile yields of sawdust samples in CO_2 highlighting the effect of devolatilisation temperature and particle size

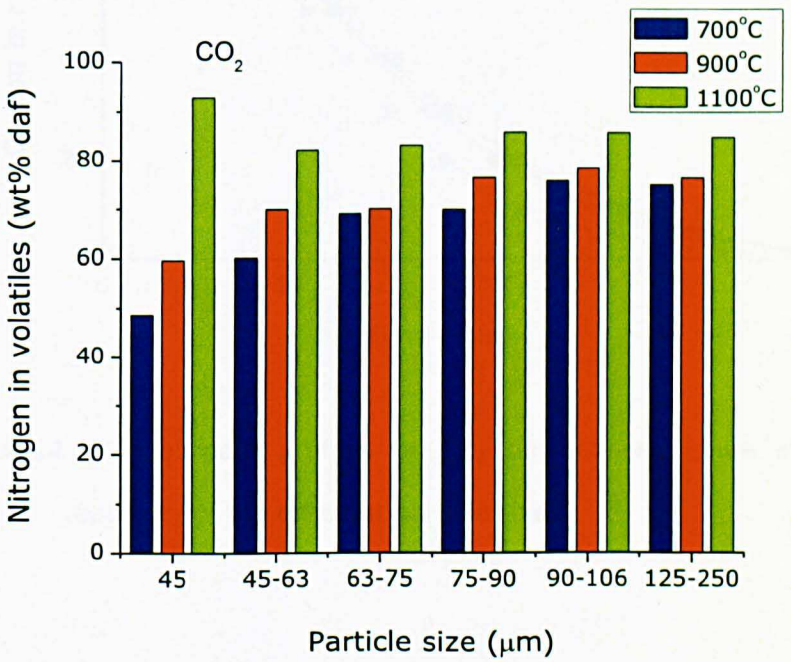

Figure 4.13 Nitrogen partitioning behaviour of biomass fuel under oxy-fuel conditions for devolatilisation temperatures 700°C, 900°C and 1100°C for all particle sizes

4.11 TGA CHAR BURNOUT CHARACTERISTICS UNDER OXY-FUEL CONDITION

The burnout characteristics of the chars produced at 700°C for all the particle sizes are presented in Figure 4.14 and Table 4.7 in order to understand reactivity and particle size variability in CO_2. Like the behaviour exhibited under air fired condition, no significant particle size variability was observed except for the smallest particle size (<45 μm) that exhibited slightly faster burnout.

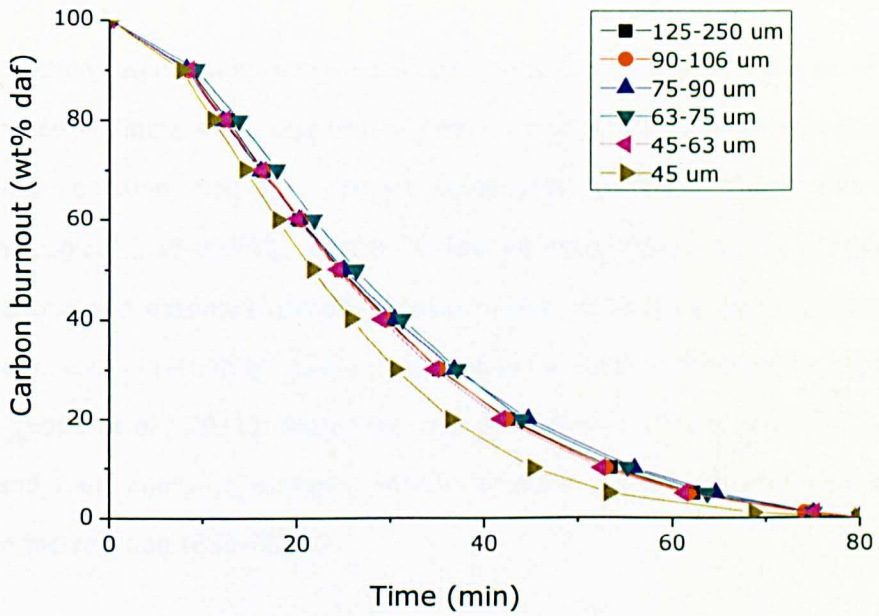

Figure 4.14 TGA burnout profiles of CO_2 devolatilised chars showing the reactivity of the different particle sizes.

Table 4.6 Reactivity ranking at a burnout temperature of 375°C

Particle size (μm)	1st order rate constant (min^{-1})	90% carbon burnout (min)
<45	0.0629	45.20
45-63	0.0536	52.40
63-75	0.0512	55.20
75-90	0.0487	56.00
90-106	0.0526	53.00
125-250	0.0522	53.50

4.11.1 *TGA Combustion regime study*

The combustion regime was also investigated under oxy-firing and the results are presented in Figure 4.15. Like the air fired char combustion, the combustion in oxy-fuel condition also had distinct combustion regimes. There was a horizontal region (325-425°C), similar to the air combustion where intrinsic kinetic control was assumed. Results from previous researchers have revealed that the combustion rate in air-coal was similar to oxy-coal in the kinetic control regime I (Edge et al., 2011). After this, was the diffusion control region (450-575°C) and then finally to a region where complete mass transfer limitation controlled the reaction (650-750°C).

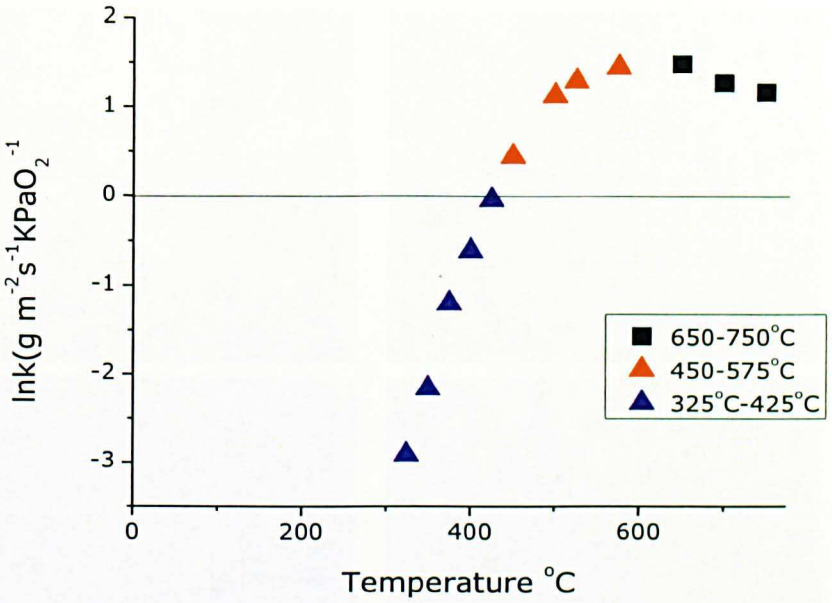

Figure 4.15 Reaction regimes for sawdust oxy-fuel combustion, showing transitions between the combustion regimes

Next of interest was the apparent kinetic parameters exhibited at the operating temperature range (325-425°C). From the results in Table 4.8, it was observed that the activation energies were similar (95-98) except for the smallest particle size which exhibited slightly higher apparent activation energy of 101 KJ/mol. The activation energies obtained also reaffirmed the insignificant particle size variability exhibited during the char burnout.

PAGE MISSING IN ORIGINAL

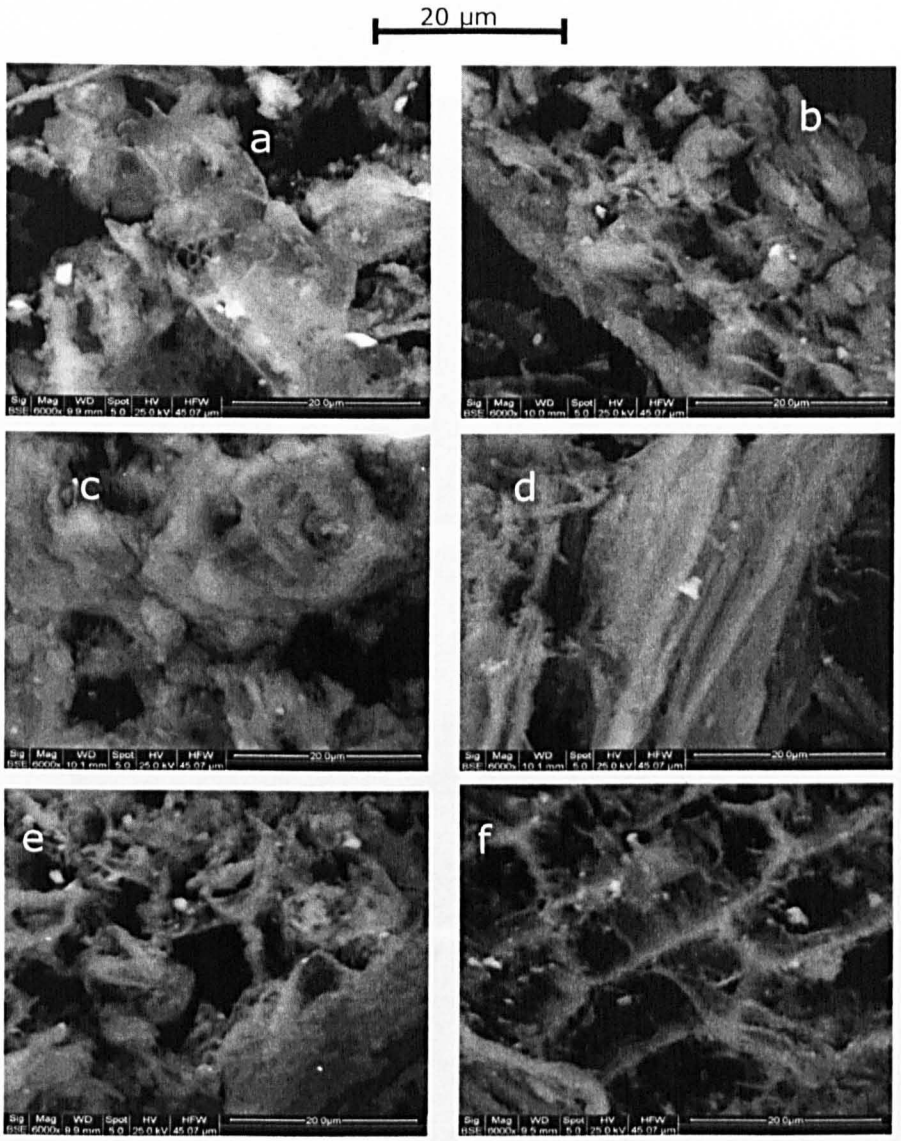

Figure 4.16 SEM images of chars produced in CO_2 at 700^{0}C; (a)_<45 µm; (b)_45-63 µm; (c)_63-75 µm; (d)_75-90 µm; (e)_90-106 µm and (f)_125-250 µm.

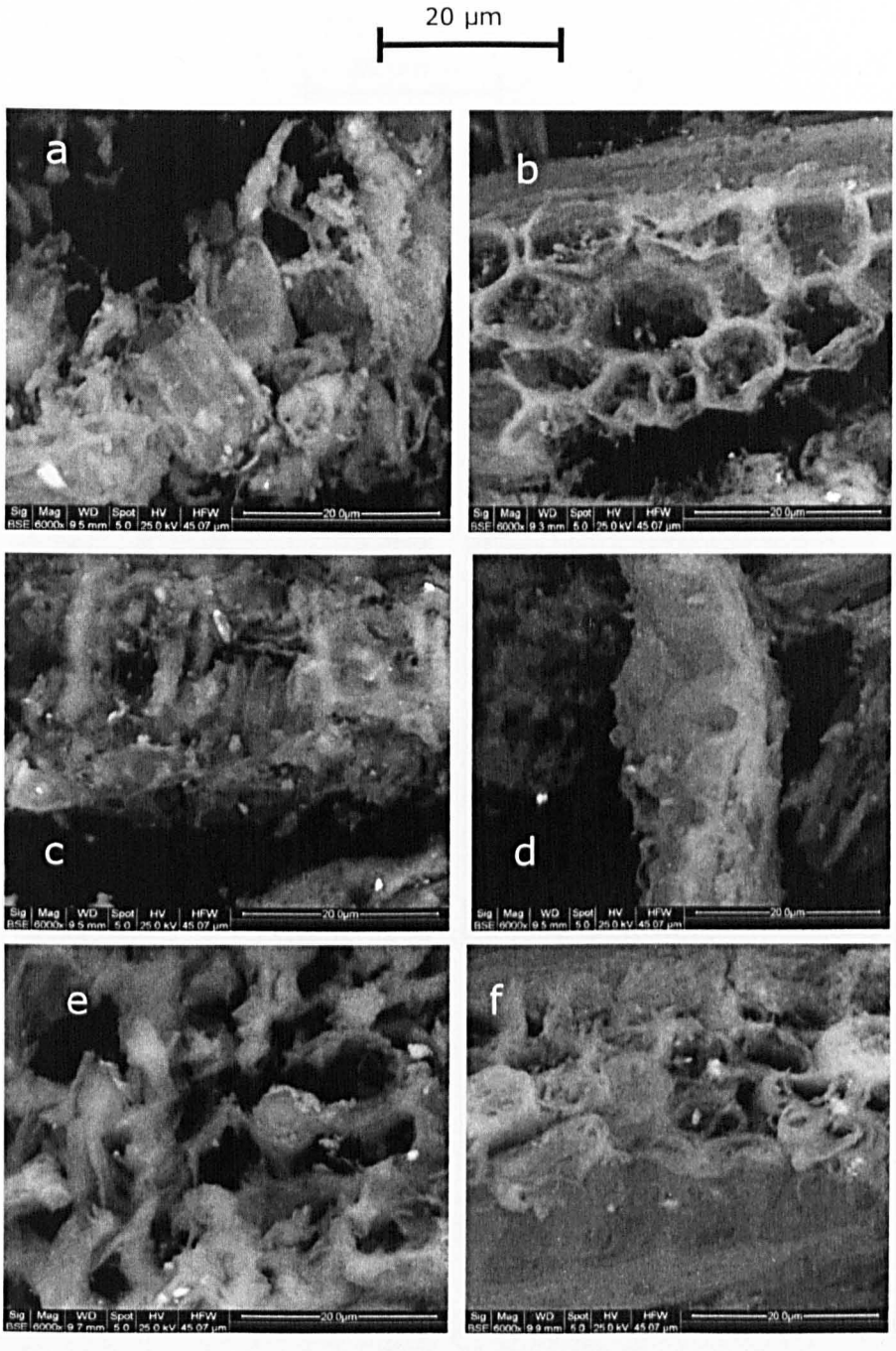

Figure 4.17 SEM images of chars produced in CO_2 at 900^{0}C. (a)_<45 µm; (b)_45-63 µm;(c)_63-75 µm; (d)_75-90 µm; (e)_90-106 µm and (f)_125-250 µm

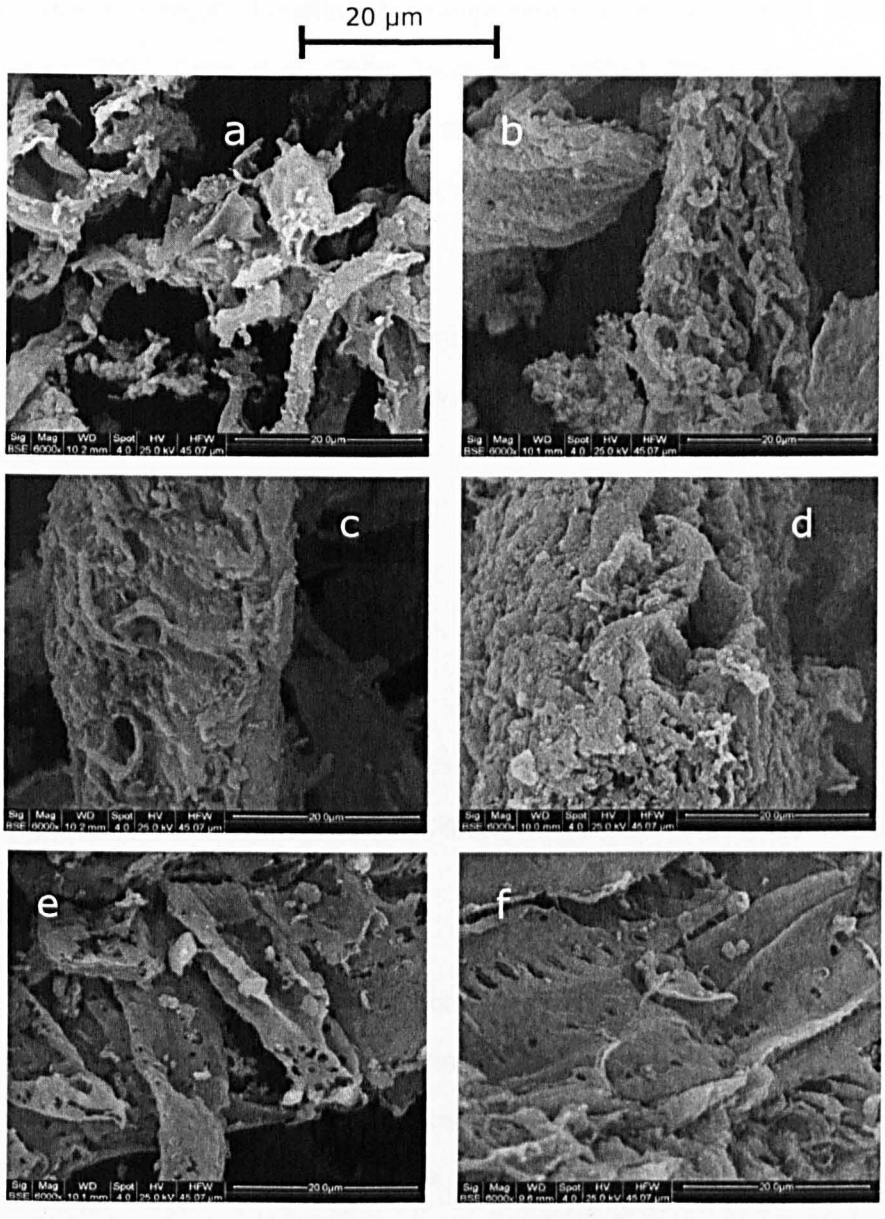

Figure 4.18 SEM images of chars produced in CO_2 at 1100^{0}C. (a)_<45 µm; (b)_45-63 µm; (c)_63-75 µm; (d)_75-90 µm; (e)_90-106 µm and (f)_125-250 µm

In Figure 4.18, the chars produced at 1100°C exhibited vascular bundles probably as a result of melting, rearrangement and re-solidification (Borrego and Alvarez, 2007, Cetin et al., 2004, Joyce et al., 2006). This compacted nature of the chars and reduced pore sizes restrict oxygen diffusion into carbon active sites and consequently could lead to reduction in combustion reactivity (Biagini et al., 2008a).

Additionally, inorganic minerals were not dispersed on all the char surfaces probably due to transformation and volatilisation of such metals as temperature increased.

4.13 CONCLUSIONS

1. Devolatilisation characteristics of sawdust under air and oxy fired conditions have been investigated at different temperatures with six particle size fractions.

2. There was no significant effect of temperature on volatile yield in N_2 for all the particle sizes at the three temperatures investigated. In the case of devolatilisation in CO_2 atmosphere, lower volatile yields were observed at 700°C. This was because there was no contribution of CO_2-char gasification reaction and mass transfer retardation of volatiles. However, at 1100°C the volatile yields in CO_2 increased significantly more than in N_2. This was attributed to the contribution of CO_2-char gasification reaction.

3. The release of nitrogen into volatiles is proportional to the yields of volatiles for both air and oxy-fuel conditions. However, due to the higher

volatile yields in CO_2 at 1100°C, more nitrogen was released and therefore less nitrogen remained in the chars. This implies that less NOx will be formed during char combustion in oxy-coal conditions in high temperature combustion systems.

4. From the char combustion results obtained at the two atmospheres, it was revealed that char burnout in oxy-conditions were slightly lower than in air fired condition at 375°C. This was probably because of the lower diffusivity of O_2 in CO_2 and the poor thermal conductivity of CO_2 at low burnout temperature of 375°C.

5 DEVELOPING A METHOD TO DETERMINE BIOMASS VOLATILE YIELDS IN THE DROP TUBE FURNACE (DTF)

5.1 SUMMARY

The first part of the DTF analysis was to investigate suitable particle size which would be used for the DTF analysis. The reproducibility and repeatability of the DTF experiment procedure was first assessed. Accurate method of measuring biomass volatile yields on the DTF was investigated. One of the common methods of calculating solid fuel conversion is the use of total ash as a tracer. Therefore, total ash was used as tracer in calculating sawdust conversion in the DTF. However, because of the high reactivity of sawdust fuel and the high temperatures involved in the DTF, possible volatilisation of the alkali and alkaline earth metals may occur especially at higher temperatures and longer residence times. As such, possible errors could be expected when using the total ash as a tracer. Therefore, silica was introduced as a tracer to calculate the volatile yields at 1100°C and 1300°C and the comparison of the results are presented. Finally, the effect of carrying out devolatilisation in slightly oxidising environment (1% O_2 concentration) on volatile yield was then investigated.

5.2 INTRODUCTION

Measuring solid fuel conversion during devolatilisation in entrained flow reactors such as the DTF has been widely carried out using ash in the resultant char to determine conversion (Borrego et al., 2009, Shuangning et al., 2006, Simone et al., 2009). This method, called the ash tracer technique has been used by researchers because of the difficulty in completely collecting the char during devolatilisation. Additionally, formation of tars due to slightly oxidising

environment under which the reactions are carried out can lead to char loss (Ballantyne et al., 2005). Therefore the ash tracer method compensates for incomplete collection of the char particles because it is assumed that the ash concentration in the char sample collected is the same as in the char particles lost. The assumption simply implies that the ash forming species did not volatilise during devolatilisation or the extent of volatilisation is not significant as to affect the ash balance (Ballantyne et al., 2005).

While this could be true for most coals, the applicability of this technique could be difficult for most biomass. This is because of the low ash content, volatilisation of ash components (Simone et al., 2009) and high conversion rate during devolatilisation especially in a slightly oxidising atmosphere. This could lead to some systematic errors in obtaining the conversion either by under estimating the conversion rate due to uncertainty in the ash measurements or overestimating it using mass of char collected.

In the conventional ASTM standard method, ash content is determined at low temperature and low heating rate which reduces the extent of volatilisation of the ash forming species. However, the high heating rate and high temperature in the DTF significantly differ from the standard ash test conditions and these can accelerate volatilisation of alkali and alkaline earth metals (AAEM) (Ren et al., 2011) which are the major ash forming minerals in biomass fuels. Additionally, gas atmosphere during devolatilisation could also contribute to high volatilisation of the ash forming species in biomass.

The available literature shows that the viability of the ash tracer method to calculate the pyrolysis conversion is sceptical because of the volatile ash components which may volatilise during the high temperature DTF operating

conditions (Borrego et al., 2009) especially for biomass fuel which has low ash content. In previous study using low ash content coals, modified ash tracer technique has been used to determine the conversion in entrained flow reactors because the conventional ash tracer method was not appropriate. For example, Ballantyne et al (2005) applied an inert artificial ash (perlite) to a low ash Victorian brown coal during devolatilisation to avoid inaccuracy or uncertainty in the conversion calculations due to volatilisation of alkali and alkaline earth metals. The perlite was added to the coal feed and fed into the DTF. The conversion based on mass of collected was higher than in modified ash tracer method due to incomplete collection of char during DTF devolatilisation (Ballantyne et al., 2005). Therefore, the investigation of the potential systematic errors associated with calculating the conversion of biomass devolatilisation in the DTF in this study became necessary.

5.3 PARTICLE SIZE VARIABILITY, REPRODUCIBILITY AND REPEATABILITY OF DTF CHAR PRODUCTION

The initial experiments were carried out at 900°C for 200, 400 and 600 ms to determine the experimental conditions and the particle size variability. The devolatilisation process was carried out at 1 bar under slightly oxidising condition at 1% O_2 concentration. The TGA burnout of the chars showed that there was no significant particle size variability as earlier been observed during TGA analysis. However, the char yields of DTF for the smaller particle size decrease rapidly with increase in residence times due to rapid volatile release as can be seen in Table 5.1. This could lead to poor reproducibility of the experimental procedure in terms of char collection efficiency. Additionally, smaller particle size fractions tend to block the screw feeder and the feed probe of the DTF. As a result, the

largest particle size (125-250μm) was taken to be the suitable particle size for DTF experiments.

Table 5.1 DTF Experimental procedure and particle size variability at 900°C

Particle size (μm)	Char Yield (g/g) N_2 (based on mass of sawdust feed)		
	200 ms	400 ms	600 ms
125-250	0.226	0.115	0.040
90-106	0.082	0.041	0.018
75-90	0.049	0.036	0.013
63-75	0.048	0.025	0.016
45-63	0.043	0.031	

*char yield =mass of char collected divided by mass of biomass feed

Next, it was necessary to investigate the effect of devolatilisation temperature on char yield which will subsequently affect char collection efficiency. Therefore, devolatilisation was carried out at 1100°C and 1300°C 200 ms and the reproducibility of the char production was assessed. The chars were produced in duplicate and the char yield was calculated based on the starting sawdust mass fed into the DTF. The results are presented in Table 5.2. From the results in Table 5.2, it can be observed that char reproducibility decreased with increase in devolatilisation temperature. At 1100°C, the char yield for the two runs produced a standard deviation of 0.011 from the mean, resulting in about 10% error. However, at 1300°C, deviation from the mean was 0.013 which resulted in about 16% error. The high percentage errors obtained could be due incomplete collection of chars during the experiments. This could also be associated with the DTF operating procedure since its parameters such as inlet gas flow rate, exhaust gas flow and feed flow rate were manually operated. Additionally, accuracy of measuring 1% oxygen concentration for each run could lead to poor

char collection efficiency. Nevertheless, the ash contents of the chars gave percentage errors less than 2 wt% for both temperatures.

Furthermore, the repeatability of the chars produced was also assessed by carrying TGA burnout test for the 1100°C and 200 ms char and the results are presented in Table 5.3. TGA combustion of the DTF char gave a reasonable repeatability data resulting in very small reactivity variation.

The efficiency of char collection from the furnace at the end of each run was then calculated from the ash of the parent fuel, those of the chars produced and the char yield. The ash contents of sawdust and the DTF chars are presented in Table 5.4 while the mass of char obtained and the char collection efficiency are presented in Table 5.5 for both gas conditions. The ash tracer method was used to calculate the volatile matter using the equation 3.13

As expected, mass of char collected decreased with increasing devolatilisation temperature and with increase in residence time (Table 5.4). This was because at higher temperatures, more volatiles were released leading to lower residual mass. Subsequently, the char collection efficiency decreased with increasing devolatilisation temperature. This means that char collection efficiency is a relative measure depending on amount of volatile yield and the loss of ash.

Table 5.2 Reproducibility of DTF char production method

DTF condition	Char yield as collected (g/g)					Ash content (wt % db)				
	1	2	mean	Standard deviation	% Error	1	2	mean	Standard deviation	% Error
1300°C 200 ms	0.088	0.070	0.082	0.013	16.1	11.54	11.27	11.41	0.22	1.9
1100°C 200 ms	0.108	0.124	0.116	0.011	9.8	7.74	7.94	7.84	0.14	1.8

* % error= standard deviation divided by the mean x 100.

Table 5.3 Repeatability of 1100°C and 200 ms sawdust DTF char in isothermal TGA burnout at 375°C

TGA Run	Rate constants (min^{-1})	(90% burnout time (min)
1	0.0998	25.30
2	0.1193	23.40
3	0.1160	24.50
4	0.1211	23.50

Table 5.4 DTF N_2 and CO_2 char collection efficiency (8 g starting mass)

Gas atmosphere	Particle size (μm)	Residence Time (ms)	Char Yield (g/g)			% char Collection efficiency		
			900°C	1100°C	1300°C	900°C	1100°C	1300°C
N_2	125-250	200	0.23	0.11	0.07	63	70	66
		400	0.11	0.05	0.02	65	60	52
		600	0.04	0.03	0.01	50	39	23
CO_2	125-250	200	0.08	0.06	0.05	45	59	48
		400	0.09	0.02	0.02	56	36	32
		600	0.03	0.01	-	50	23	-

Table 5.5 Ash contents of parent sawdust and DTF chars at different operating conditions

Gas atmosphere	Particle size (μm)	Resident time (ms)	Sawdust feed Ash (wt% db)	DTF char Ash content (wt% db)		
N_2				900°C	1100°C	1300°C
	125-250	200	1.2	3.2	7.9	11.6
		400	1.2	7.4	15.4	16.9
		600	1.2	14.8	21.2	24.4
CO_2		200	1.1	6.4	11.5	12.6
	125-250	400	1.1	8.2	19.3	21.3
		600	1.1	17.4	21.8	

On the other hand, the ash content of the chars increased with increasing temperature and residence times due to concentration of the ash forming inorganics. Using the conventional ash tracer method, the volatiles yields were found to increase with increasing temperature.

However, it was necessary to assess the applicability of the ash tracer method to calculate volatile yields for highly reactive biomass sample especially at high temperatures. To do this, the volatile yields obtained using ash tracer was compared to the volatile yields using the mass of char collected at the end of the runs and the results are presented in Tables 5.6 and 5.6. From the comparison of the results in Tables 5.6 and 5.7, it might be possible that the use of the ash tracer method may be under estimating volatile yields and using mass of char collected may also be over estimating volatile yields.

Table 5.6 Comparison of sawdust DTF volatile yields in 99% N_2/1 % O_2 and mass of char collected

Sawdust	Conversion by ash tracer (wt% daf)			Conversion by mass of char collected (wt% total volatile)		
Resident time	900°C	1100°C	1300°C	900°C	1100°C	1300°C
200ms	63	86	91	77	89	93
400ms	85	93	94	89	95	98
600ms	93	96	96	96	98	99

Table 5.7 Comparison of sawdust DTF volatile yields in 99% CO_2/1 % O_2 and mass of char collected

Sawdust	Conversion by ash tracer (wt% daf)			Conversion by mass of char collected (wt% total volatile)		
Residence time	900°C	1100°C	1300°C	900°C	1100°C	1300°C
200ms	83	91	92	92	94	95
400ms	86	95	96	92	98	98
600ms	94	96	n/a	97	99	n/a

5.4 A NEW METHODOLOGY ESTABLISHED FOR CALCULATING DTF VOLATILE YIELDS FOR LOW ASH SAMPLES

In order to ascertain which explanation will be true for the calculated volatile yields in Tables 5.6 and 5.7, a methodology was developed and validated to allow the calculation of DTF volatile yields where conventional ash tracer method may not be applied with confidence. An artificial ash (silica) was used as a tracer, adopting method used by Ballantyne et al (2005).

5.4.1 *Experimental*

The particle size of the silica used was the same as the sawdust particle size (125-250 μm). The mass loss of the silica at high temperature was tested in the TGA before carrying out the DTF experiments. About 5 mg of silica was added to the TGA crucible and heated to 110°C at 50°C/min in nitrogen to remove moisture. It was then heated to 800°C at 50°C/min in air and held for 30 min till no further weight loss. From the TGA analysis, the silica was found to retain 90.48% of its weight.

For the DTF test, the silica was heated to 800°C in a muffle furnace and kept for 4hr. it was found that the silica also retained 90.30% of its weight. To ensure that the DTF experiment did not lead to further weight loss in the silica sample, 5-10 mg of the oven dried silica was heated in the TGA to 800°C in air and held for 30 minutes. There was no weight loss observed. Again, 2 g of the oven dried silica was feed into the DTF at 1300°C and 600 ms in nitrogen and CO_2 respectively and there was no further weight loss. This means that the silica was adequate as an external ash for this test. For each DTF run, the dried silica and sawdust mixture was prepared (10/90 wt%) and thoroughly mixed with using

spatula before feeding into the DTF. The feed ash content (silica/sawdust) was determined using standard ash determination procedures in a muffle furnace at 550°C. The DTF volatile yields for the silica ash tracer method were calculated using equation 5.2.

$$V_{DTF} = \frac{10^4 \times (A_1 - A_f)}{A_1 \times (100 - A_f)} \quad (\%\ \text{daf}) \qquad (5.2)$$

Where A_1 is the ash content of the silica/sawdust DTF char (wt% dry basis), A_f is the ash content of the initial silica/sawdust feed as determined from the muffle furnace (wt% dry basis).

5.5 COMPARISON OF VOLATILE YIELDS BETWEEN TOTAL ASH TRACER, SILICA TRACER AND MASS OF CHAR COLLECTED

Figures 5.1 and 5.2 present the volatile yields of sawdust using silica as a tracer in comparison to the results obtained previously using total ash and mass of char collected. From Figures 5.1 and 5.2, it can be seen that at 1100°C in N_2 and CO_2, the volatile yields obtained at all residence times using the silica tracer method was comparable to the volatile yields obtained using the total ash as tracer. This suggested that due to low ash volatilisation at that temperature, the ash tracer method could be used to evaluate the volatile yields. However, at 1300°C (Figures 5.3 and 5.4) for all residence times in N_2 and CO_2, the volatile yields obtained with the silica method were higher than the values obtained using the conventional ash tracer method and lower than the values obtained using the mass of char collected. This suggested that at higher temperatures where some ash forming metal volatilisation occurred, the ash tracer method would not be applied with confidence to calculate DTF volatile yields of low ash biomass samples.

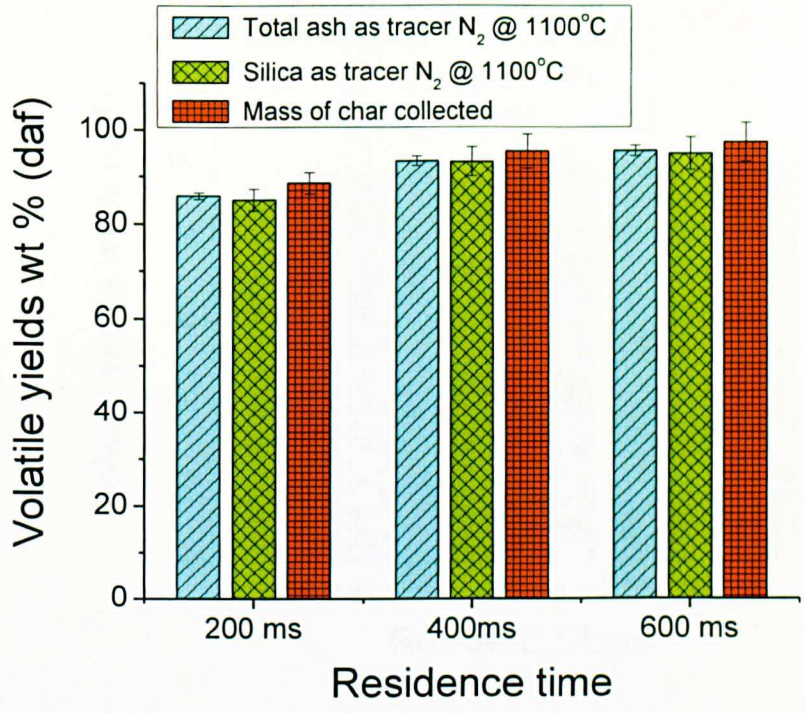

Figure 5.1 Comparing volatile yields using total ash, silica and the mass of char collected at the end of the experiment in 99% N_2/1% O_2 at 1100°C

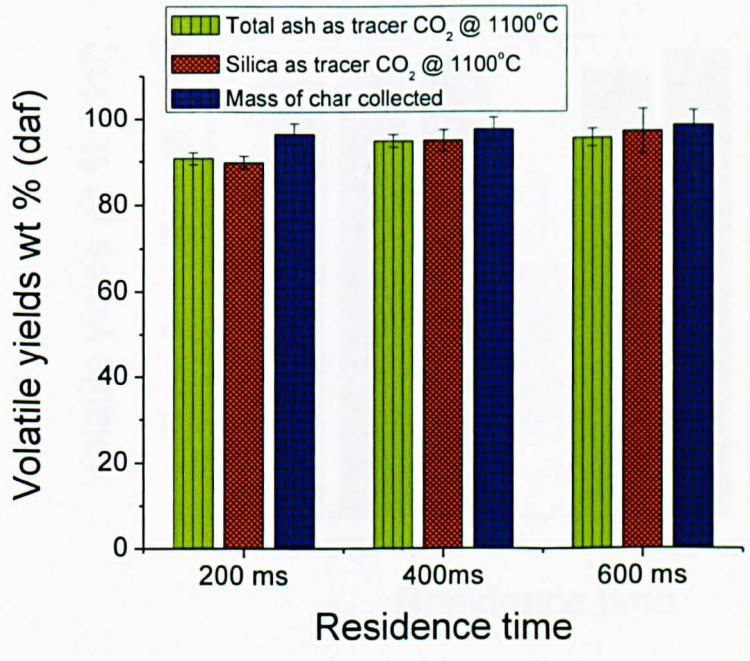

Figure 5.2 Comparing volatile yields using total ash, silica and the mass char collected at 99% CO_2/1% O_2 at 1100°C

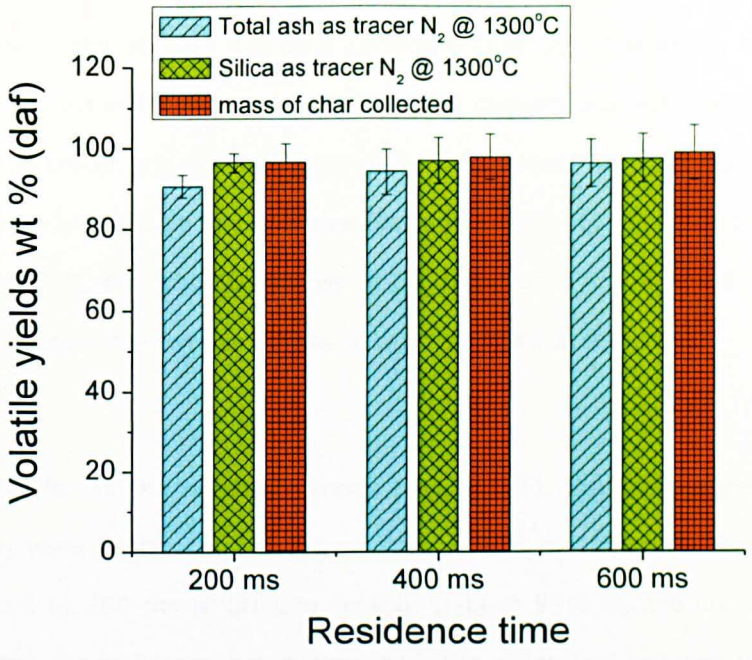

Figure 5.3 Comparing volatile yields using total ash, silica and the mass char collected at the end of the experiment in 99% N_2/1% O_2 1300°C

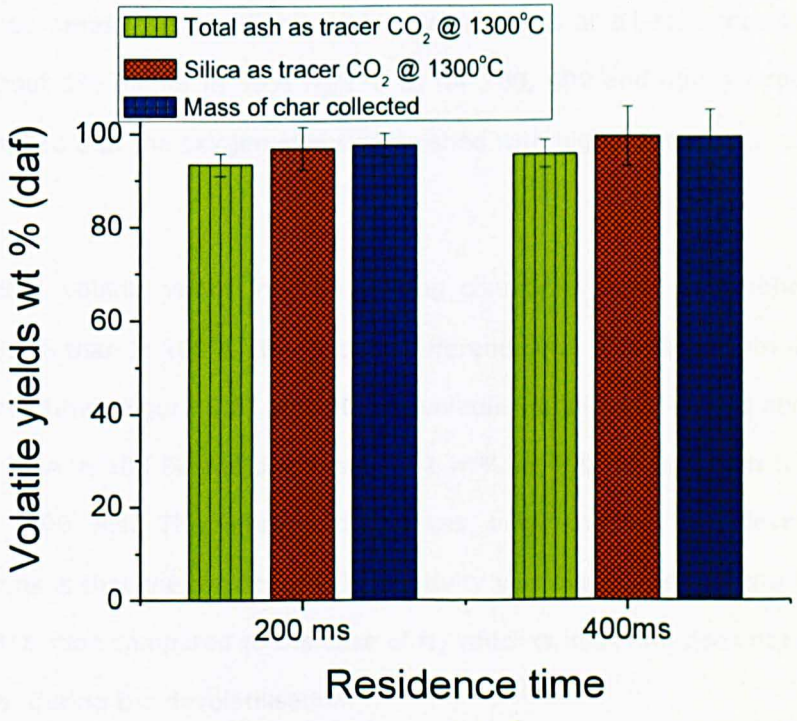

Figure 5.4 Comparing of volatile yields using total ash, silica and the mass of char collected at 99% CO_2/1% O_2 at 1300°C

Next of interest was to investigate the effect of carrying out DTF devolatilisation of sawdust under slightly oxidising condition (1% O_2). Therefore, experiments were carried out in 100% N_2 or CO_2. First, the conversions were calculated using total ash as tracer and secondly, using the silica tracer method. Figures 5.5 and 5.6 compare the volatile yields of sawdust under 99% N_2/1% O_2 and 100% N_2 at 1100°C for 200, 400 and 600 ms using the total ash tracer method. Figures 5.7 and 5.8 compare the two conditions using the silica tracer method.

At 1100°C for all the residence times (Figure 5.5), the volatile yields in 99% N_2/1% O_2 were slightly higher than volatile yields in 100% N_2. This was more pronounced at 200 ms where the volatile yield in 99% N_2/1% O_2 was about 8 wt% higher. As residence times increased, the difference reduced to about 2.5 and 2 wt% higher for 400 ms and 600 ms respectively than in 100% N_2. These results demonstrated that the 1% O_2 concentration used during devolatilisation contributed to higher weight loss of the sample. However, at 1300°C for all the residence times, the trend changed. Volatile yields at all residence times were only about 1% higher in 99% N_2/1% O_2 for 200, 400 and 600 ms respectively. This implied that the oxygen effect diminished with higher temperatures.

At 1100°C volatile yields in the oxidising conditions were also higher in 99% CO_2/1% O_2 than in 100% CO_2, but the difference also decreased with increase in residence time (Figure 5.6). At 200 ms, volatile yield in 1% O_2 was about 5 wt% higher than in 100 % and decreased to 2 wt% at 400 ms and then to less than 1% at 600 ms. The smaller differences between the two devolatilisation conditions is that the impact of CO_2 reactivity was also evident in the 100% CO_2 devolatilisation compared to the case of N_2 which is inert and does not react with the char during the devolatilisation.

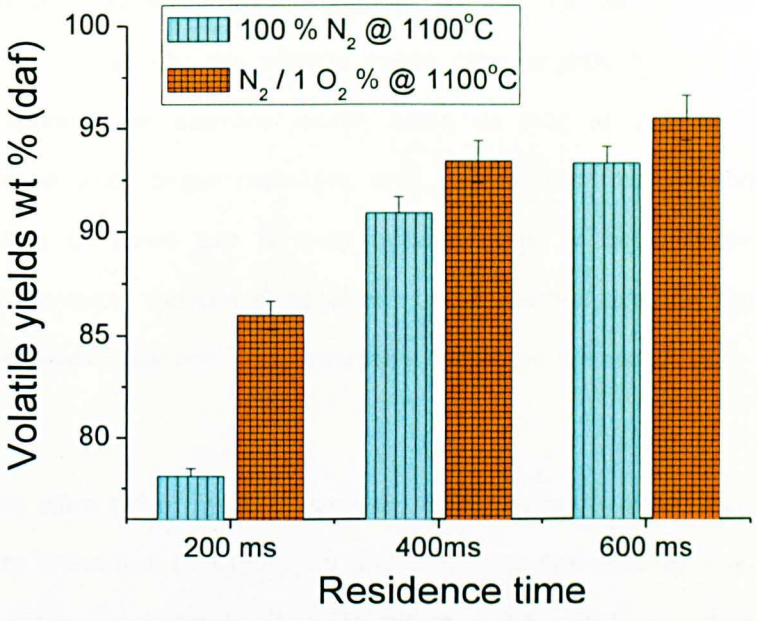

Figure 5.5 Comparison of DTF Volatile yields in 99% N_2/1% O_2 and 100% N_2 atmospheres at 1100°C using total ash tracer

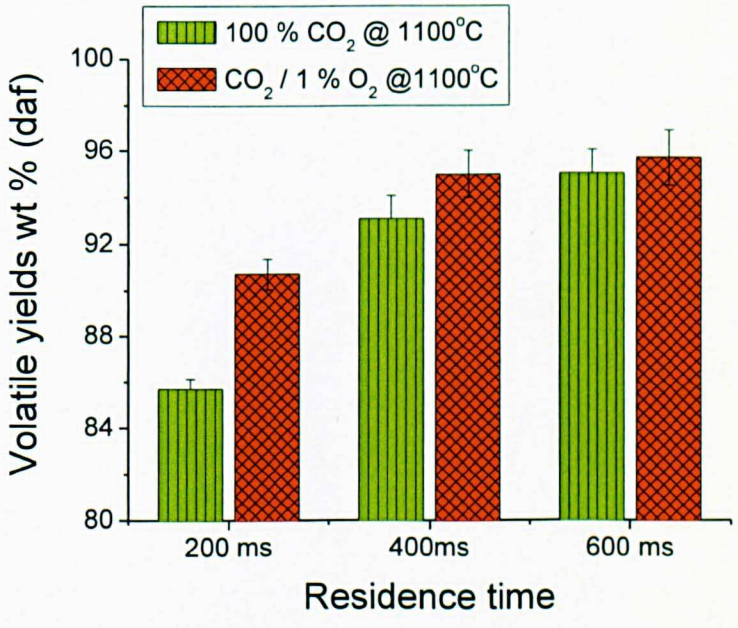

Figure 5.6 Comparison of DTF Volatile yields in 99% CO_2/1% O_2 and 100% CO_2 atmospheres at 1100°C using total ash tracer

Volatile yield in 100% N_2 and CO_2 were also lower than in 1% O_2 at 1300°C and for all residence times as seen in Figures 5.7 and 5.8. However, at 1300°C for 400 ms in Figure 5.8, the volatile yields were slightly higher in 100% CO_2 devolatilisation. One possible reason could be that at 1300°C with 1% O_2 concentration and longer residence time, there could be possible enhanced volatilisation of some ash forming minerals due to both oxygen and CO_2 reactivity. As such, the conventional ash tracer method used for the calculation of volatile yields could not have accurately measured the conversion.

Hence, the silica tracer method was used to calculate the volatile yields and the results are presented in Tables 5.8 and 5.9. From the results, it was observed that the ash tracer method still underestimated DTF volatile yields and the using mass of char collected also overestimated it. The silica tracer method estimated acceptable values for both atmospheres. From the results obtained using the silica tracer method for both 100% gas and in oxidising conditions, it was apparent that the maximum DTF volatile yield for sawdust was between 96-97 wt% on dry and ash free basis in N_2 and between 96-98 wt% in CO_2.

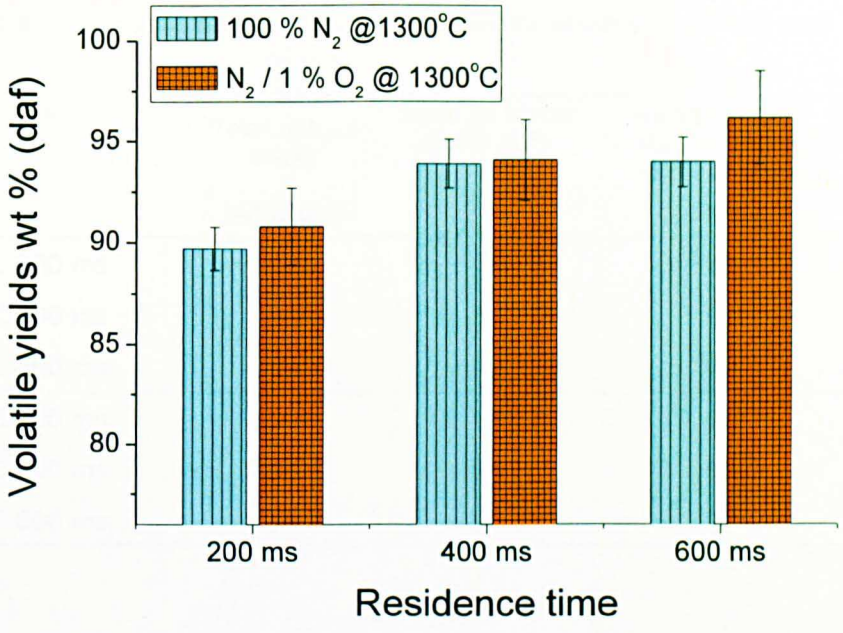

Figure 5.7 Comparison of DTF Volatile yields in N_2/1% O_2 and 100% N_2 atmospheres at 1300°C using total ash tracer

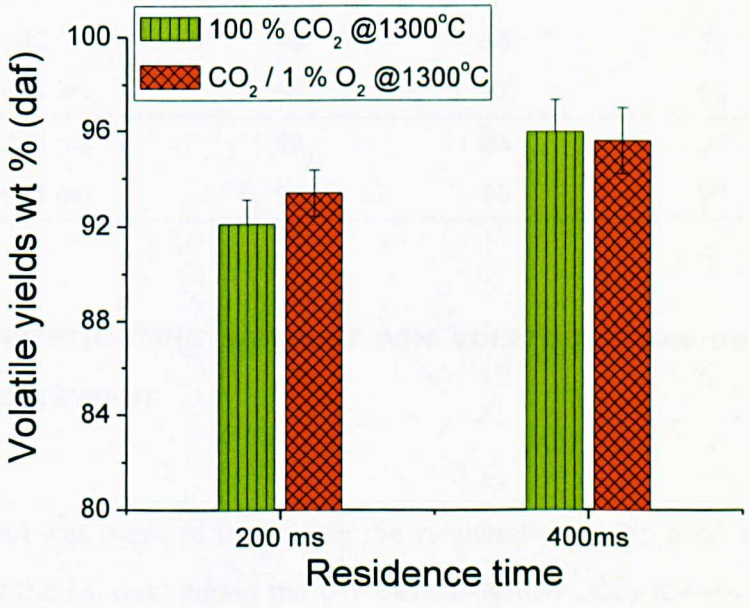

Figure 5.8 Comparison of DTF Volatile yields in 99% CO_2/1% O_2 and 100% CO_2 atmospheres at 1300°C using total ash tracer

Table 5.8 DTF volatile matter yields in nitrogen for sawdust (125-250 μm)

100% N_2	Total ash as tracer (wt% daf)	Silica as tracer (wt% daf)	Using mass of char collected without silica (wt% daf)
1100°C 200 ms	78	78	89
1100°C 400 ms	91	94	96
1100°C 600 ms	93	96	97
1300°C 200 ms	93	96	95
1300°C 400 ms	94	96	97
1300°C 600 ms	94	97	97

Table 5.9 DTF volatile matter yields in CO_2 for sawdust (125-250 μm)

100% CO_2	Total ash as tracer (wt% daf)	Silica as tracer (wt% daf)	Using mass of char collected without silica (wt% daf)
1100°C 200 ms	86	88	93
1100°C 400 ms	93	96	98
1100°C 600 ms	95	97	98
1300°C 200 ms	92	96	97
1300°C 400 ms	96	98	99

5.6 INVESTIGATING SAWDUST ASH VOLATILISATION DURING DTF EXPERIMENT

An attempt was made to investigate the volatilisation of the alkali and alkaline metals of the sawdust during the DTF devolatilisation using ICP-MS. Table 5.10 presents the alkali and alkaline metals contained in the ash of sawdust sample

while Tables 5.11 and 5.12 are the results of the metals contained in the DTF chars produced in nitrogen and CO_2 respectively calculated on the basis of the starting biomass. In Tables 5.11 and 5.12, it was observed that at 200 ms and for all the temperatures, Na appeared to be more concentrated than in the starting biomass. One possible reason is that the distribution of the different elements in the char may be different and taking a portion of the char may vary the elemental composition. Teixeira et al (2011) studied the elemental balance and partitioning in ash stream of biomass and biomass/coal blends in a fluidised bed and observed that the recovery ratios for some ash forming elements were higher.

Despite the uncertainties in over quantification, the decrease in the concentration of the alkali and alkaline elements with increasing temperature and residence time observed in Tables 5.11 and 5.12 suggested that volatilisation occurred. Furthermore, the low concentration of the metals at 1300°C and 600 ms in Tables 5.11 and 5.12 also indicated that there could be uncertainties in carrying out mass balance based on starting sawdust. This is because high volatile matter yields or low char yields can lead to systematic errors. This is clearly seen in Tables 5.8 and 5.9 where less than 10% char yields led to on underestimation of volatile matter yield using the ash tracer method.

Table 5.10 Alkali and alkaline earth metals present in raw sawdust sample

Elements	concentration wt% based on raw sawdust
Na	0.12
Mg	0.09
K	0.21
Ca	0.75
Al	0.04
Fe	0.04

Table 5.11 ICP-MS results showing alkali and alkaline-earth mineral contents retained in sawdust DTF chars in nitrogen atmosphere based on starting biomass (wt% per mass of biomass fed, as received basis)

Elements	200 ms			400 ms			600 ms		
	900°C	1100°C	1300°C	900°C	1100°C	1300°C	900°C	1100°C	1300°C
Na	0.69	0.32	0.17	0.27	0.10	0.08	0.12	0.06	0.06
Mg	0.21	0.13	0.05	0.10	0.05	0.05	0.06	0.03	0.02
K	0.20	0.11	0.11	0.16	0.13	0.10	0.15	0.08	0.02
Ca	0.87	0.60	0.36	0.62	0.40	0.43	0.45	0.36	0.22
Al	0.02	0.01	0.01	0.01	0.00	0.00	0.02	0.02	0.01
Fe	0.03	0.02	0.01	0.02	0.01	0.01	0.01	0.01	0.01

Table 5.12 ICP-MS results showing alkali and alkaline-earth mineral contents retained in sawdust DTF chars in CO_2 atmosphere based on starting biomass (wt% per mass of biomass fed, as received basis)

Sample	200 ms			400 ms			600 ms	
	900°C	1100°C	1300°C	900°C	1100°C	1300°C	900°C	1100°C
Na	0.31	0.17	0.15	0.24	0.08	0.09	0.09	0.04
Mg	0.12	0.07	0.07	0.09	0.03	0.07	0.05	0.04
K	0.22	0.14	0.15	0.15	0.11	0.11	0.12	0.06
Ca	0.75	0.45	0.54	0.56	0.28	0.66	0.35	0.31
Al	0.02	0.02	0.01	0.00	0.00	0.01	0.00	0.00
Fe	0.01	0.01	0.01	0.01	0.02	0.01	0.01	0.01

5.7 CONCLUSIONS

1. A new methodology has been developed for the determination of biomass volatile matter yields in the DTF. The method used the principle of the conventional ash tracer method by adding silica to mix with the sawdust feed to give high accurate measure of volatile matter yields.

2. The volatile contents obtained with silica at 1300°C were between the values obtained from the ash tracer method and those obtained based on the mass of char collected from each experimental run. This suggested that conventional ash tracer method will underestimate high temperature volatile yield for biomass samples.

3. Devolatilisation in 100% N_2 exhibited slightly lower volatile matter yields than that carried out in 99% N_2/1% O_2. This implied that oxygen reactivity contributed to higher volatile yields. In the case of CO_2, the differences between the two conditions were smaller than the values observed for N_2 devolatilisation.

4. Studying sawdust elemental mass balances for the alkali and alkaline earth metals during the DTF experiments gave some uncertainties. However, the decrease in concentration of alkali and alkaline metals with increasing temperature is an indication that volatilisation occurred.

6 COMPARATIVE STUDY OF THE TGA COMBUSTION REACTIVITY OF SAWDUST CHARS PRODUCED BY TGA AND IN THE DTF

6.1 SUMMARY

Thermogravimetric analysis (TGA) has been widely used to obtain combustion reactivity data for solid fuels. However, fundamental information relating such data to systems that operate under conditions closer to those encountered in industrial-scale pulverized combustion – such as a drop tube furnace (DTF) is scarce, especially for certain types of biomass. This chapter therefore compares the TGA combustion reactivity of TGA and DTF devolatilised sawdust chars. The implications of devolatilisation temperature, heating rate and residence time were considered. It was observed that the TGA burnout profile of the 1300°C and 600 ms DTF char was similar to the 700°C TGA char and these two chars consequently formed the basis of the subsequent comparison. However, during combustion, the DTF char showed a lower maximum rate of mass loss than the TGA char. This might be due to the differences in heat treatment during devolatilisation. Examining the scanning electron microscope (SEM) images revealed that the TGA chars retained a cell matrix structure with a visible macropore network. In contrast, the DTF chars displayed swollen surfaces with distributed pore networks, resulting in higher BET surface areas. The activation energy of the DTF char was smaller than that of TGA char, demonstrating the presence of greater internal diffusion control during TGA burnout. Finally, a reproducibility and repeatability study of the char production methods was also undertaken. Char from the DTF was thus found to be significantly more variable than that from the TGA, probably because of the large number of process variables involved in its operation. The variation between Activation energy and

the log of the pre-exponential factor for sawdust char burnout was found to be less than coal char burnout signifying that at low temperatures, sawdust would burn somewhere closer to intrinsic kinetic control regime than coal.

6.2 INTRODUCTION

Thermo-gravimetric analysers (TGA) and drop tube furnaces (DTF) have been widely used to study the combustion behaviour of solid fuels and their chars. Whether TGA combustion reactivity of solid fuels can be correlated with their DTF counterparts is essential for the application of TGA parameters in industrial scale pulverized fuel (pf) combustion systems. This is because the high temperatures and relatively short heat treatment times experienced in a pf combustion system could influence char morphology and hence intrinsic char combustion reactivity may differ. Nevertheless, the fundamental information obtained from the TGA combustion profiles can be used for an initial evaluation of the combustion behaviour at the industrial scale.

For biomass fuel, it is overly important to understand the TGA fundamental char combustion reactivity data and extrapolate to systems that simulates closely to industrial boilers for design and optimization of biomass fired boilers because of the wide spread use of biomass for co-firing in pf systems for power generation (Basu et al., 2011, Berggren et al., 2008) and the subsequent movement towards 100% biomass fired boilers (Bain et al., 1998, Demirbas, 2005, van den Broek et al., 1996). The reason is that biomass firing is considered as an environmentally safe way of providing energy (Narodoslawsky and Obernberger, 1996) and thereby decarbonizing the energy sector (Ekins, 2004) while co-firing is aimed at reducing greenhouse gas emissions (Domenichini et al., 2011, Huang et al., 2006, McIlveen-Wright et al., 2011) in order to meet low emission

target. Although there is wide difference between its operating conditions and those in industrial setup, TGA provides a simple, cheap, fast, small-scale and reliable way of obtaining the burnout profiles of fuels (Aboulkas et al., 2008, Otero et al., 2008, Park et al., 2009, Varol et al., 2010).

In char reactivity studies, the isothermal method is mostly used for reactivity data analysis because it is straightforward (Sima-Ella et al., 2005b). On the other hand, the non-isothermal method in which the sample is linearly heated is quicker but more complicated in reactivity data analysis (Sima-Ella et al., 2005b). This analysis is carried out under different conditions (e.g. temperature, heating rate, residence time and gas atmosphere) and it can therefore provide results relevant to any fuel combustion system (Miranda et al., 2008).

These operating conditions determine the rate controlling steps during combustion such that when the reactant gas is able to diffuse easily into the reacting surface through the pore network without instantly reacting, then regime I condition is prevailing, to where pore diffusion control have comparable control (regime II) and finally to completely mass transfer restricted regime (regime III) where reaction takes place at the external surface of the char (Jess and Andresen, 2010, Szekely et al., 1976). On the other hand, DTF and other entrained flow reactors operate more closely to the conditions prevailing in an industrial process with short resident times, high temperature and heating rates (Biswas et al., 2006). Such operating conditions also influence structural changes in the char during devolatilisation (Cloke et al., 2003, Yu et al., 2007).

Some studies in the past have investigated the combustion reactivity of biomass chars under conditions that are relevant to industrial systems. For example, Adanez et al (2001) investigated the combustion reactivity of biomass char in

TGA and compared it to that of a fluidized bed combustion (FBC) system. The results revealed that the extrapolation of the TGA reactivity data to the FBC was difficult because of the structural differences exhibited by the chars during combustion. However, the chars were devolatilized in different equipment prior to the actual experiment. Wornat et al (1996) investigated the combustion rate of biomass char in an entrained flow reactor at 12 mole% O_2 and gas temperature of 1600°K. It was observed that the burning rate of the char decreased as conversion proceeded due to the removal of reactive carbon and the catalytic inorganic metals. This study only considered the overall burning rate of the char. Furthermore, Meesri et al (2003) carried out sawdust char combustion in a DTF at 10 mole% O_2 and 1473K. The results revealed that sawdust char combustion took place under regime II, dominated by chemical reaction and diffusion control limitation. Again, this study only gave the reactivity data of sawdust char in the DTF without considering the relevance of TGA fundamental data to pf combustion conditions.

Previous work at the University of Nottingham conducted a comparative TGA study of the combustion reactivity of TGA and DTF devolatilized chars from a single bituminous coal (Le Manquais et al., 2009). During this, it was observed that optimised devolatilisation procedures could be used to generate corresponding TGA burnout rates between the two char types for particle size ranges of <75 μm. But, with larger particles, a reactivity divergence was evident and the TGA chars became less combustible than their DTF counterparts. Scanning electron microscope (SEM) images and internal BET surface areas indicated that this was because of incompatible char morphologies. Thus, while chars produced under the conditions of TGA pyrolysis strongly resembled raw coal and displayed an undeveloped pore network; the DTF chars were highly porous and extensively swollen.

As a result of the findings and because of the increasing popularity of biomass as a fuel for power generation, (Chiaramonti et al., 2007, Evans et al., 2010, Moon et al., 2011, Pihl et al., 2010, Tous et al., 2011), there is merit in performing an equivalent investigation with different forms of biomass. This study therefore compares the combustion reactivity of TGA and DTF sawdust chars and the effect of devolatilisation conditions on char combustion behaviour is examined. The combustion characteristics of the chars are explained in terms of their burnout characteristics, physical properties such as char morphology, structural features and porosity. Reproducibility and the repeatability of the char production methods are examined to assess the possible errors associated with the data spread. Since fuel particle size influences the devolatilisation behaviour and the subsequent char morphology, the effect of particle size was also investigated. Finally, the reaction regime and the reactivity of the chars are investigated in terms of activation energy and pre-exponential factors.

6.3 EXPERIMENTAL PROCEDURES

6.3.1 *Samples*

The biggest particle size (125-250 μm) used for this comparison for the reasons stated in chapter 5. The properties of this particle size fraction are given in Table 4.1.

6.3.2 *TGA*

Details of method used are described in section 3.2.2.3. The model equations used to obtain kinetic parameters are also described in 3.2.2.6.

6.3.3 *DTF*

DTF chars were produced at devolatilisation temperature of 1300°C, 200, 400 and 600 ms using the method described in section 3.4.1.

6.4 COMPARISON OF DEVOLATILISATION PROCEDURE

It was difficult directly to compare TGA and DTF chars because, although conventional TGAs can easily achieve the temperatures of a PF boiler, heating rates are only hundreds or thousands of degrees Celsius per minute, whereas tens or hundreds of thousands of degrees Celsius per minute can be achieved on the DTF or in an industrial PF system. However, some interesting observations can be made by creating DTF and TGA chars that ostensibly appear to have comparable TGA burnout profiles. To do this, it was first necessary to alter the TGA devolatilisation heating procedure so that it produced chars with burnout profiles matching those from the DTF. DTF devolatilized chars were produced at 1300°C using 200, 400 and 600 ms residence times and these were compared with TGA devolatilized chars at 700, 900 and 1100°C. The reaction rate constants and 90% carbon conversion time of the TGA and DTF chars are presented in Table 4.

It was observed that char produced at 200 ms was more reactive, having a shorter burnout time and a higher combustion rate. As residence time increased, the reactivity of DTF char reduced indicating that the char has undergone thermal annealing and deactivation. On the other hand, the TGA chars showed decreased reactivity at higher temperatures, signifying that char deactivation was also dependent on the severity of the heat treatment. From these results, the reactivity 700°C TGA char was found to be similar to 1300°C, 600 ms DTF

char and this suggested that 700°C TGA char and 600 ms DTF chars might form a suitable basis for further comparison. The burnout profiles of the TGA and the DTF devolatilised chars are presented in Figure 6.1.

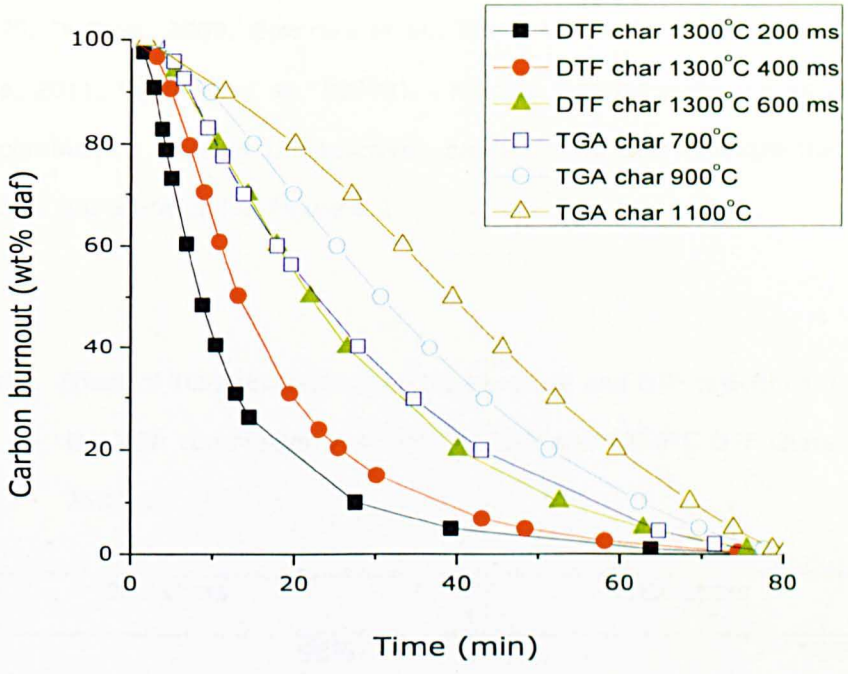

Figure 6.1 Carbon burnout profiles of TGA chars at different devolatilisation temperatures and DTF chars at different heating rates

From Table 6.1, it is evident that the 200 and 400 ms 1300°C DTF chars are more reactive than the 700°C TGA char, exhibiting faster burnout times. This could be as a result of the 1% oxygen introduced into the system during the DTF devolatilisation which might have activated the char and enhanced accessibility of oxygen into the char active sites. Another possible reason could be that due to the short residence times experienced in 200 and 400 ms, incomplete devolatilisation could take place. This would have led to residual hydrogen being retained in the chars (Le Manquais et al., 2009). However, at 1300°C 600 ms,

the DTF char reactivity was similar to that of the TGA 700°C char. Higher devolatilisation in the TGA produced chars that were less reactive than the DTF chars indicating char deactivation or thermal annealing effect. This effect usually reduces the accessibility of oxygen into the active sites of the char due to structural modification of char and hence loss of combustion reactivity (Cai et al., 1996, Di Blasi, 2009, Guerrero et al., 2005, Lu et al., 2002, Senneca and Salatino, 2011, Senneca et al., 2007b). . Next, it was necessary to assess the chars' combustion rates or the reactivity profiles to further evaluate the chars and results are presented in Figure 6.2.

Table 6.1 Effect of TGA devolatilisation temperature and DTF residence time on the TGA combustion reactivity of TGA and 1300°C DTF chars (125-250μm).

DTF chars			TGA chars		
Residence time (ms)	1st order rate constant	90% carbon burnout time	Temp °C	1st order rate constant	90% carbon burnout time
200	0.079	27.6	700	0.056	48.5
400	0.067	36.9	900	0.044	62.6
600	0.051	52.6	1100	0.045	61.7

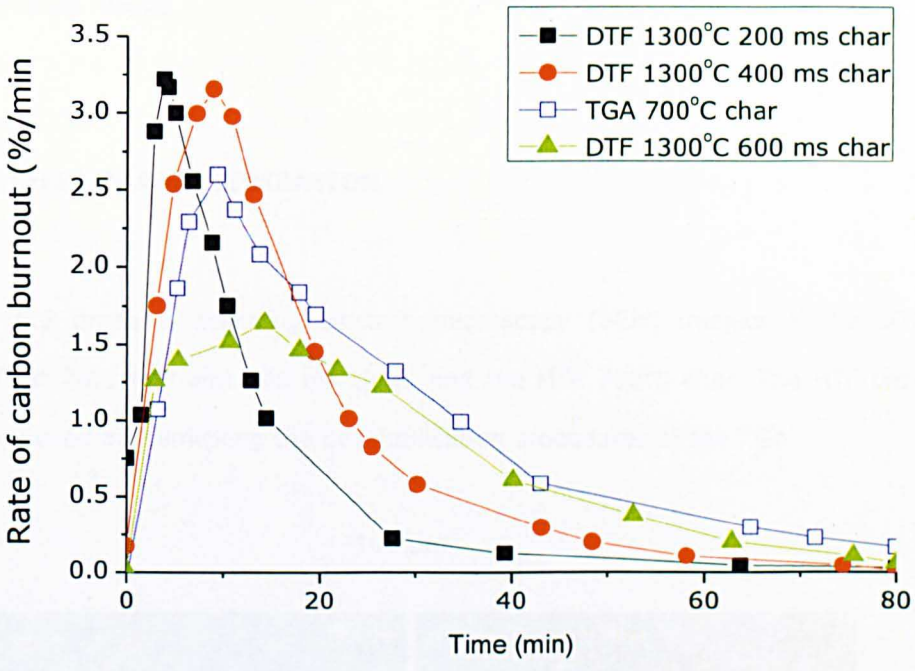

Figure 6.2 Rate of carbon burnout at 375°C for TGA 700°C char and 1300°C DTF chars at different residence times

Figure 6.2 shows the maximum rates of weight loss of DTF chars compared to their TGA counterpart. The 200 and 400 ms chars exhibited faster instantaneous burnout rates while the 600 ms char exhibited the smallest burnout rate with the slowest burnout pattern. Surprisingly, the combustion rate of TGA 700°C char, which had a similar burnout profile to the 600 ms DTF char in Figure 6.1, had a much higher peak combustion rate though the rate was slightly slower at the later end of the combustion. Firstly, this could be as a result of alterations to the physical structure of the char obtained from the unequal heating rates experienced by the samples during devolatilisation. Another possible reason is that since devolatilisation is likely to be incomplete in the TGA devolatilisation, volatiles could be retained in the char and burnt early in the subsequent combustion. Thirdly, the DTF 600 ms char would have been deactivated due to the longer residence time experienced during the heat treatment. Further

analyses were therefore required to understand the morphological changes behind these results.

6.5 CHAR CHARACTERIZATION

Figure 6.3 presents scanning electron microscopy (SEM) images of the DTF 1300°C at 200, 400 and 600 ms chars and the HTF 700°C char. The HTF char was produced by mimicking the devolatilisation procedures of the TGA.

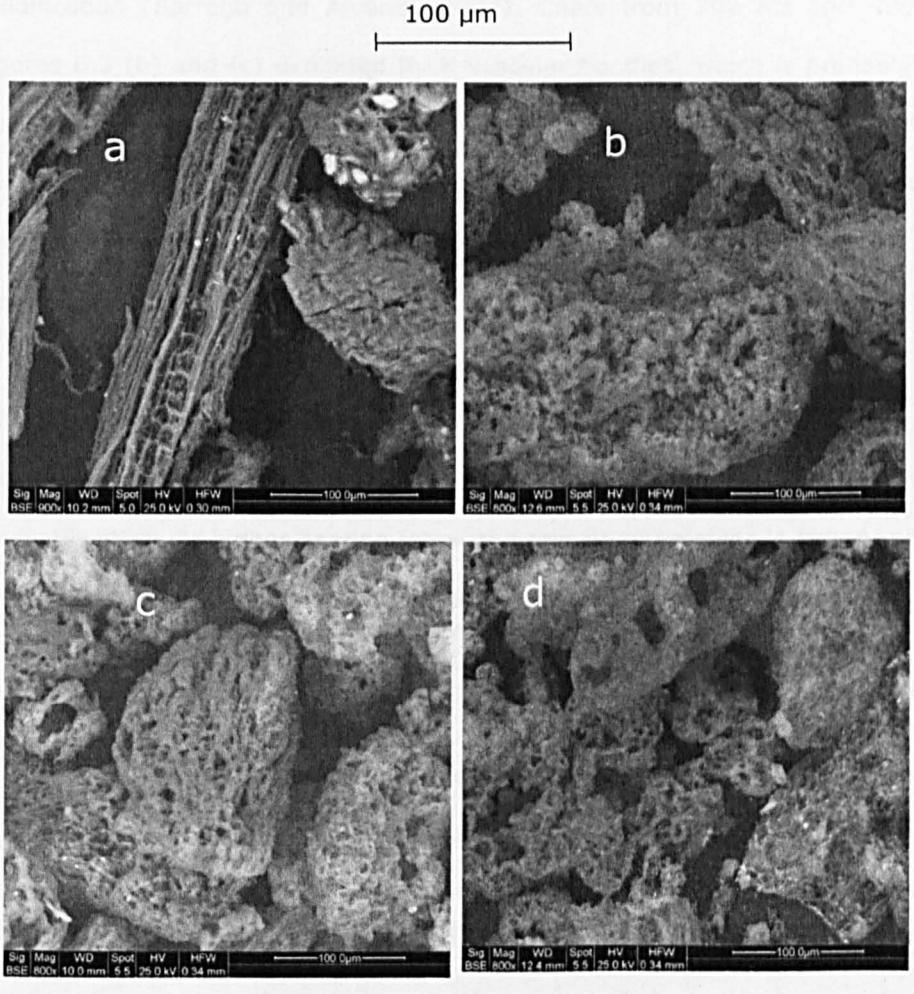

Figure 6.3 SEM images of sawdust chars obtained at devolatilisation (a) HTF 700°C at 150 °C/min and DTF 1300°C for (b) 200 ms, (c) 400 ms and (d) 600 ms.

The char produced at 700°C in HTF, Figure 6.3 (a), did not experience much melting and/or swelling. The fibrous nature of the cells is clearly visible, but there are some evident cavities along the cell structure. This is probably due to some form of degassing or the release of volatile matter through the pores (Cetin et al., 2004). However, in Figures 6.3 (b) to (d), there is significant variation in the structure of the DTF devolatilized chars. The sawdust's cellulose structure was completely melted and the cells have lost their fibrous nature and structural distinction due to swelling, melting, rearrangement and re-solidification (Borrego and Alvarez, 2007). Chars from 200 ms and 400 ms, Figures 6.3 (b) and (c) exhibited thick vascular bundles, which is probably as a result of the melting and fusing of particles (Cetin et al., 2004, Joyce et al., 2006). They are irregular in shape with an abundance of pores, again due to degassing. The 600 ms char has similar characteristics, but exhibited an even more porous surface.

The differences in morphology of the TGA and DTF devolatilized chars are as a result of the differences in heating rates experienced by the samples during devolatilisation. At higher heating rates, the release of volatiles is faster and this could lead to the chars possessing larger surface areas with a higher availability of actives sites though thermal annealing is likely to occur.

A cross-sectional porosity assessment of the chars is needed to provide a better understanding of the changes that occurred to the sawdust's internal char structure. Hence, Table 6.2 presents the BET surface areas of HTF char produced at 700°C and the DTF char produced at 1300°C and 600 ms. In Table 6.2 the BET surface area of the DTF char is greater than that of the HTF char. This is as expected, because due to rapid heating and the subsequent loss of volatile matter, the DTF chars would possess a greater population of pores and, as such,

larger internal surface areas. This indicates that the larger BET surface area exhibited by the DTF char could also be due to a potential activating effect from the 1% oxygen used during devolatilisation. However, this did not translate into higher maximum burnout for the DTF char probably due to thermal annealing caused by char structural ordering during the heat treatment (Lu et al., 2002).

In addition, cross-sectional optical images of the chars are displayed in Figure 6.4. Images a, b and c are DTF chars from 1300°C for 200, 400 and 600 ms respectively. They have well developed pore networks because of the fast heating rate and rapid loss of volatiles experienced during devolatilisation. Like industrial coal chars, which do not conform to a single configuration, (Le Manquais et al., 2009) these bio-chars have a combination of porous networks. They mainly consist of type I and II char particles with > 80% and > 50% porosity respectively, (Le Manquais et al., 2009, Yu et al., 2007, Cloke et al., 2003, Sørensen et al., 2000) due to swelling and the extensive release of volatiles. These include cenospheres, tunuisphere, tenuine networks and mesosphere structures. Several degassing vesicles are found in their walls. The 600 ms char also appears to have thinner walls than the 200 and 400 ms chars, which is probably due to more extensive volatile release as a result of longer devolatilisation times.

Table 6.2 BET surface areas of HTF char produced at 700°C, 150°C/min and DTF devolatilized char at 1300°C and 600 ms (125-250 μm)

Sample	BET surface areas (m^2 / g daf)	Pore sizes (nm)
HTF char	322	5
DTF char	339	6

Conversely, image 6.4d shows the HTF sample from 700°C which demonstrates type II and III pore networks with >50% and approximately 50% porosity respectively . The char consists of particles that are not fully devolatilized.

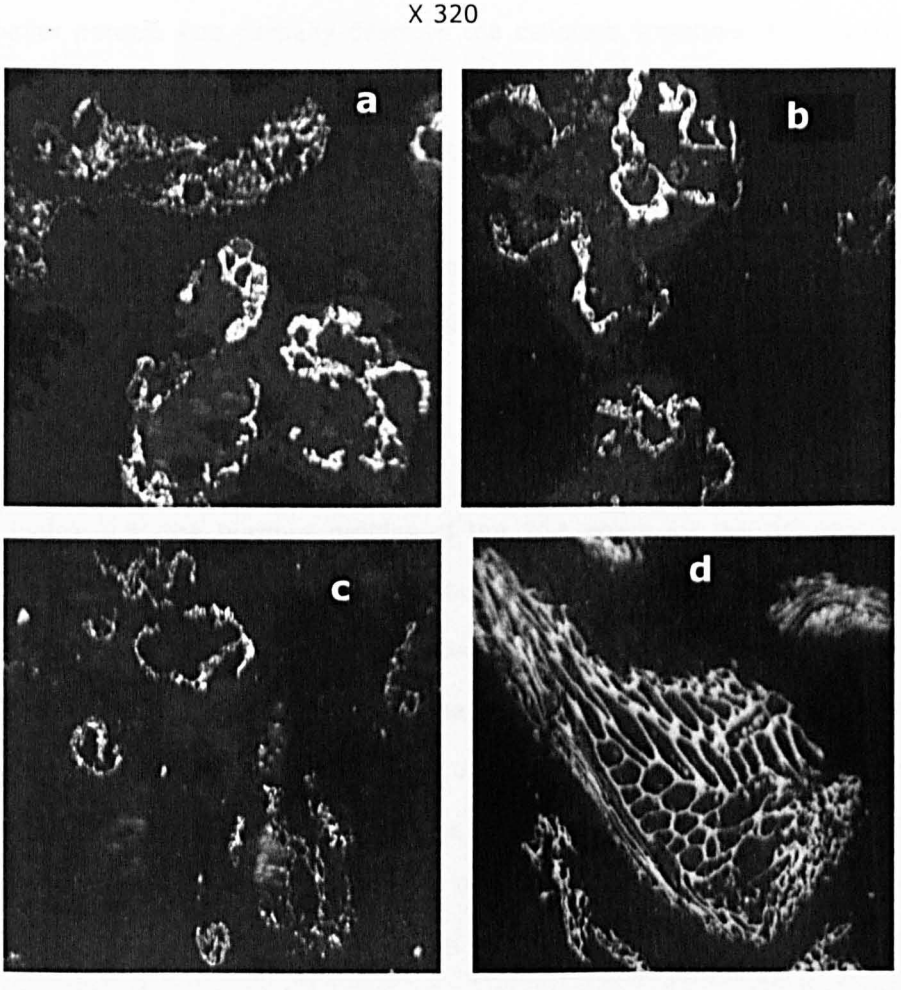

Figure 6.4 Cross sectional optical images of DTF chars showing pore distribution within the char structure at 1300°C (a) 200 ms, (b) 400 ms, (c) 600 ms and (d) HTF 700°C

6.6 INFLUENCE OF PARTICLE SIZE ON COMBUSTION REACTIVITY

Experiments were undertaken to understand the influence of particle size on combustion reactivity. Six particle size fractions were used and their TGA burnout profiles are presented in Figure 6.5. The milling of biomass sample into smaller particle size partially destroys the cellulose structure. This could cause the different particle size fractions to exhibit different characteristics, in particular pore structure, surface area and ash forming elements (Vassilev et al., 2010). During devolatilisation, the intra-particle mass transfer resistance increased with increasing biomass particle size and this can cause variations in char structure (Asadullah et al., 2009) and subsequently, the char burnout propensity.

In Figure 6.5, the burnout profiles of the TGA chars for the different particle sizes are presented. The smallest particle size fraction (<45 μm) was observed to burn faster, having faster burnout time while the biggest particle size fraction (125-250 μm) took slightly longer time to burn out. Nevertheless, even though intrinsic reactivity can be achieved using smaller particle size, the biggest particle size fraction (125-250 μm) was used in the DTF because char yield from the smallest particle sizes would be very small and this would lead to poor reproducibility. Additionally, very small particle size fraction (<45 μm) will lead to bridging and sloughing in the screw feeder of the DTF (Le Manquais et al., 2009).

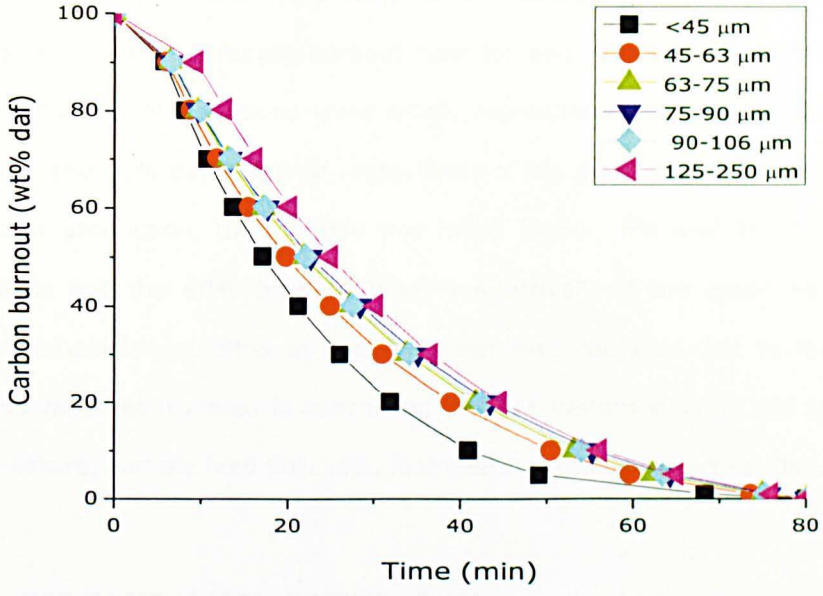

Figure 6.5 TGA char burnout profiles at 375°C of the different particle sizes devolatilized at 700°C, 150°C/min

Table 6.3 Variability of TGA isothermal char burnout at 375°C in terms of standards deviation using single particle size 125-250 μm

Method	Mean		Standard deviation	
	1st order rate constants (min^{-1})	90 % burnout time (min)	1st order rate constants (min^{-1})	90 % burnout time (min)
TGA	0.055	49.4	±0.002	±1.3
DTF	0.050	51.9	±0.001	±4.6

The reproducibility and repeatability of TGA and DTF chars are presented in Table 6.3 in terms of rate constants and 90% carbon burnout. This assessment was carried out to measure the possible errors that could affect the reactivity

data from the two operating regimes. The reproducibility and repeatability of the char production methods were assessed by calculating the standard deviation across results from 3 repeat burnout runs for each process. For the TGA char, the coefficients of variations were small, representing about 3% for the rate constant and 90% burnout time respectively of the mean values recorded. In the DTF char production, the variable was much higher, 3% and 9% for the rate constants and the 90% burnout times respectively of the mean values. The higher variability exhibited by the DTF char rate could be due to the several process variables involved in controlling the DTF system such as gas flow rates, gas pressure, sample feed flow rate, fast heating rate and short residence time.

6.7 TGA COMBUSTION REGIME STUDY

Having established the variability data for both operating conditions, it was important to study the combustion reactivity of the chars. Intrinsic kinetic parameters are obtained when a char burns under chemical control (i.e. reaction regime I); where diffusion and mass transfer resistances are absent. The kinetic parameters were calculated from the slope and intercept of the Arrhenius plot in Figure 6.6. The DTF char, which had a larger BET surface area but lower maximum rate of combustion, has a lower activation energy and pre-exponential factor than the TGA char. This reaffirms that the DTF char has undergone thermal deactivation. The thermal deactivation can be caused by a loss of intrinsic reactivity due to loss of active sites on the char surface or by a loss of surface area that is available for reaction (Tremel and Spliethoff, 2013).

As such, the DTF char combustion is dominated by internal pore diffusion control (regime II). Nevertheless, the activation energy obtained in this study is comparable to that obtained in previous study in a DTF (Meesri and Moghtaderi, 2003). In summary, while pore diffusion is the rate limiting step in the

combustion of the DTF char, leading to burnout under regime II conditions, some form of pore diffusion limitation still controls the rate of TGA char burnout preventing it from burning under true kinetic control regime.

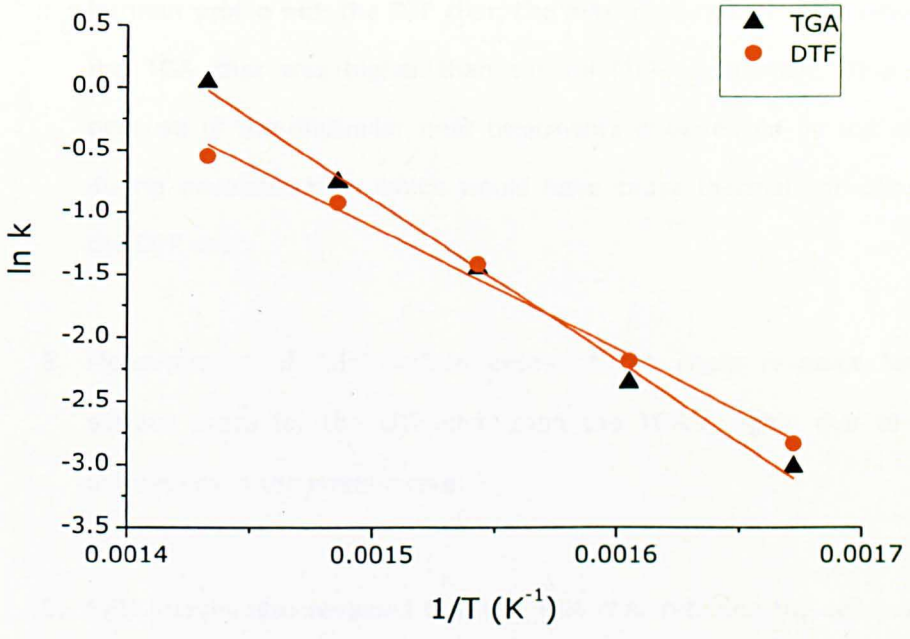

Figure 6.6 Arrhenius plots used to obtain kinetic parameters for TGA and DTF

Table 6.4 Comparison of the Kinetic parameters of TGA char at 700°C, 150°C/min and DTF devolatilized char at 1300°C and 600 ms (125-250 μm)

Operating condition	DTF char			TGA char			
	E	A	R^2		E	A	R^2
1300°C 600 ms	82	8.1×10^5	0.99	700°C	107	1.04×10^8	1.00

6.8 CONCLUSIONS

1. The burnout characteristics of TGA char produced at devolatilisation temperature of 700°C and heating rate 150°C/min correlated with DTF char produce at 1300°C and 600 ms and as such comparison was based on those chars. While the TGA char exhibited somehow similar burnout profile with the DTF char, the maximum rate of combustion of the TGA char was higher than the its DTF counterpart. This was because of the dissimilar heat treatments experienced by the chars during devolatilisation which would have cause thermal annealing in the DTF char.

2. Measurement of BET surface areas of the chars revealed larger surface areas for the DTF char than the TGA's, again due to the differences in the heating rate.

3. SEM images also revealed that the TGA char retained the cell matrix of the parent while the DTF char experienced complete melting of the cellulose structure. Subsequently, optical images analysis of the internal structures of the chars revealed mixed porous chars of type I and II for the DTF chars, having wide pores with thin walls especially the 600 ms char while the HTF char exhibited a mix dense, porous and thick wall with macropore network falling under type II and III char networks.

4. These results suggest that in reality, TGA cannot be used to imitate the devolatilisation characteristics of the DTF due to the lower heating rate. Nevertheless, significant information has been obtained for the application of biomass as a pulverised fuel in biomass fired boilers.

7 IMPACT OF CO_2 ON BIOMASS DEVOLATILISATION, NITROGEN PARTITIONING AND CHAR COMBUSTION IN THE DROP TUBE FURNACE

7.1 SUMMARY

This chapter investigates and presents the results of the devolatilisation and combustion behaviour of sawdust in CO_2 in a drop tube furnace (DTF) compared to conventional air fired condition. The implications of devolatilisation temperature and residence time on volatile yield and char burnout were investigated. Also, the influence of CO_2 on nitrogen partitioning between volatiles and residual char was considered. From the results, it was observed that higher volatile yields were observed in CO_2 compared to nitrogen condition attributable to CO_2-char gasification reaction. The higher volatile yields were pronounced at the early stage of combustion (200 ms) for the devolatilisation temperatures but more pronounced at 900°C. Fuel-N transformation into volatile phase was proportional to volatile yield in both CO_2 and nitrogen conditions. While significant higher volatile yield was obtained at 900°C under CO_2 in DTF than in N_2, lower volatile yield was obtained in TGA under CO_2 than in N_2 indicating the implications of heating rate on CO_2 volatile yield. Scanning electron microscope (SEM) images revealed higher porosity of the CO_2 chars than those of the N_2 chars resulting in the higher internal surface areas exhibited by the CO_2 chars. In DTF re-firing, burnout of sawdust char was observed to be faster in oxy-fired than in air fired condition.

7.2 INTRODUCTION

The power industry is faced with continuous demand to reduce CO_2 emissions from their operations and this has resulted in developing technologies to reduce the emissions. Oxy-fuel combustion is an advancing technology aimed at achieving near zero emissions and the oxy-biomass combustion is a way forward to achieving negative CO_2 emissions in the power industry. This is because biomass is carbon neutral, sustainable and will lead to reduction in net CO_2 emissions (Tous et al., 2011). While different fundamental issues of oxy-fuel coal combustion is being tackled and pilot plants are being tested, little is known about the behaviour of biomass under oxy-fuel combustion.

Few Studies have investigated the pyrolysis and combustion behaviour of some biomass samples using TGA analysers. For instance, The results have shown that at temperatures below 900°C, volatile yield in CO_2 was lower (Yuzbasi and Selçuk, 2011). This is because at such relatively low temperatures, CO_2 behaves as an inert gas. However, higher volatile yields were observed as temperature increased due to CO_2-char gasification reaction. It results of these findings revealed some fundamental information about biomass oxy-fuel condition which can be used for an initial evaluation of the combustion behaviour at the industrial scale.

On the other hand, oxy-coal combustion has been extensively investigated and has given useful information. For example, the fundamental studies carried out by Wall gave an insight into the devolatilisation behaviour of coal under oxy-fuel condition compared to air fired condition (Wall, 2005). Investigation of 4 coals under oxy-combustion revealed that volatile yields were higher than in conventional air fired condition. This gave an insight to further research in the

nitrogen partitioning between volatiles and char and the residual char burnout characteristics under oxy-firing. Sun and Snape (2009) studied the devolatilisation, nitrogen partitioning characteristics and the residual char burnout of 6 coals under air and oxy conditions in drop tube furnace. It was found also that devolatilisation in CO_2 gave notably higher volatile yield at 1300°C 200 ms (5-20 wt %) than in air fired condition. Such higher volatile yield was attributed to the CO_2-char gasification reaction and has also been identified by other researchers (Hahn et al., 2003, Messenböck et al., 1999, Naredi and Pisupati, 2011a, Gil et al., 2012).

For nitrogen partitioning, the results of Sun and Snape (2009) revealed that the release of nitrogen into the volatile phase was proportional to the yield of volatile. However, oxy-firing led to notably higher proportions of Fuel-N in the volatile phase due to higher volatile yield obtained in oxy-fuel condition compared to air fired condition. However, for few of the coals, the release of nitrogen appeared to be retarded slightly under oxy-fuel firing and it was attributed to selectivity of CO_2-carbon gasification reactivity. The increased nitrogen release into the volatile phase in oxy-fuel condition implies that NOx emissions can be potentially reduced during oxy-fuel combustion.

Fundamentally, the key design principle of the low NOx burners in pulverised coal combustion systems was to release as much nitrogen as possible into the gas phase so that it could be converted to molecular nitrogen rather than NO_x (Hahn et al., 2003, Taniguchi et al., 2002). However, because of the relatively low temperature involved low NOx burners (Taniguchi et al., 2002) complete fuel conversion is not easily achieved and this could lead to high concentration of carbon in the fly ash (Backreedy et al., 2003). Oxy-fuel combustion technology is able to achieve the principle of low NOx design through the high volatile yields obtained.

Subsequently, char combustion test carried out by Sun and Snape (2009) it was observed that for majority of the coals investigated, the rate of char burnout was quicker in oxy-fuel than in air firing condition. However, the combustion rate varied significantly with the different coal samples and the combustion temperatures.

Based on the fundamental TGA information on biomass fuel combustion and the behaviour of coal under oxy-fuel conditions in combustion systems simulating closer to industrial really, it became necessary to investigate CO_2 effect of devolatilisation characteristics of biomass. Although coal and biomass fuels are very dissimilar, a good deal of insight into oxy-biomass combustion behaviour can be derived from the oxy-coal investigations (Dare et al., 2001). This chapter investigates the devolatilisation behaviour of sawdust in a DTF under air and oxy-fuel conditions. The implication of gas atmosphere, devolatilisation temperature, residence time and heating rate on volatile yields are examined. Characterisation of fuel-N_2 partitioning between volatiles and residual char is examined. Physical properties of the chars are investigated to highlight their influence on char burnout. Finally, the burnout of the devolatilised chars is investigated at different temperatures in both atmospheres.

7.3 Experimental procedure

7.3.1 *TGA analysis*

Details of method used are described in section 3.2.2.6. The model equations used to obtain kinetic parameters are also described in 3.2.2.6. The largest particle size used for this investigation was 125-250 μm. The properties of this particle size is given in Table 4.1.

7.3.2 *DTF analysis*

DTF chars were produced at a temperature of 1300°C for 200, 400 and 600 ms using the method described in section 3.5.2.

7.3.3 *DTF re-firing*

Part of the DTF chars produced at 900, 1100 and 1300°C in N_2 and CO_2 were then re-fired at 900, 1100 and 1300°C respectively in 5% oxygen in N_2 and CO_2 (mol mol^{-1}) for 200 ms. Also, chars produced at 1300°C under both atmospheres in 400 and 600 ms were re-fired to investigate the effect of furnace residence time on char burnout. The residues were collected and weighed. The ash contents of the residues were also assessed. The conversion was calculated using the old ash tracer method. This is because the ash content of the char is higher concentration of ash unlike the parent sawdust so that ash volatilisation would not affect the concentration of the residual ash.

7.4 IMPACT OF DEVOLATILISATION TEMPERATURE AND RESIDENCE TIME ON VOLATILE

The volatile yields at three different temperatures of 900, 1100 and 1300°C and residence times of 200, 400 and 600 ms are presented in Figure 7.1. As can be seen from Figure 7.1, the volatile yields are generally higher than the volatile yield obtained in proximate analysis in Table 4.1 in chapter 4 except for the 900°C and 200 ms where the DTF volatile yield was found to be lower than the value obtained in the TGA proximate analysis. The higher volatile yield obtained in the DTF was because at higher temperature and high heating rate, the residual volatiles are released from the sample thereby contributing to the increase in the volatile yields. However, the impact of CO_2 on volatile yield was found to be more pronounced at all temperatures and residence times than N_2

conditions. For example, at 900°C and 200 ms, the volatile yield in oxy condition was about 82 wt% which is about 19 wt% higher than the yield obtained in N_2. The yield of volatiles increased with increase in devolatilisation as expected. In both CO_2 and N_2 conditions, the volatile yield depended not only on devolatilisation temperature but also on residence time. Higher yields of volatiles were generated from the devolatilisation tests in oxy-conditions and this was attributable to the contribution of CO_2-char gasification reaction. However, the difference in volatile between oxy and air fired conditions became smaller as temperatures increased from 900 to 1300 °C, and residence time from 200 to 600 ms. This behaviour exhibited by biomass oxy-firing is due to the extremely low yield of bio-chars at higher temperatures and residence times and hence the relatively lower significance of CO_2-char gasification reactions.

However, this trend was quite different from that observed for oxy-coal combustion (Naredi and Pisupati, 2011a, Sun and Snape, 2009). For example, oxy-coal devolatilisation investigation carried in the DTF by Sun and Snape (2009) revealed that at lower temperatures, 900 and 1100°C, the impact of CO_2 on volatile yield was small for most coals. This was attributed to higher mass transfer resistance of primary volatiles in CO_2 than in N_2. At temperature greater than 1100°C, CO_2-char gasification was highly promoted leading to higher yield of volatiles. On the contrary, for results obtained by Borrego and co-workers (Borrego et al., 2009), lower volatile yields were observed in a CO_2 atmosphere than in nitrogen. They attributed it to the participation CO_2 in cross linking reaction at the surface of the particle during devolatilisation that prevented rapid volatile release.

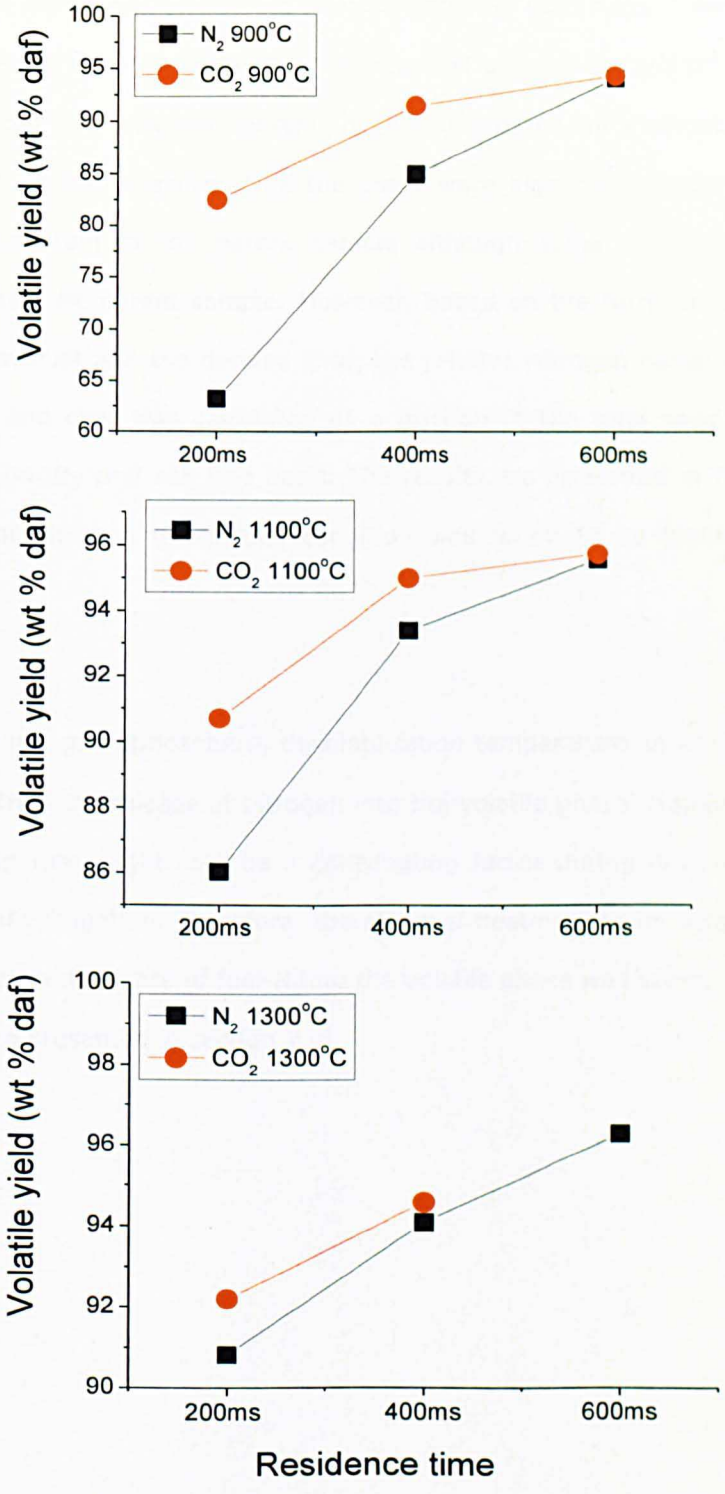

Figure 7.1 Sawdust DTF volatile yield in nitrogen or CO_2 highlighting the effect of temperature and residence time.

7.5 NITROGEN PARTITIONING IN CO_2

The partitioning of nitrogen between volatiles and residual chars has significant impact on NOx emissions during devolatilisation of solid fuels. Table 7.1 presents the elemental nitrogen contents of the sawdust and the derived DTF chars on dry basis. From the nitrogen content in char determine by elemental analysis in Table 7.1, it was observed that the chars were higher or comparable with the nitrogen content of the parent sample although some appear to be slightly higher than the parent sample. However, based on the Nitrogen content of the parent sawdust and the derived char, the relative nitrogen partitioning between volatiles and char was calculated as a fraction of the total sawdust contained nitrogen on dry and ash free basis. The results are presented in Table 7.2. The release of nitrogen under CO_2 condition was found to be higher than in N_2 condition.

In summary, gas atmosphere, devolatilisation temperature as well as residence time controls the release of nitrogen into the volatile phase. However, the effect of heating rate might also be a contributing factor during devolatilisation and requires investigation. Therefore, the effect of heating rate on volatile yield and the subsequent release of fuel-N into the volatile phase was investigated and the results are presented in section 7. 6.

Table 7.1 Elemental nitrogen contents of sawdust and DTF chars at different devolatilisation conditions (wt % daf).

	Parent sample	0.42	
DTF chars	N_2 / 1% O_2		
Temperature °C	200 ms	400 ms	600 ms
900°C	0.50	0.51	0.45
1100°C	0.37	0.64	0.63
1300°C	0.36	0.63	0.63
	CO_2 /1% O_2		
900°C	0.37	0.37	0.41
1100°C	0.43	0.47	0.23
1300°C	0.51	0.48	

Table 7.2 Proportion of fuel-N in volatiles (wt% daf).

Enviroment	Particle size (μm)	Resident Time (ms)	Proportion of fuel-N in volatiles		
			900°C	1100°C	1300°C
N_2	125-250	200	57	88	92
		400	82	90	91
		600	93	93	95
CO_2	125-250	200	84	91	92
		400	88	94	94
		600	94	98	-

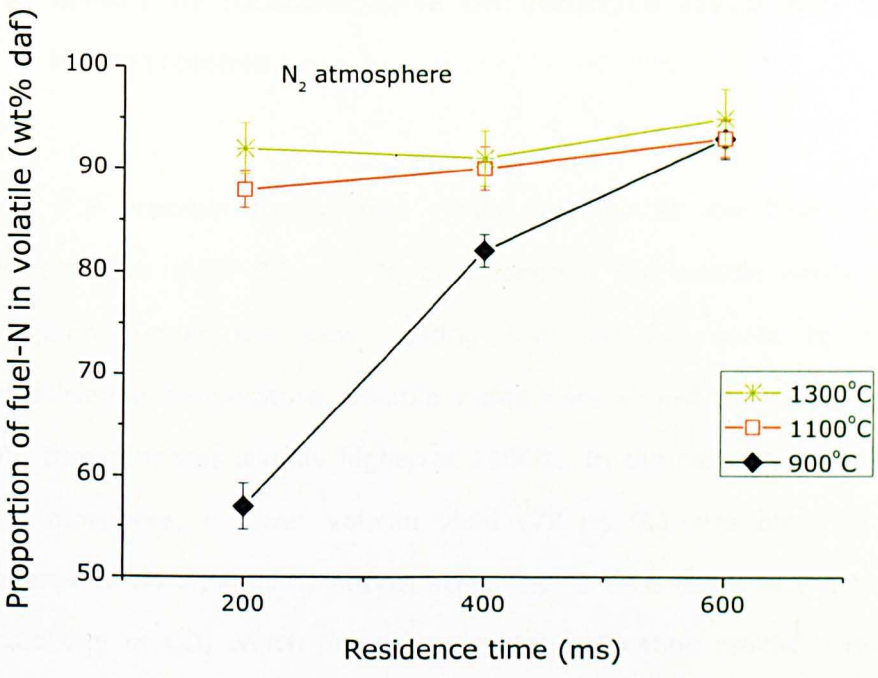

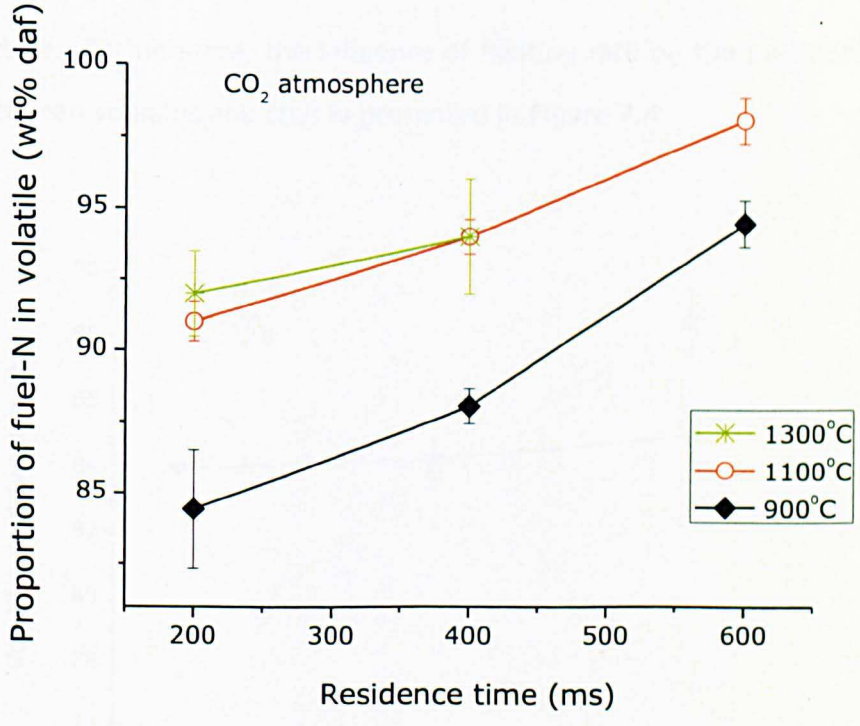

Figure 7.2 Comparison of nitrogen partitioning behaviour of sawdust in CO_2 and N_2 atmospheres during devolatilisation at 900, 1100 and 1300°C at residence times 200, 400 and 600 ms.

7.6 EFFECT OF HEATING RATE ON VOLATILE YIELD AND NITROGEN PARTITIONING

Figure 7.3 presents the volatile yields obtained at low heating rate TGA devolatilisation under CO_2 and N_2 atmospheres. The volatile yields in nitrogen atmosphere under the slow heating rate did not seem to depend on devolatilisation temperature. Volatile yields were almost the same for 700 and 900°C though it was slightly higher at 1100°C. In the case of devolatilisation in CO_2 atmosphere, a lower volatile yield (77 wt %) was obtained at 700°C compared to 84 wt% in N_2 atmosphere. This is as a result of the low thermal conductivity of CO_2 which did not promote gasification reaction. However, at 1100°C, there was a rapid increase in volatile yields in CO_2. The extra mass loss observed in oxy condition at that temperature was due to CO_2-char gasification reaction. Furthermore, the influence of heating rate on the partitioning of fuel-N between volatiles and char is presented in Figure 7.4.

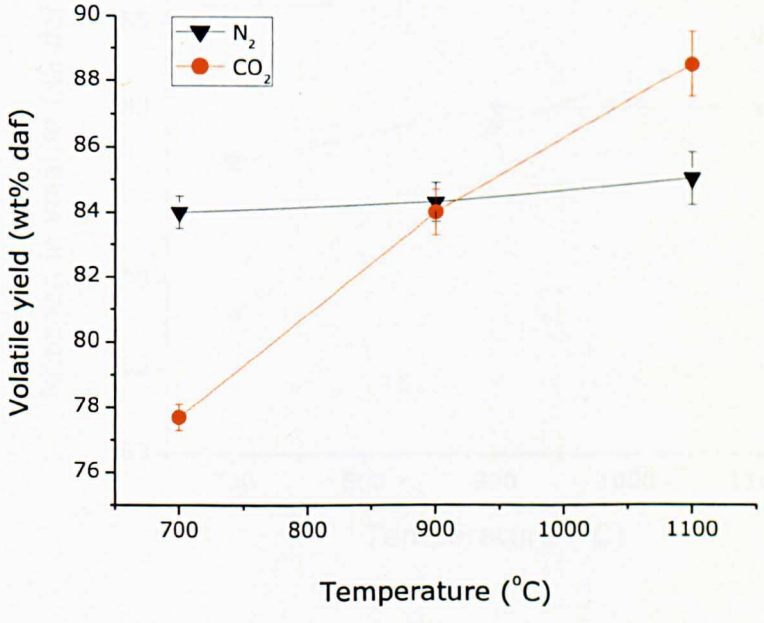

Figure 7.3 Low heating rate TGA Volatile yield under CO_2 and N_2 atmospheres

Like the higher heating rate DTF devolatilisation, the release of fuel-N into the gas phase correlated with increasing volatile yields. However, the release of fuel-N into the gas phase at temperatures below 1100°C seemed to be retarded in CO_2. The low impact of CO_2 is again as a result of the fact that CO_2 is less reactive at low temperatures due to poor thermal conductivity especially at slow heating rate. As such, CO_2 gasification reaction was not promoted. Then as temperature increased to 1100°C, a rapid released of fuel-N in the volatile phase was observed and this is again attributed to CO_2-char gasification reaction (Arias et al., 2008, Rathnam et al., 2009, Wall et al., 2009). In DTF, significant release of volatiles in CO_2 was observed even at the lowest temperature (900°C) as seen in Figure 7.1 whereas in the low heating rate condition the impact of CO_2 was not significant between 700 and 900°C. These results revealed that volatile yield and fuel-N partitioning between volatiles and char do not only depend on gas atmosphere and temperature but also on heating rate.

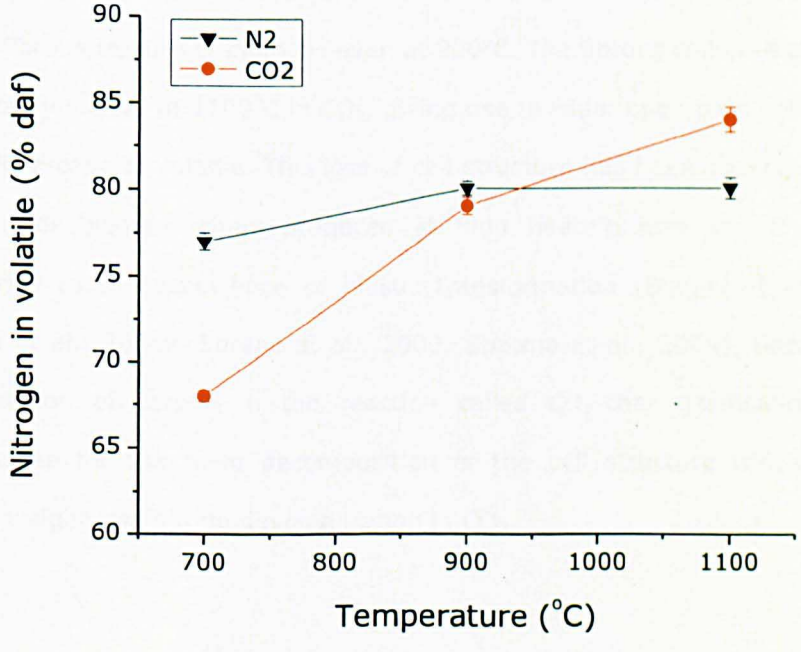

Figure 7.4 The effect of heating rate on fuel-N partitioning behaviour of sawdust in CO_2 and N_2

7.7 CHARACTERISATION OF DEVOLATILISED CHARS

Having understood the devolatilisation behaviour and the nitrogen partitioning characteristics of sawdust in DTF and the subsequent comparison with the low heating rate devolatilisation, the morphological changes of the DTF chars under the different gas atmospheres were studied. This is important because such structural changes impacted on the chars due to rapid volatile yield will affect the combustion reactivity of the resultant chars. Therefore, 900, 1100 and 1300°C chars generated from the DTF at 200 ms in CO_2 and N_2 atmospheres were characterised using a scanning electron microscope (SEM) and the results are presented in Figure 7.5. Chars produced at 900°C in N_2 showed some porosity but still retains the fibrous texture of the parent biomass. This might be the reason for the low volatile yield obtained at that temperature and atmosphere in Table 7.2 and Figure 7.1. However, at 1300°C, the fibrous nature of the parent sample melted and formed lumped irregular shape surfaces with wider pore networks. In the case of chars produced in a CO_2 atmosphere, bulk porosity was more pronounced and the there is evidence of thermal breakdown of the fibrous texture of biomass even at 900°C. The fibrous cellulose cell texture completely melted at 1100°C in CO_2, giving rise to wider open pore networks due to rapid escape of volatile. This loss of cell structure has been observed in other studies for biomass chars produced at high heating rate and it has been attributed to the occurrence of plastic transformation (Biagini et al., 2008b, Biagini et al., 2008a, Lorenz et al., 2000, Sharma et al., 2004). Secondly, the participation of carbon in the reaction called CO_2-char gasification is also responsible for the rapid decomposition of the cell structure which leads to higher weight loss during devolatilisation in CO_2.

Further increase in temperature to 1300°C resulted in the disappearance of the bulk porosity observed at 1100°C. The char was dominated by minerals and ash

showing various degrees of rounding/curving features, due to the more pronounced CO_2-char gasification reactions at such higher temperatures. Additionally, it appeared that there was rapid volatilisation of the mineral matter, re-deposition and re-distribution of such minerals on the surface of the 1300°C CO_2 char. In summary, the CO_2 chars exhibited more swollen structures typical of more reacted surfaces.

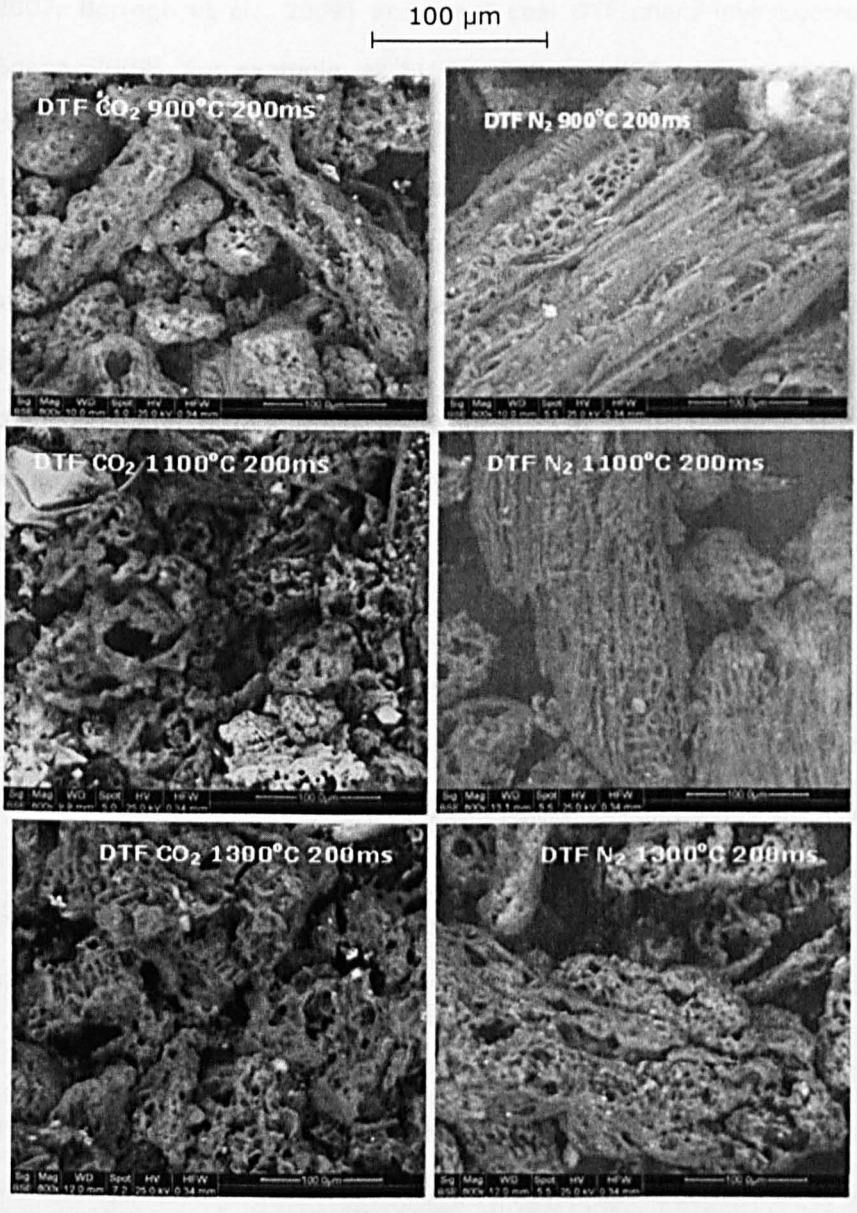

Figure 7.5 Morphology of DTF devolatilised sawdust chars in N_2 and CO_2

Figure 7.6 presents the BET surface areas of the chars at different temperatures and residence times expressed on dry ash free basis. It can be observed that the BET surface areas of the oxy-chars are higher than their counterparts in air fired condition for the two temperatures and at all the residence times investigated. The higher surface areas in CO_2 devolatilised chars are due to the activation by the CO_2-char gasification reaction. Similar higher surface areas in CO_2 have been observed for biomass DTF chars especially wood chips (Borrego and Alvarez, 2007, Borrego et al., 2009) and for 6 coal DTF chars investigated (Sun and Snape, 2009). For example, at 1100°C 200 ms, BET surface areas for the CO_2 char was 11 $m^2 g^{-1}$ while that of N_2 was about 2 $m^2 g^{-1}$. A rapid increase in surface area was observed as residence time increased. Increasing the residence time widens the temperature of primary devolatilisation (Hasan Khan Tushar et al., 2012) and this would have led to the release of residual volatiles and subsequently, further evolution of the internal structure of the char. The CO_2 chars exhibited surface areas of 62 $m^2 g^{-1}$ and 96 $m^2 g^{-1}$ for 400 and 600 ms respectively while the N_2 chars recorded 26 $m^2 g^{-1}$ and 67 $m^2 g^{-1}$ for 400 and 600 ms respectively.

Similarly, at 1300°C the BET surface areas increased much more than the 1100°C chars. The BET surface area for the oxy-chars at 1300°C and 400 ms was about 4 times higher than for the 1100°C and 400 ms oxy-char. It was over 8 times higher than the 1300°C and 400 ms N_2 chars. The observed difference in the surface areas between the N_2 and the oxy-chars is attributed to the CO_2-char gasification reaction which seems to have activated the resultant oxy-chars.

In summary, devolatilisation temperatures, gas atmosphere and residence time affect the porosity of chars. The differences in the porosity of chars produced will also affect their combustion reactivity. Hence, the combustion characteristics of

these chars under both conditions are assessed by re-firing the char in each atmosphere with 5% O_2 concentration.

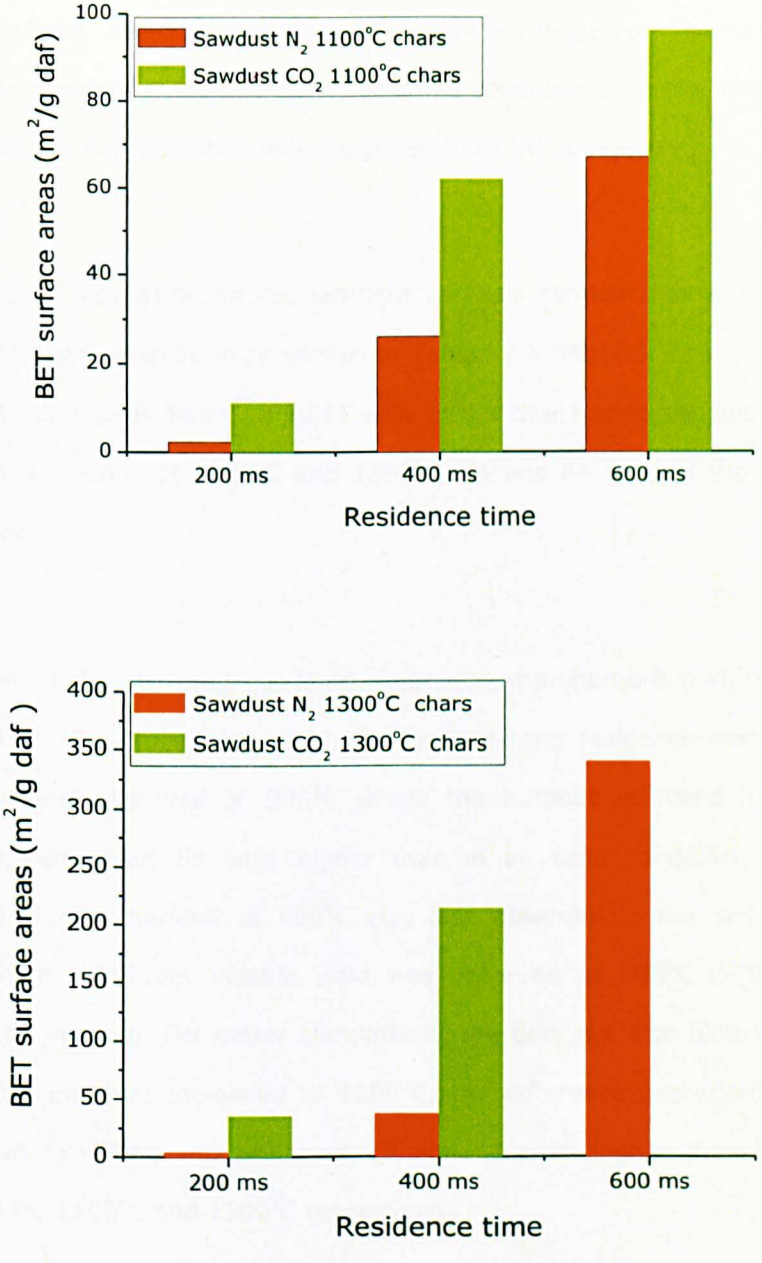

Figure 7.6 Surface areas of DTF chars by BET measurements

7.8 DTF RE-FIRING

In the case of biomass, the combustion of char is a minor part of the biomass combustion process because most of the mass is lost during devolatilisation especially with small particle sizes. Char formation is only about 10% so that unburnt carbon in ash is generally not an issue (Chui et al., 2003). However, understanding biomass char burnout is necessary for co-firing tests. As such, the burnout of the selected sawdust chars was investigated. The char burnout experiments were carried out using the same condition as in the devolatilisation test but the O_2 concentration was increased from 1% to 5% v/v.

The effect of gas atmosphere, temperature and residence time on the char combustion performance is presented in Tables 7.4 and 7.5. From Table 7.4, it was observed that at 900°C, only 11 wt% of the char has combusted in air fired condition. However, at 1100°C and 1300°C, 74 and 81 wt% of the chars have combusted.

Compared to the air firing condition, improved char burnout performance was observed in CO_2 atmosphere at all temperatures and residence times. A major difference was observed at 900°C where the burnout achieved in oxy-firing condition was about 69 wt% higher than in air fired condition. This trend observed in char burnout at 900°C was also observed in the devolatilisation stage where significant volatile yield was observed at 900°C in CO_2 due to gasification reaction. For better comparison, the data are also plotted in Figure 7.7. As temperature increased to 1300°C, the difference decreased, but char burnout in oxy-firing was still over 15 and 10 wt% higher than in air fired condition for 1100°C and 1300°C respectively.

Table 7.3 DTF re-firing characteristics of sawdust char at different temperatures for 200 ms under air and oxy-fuel conditions

	Char burnout (wt % daf)	
Temperature	N_2 / 5% O_2	CO_2 / 5% O_2
900°C	11	80
1100°C	74	92
1300oC	81	95

Table 7.4 The effect of residence times on sawdust char re-firing under air and oxy-fuel conditions at 1300°C

	Char burnout (wt % daf)	
Residence time	N_2/ 5% O_2	CO_2/ 5% O_2
200 ms	81	95
400 ms	82	96
600 ms	89	

The increase in residence time also increased the burnout propensity of the chars. From Table 7.5 and Figure 7.8 demonstrated the effect of residence time on the char burnout. Again, higher burnout trends were observed for oxy-biomass chars for all the residence times considered. This higher burnout trend in oxy-firing condition was also observed during coal char combustion (Naredi and Pisupati, 2011a, Sun and Snape, 2009) and it was attributed to CO_2-char gasification reaction. Additionally, the ash contents of the re-fired chars are presented in Table 7.6 to further explain the extent of combustion obtained. Overall, the improved char porosity observed in Figure 7.6 explained the burnout

performance obtained in oxy-condition in addition to CO_2-char gasification reaction. Also, the catalytic activity of biomass inherent alkali and alkaline metals could play possible role in the combustion reactivity of the chars.

Subsequently, while nitrogen yield in the volatile phase is important due to NOx reduction through staging as earlier discussed, the release of residual nitrogen into the gas phase during char combustion is also an important issue in pulverised fuel combustion. However, it was observed in Figure 7.2 that over 80-98 wt% of the sawdust bound nitrogen was transformed into the volatile phase especially at higher temperatures and residence times. As such, the partitioning of the nitrogen in the unburnt residue was not investigated.

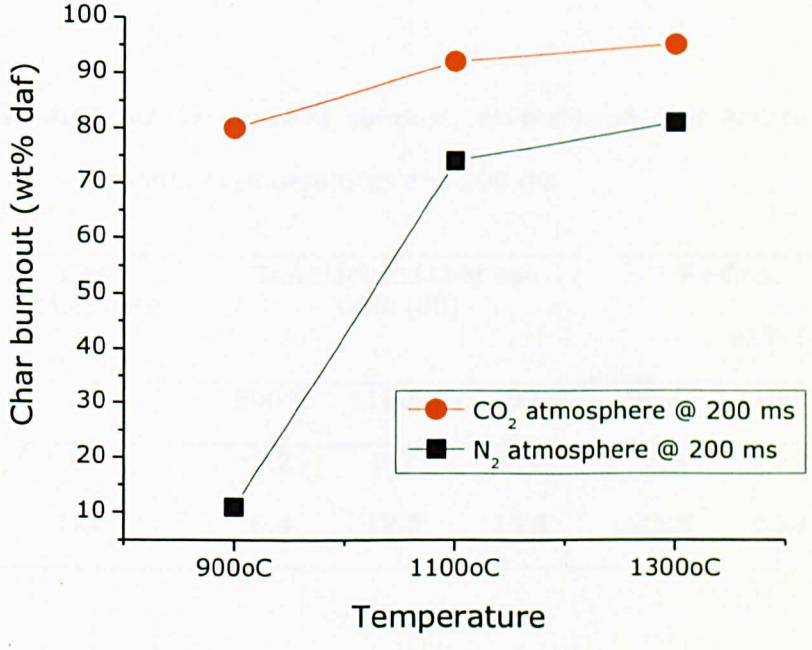

Figure 7.7 Comparison of burnout characteristics of sawdust chars at different furnace temperatures under air and oxy-fuel conditions

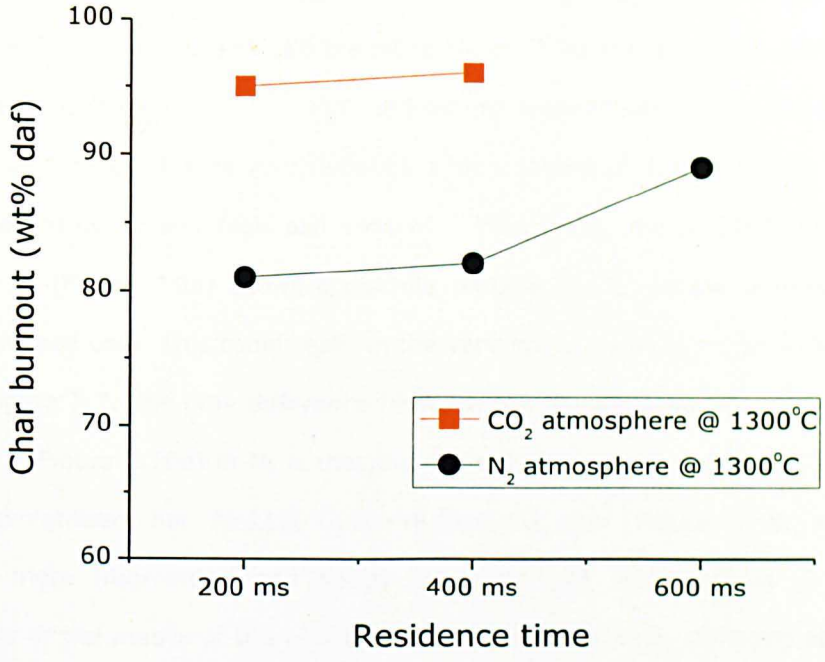

Figure 7.8 Comparison of burnout characteristics of sawdust chars at different residence time

Table 7.5 Ash contents of sawdust, devolatilised char and re-fired chars at different temperatures and 200 ms

Gas atmosphere	Devolatilised char ash wt% (db)			Re-fired char ash wt% (db)		
	900°C	1100°C	1300°C	900°C	1100°C	1300°C
N_2	3.2	8.2	7.9	3.6	25.2	30.7
CO_2	6.4	12.5	13.4	25.8	63.1	77.4

7.9 CHARACTERISATION OF DTF RE-FIRED CHARS

The morphological changes exhibited by the residues after re-firing were examined and compared to the initial chars. In addition, the morphology of the

parent sawdust was also included in order to have a better basis for the comparison (Figure 7.9a). Figure 7.9b and c are the devolatilised and re-fired chars in CO_2 at 900°C and 200 ms while Figure 7.9d and e are the devolatilised and re-fired chars in N_2 at 1100°C and 200ms respectively. The re-fired char at 900°C under CO_2 (Figure 7.9c) exhibits a high degree of fragmentation, possible mineral inclusion and high ash content. Meanwhile, the re-fired 900°C char under N_2 (Figure 7.9e) shows a discrete particle shape, mostly resembling the devolatilised char. This could reaffirm the very low burnout recorded in Table 7.3 and Figure 7.7. The only difference between the devolatilised (Figure 7.9d) and re-fired (Figure 7.10e) in N_2 is that the re-fired char possessed more pores than the devolatilised char. At 1100°C, the re-fired CO_2 char (Figure 7.10b) showed a much more fragmented and floppy structure with redistribution of mineral matters in the matrix of the residue. The re-fired char in N_2 condition at 1100°C (Figure 7.10d) also experienced a high degree of fragmentation with evidence of ash distributed across the surface of the residue. This reaffirmed the high percentage burnout exhibited by the N_2 char at this temperature (74 wt %) in Table 7.3. The effect of residence time on char burnout was also demonstrated in Figures 7.11 and 7.12 using the highest temperature of 1300°C and different residence times in CO_2 and N_2 atmospheres respectively.

The re-fired in CO_2 at 1300°C and 200 ms in Figure 7.11b was almost completely combusted and the ash covering the char surface. The 400 ms char (Figure 11d) also experienced high ash formation due to high burnout of the char. For the 1300°C and 200 ms re-fired char in in nitrogen (Figure 7.12b), the ash is concentrated on some part of the char surface. The ash content increased as residence time increased to 400 ms (Figure 12 d). At 600 ms, ash content appeared to have reduced probably due to volatilisation some ash forming minerals.

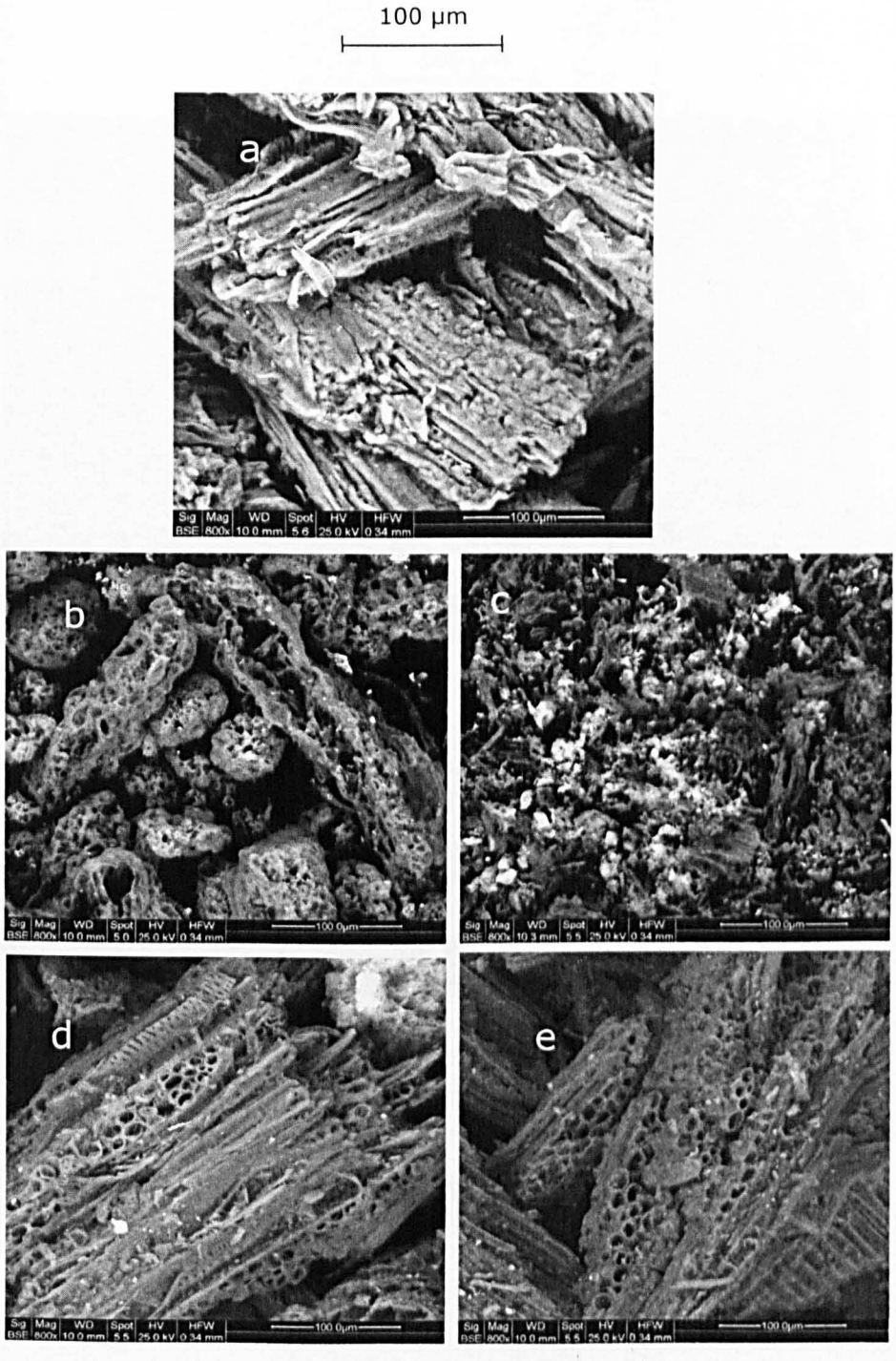

Figure 7.9 SEM images of parent sawdust, DTF devolatilised char and re-fired residue under N2 and CO_2 atmospheres at 900°C 200 ms: (a)_parent sawdust (b)_devolatilised CO_2 char; (c)_re-fired CO_2 residue; (d) _devolatilised N_2 char; (e) _re-fired N_2 residue

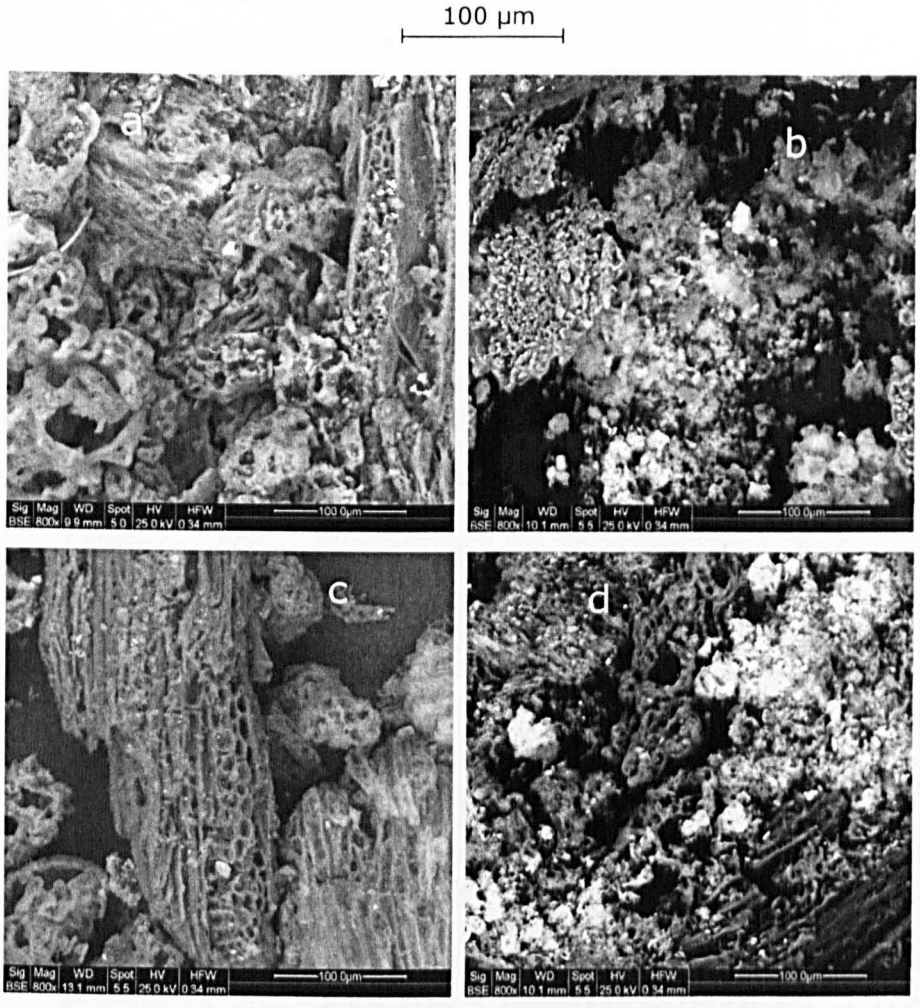

Figure 7.10 SEM images of DTF devolatilised char and re-fired residue under N_2 and CO_2 atmospheres at 1100°C 200 ms: (a) _devolatilised CO_2 char; (b)_ re-fired CO_2 residue; (c)_ devolatilised N_2 char; (d)_re-fired N_2 residue;

In conclusion, the char burnout during DTF re-firing demonstrated that due to CO_2-char gasification reaction, re-firing char under CO_2 exhibited significant very high burnout compared to re-firing under N_2 at the temperatures considered for

the selected chars. Also, like devolatilisation, char burnout was also affected by temperature and residence time.

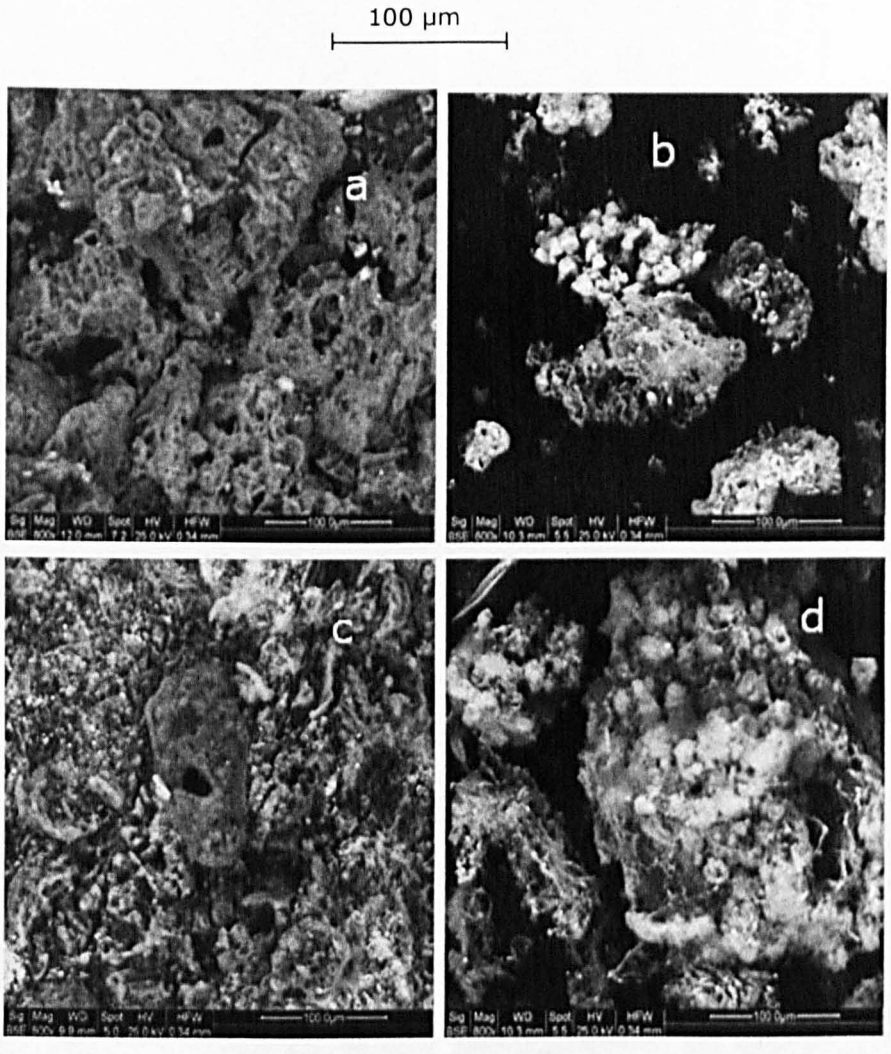

Figure 7.11 SEM images of DTF devolatilised char and re-fired residue under CO_2 atmospheres at 1300°C 200 and 400 ms: (a) _devolatilised CO_2 200 ms char; (b)_ re-fired CO_2 200 ms residue; (c)_devolatilised CO_2 400 ms char; (d)_re-fired CO_2 400 residue;

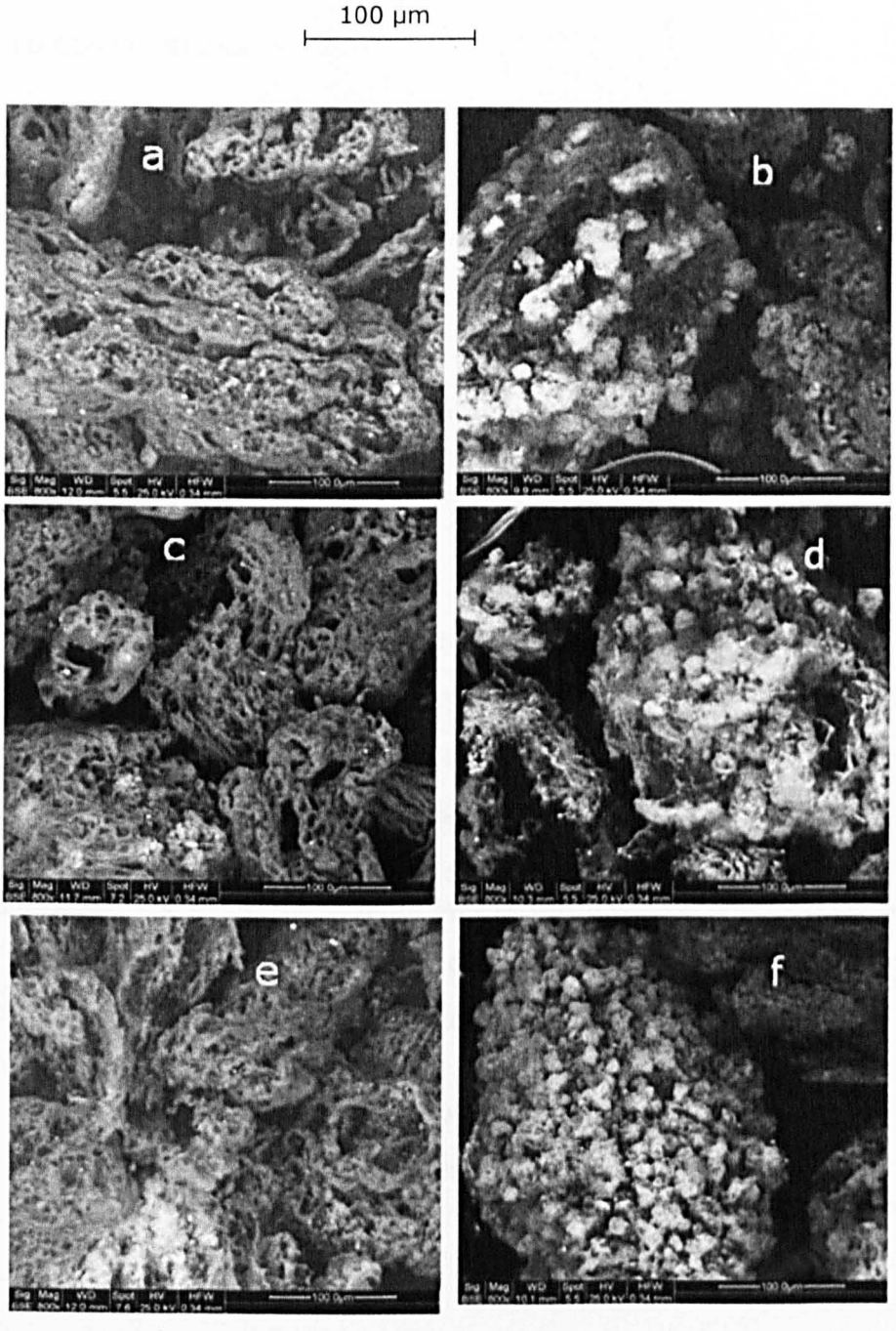

Figure 7.12 SEM images of DTF devolatilised char and re-fired residue under N_2 atmospheres at 1300°C 200, 400 and 600 ms: (a) _devolatilised 200 ms char; (b)_ re-fired 200 ms residue; (c)_ devolatilised 400 ms char;(d)_re-fired 400 ms residue; (e)_devolatilised 600 ms char; (f)_re-fired 600 ms residue

7.10 CONCLUSIONS

1. Compared to N_2, sawdust devolatilisation in CO_2 led to significant higher volatile yields especially at the early stages of devolatilisation (200 ms). However, the impact of CO_2 on volatile yields decreased with increase in temperature and residence time, behaving quite differently from most coals investigated previously by other researchers.

2. Oxy-biomass devolatilisation also led to higher proportion of fuel-N_2 released into the gas phase due to the higher volatile yield. Again, this was more pronounced at the early stage of devolatilisation, at lower temperature and residence times. Devolatilisation in CO_2 produced chars with higher surface areas due to the activating effect of CO_2 as a result of CO_2-char gasification results.

3. Improved char burnout was observed in CO_2 atmosphere than in N_2 atmosphere at all the combustion temperatures considered.

4. SEM images of the CO_2 devolatilised chars developed more porous chars recording higher BET surface areas than the N_2 chars.

8 IMPACT OF BIOMASS CHAR ON COAL CHAR BURN-OUT UNDER AIR AND OXY-FUEL CONDITIONS

8.1 SUMMARY

Although biomass co-firing is now well established in pulverised fuel (PF) combustion under conventional air-fired conditions, there is little information available on how biomass will behave in oxy-fuel firing. Using thermogravimetric analysis (TGA) and a drop tube furnace (DTF), this study examines the impact of co-firing biomass and coal under oxy-fuel conditions compared to normal air firing, with the emphasis on the potential catalytic effect of the biomass alkali and alkaline metals on coal char burnout. Individual chars and their blends prepared from sawdust, pinewood and a South African coal in the DTF and under slow-heating conditions have been used in TGA char burnout tests. The results demonstrate that the coal/biomass char blends burned off significantly faster than predicted under both oxy-fuel and air-firing conditions, and this synergistic catalytic effect was found to be considerably more pronounced in oxy-fuel conditions. In particular, the biomass/coal char blends from devolatilisation in CO_2 burn off approximately two times faster than those prepared under nitrogen. To further examine the catalytic effect, the raw sawdust sample was first extracted with 5M hydrochloric (HCl) acid to remove the alkali and alkaline metals before the char preparation and subsequent char burnout tests. It was found that the removal of the alkali and alkaline metals led to the almost complete loss of the catalytic effect as observed with the untreated sawdust derived char samples. The results indicate that biomass having relatively high contents of alkali and alkaline metals can serves as effective combustion catalysts to improve char burn-out performance, particularly for less reactive coals, such as the South African coal investigated here.

8.2 INTRODUCTION

For effective utilisation of coal and various biomass feedstocks in pulverised fuel (PF) for power generation, compatibility of the fuels during co-combustion is preferable because of the potential chemical interactions between the two different types of fuels that may impact upon coal char burnout, fouling and corrosion and in particular the ability of fly ash to meet specifications for other uses. This is particularly true in the case of co-firing biomass at high ratios, which has recently drawn greater focus due to the growing concerns over the climate-forcing carbon emissions from coal-fired power plants (Fernando, 2012). In addition, the potential catalytic effect of biomass alkali and alkaline metals on coal combustion is potentially important as complete coal char burnout becomes more difficult nowadays to achieve, because of a combination of the increasing amount of unreactive inertinite in internationally traded coals and the use of low NO_x burners (Carroni et al., 2002, IEA and Report:).

Catalytic combustion of pulverised fuels as a means to improve PF combustion efficiency has been the topic of many investigations where the catalytic activity of a range of combustion additives have been examined in considerable detail, such as alkali, alkaline-and transition metal compounds (Gong et al., 2010, Le Manquais et al., 2012, Le Manquais et al.,.2011b, Li et al., 2007, Ma et al., 2006, Wu et al., 1998). Combustion catalysts can be mixed with pulverised fuel via grinding or impregnation, which can improve combustion performance by decreasing ignition temperature and increasing combustion rates. Alkali and alkaline metals have been used as catalysts to promote PF combustion (Le Manquais et al., 2012, Wu et al., 1998), and the results showed that they all catalyse coal combustion at varying degrees although their catalytic performance may vary considerably with individual elements and their chemical forms. However, these types of catalysts can contribute to some major operational

problems, such as fouling, slagging and corrosion. Therefore, other metal compounds, such as some rare and transitional metal oxides have been examined as alternative catalysts (Gong et al., 2010, Le Manquais et al., 2011b, Li et al., 2007, Ma et al., 2006).Using thermogravimetric (TGA) analysis and with CeO_2 and Fe_2O_3 as the catalysts, Gong et al (2010) examined the combustion reactivity of pulverised coals of different ranks varying from lignite to anthracite, and the results demonstrated that the two additives can significantly improve the combustion rate of all coal chars, particularly for coals of higher ranks. The catalytic effect of a group of transitional and rare metals was also evaluated by Le Manquais et al (2011b). It was found that while all examined catalysts showed consistent catalytic activity in both TGA and drop tube furnace (DTF) studies, copper(I) chloride, silver chloride and copper nitrate were identified as the most successful catalysts though a definitive reactivity ranking was found difficult to establish. Similar catalytic activity was also obtained for other metal compounds, such as MnO and BaO [9] and CuO, FeO_3 and ZnO (Li et al., 2007). Although further investigations are needed, it seems that the catalytic effect of metal compounds arises from the improved oxygen transfer behaviours due to the oxygen storage and redox properties of these metal oxides during the combustion process (Li et al., 2007).

However, the use of external combustion additives may prove too costly for practical applications in power generation industry. Biomass contains alkali and alkaline metals that have been known to catalyse coal gasification and combustion at appreciable levels during co-firing process (Fermoso et al., 2010b, Jones et al., 2007, Kastanaki and Vamvuka, 2006, Molcan et al., 2009, Sahu et al., 2010, Zhu et al., 2008). Thus, these may serve as an important source of cost-effective natural source of combustion catalysts, and this is particularly important in the case of co-firing biomass at high ratios for PF power generation, a strategy that has drawn greater focus in recent years as a means to mitigate

carbon emissions (Fernando, 2012). For instance, Jones et al (2007) found that for air firing, the impregnation of potassium onto a HCl-demineralised willow biomass led to significantly improved combustion behaviour of the biomass chars, highlighting the catalytic effect of potassium during biomass combustion. Kastanaki et al (2006) investigated the combustion reactivity of coal-biomass char blends at temperatures up to 850°C with a TGA. The results showed that the combustion behaviour of the char blends was greatly influenced by the rank of individual coals and the properties and amount of each biomass component present in the blend, with the synergistic effect of biomass on coal combustion being greater for lignite than for hard coal derived chars. The characterisation of biomass co-firing conducted by Molcan et al (2009) on a 3 MW_{th} Combustion Facility reveals that biomass addition to coal can improve coal combustion efficiency as highlighted by the higher char burnout levels and lower CO concentrations obtained in all co-firing cases examined. In addition, lower SO_x and NO_x emissions can also be achieved in general as a co-benefit of biomass co-firing (Sami et al., 2001).

While most of these studies were conducted under conventional air-fired conditions and at lower co-firing ratios, little information is available to date on the potential impact of co-firing biomass and coal in oxy-fuel conditions. As part of a larger research programme to address the fundamental knowledge gap of oxy-fuel combustion, this chapter presents TGA and DTF results comparing air and oxy-fuel co-combustion of coal and biomass chars at different blending ratios, with the focus on the potential catalytic effect of biomass-contained minerals on char burnout performance.

8.3 EXPERIMENTAL

The overall experimental approach is presented in Figure 8.1.

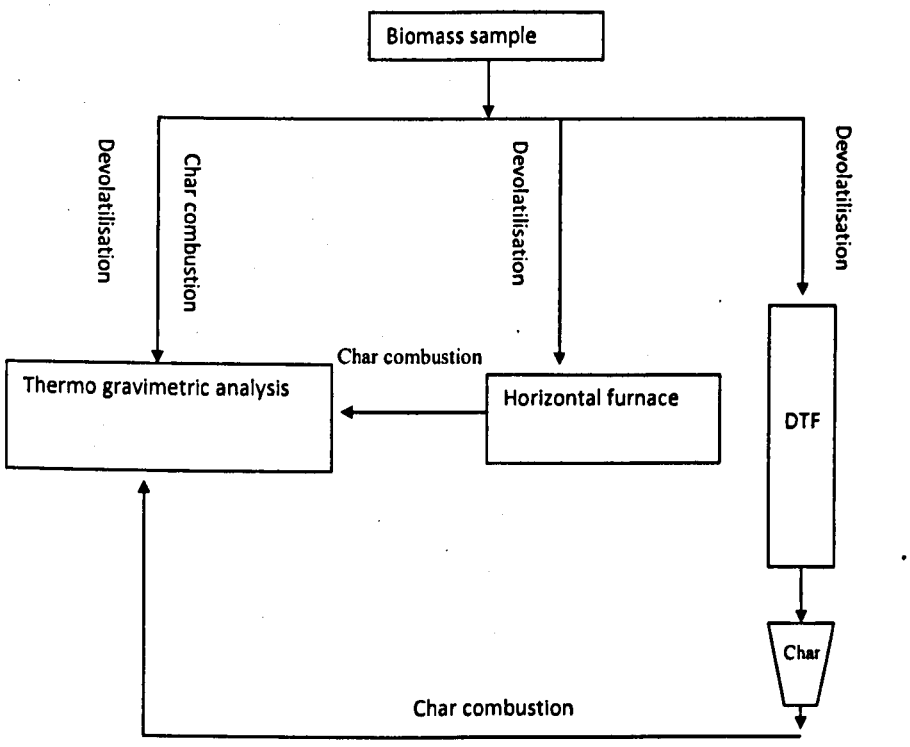

Figure 8.1 Schematic diagram of the experimental approach

8.3.1 *Samples*

Two biomass materials, namely sawdust and pine wood and a South African bituminous coal, Kleinkopje (KK), were used in this study. The properties of these samples are presented in Table 8.1. A particle size range of 125-250 μm was used for the biomass samples and 53-75 μm for the coal sample, respectively. The reason of using larger particle size fraction for the biomass samples was to produce chars having particle sizes similar to those of coal-derived chars.

8.4 COMBUSTION REACTIVITY OF SLOW HEATING RATE SAWDUST AND COAL CHAR BLEND

Figure 8.2(a, b) show the burnout profiles of the HTF sawdust and coal chars and their 50:50 blends under air and oxy-fuel conditions, respectively. The results indicate that the HTF sawdust/coal char blends burn off considerably quicker than what is predicted for the individual chars when they are burned separately, being consistent with the results reported in other investigations (Jones et al., 2007, Kastanaki and Vamvuka, 2006). However, it is interesting to note that the catalytic effect observed for the sawdust char blend appears to be more pronounced in the oxy-fuel conditions. This is further highlighted in Table 8.1 by the burnout rate constants and the reaction times to 90% burnout levels for different chars and their blends. The time to 90% burnout for the 50:50 sawdust/coal char blend prepared under oxy-fuel conditions is *ca.* 21 min, which is less than half of the time of 48 min needed for the coal char to achieve the same burnout level. This compares to the burnout times of the chars prepared in nitrogen of ca. 22 min for the char blend versus ca. 39 min for the coal char. To investigate whether other biomass fuels can behave in a similar manner as the sawdust, a pinewood char and its blend with the coal char were produced and combusted under the same conditions. The results for the pinewood sample are presented in Figure 8.2(c, d). It is evident that the pinewood chars also exhibit similar catalytic effect on coal char burnout performance.

The difference between the experimental and predicted burnout profiles for the char blends highlights the synergetic interactions that occurred during the co-combustion process. Synergy is when two or more fuel components functioning together to produce a total effect that is greater than the sum of the individual components when they are applied separately. The likely explanation for the improved coal char burnout propensity lies in the mineral matter present in the

biomass samples. Most biomass fuels contain significant levels of alkali, alkaline and transitional metals (e.g. Na, K and Ca etc.), which are known catalysts for both combustion and gasification (Brown et al., 2000, Haykiri-Acma and Yaman, 2010, Zhang et al., 2007). The catalytic effect of biomass-contained minerals on coal char burnout will be discussed later in section 3.4. The improved char burnout arising from biomass char blending (Figure 8.2) may suggest that any biomass fuels containing alkali and alkaline metals will potentially improve the combustion performance of coal.

Compared to the improved coal char burnouts in air, it is suggested that the further improved char burnout rates observed for oxy-fuel conditions are attributable to a combination of char combustion and CO_2/char gasification reactions both catalysed by the alkali and alkaline minerals contained in the biomass samples. In particular, the CO_2/char gasification reactions that take place simultaneously in oxy-fuel combustion can lead to significantly higher porosity of residual chars being developed (Davidson and Santos, 2010), this giving rise to increased access of oxygen and other reactants to the carbon residues.

It is also interesting to note that the catalytic effect of biomass char blending on coal char combustion appears to be significantly larger for the less reactive coal char prepared at the higher temperatures of 900 and 1100°C, compared to the char produced at 700°C. It was found previously that the effect of biomass co-firing was more pronounced for lignite than for bituminous coals due to the compatible active reaction temperatures of lignite and biomass chars during co-combustion (Kastanaki and Vamvuka, 2006). However, the results obtained here tend to suggest that the chemical nature and mobility of biomass-contained mineral matters, as opposed to the compatibility of the fuels, can be potentially

more important in terms of their induced catalytic activity particularly in the case of biomass/coal co-combustion in oxy-fuel conditions.

Table 8.1 Comparison between the combustion reactivity of low heating rate sawdust and coal chars and their blends

Samples	N_2 chars and air firing		CO_2 chars and oxy-fuel firing	
	Rate constants (min^{-1})	Time to 90 % burnout (min)	Rate constants (min^{-1})	Time to 90 % burnout min)
Sawdust char	0.4901	6.60	0.3325	7.85
Kleinkopje char	0.7340	38.70	0.0526	48.00
50:50 blend	0.1002	22.15	0.1089	20.65
Predicted blend	0.0829	25.60	0.0720	31.60

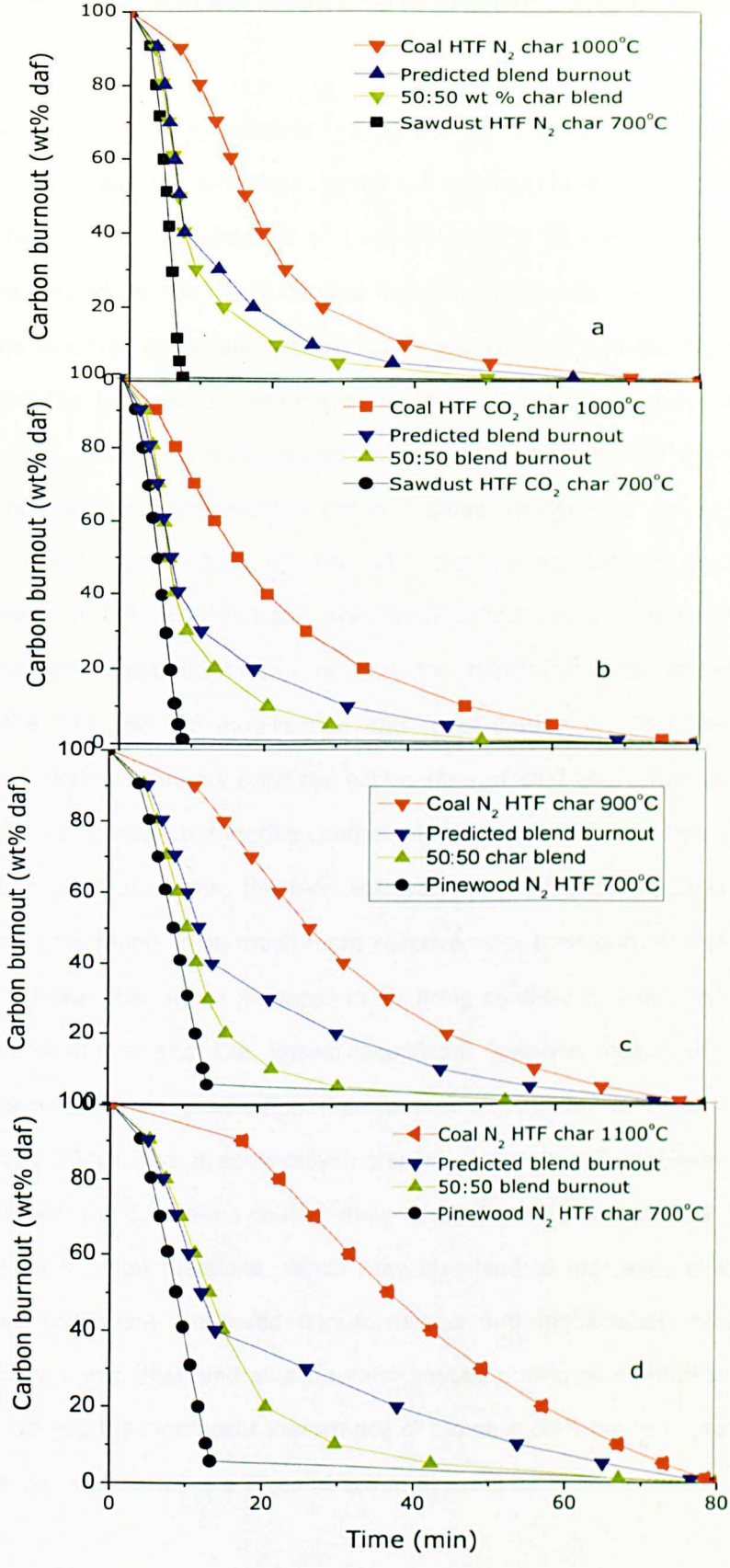

Figure 8.2 TGA burnout profiles in air of HTF sawdust, pinewood, coal chars and their blends prepared in air firing and oxy-fuel conditions at different temperatures

8.5 COMBUSTION REACTIVITY OF DTF SAWDUST AND COAL CHARS

DTF is a useful tool to investigate the combustion characteristics of pulverised fuels under well-defined conditions, which are comparable to those in a PF power plant. The catalytic performance of biomass char in co-combustion was thus further examined for the chars derived from devolatilisation in N_2 and oxy-fuel conditions in a DTF at variable temperatures and residence times. Figure 8.4(a, b) present the burnout characteristics for these DTF char samples. Improved char burnout rates at varying degrees were observed for all DTF coal/biomass char blend samples. Compared to the HTF chars, however, a generally larger catalytic effect was evident for the DTF chars generated at much higher temperatures in both air-firing and oxy-fuel conditions. This could be due to the higher surface areas developed in the coal char as a result of the higher heating rate in the DTF and the mobilisation and redistribution of biomass-contained alkali and alkaline minerals onto the active sites of coal char. This could allow these minerals to stay in effective contact with the coal char and hence act as a combustion catalyst. Again, the biomass/coal char blends prepared in oxy-fuel conditions were found to be much more reactive, with their burn-off rates nearly two times faster than those prepared in air-firing conditions. Given the elevated CO_2 concentrations and the known significant catalytic effect of biomass-contained minerals on gasification (Fermoso et al., 2010b, Jones et al., 2007, Zhu et al., 2008), the dramatically increased reactivity of coal/biomass char blends in oxy-fuel conditions could mainly result from a preferentially catalysed CO_2/char gasification reactions, which may also lead to increased char surface areas and potentially improved transformation and mobilisation of biomass-contained catalytic alkali and alkaline-earth metals during co-combustion. These results highlight the significant importance of biomass co-firing in improving coal combustion performance in a PF combustion system.

8.5.1 *Effect of biomass blending ratios on char reactivity*

The effect of biomass char blending ratios on coal char combustion reactivity is demonstrated in Figure 8.3. While limited but still appreciable improvement in char burnout was observed for the 10:90 biomass/coal char blend, the catalytic activity increased notably with increasing proportions of bio-char in the blends from 10 wt % to 25 and 50 wt%. Close examination of the 90% char burnout times for different samples (Table 8.2) reveals that the decrease in char burnout times or increase in char burnout rates is almost proportional to the amount of bio-char present in the blends, being consistent with the proportionally increased concentrations of biomass-contained catalytically active metals in the blends. Although further investigations are needed, the results obtained highlight the significant potentials of biomass co-firing in catalysing coal combustion, and this is particularly important in the case of enhanced biomass co-firing in PF combustion, which has been regarded in a recent IEA report as being an effective strategy to mitigate CO_2 emissions from coal-fired power generation (Fernando, 2012). It is noteworthy that to some extent, the significantly further improved oxy-char burnout performance compares well to the enhanced co-gasification behaviour of biomass and coal as observed in other investigations where biomass present in high proportions acts as either a catalyst or accelerates coal devolatilisation (Park et al., 2010, Sharypov et al., 2007, Straka et al., 2004, Zhang et al., 2007).

Table 8.2 Effect of biomass/coal char blending ration on co-combustion reactivity

Sample	1st order rate constants (min^{-1})	Time to 90% Burnout min)
25:75 biomass/coal N_2 char blend	0.0725	34.00
10:90 biomass/coal N_2 char blend	0.0601	43.00

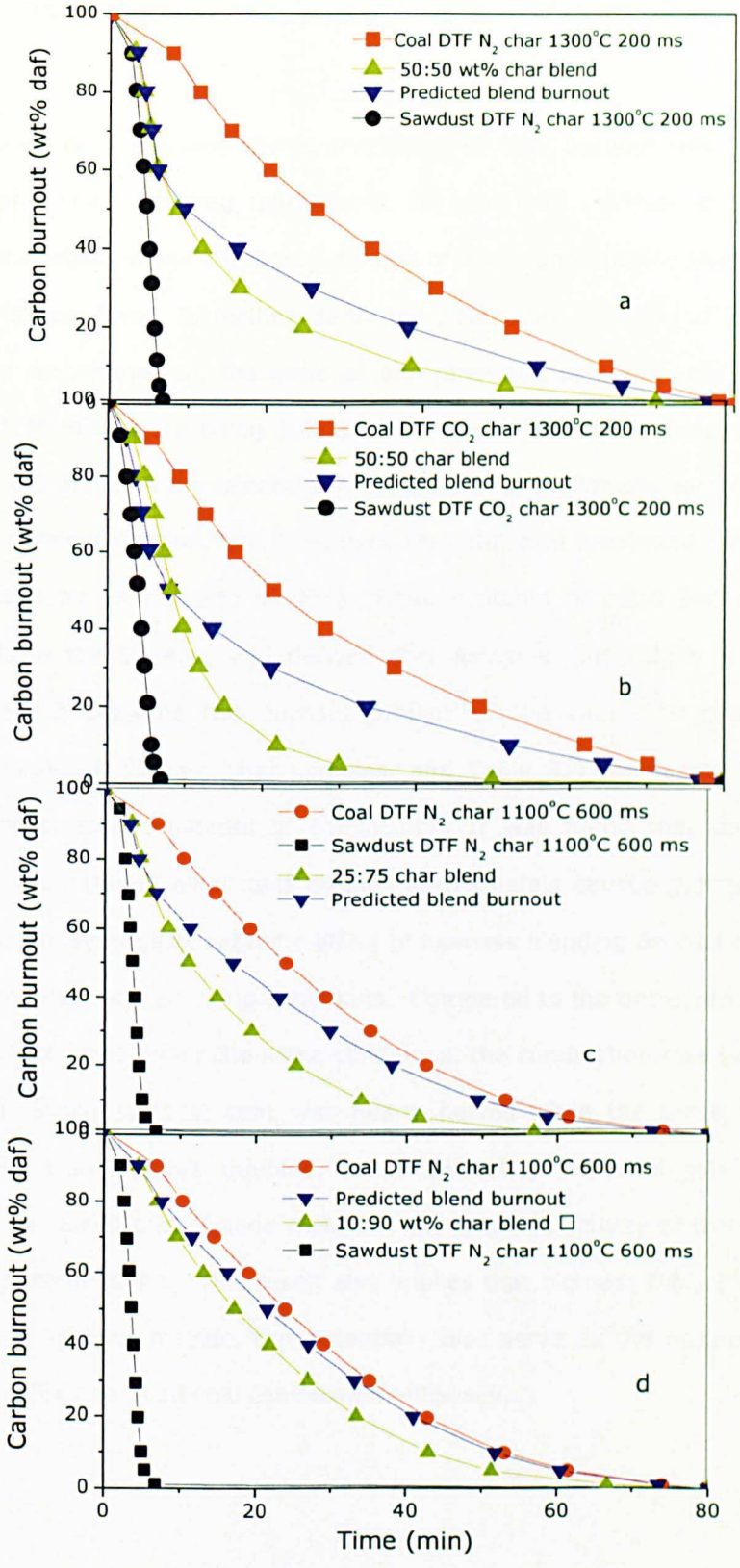

Figure 8.3 TGA burnout profiles of DTF biomass and coal chars and their blends highlighting the effect of different gas atmospheres and biomass blending ratios during co-firing

8.6 EFFECT OF BIOMASS DEMINERALISATION ON CHAR COMBUSTION REACTIVITY

As have been discussed above, the improved char burnout rates as a result of biomass char blending particularly for oxy-fuel combustion are possible demonstration of the catalytic activities of alkali and alkaline metals present in the biomass fuels. To further clarify the potentially vital role of these minerals during co-combustion, the sawdust and pinewood samples were demineralised with 5 M HCl before being subjected to devolatilisation to generate the chars. Table 8.3 presents the mineral compositions of both biomass samples before and after demineralisation. It is evident that the acid treatment led to dramatic decrease by an average of 90% in the contents of alkali and alkaline-earth metals in the biomass and derived char samples, particularly K, Na and Ca. Figure 8.3 presents the burnout profiles of the coal char blends with the demineralised biomass char samples, and Table 8.4 compares their apparent first order rate constants of combustion. It was found that the removal of biomass-contained alkali and alkaline-earth metals caused almost a complete loss of the synergistic catalytic effect of biomass blending on coal combustion in both oxy-fuel and air-firing conditions. Compared to the untreated biomass char blends prepared under the same conditions, the combustion rate constant of the demineralised sawdust char was nearly halved while the times to 90% char burnout were almost doubled, thus confirming the vital role of biomass-contained alkali and alkaline metals in the catalytic activity of biomass co-firing on coal combustion. This result also implies that biomass fuels containing high levels of mineral matters can potentially also serve as the natural combustion catalyst for improved coal combustion efficiency.

Table 8.3 Alkali and alkaline-earth mineral contents of char and ash samples derived from raw and HCl-leached biomass samples

Sample	Mineral content, wt % (dry basis)			
	Na	Mg	K	Ca
Biomass ash samples				
Raw sawdust	0.12	0.09	0.21	0.75
5M HCl washed sawdust	0.02	0.02	0.008	0.006
Raw pinewood	0.46	0.61	2.95	8.21
5M HCl washed pinewood	0.16	0.02	0.02	0.12
Biomass char samples				
Raw sawdust	0.0084	0.0063	0.015	0.053
5M HCl washed sawdust	6.28×10^{-5}	6.28×10^{-5}	2.51×10^{-5}	1.88×10^{-5}
Raw pinewood	0.06	0.08	0.41	1.12
5M HCl washed pinewood	0.009	0.001	0.001	0.007

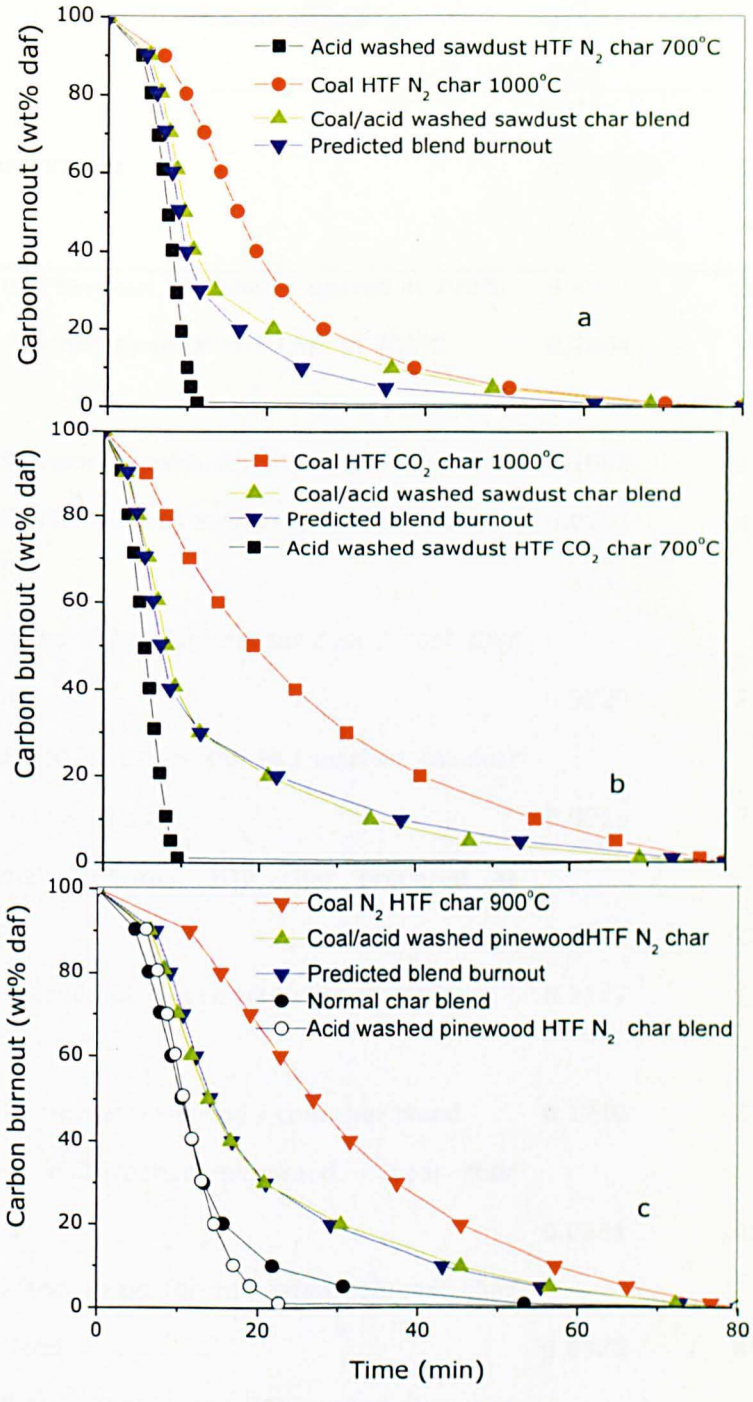

Figure 8.4 TGA burnout profiles of coal and demineralised sawdust and pinewood chars and their blends derived from devolatilisation in air-firing conditions

Table 8.4 TGA char burnout reactivity of individual biomass chars and their blends with coal char before and after biomass demineralisation treatment with 5M HCl

Char samples	Rate constants (min^{-1})	Time to 90% burnout
Normal sawdust HTF char prepared at 700°C	0.4901	6.60
HCl-leached sawdust HTF char at 700°C	0.2884	11.70
50:50 normal sawdust / coal char blend	0.1002	22.15
50:50 HCl-leached sawdust / coal char blend	0.0501	43.00
Predicted value for the sawdust / coal char blend	0.0829	25.60
Predicted value for the HCl-leached sawdust / coal char blend	0.0918	25.10
Normal pinewood HTF char prepared at 700°C	0.2323	12.70
HCl-leached pinewood HTF char at 700°C	0.2147	17.00
50:50 normal pinewood / coal char blend	0.1210	21.80
50:50 HCl-leached pinewood / coal char blend	0.0531	45.40
Predicted value for the pinewood/coal char KK blend	0.0522	44.50
Predicted value for the HCl-leached pinewood / coal char blend	0.6015	39.80

8.7 CONCLUSIONS

1. The biomass/coal char blends burn off significantly faster than the unblended coal chars in both air and CO_2, highlighting the catalytic activity of biomass char blending on coal combustion reactivity.

2. The catalytic effect increases dramatically with increasing proportions of biomass char in the blends. The catalytic effects were found to be considerably more pronounced in CO_2-rich or oxy-fuel conditions, with the coal and biomass char blends being able to burn off almost up to twice faster than the unblended coal chars.

3. Under oxy-fuel conditions, the CO_2/char gasification reactions appear to be preferentially catalysed with biomass blending. This may lead to increased char surface areas and enhanced transformation and mobilisation of biomass-contained catalytic active mineral matters, which may together account for the particularly improved char burnout performance of the char blends in oxy-fuel conditions.

4. The removal of alkali and alkaline- metals from biomass resulted in the nearly complete loss of the catalytic activity of biomass char, confirming they were responsible for the catalytic activity.

These findings suggest that co-firing with high biomass ratios can potentially be a strategy to improve the char burn-out performance in PF combustion

9 SYNERGETIC EFFECTS OF BIOMASS ON COAL VOLATILE YIELDS

9.1 SUMMARY

In chapter 8, the potential catalytic impact of alkali and alkaline metals inherent in biomass char on coal char burnout was examined. However, from application point of view, co-firing deals with blending of the original fuels. This chapter therefore presents the synergetic effects of biomass and coal during devolatilisation in the TGA and DTF. The devolatilisation characteristics of the blends are presented in terms of volatile yields and morphological changes of the chars.

9.2 INTRODUCTION

The interaction between biomass and coal has been investigated extensively during co-pyrolysis (Blesa et al., 2003, Haykiri-Acma and Yaman, 2007, Haykiri-Acma and Yaman, 2008a, Moghtaderi et al., 2004, Park et al., 2010, Sonobe et al., 2008, Wagenaar and Van den Heuvel, 1997, Wang et al., 2009) under conventional air-fired conditions. Little information is available on biomass/coal interaction under CO_2 condition especially at high heating rate and high temperature environment. A study of biomass/coal co-pyrolysis under oxy-fuel conditions was carried out by TGA. The results revealed that there was no interaction between the fuels in nitrogen and CO_2 conditions except at higher oxygen concentration in CO_2 (Yuzbasi and Selçuk, 2011).

This chapter therefore investigates the co-devolatilisation of sawdust and coal in a DTF in order to examine possible interaction between sawdust and coal in

combustion system closer to pulverised fuel combustion system and compares to TGA.

9.3 EXPERIMENTAL

Weighed amounts of sawdust and coal (50:50 wt%) were mixed thoroughly and fed into the DTF using 1% O_2/99% N_2 and 1% O_2/99% CO_2 for devolatilisation under air and oxy-fuel fired condition respectively. The volatile yields were then determined using the ash tracer method (equation 3.13). Details of DTF devolatilisation operation has been described in section 3.5.2. Volatile yields were determined using the conventional ash tracer method.

9.4 SAWDUST/KLEINKOJPE DTF VOLATILE YIELDS

Figure 9.1 presents the volatile yields for Kleinkopje, a relatively high rank coal under CO_2 and N_2. These results were previously obtained by previous workers (Sun and Snape, 2009). At 900°C and 200 ms, the volatile yield in CO_2 condition was lower than in N_2 atmosphere. This is an indication of mass transfer resistance of the primary volatiles in CO_2 than in N_2. This implied that at such temperature, CO_2 did not have much impact on the volatile yield of Kleinkopje. Secondly, gasification reaction was not promoted. This behaviour exhibited by Kleinkopje was quite different from the sawdust as earlier been observed. The possible reason for the higher yield recorded for sawdust at 900°C and 200 ms might be the higher reactivity of biomass towards CO_2 (Irfan, Arami-Niya et al. 2011). However, as temperature was increased to 1100°C and 1300°C the impact of CO_2 on coal volatile yields became significant. The higher volatile yields in CO_2 are due to the contribution of CO_2-char gasification reaction, consistent with results of other researchers (Yuzbasi and Selçuk, 2011).

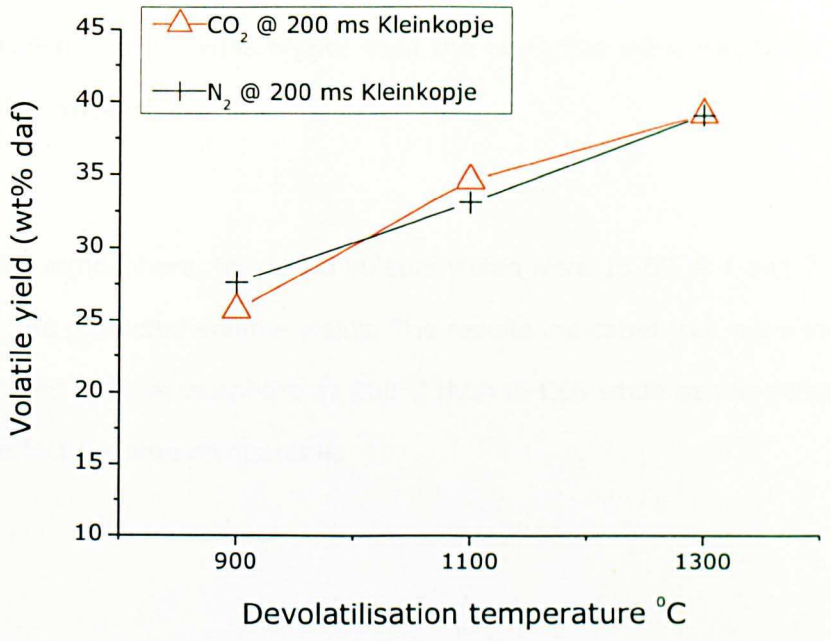

Figure 9.1 Kleinkojpe DTF volatile yields under N_2 and CO_2 at different devolatilisation temperatures and 200 ms (Sun and Snape, 2009)

9.5 SYNERGETIC EFFECTS FOR DTF VOLATILE YIELDS DURING CO-DEVOLATILISATION

Figures 9.2 and 9.3 present the volatile yields of the individual fuels, their blends and the synergetic effect observed during the co-devolatilisation under N_2 and CO_2 conditions respectively. As can be seen from both Figures, the experimental values of the volatile yields obtained under both atmospheres were higher than the predicted values. These significant higher volatile yields indicate that there was interaction between the fuels during devolatilisation. Also, the addition of biomass to coal increase coal volatile yields from 30 wt% to about 70 wt%.

Furthermore, to have a better understanding of the influence of gas atmosphere on the compatibility of the fuels, the synergetic effects under N_2 and CO_2

condition were compared and the results are presented in Figure 9.4. For example, in the N_2 atmosphere, volatile yields in the experimental was about 19.4, 9.6 and 8.3 wt% higher than the predicted values at 900°C, 1100°C and 1300°C respectively.

In CO_2 atmosphere, the blend volatile yields were 13.67, 9.1 and 7.6 wt% higher than the predicted volatile yields. The results indicated that more interaction was observed in N_2 atmosphere at 900°C than in CO_2 while as temperature increase, the effect became comparable.

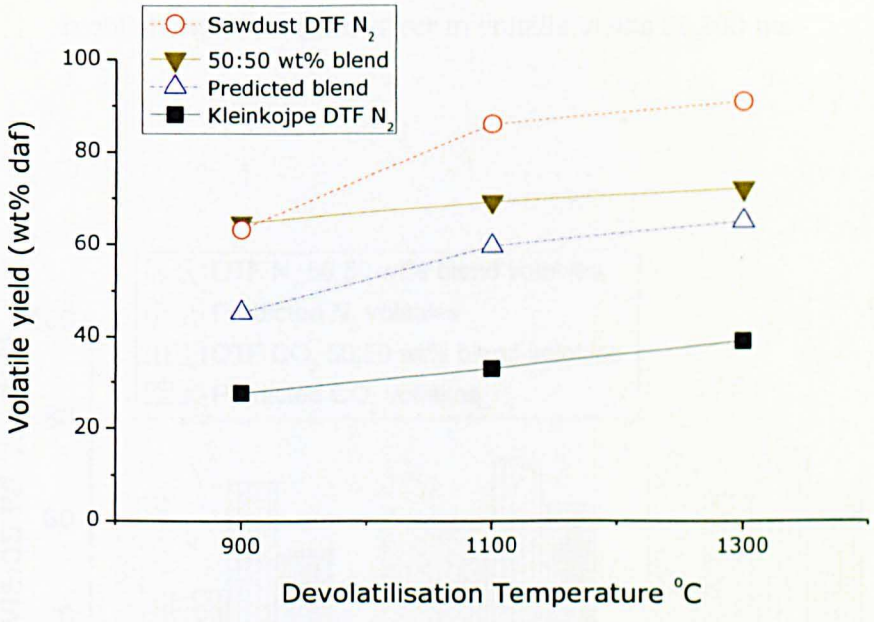

Figure 9.2 DTF co-devolatilisation of sawdust and Kleinkojpe in N_2, highlighting synergetic effect in volatile yields at 200 ms

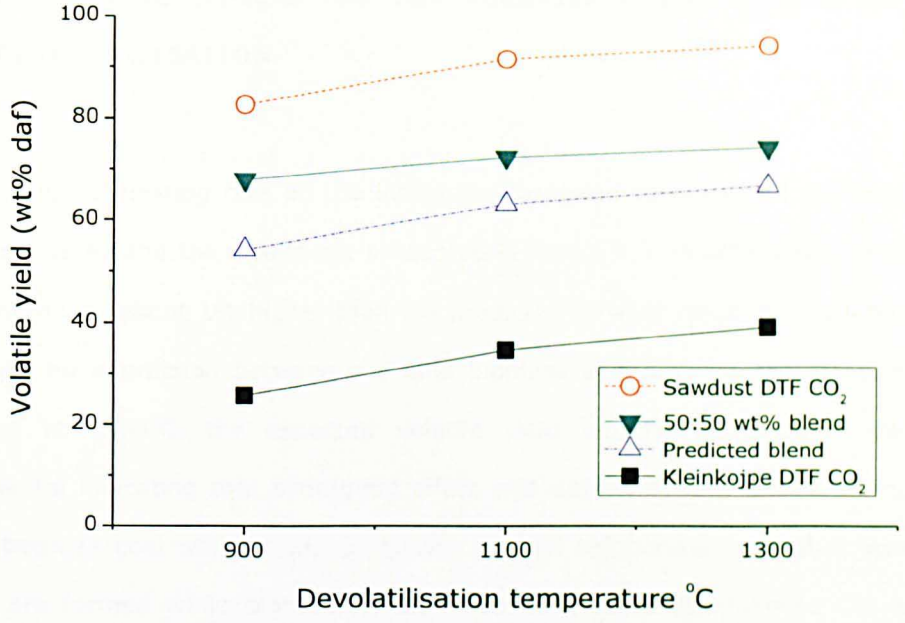

Figure 9.3 DTF co-devolatilisation of sawdust and Kleinkojpe in CO_2, highlighting synergetic effect in volatile yields at 200 ms

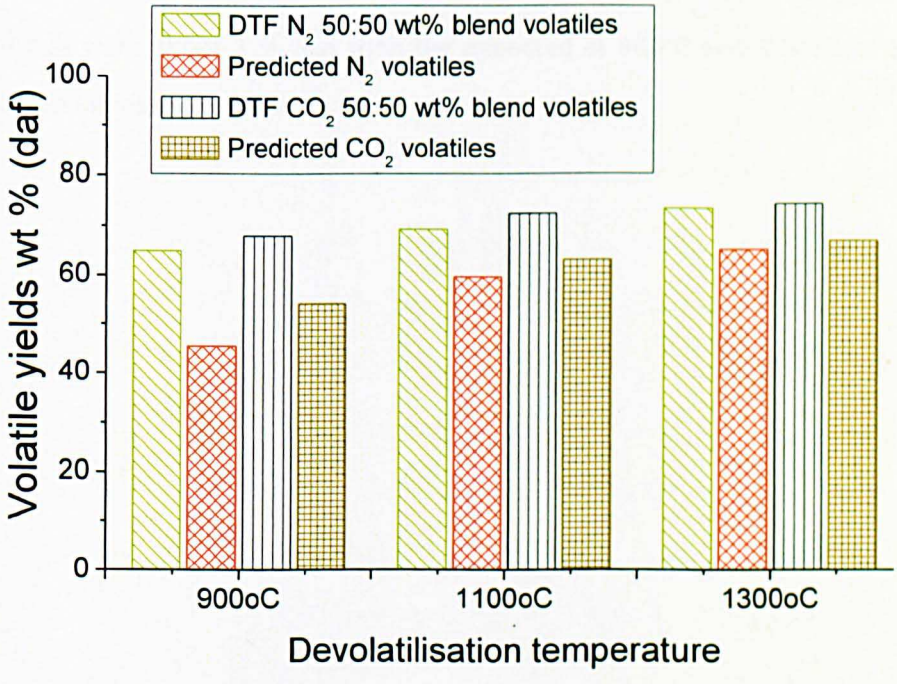

Figure 9.4 Comparing the synergetic effects of sawdust/Kleinkojpe DTF blends under N_2 and CO_2 at 200 ms

9.6 SYNERGETIC EFFECTS FOR TGA VOLATILE YIELDS DURING CO-DEVOLATILISATION

The influence of heating rate on the interaction between sawdust and coal was also investigated and the results are presented in Figure 9.5. Volatile yields in N_2 atmosphere was about 1% higher than the predicted or what would be expected if the was no interaction between coal and biomass at 900°C. As temperature increased to 1100°C, the expected volatile yield became higher than the experimental indicating that synergetic effect was absent at that temperature. This is because coal will decompose slowly at such temperatures so that less volatile are formed while biomass would have completely decomposed. As a result, there was no interaction between biomass volatile and those of coal. Similar results have been obtained by previous researchers (Kastanaki et al., 2002, Meesri and Moghtaderi, 2002, Moghtaderi et al., 2004).

In the case of devolatilisation in CO_2 also (Figure 9.5), lower volatile yields were obtained than the predicted indicating that there was no synergy. The volatile yields in CO_2 were about 3 % less than the expected at 900°C and 2.5% less as temperature increased to 1100°C.

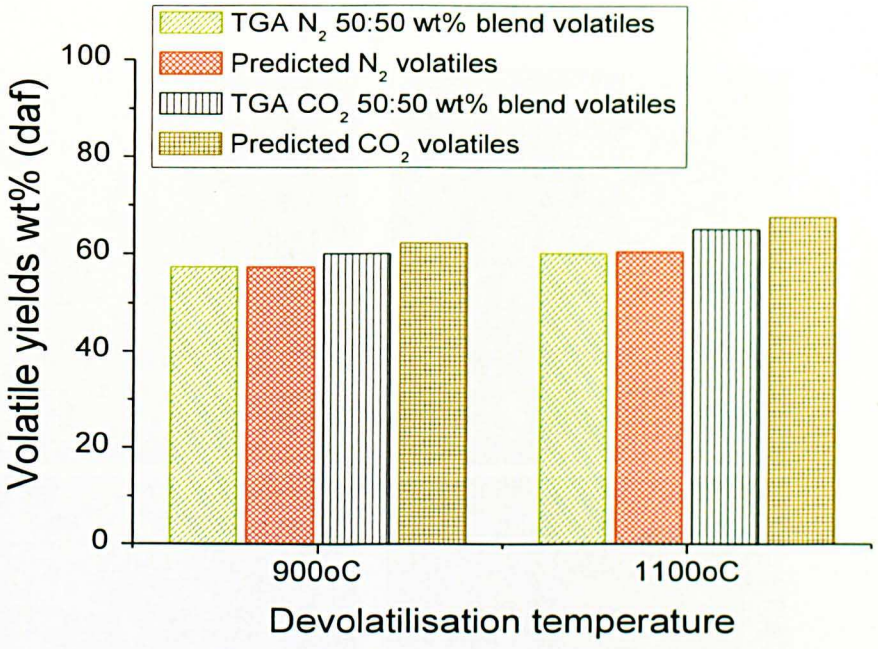

Figure 9.5 Comparing the synergetic effects of sawdust/Kleinkojpe TGA blends under N_2 and CO_2

9.7 CHARACTERISATION OF CO-DEVOLATILISED CHARS

Figure 9.6 presents SEM images of sawdust and Kleinkojpe blend chars generated from the DTF at 1100 and 1300°C at residence time of 200 ms under N_2 and CO_2. All the chars showed significant swelling with porous structures. At 1100°C, (Figure 9.6a and c) the surfaces of both chars are dominated by the minerals (ash). As temperature increased to 1300°C, there seemed to be a re-distribution of the minerals in the CO_2 char (Figure 9.6b). The 1300°C CO_2 char also became more significantly porous than the 1100°C CO_2 chars. This could be due to increased CO_2-char gasification reaction. Meanwhile, the chars generated under N_2 atmospheres at 1300°C appeared to contain more ash distributed round the surface of the char.

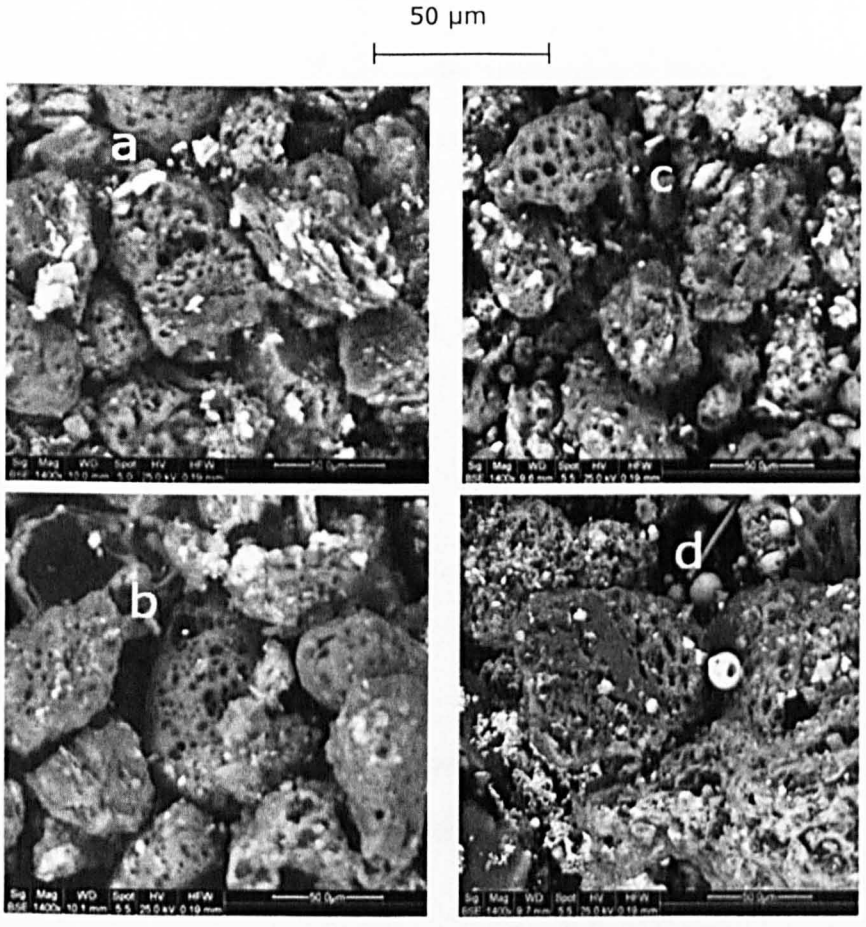

Figure 9.6 SEM images of sawdust and Kleinkojpe blend DTF chars generated at different temperatures and 200 ms: (a)_1100°C CO_2; (b)_ 1300°C CO_2; (c)_1100°C N_2; (d)_1300°C N_2

9.8 TGA BURNOUT CHARACTERISTICS OF DTF CO-DEVOLATILISED SAWDUST AND COAL CHAR BURNOUT

The burnout profiles of the chars generated at 1300°C and 200 ms in CO_2 are presented in Figure 9.7. Like what was observed in chapter 8 with the char-char blend burnout, co-devolatilisation also led to improved coal char burnout as seen in Figure 9.7. This means that co-firing biomass and coal will be beneficial to coal combustion efficiency.

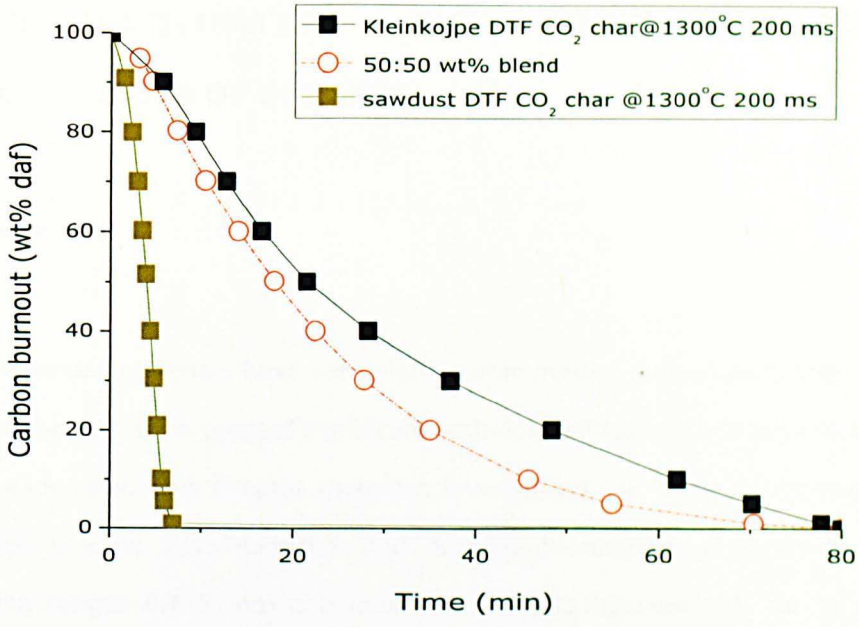

Figure 9.7 TGA burnout profiles of DTF sawdust, coal and 50:50 wt% blend co-devolatilised chars produced at 1300°C and 200 ms.

9.9 CONCLUSIONS

1. Co-devolatilisation of sawdust and biomass in the DTF led to higher volatile yields, but more pronounced in CO_2.

2. There was no synergy between the sawdust and coal in the TGA devolatilisation due to the fact that biomass decomposed faster than coal.

3. The devolatilised chars at 1100°C exhibited ash deposition on the surfaces of the chars. As temperature in increased to 1300°C, the ash seemed to have been redistributed or possibly, some of the ash forming metals would have volatilised in oxy-firing. More ash was still visible on the surface N_2 char even at 1300°C.

10 EFFECT OF MOISTURE CONTENT AND PARTICLE SIZE ON DEVOLATILISATION AND CHAR BURNOUT CHARACTERISTICS OF BIOMASS

10.1 SUMMARY

Many raw biomass materials have very high volatile matter content compared to coals and their utilisation present significant technical difficulties, and tend to be relatively expensive. This chapter therefore investigates the effect of moisture and particle size on devolatilisation and burnout characteristics of sawdust. Particle size ranges 0.6-5 mm and moisture contents between 10- 50 % at furnace temperature of 1300°C were investigated at different residence times. From the results, it was observed that a combination of particle size and moisture content affected the devolatilisation process. For particle size >0.6 mm, the density of the particles is greater than the entrained gas velocity so the particles dropped to the collector probe faster. This resulted to incomplete devolatilisation. However, the effect of moisture was greater than particle size. With moisture content >10 %, incomplete devolatilisation was observed. This was because most of the heat in the furnace was used to evaporate the water. For burnout test, particle size >6 mm with moisture content >10 % had lower burnout value than particle size <6 mm and 10 % moisture content. Overall, moisture content still played significant role because the water content had to be completely driven off before complete burnout could be achieved.

10.2 INTRODUCTION

As more and more attention is being given to increasing the share of biomass fuels for heat and power generation (EREC, 2011, Tous et al., 2011), there has been increasing industrial interest in the combustion of pre-milled biomass materials in pulverised combustion systems, both in the co-firing of biomass with pulverised coal and more recently, in the suspension firing of 100% biomass. The efficiency of biomass combustion system depends on the moisture content of the fuel. Since the vaporisation uses energy released from the combustion process, it potentially lowers the temperature in the combustion chamber, which slows down the combustion process. This is because energy is needed to reduce the moisture content of the fuel (drying) before combustion starts. Dry biomass materials, therefore, do not need to be milled to the very fine, sub-millimetre particle sizes before firing or co-firing. This means that there is a relationship between biomass particle drying, devolatilisation rates and the char burnout levels, biomass particle size distribution and the total moisture content of biomass being fired. However, at industrial scale or in bigger combustion test rigs, it is difficult to achieve a sufficiently good level of control over such key fuel quality parameters. Therefore, a fundamental study was necessary to provide the basic process kinetic data which might be useful for CFD modelling of biomass combustion processes with varying moisture contents using the DTF.

10.3 THE DEVOLATILISATION TESTS

The analysis data for the products of the devolatilisation tests at 1300°C for a residence time of 200, 400 and 600 ms are presented in Tables 10.1 and 10.2, 10.3 and 10.4 and 10.5 and 10.6 respectively.

Looking in the first instance at the product moisture contents, there are a number of clear trends in the data. The moisture contents of the DTF products increased both with increasing feed material moisture content and with increasing particle size, as follows:

200 ms 3.8-6.8% H_2O (Table 10.1),

400 ms 3.3-6.6% H_2O (Table 10.3), and

600ms 1.2-6.8% H_2O (Table 10.5)

This is much as would be expected. It is also clear that even for the 0.6 mm fraction at an original moisture content of 10%, there was still some residual water, i.e. some of the larger wood particles in this size fraction had not completely dried out. The residual moisture level was clearly dependent on the residence time, as would be expected; i.e. after 200 ms, the residual moisture content was around 4%, whereas after 600 ms this had decreased to around 1.2%. It should be noted that the samples with very low very low values may also be affected by some moisture pick-up from the atmosphere during storage and handling.

The ash contents of the product chars also decrease with increasing moisture content and particle size, as would be expected. This indicated that decreasing

amounts of volatile organic material were lost from the larger, wetter particles during the drop tube experiments. This again, is much as would be expected. The volatile matter and fixed carbon contents of the drop tube product materials, both on an as produced basis and on a dry ash free basis, are also presented in Tables 10.1, 10.2, 10.3, 10.4, 10.5 and 10.6.

It is also possible, by using the ash contents of the materials as a tracer to provide an estimate of the extent of devolatilisation that occurred during the drop tube experiments. It should be noted, however, that the ash content of the parent sawdust material was relatively low, less than 0.5%, and this introduces significant errors into the use of the ash content as a tracer in this way as earlier noted in chapter 5 using smaller particle sizes with moisture content less than 10%. It should also be noted, as stated above, that some feeding difficulties were experienced with some of the samples, and particularly the wetter samples with the larger top sizes, and that this may have introduced further errors into the measurement of the % devolatilisation and % burnout, due to hang up of the feed material and inconsistencies in the conditions experienced by the particles.

The % devolatilisation values, expressed as a percentage of the original volatile matter measured wood pellets, are also presented in Tables 10.4a, 10.5a and 10.6a for the three different residence times, respectively. These values have been plotted against the original moisture content of the sawdust samples, for the 200, 400 and 600 ms residence times, in Figures 10.1, 10.2 and 10.3 respectively. It can be seen from the data on these plots that the % devolatilisation tended to decrease with increasing original moisture content and increasing particle top size, as would be expected. The trends are distorted to

some extent by the feeding difficulties that were experienced, particularly with the larger, wetter particles. These data indicate that, at a residence time of 600 ms at 1300°C, the % devolatilisation at the 600 ms residence time decreased with increasing top size, and depending on the original moisture content, as follows:

- 84-88% at 0.6 mm
- 46-73% at 1.18 mm
- 30-58% at 2 mm
- 47-64% at 3.15 mm, and
- 52-58% at 5 mm.

At 400 ms residence time, the values were:

- 45-79% at 0.6 mm
- 37-58% at 1.18 mm
- 40-67% at 2 mm, and
- 60-64 % at 3.15 mm.

At 200 ms residence time, the values were:

- 40-72% at 0.6 mm
- 43-50% at 1.18 mm
- 46-49% at 2 mm,
- 14-37% at 3.15 % and
- 28-43% at 5 mm

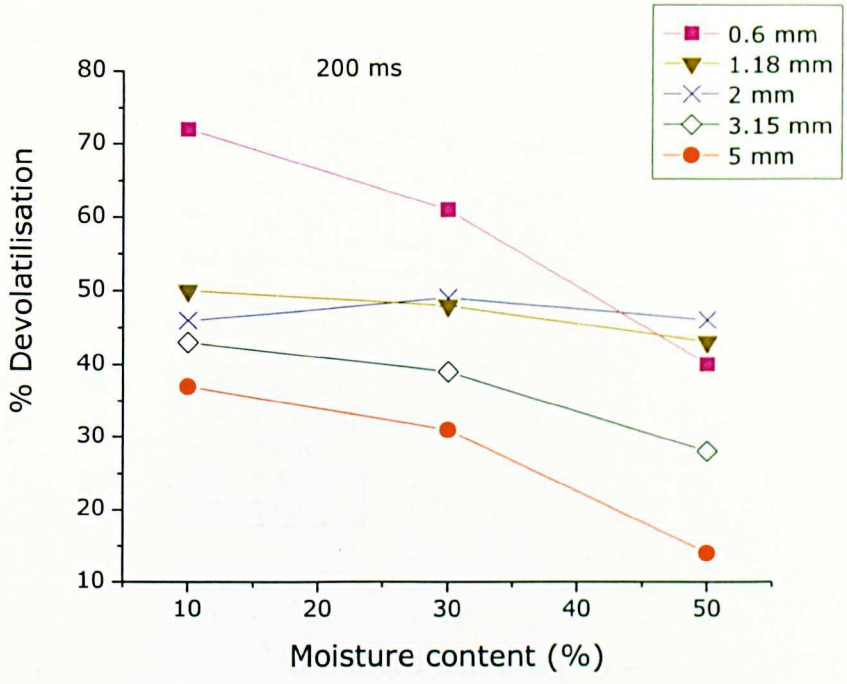

Figure 10.1 The calculated % devolatilisation values plotted against the moisture content for the tests with a residence time of 200 ms.

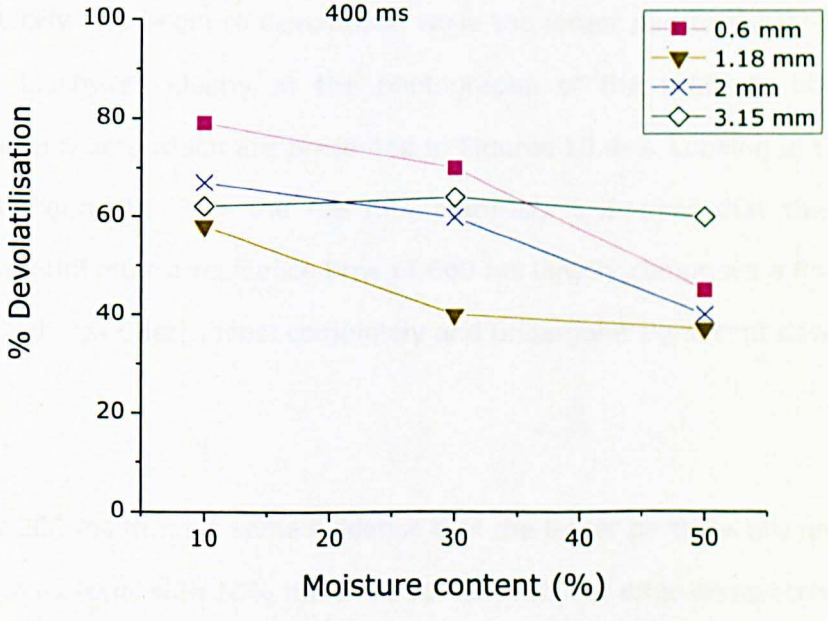

Figure 10.2 The calculated % devolatilisation values plotted against the moisture content for the tests with a residence time of 400 ms.

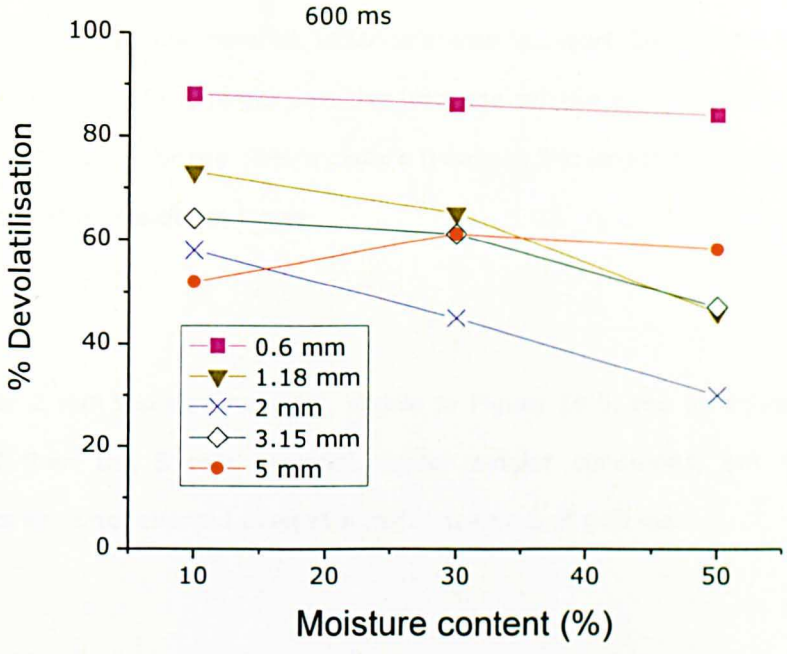

Figure 10.3 The calculated % devolatilisation values plotted against the moisture content for the tests with a residence time of 600 ms.

Clearly, the drying and devolatilisation processes are occurring simultaneously as the biomass particles pass through the hot zone. The finer particles dry relatively quickly and begin to devolatilise while the larger particles were still drying. This is illustrated clearly in the photographs of the products of the drop tube experiments which are presented in Figures 10.4-6. Looking in the first instance at Figure 10.4 for the 0.6 mm material, it is clear that the 10% moisture material after a residence time of 600 ms largely comprises a fine black powder, which has dried almost completely and undergone significant devolatilisation.

At 200 ms there is some evidence that the larger particles are not charred at all. The material with 50% moisture content had not dried completely even after 600 ms in the hot zone, and there is evidence that the larger particles are largely uncharred.

For the 5 mm top size material, which is shown in Figure 10.6, there is evidence of some charring of the larger particles from the sample with 10% moisture at all residence times. For the 50% moisture material, the larger particles are largely uncharred at all residence times.

With the 2 mm top size material, shown in Figure 10.5, the particles are more charred than the 5 mm material, under similar conditions, but the larger particles were not charred even at a residence time of 600 ms.

Table 10.1 Properties of the DTF chars from devolatilisation at a residence time of 200ms

Particle size, mm	Moisture, % w/w	Proximate analysis of DTF chars, (wt %, as produced)				DTF % Volatiles
		Moisture	Volatile	Ash	Fixed carbon	Based on original biomass
0.6	10%	3.83	74.97	1.88	19.32	72
	30%	4.83	76.68	1.36	17.13	61
	50%	4.62	77.95	0.88	16.55	40
1.18	10%	4.62	76.34	0.89	18.15	50
	30%	5.91	77.89	0.86	15.34	48
	50%	5.74	79.37	0.79	14.10	43
2	10%	4.68	78.41	0.87	16.04	46
	30%	5.78	79.19	0.91	14.12	49
	50%	6.20	78.89	0.87	14.04	46
3.15	10%	3.82	75.76	0.7	19.72	37
	30%	5.51	78.25	0.64	15.60	31
	50%	6.57	80.09	0.51	12.83	14
5 mm	10%	5.68	76.93	0.73	16.66	43
	30%	6.08	77.85	0.69	15.38	39
	50%	6.83	79.10	0.58	13.49	28

Table 10.2 Properties of the DTF chars from devolatilisation at a residence time of 200ms

Particle size, mm	Moisture, % w/w	Proximate analysis of DTF chars, wt % (dry and ash free basis)	
		Volatile	Fixed carbon
0.6	10%	79.51	20.49
	30%	81.74	18.26
	50%	82.49	17.51
1.18	10%	80.79	19.21
	30%	83.55	16.45
	50%	84.91	15.09
2	10%	83.02	16.98
	30%	84.87	15.13
	50%	84.89	15.11
3.15	10%	79.35	20.65
	30%	83.38	16.62
	50%	86.19	13.81
5	10%	82.20	17.80
	30%	83.50	16.50
	50%	85.43	14.57

Table 10.3 Properties of the DTF chars from devolatilisation at a residence time of 400ms

Particle size, mm	Moisture, % w/w	Proximate analysis of DTF chars (as produced), wt %				DTF % Volatiles
		Moisture	Volatile	Ash	Fixed carbon	Based on original biomass
0.6	10%	3.32	66.51	2.51	27.66	79
	30%	4.63	71.42	1.72	22.23	70
	50%	5.65	75.97	0.96	17.42	45
1.18	10%	4.75	73.39	1.07	20.79	58
	30%	4.05	76.58	0.75	18.62	40
	50%	5.77	77.69	0.71	15.83	37
2	10%	3.28	73.60	1.42	21.7	67
	30%	4.63	76.48	1.18	17.71	60
	50%	4.86	77.85	0.78	16.51	40
3.15	10%	3.55	74.78	1.16	20.51	62
	30%	4.07	77.62	1.20	17.11	64
	50%	6.57	77.74	1.09	14.6	60

Table 10.4 Properties of the DTF chars from devolatilisation at a residence time of 400ms

Particle size, mm	Moisture, % w/w	Proximate analysis of DTF chars, wt % (dry and ash free basis)	
		Volatile	Fixed carbon
0.6	10%	70.63	29.37
	30%	76.26	23.74
	50%	81.35	18.65
1.18	10%	77.93	22.07
	30%	80.44	19.56
	50%	83.07	16.93
2	10%	77.23	22.77
	30%	81.20	18.80
	50%	82.50	17.50
3.15	10%	78.48	21.52
	30%	81.94	18.06
	50%	84.19	15.81

Table 10.5 Properties of the DTF chars from devolatilisation at a residence time of 600ms

Particle size, mm	Moisture, % w/w	Proximate analysis of DTF chars, wt % (as produced)				DTF % Volatiles
		Moisture	Volatile	Ash	Fixed carbon	Based on original biomass
0.6	10%	1.23	59.16	4.12	35.49	88
	30%	2.17	66.42	3.63	27.78	86
	50%	3.13	70.06	3.38	23.43	84
1.18	10%	0.97	68.75	1.65	28.63	73
	30%	1.68	73.69	1.28	23.35	65
	50%	1.96	74.83	0.83	22.38	46
2	10%	1.93	74.69	1.12	22.26	58
	30%	4.98	76.47	0.85	17.70	45
	50%	5.05	76.88	0.67	17.40	30
3.15	10%	4.07	76.16	1.21	18.56	64
	30%	4.61	77.16	1.12	17.11	61
	50%	6.39	77.96	0.83	14.82	47
5	10%	4.11	76.49	0.87	18.53	52
	30%	6.23	77.13	1.07	15.57	61
	50%	6.79	77.85	1.00	14.36	58

Table 10.6 Properties of the DTF chars from devolatilisation at a residence time of 600ms.

Particle size, mm	Moisture, % w/w	Proximate analysis of DTF chars, wt % (dry and ash free basis)	
		Volatile	Fixed carbon
0.6	10%	62.50	37.50
	30%	70.51	29.49
	50%	74.94	25.06
1.18	10%	70.60	29.40
	30%	75.94	24.06
	50%	76.98	23.02
2	10%	77.04	22.96
	30%	81.20	18.80
	50%	81.54	18.46
3.15	10%	80.41	19.59
	30%	81.85	18.15
	50%	84.03	15.97
5	10%	80.50	19.50
	30%	83.20	16.80
	50%	84.43	15.57

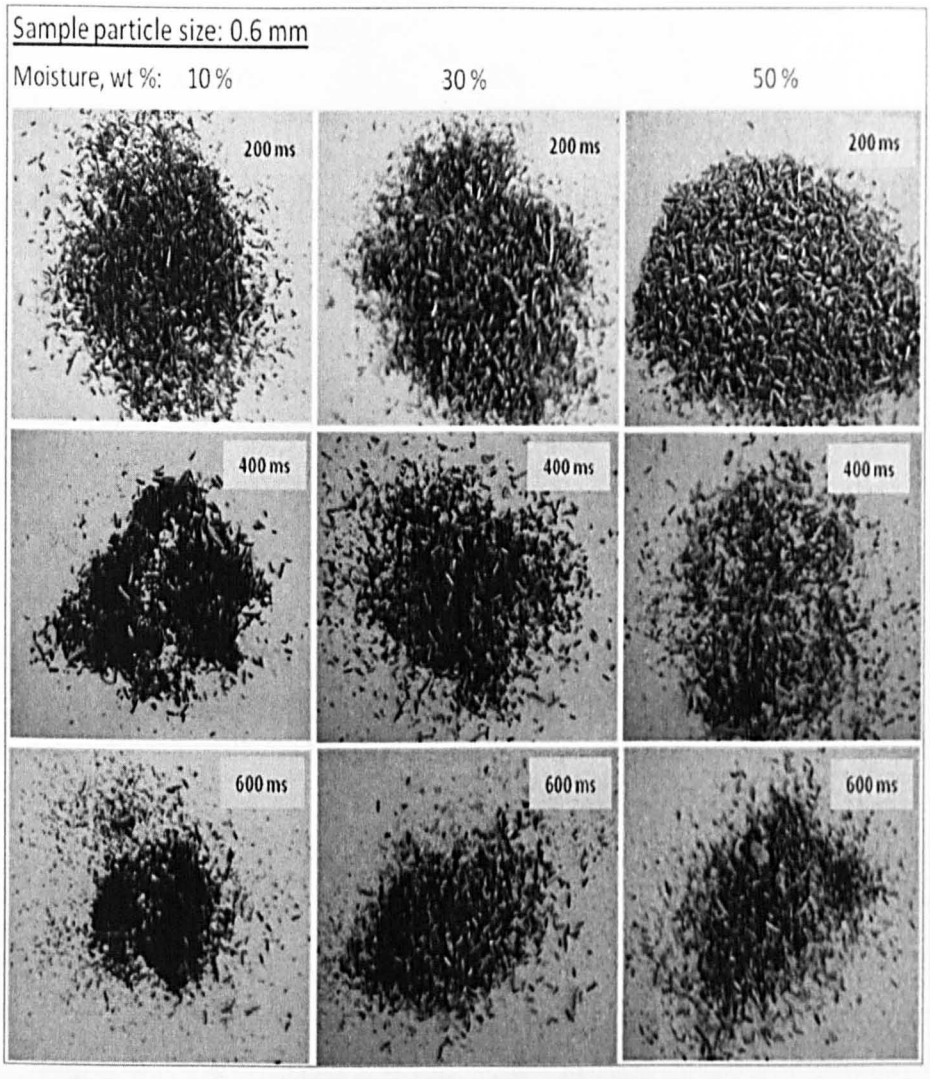

Figure 10.4 Photographs of the char from the devolatilisation test products for the 0.6 mm top size material with 10, 30 and 50% moisture and after residence times of 200, 400 and 600 ms.

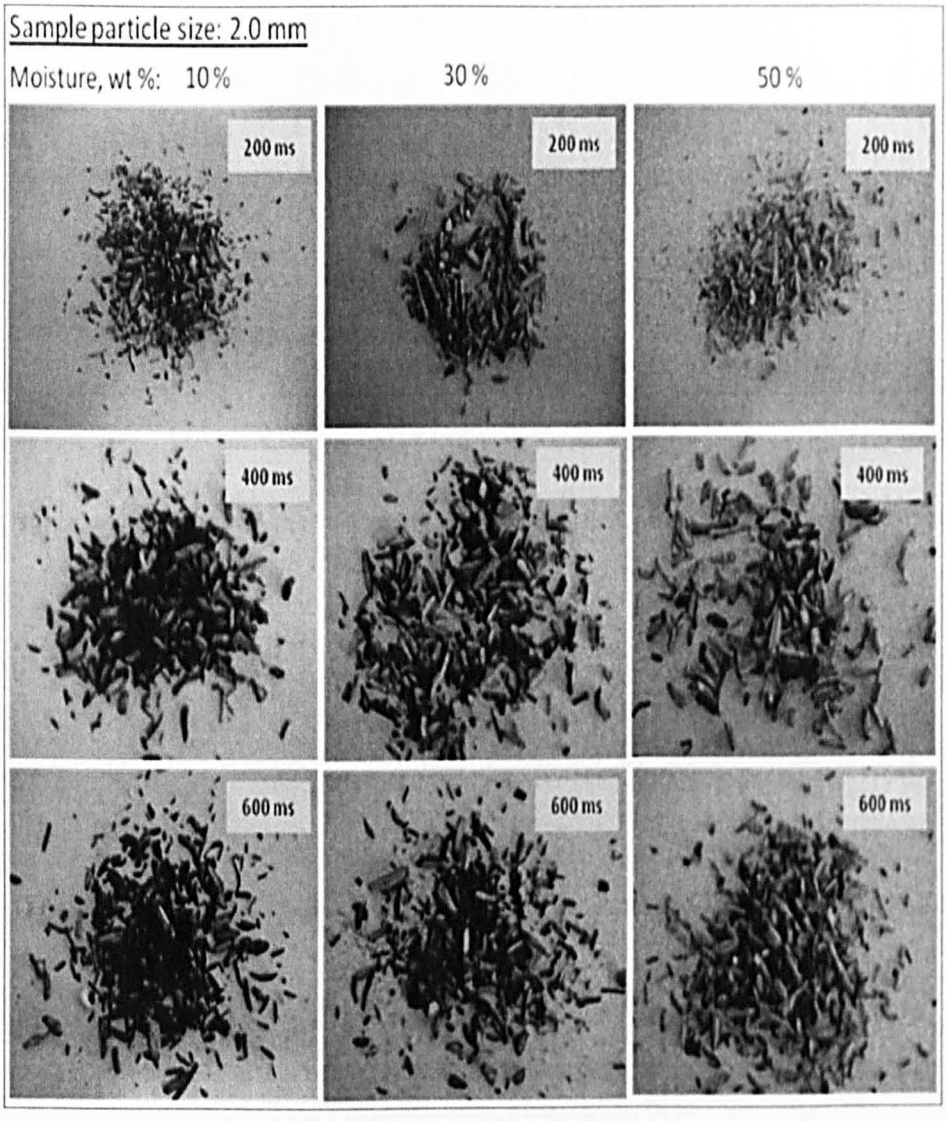

Figure 10.5 Photographs of the char from the devolatilisation test products for the 2.0 mm top size material with 10, 30 and 50% moisture and after residence times of 200, 400 and 600 ms.

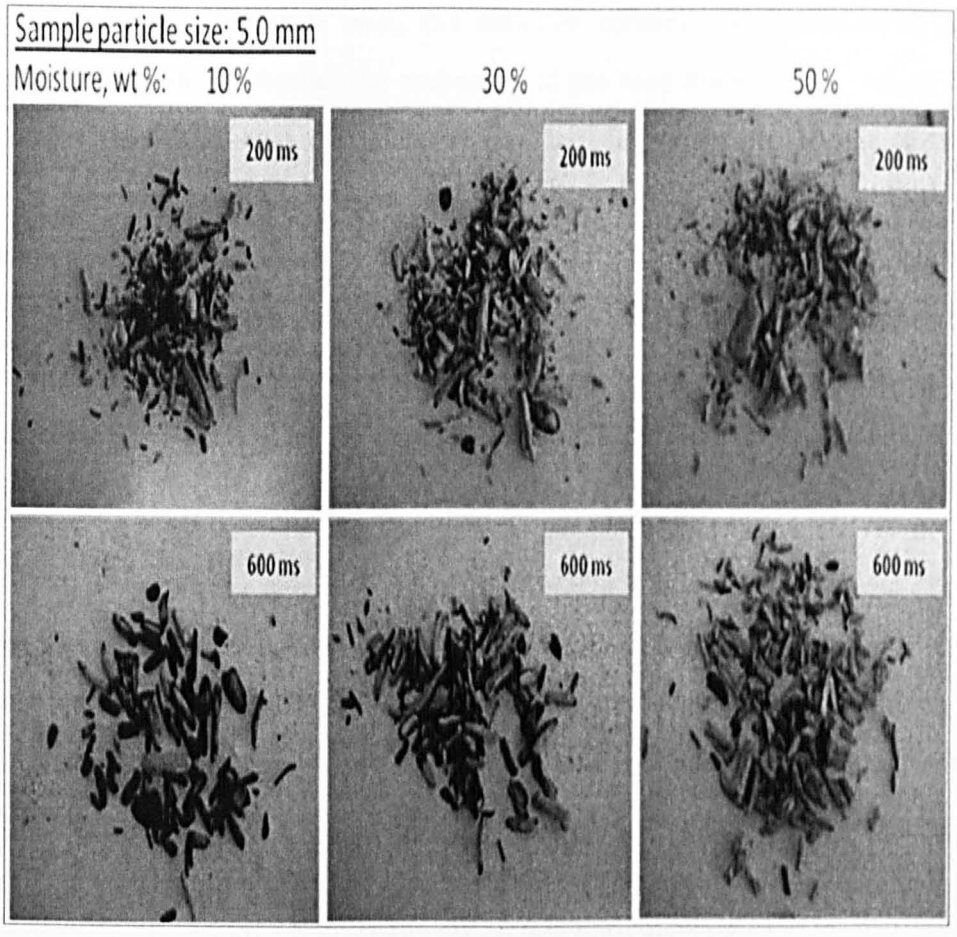

Figure 10.6 Photographs of the char from the devolatilisation test products for the 5.0 mm top size material with 10, 30 and 50% moisture and after 200, and 600 ms residence times.

10.4 THE CHAR COMBUSTION TESTS

As stated above, the combustion tests were performed under similar test conditions, but elevated oxygen concentrations, to provide the char burnout data, as a percentage by mass of the organic material, i.e. volatiles and fixed carbon, in the original sawdust samples. The results are listed in Table 10.7, and the % burnout values have been plotted against the residence time in Figure 10.7.

As with the devolatilisation tests, the moisture contents of the resultant char materials generally reflected the properties of the feed materials i.e. values for the chars from the <0.6 mm material with an initial moisture content of 10% were in the range 3-5%, whereas the values for the <2 mm material with an initial 40% moisture were in the range 6.5-7.2 %. Clearly there was still significant residual moisture after a residence time of 600 ms, indicating that the larger particles had not dried out and no devolatilisation and combustion had occurred.

The % burnout values generally reflect the top size and moisture contents of the feed materials, i.e. the % burnout value for the <0.6 mm material with 10% moisture, at a residence time of 600 ms, was 91%, whereas the value for the <2 mm material with 40% moisture at a residence time of 200 ms was only around 60%.

Table 10.7 Properties of the residues from DTF biomass burnout tests at 1300°C and residence times of 200, 400 and 600 ms.

size, mm	moisture content wt%	time, ms	Proximate analysis of DTF chars, wt % (as produced)				% burnout
			Moisture	Volatile	Ash	FC	Based on original biomass
0.6	10%	200	4.74	73.12	1.44	20.70	64
		400	3.78	65.14	2.03	29.05	74
		600	3.13	58.59	5.35	32.93	91
	40%	200	5.98	76.16	1.29	16.57	59
		400	5.00	73.28	1.23	20.49	57
		600	3.99	70.36	2.06	23.59	75
2	10%	200	5.70	73.02	0.99	20.29	53
		400	4.10	72.45	1.13	22.32	59
		600	4.16	70.29	1.32	24.23	65
	40%	200	6.55	77.56	1.16	14.73	60
		400	7.18	75.78	0.87	16.17	46
		600	6.51	73.09	1.21	19.19	61

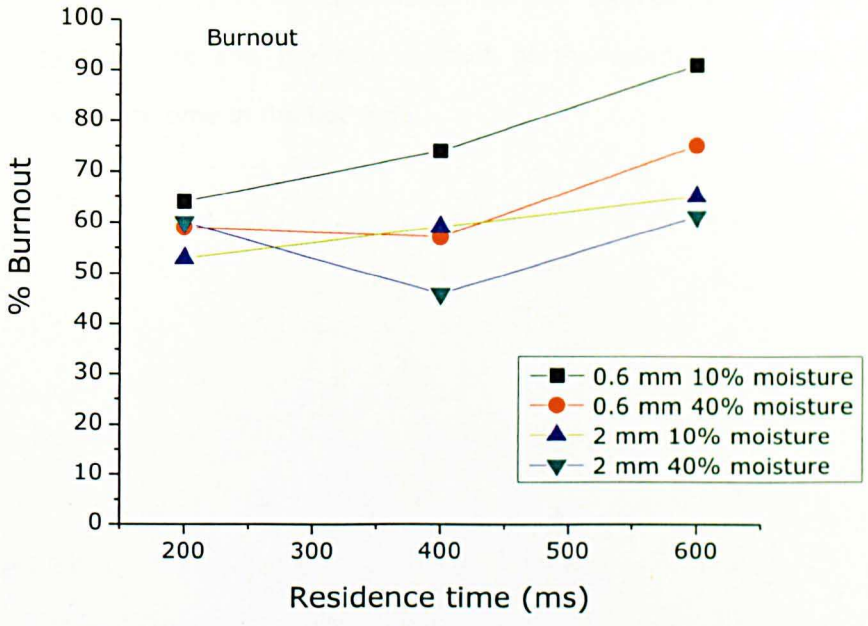

Figure 10.7 The % burnout values plotted against the residence times.

10.5 CONCLUSIONS

1. It is clear from the data presented above that the top size and the total moisture content of the sawdust particles and the drop tube residence time all had a significant impact on the devolatilisation and burnout of the sawdust particles.

2. The burnout values for the >0.6 and <2 mm materials were relatively low even at a residence time of 600 ms. Only the 0.6 mm 10% material at the 600 ms residence time provided higher devolatilisation and burnout.

3. The drop tube experiments were carried out at a peak hot zone temperature of around 1300°C, which is a little lower than would be

experienced in a pulverised fuel flame, however the results do indicate the sensitivity of the devolatilisation and combustion processes to the particle size and moisture content of the sawdust particles and the residence time in the hot zone.

11 GENERAL DISCUSSION AND RELEVANCE OF THIS STUDY

11.1 INTRODUCTION

The power generation sector is facing an increasing demand to cut its greenhouse carbon emissions due to the global concerns over climate change. Oxy-fuel combustion, which involves the combustion in O_2 and/or CO_2-enriched atmosphere, has been regarded as one of the viable CCS options which will enable the continuous use of fossil energy for power and heat generation. However, due to the dramatic change of the combustion environment, some fundamentally important issues have to be addressed adequately in order to aid the successful development and deployment of oxy-fuel firing technology. This PhD study presents experimental investigations into the combustion fundamentals of coal, biomass and their blends in oxy-fuel conditions in comparison to conventional air firing conditions. The experiments have been performed in TGA, DTF and a horizontal tube furnace simulating TGA conditions, supported by a range of characterisations with ICP-MS, SEM-EDAX and BET measurements etc.

11.2 TGA Characterisation of raw feedstock and/or chars

The fundamental studies carried out with TGA at low heating rates demonstrated that there exist fundamental differences in the devolatilisation and subsequent char burnout behaviour of sawdust under oxy-fuel and conventional air firing conditions.

The lower diffusivity of primary volatiles in CO_2 than in N_2 resulted in lower volatile matter yields at 700°C than in nitrogen. However, volatile yields obtained in CO_2 became significantly higher than those in N_2 with increasing temperatures to 1100°C. The higher volatile yields obtained for oxy-fuel conditions occurred as a result of CO_2-char gasification reaction, due to the rapidly increased CO_2 reactivity with the increasing temperatures.

TGA characterisation of the intrinsic reactivity of coal and biomass chars at lower temperatures (<500 °C) in TGA demonstrated that char burnout in oxy-firing condition was slightly lower compared to air firing, due to a combination of the lower O_2 diffusivity in CO_2 than in N_2 and the lower CO_2 reactivity at these temperatures. This partly explains why the ignition temperatures of fuels is higher in oxy-fuel than in air firing conditions at the same oxygen level or otherwise, higher O_2 concentration are needed in order to achieve similar fuel ignition or combustion performances in oxy-combustion.

The results also revealed that the proportion of nitrogen released into the volatile phase increased with increasing volatile yield for both air and oxy-firing conditions. However, more nitrogen was released into the volatile phase in oxy-fuel condition at 1100°C than in air firing condition signifying the potential importance of oxy-biomass firing or co-firing in industrial systems where combustion takes place at high temperatures.

11.3 DTF Testing of oxy-coal/biomass co-combustion

An innovative methodology was developed and validated in this work for the determination of biomass volatile matter yields in the DTF for those fuels containing extremely low ash contents, such as the biomass samples used in this

study. This method was based on the principle of the conventional ash tracer method, which has widely been used for coals which usually have much higher ash contents than biomass fuels, by doping high temperature calcined silica to the biomass feed to artificially increase the 'ash' contents of these samples.

The effect of using slightly oxidising environment (1% O_2), which is a common practice in DTF devolatilisation tests, was found to influence the volatile yields. It was observed that the volatile yields obtained in a gas stream containing 1% O_2 were higher than those without the addition of 1% O_2, and this effect became more pronounced with increasing residence times from 200 to 600 ms.

Coupled with other characterisation, a large number of DTF tests have been carried out in this study under a wide range of conditions, including different temperatures, residence times and variable coal/biomass co-firing ratios in both air and oxy-fuel conditions. Therefore, this presented work has led to improved fundamental knowledge and understanding of the oxy-fuel co-combustion of coal and biomass fuels in some fundamental important aspects, such as fuel devolatilisation, char burnout, nitrogen partitioning and biomass-contained mineral transformation and related possible synergistic catalytic effect on coal combustion.

11.4 Comparing TGA and DTF Experimental Results

An effort has been made trying to extrapolate the reactivity data of TGA chars to those of DTF char. It was found that the burning rate of DTF chars was considerably higher than those of their TGA counterpart, due to their dissimilar physical characteristics. SEM images and BET surface areas of these chars revealed differences in their char morphologies, reaffirming the different char properties accounting for their different burning rates. For instance, the SEM

images revealed that the TGA char retained the cell matrix of the parent biomass sample while the DTF biomass char experienced complete melting of the cellulose structure.

In addition, optical images showing the internal structures of the DTF chars revealed mixed porous structures of type I and II whilst the HTF (TGA replicated) char exhibited a mix dense and thick-walled textures of macropore network, which falls under the category of type II and III char networks. Therefore, it is evident that it will not be practicable to extrapolate TGA devolatilisation and char burnout characteristics to those of the DTF because of the large disparity in operating conditions.

11.5 DTF devolatilisation tests of biomass samples

Compared to N_2 atmosphere, sawdust devolatilisation in CO_2 at high temperatures DTF led to significantly higher volatile yields especially at the early stages of devolatilisation (200 ms). The impact of CO_2 on volatile matter yields in the DTF was higher than in nitrogen for all the temperatures and residence times examined in this work.

Like the TGA devolatilisation, the amount of fuel nitrogen released into the gaseous volatile phase was proportional to the yield of volatiles for both air and oxy-firing conditions. However, considerably higher proportions of fuel nitrogen were released into the volatile phase when devolatilisation was conducted in CO_2 than in nitrogen.

BET characterisation of the chars showed that devolatilisation in CO_2 gave rise to higher surface areas as a result of the activating effect of CO_2 due to CO_2-char gasification reaction.

11.6 The transformation and catalytic effect of Inherent biomass-contained Alkali and alkaline metals

When biomass char was blended with coal char, it was observed that the blends burn off significantly faster than the unblended coal chars in both air and oxy-firing conditions, highlighting the catalytic activity of biomass char blending on coal combustion reactivity. Further, it was also found that under oxy-firing condition, the catalytic effect was found to be more pronounced, with the coal and biomass char blends being able to burn off almost twice faster than the unblended coal chars.

Noticeably, the catalytic effect increases with increasing proportions of biomass char in the blends, suggesting that co-firing with high biomass ratios can potentially be a strategy to improve coal char burn-out performance in PF combustion.

Interestingly, the removal of alkali and alkaline metals from biomass led to dramatically reduced the reactivity of these char blends and in some cases, nearly complete loss of the catalytic activity, this confirming that these metals were responsible for the catalytic activity observed from biomass fuel blending.

11.7 DTF Co-devolatilisation of coal and biomass

Co-devolatilisation of coal and biomass samples in DTF also gave rise to higher volatile matter yields in Oxy-fuel conditions. While synergetic effect was observed for the co-devolatilisation tests in DTF, no synergy was found in the TGA conditions.

11.8 Wet biomass firing

Moisture content of biomass fuel affects its combustion behaviour. DTF firing tests of biomass samples having different particle sizes and moisture contents demonstrated that the particle size and in particular, the moisture content of the sawdust feedstock examined both had a major impact on the devolatilisation and char burnout performance of the sawdust sample. For instance, the burnout of the sawdust in the range of >0.6 and <2 mm with moisture content higher than 10% were extremely low even at 1300 °C and a residence time of 600 ms. Devolatilisation and burnout levels in excess of 90% were obtained only for the < 0.6 mm size fraction having a moisture content of less than 10 wt%.

11.9 OVERALL RELEVANCE OF THIS STUDY

11.9.1 *Devolatilisation*

This is an important aspect of solid fuel combustion because it determines the stability of the flame in the combustion system. This involves the release of gases such as CO_2 and H_2O. The concentration of these species in the flue gas is difference under oxy-fuel conditions compared to air firing. Devolatilisation behaviour and the impact of these species during oxy-fuel combustion have been investigated for the past decade. However, little information is available for oxy-biomass firing.

Therefore this data obtained in this study provides fundamental input required to model the devolatilisation behaviour of biomass fuels under oxy-firing. Also, the

innovative methodology developed will help to accurately determine volatile matter yields of biomass at high temperatures in the industrial systems.

11.9.2 *Char combustion*

The efficiency of a combustion system largely depends on the oxidation of the residual char after devolatilisation. Again, research is increasing on the burnout behaviour of coal chars under oxy-firing conditions and air firing (Gharebaghi et al., 2011a). Results obtained from such studies have been used to simulate the potential burnout behaviour in industrial burners. Also, CO_2-char gasification reactions occur during oxy-fuel firing and this has been incorporated into modelling oxy-coal combustion systems (Hecht et al., 2012). Therefore, the burnout propensity of sawdust obtained under oxy-firing will be useful input data to model the burning rate and burnout efficiency of the system.

To catalyse coal char burnout without incurring additional cost, inexpensive catalysts are needed. Addition of sawdust char to coal char improved coal char burnout due to the presence of alkali and alkaline earth metals inherent in biomass char. The burnout was significantly faster under oxy-fuel firing than under air firing. These findings pointed out that co-firing will reduce unburnt carbon in coal ash thereby making it saleable to other users.

11.9.3 *Emissions*

For conventional power plants to maintain the required generation capability using available and cost effective fuels and maintaining reliable operation and meeting emissions regulations, oxy-biomass firing or co-firing will be a viable option. NO_x formation during combustion is attributed to three reaction processes; the contribution from fuel bound nitrogen, oxidation from atmospheric nitrogen in the combustion system and interaction of hydrocarbons with atmospheric nitrogen.

The data provided nitrogen partitioning behaviour of sawdust under CO_2 and nitrogen atmosphere during devolatilisation. In predicting NO_x emissions, the data will be useful to solve a transport equation for nitric oxide (NO) concentration in the system.

11.10 INTENDED TARGET OF THE STUDY

This experimental study can directly impact the combustion modelling activities currently being conducted at the University of Nottingham and other project partners.

Other intended beneficiaries of this work are the power generation industry. Since conventional gas and coal-fired power stations will still provide most of the UK's electricity (DUKES, 2012), biomass firing or co-firing is set to become increasingly important as a means to mitigate greenhouse emissions from power generation sector. Recently, co-firing biomass at high ratios has received great focus (Fernando, 2012). The presented work has led to the improved understanding of coal and biomass co-combustion at high ratios. The significant catalytic activity found from biomass co-firing at high ratios may be of particular importance as to how the combustion efficiency of increasingly less reactive coals can be effectively improved via managed biomass co-firing.

11.11 APPLICATION OF THE DATA IN CFD MODELLING

Combustion modelling is critically important to the successful development of oxy-fuel technology. However, unlike conventional air-fired combustion, there is still a general lack of fundamental combustion data, in terms of fuel devolatilisation, char combustion, nitrogen partitioning, mineral transformation and in particular the contribution of CO_2-char gasification reactions. In terms of

the oxy-fuel combustion of coal and biomass fuels, the relevant information available for the combustion modelling is even less.

In order to predict biomass combustion performance using a CFD models in oxy-fuel combustion, biomass reactivity must be known. Inputs requirements include high temperature volatile matter release and char reactivity.

For example, the fundamental data on devolatilisation yields, amount of char formed, char composition and the burning rates of char have been obtained from both TGA and DTF. The DTF data provided can be applied in FG-DVC and model which has previously been used for biomass firing (Jones et al., 2000) and co-firing (Ma et al., 2009) to predict flame behaviour and temperature of the combustion system. Results obtained can also serve as input data for FG-Biomass codes to determine the devolatilisation behaviour of biomass. Moreover, modelling code such as Code_Saturne® has been employed to calculate combustion under oxy-coal condition considering char-CO_2 gasification reactions. This code may be applied to oxy-biomass combustion.

Furthermore the DTF data obtained in this study provide fundamental information to develop kinetic data for CFD models and extrapolate it to product formation under realistic condition. The char burnout kinetic model (CBK) is one of the modelling codes used for coal char combustion (Hurt et al., 1998). Recently, a modified version (CKB8) was used to model char burnout kinetics under oxy-fuel firing and the code is capable of predicting burnout extent in an acceptable range (Gharebaghi et al., 2011). A commercially available CFD code, ANSYS Fluent version 12.0 is also useful code for CFD modelling oxy-coal combustion. Presumably, some of these codes can be modified to model the data obtained in this study in order to design dedicated biomass oxy-firing or co-firing.

12 CONCLUSIONS AND FUTURE WORK

12.2 CONCLUSIONS

A fundamental study of co-firing biomass with coal under both air and oxy-fuel firing conditions has been conducted as a part of larger research programme to address the knowledge gaps associated with the ongoing development of oxy-fuel firing technology, which is regarded as one of new promising technologies to capture CO2 emissions from power plants. The results obtained in this study cover a range of fundamental aspects with respect to the oxy-combustion of coal and biomass over a wide range of co-firing ratios, with a particular focus on the potential synergistic effect of biomass-contained mineral matters on the overall combustion performances in terms of fuel devolatilisation and subsequent char burnouts and associated nitrogen partitioning behaviours. This experimental study has involved the use of a well-defined drop tube furnace (DTF), TGA and a horizontal tube furnace (HTF) simulating the TGA conditions for char preparation and other advanced characterisations, such as SEM-EDX, ICP-MS and BET measurements etc. This investigation has led to the following summary and conclusions:

1. A new unique methodology, named as silica tracer, has been developed and validated in this study in order to calculate more accurately the high temperature volatile yields and char burnout rates from DTF tests. Traditionally, an ash tracer methodology has long been used for calculating the volatile yields and char burnouts of coals in DTF studies. However, due to the very low ash contents of most biomass fuels, a large error can be incurred from using the traditional ash tracer method. In this new silica tracer method, high temperature calcined silica materials

having particle sizes similar to those of fuel and/or char samples was introduced into the samples as the artificial ash. The DTF results obtained from using the new methodology were found to be more re-producible and accurate as highlighted in a number of DTF tests and, more importantly, no evident effect of the silica's doping on biomass pyrolysis and combustion behaviour was found.

2. It was found that the devolatilisation of all biomass and coal samples under oxy-fuel conditions can lead to significantly higher yields of volatiles being produced compared to air-firing conditions in both DTF and HTF. However, the devolatilisation in DTF appears to be more pronounced than in HTF, due to the significantly higher temperatures and faster heating rates in the DTF reactor.

3. Both biomass and coal chars prepared from DTF and HTF burn off significantly faster in oxy-fuel than in air conditions at high combustion temperatures, highlighting the significant contribution of the CO2-enriched atmosphere to the improved char burnout performance. In addition, it was also found that under similar conditions, the chars generated from DTF is more reactive than the chars prepared in a HTF simulating TGA conditions, being indicative of the effect of the much higher heating rates in DTF on the reactivity of resultant chars.

4. The chars generated under all oxy-fuel conditions examined were found to have much higher specific surface areas than those of the chars prepared in air conditions, highlighting the significance of the char/CO_2 gasification reaction under oxy-fuel conditions. The gasification reaction can lead to more pronounced biomass/coal devolatilisation and improved char burnout performances.

5. Co-firing biomass at high ratios up to 50% in both air and oxy-fuel conditions led to significantly improved char combustion performances. It was found that the biomass/coal char blends burn off significantly faster than the unblended coal chars in both air and CO_2, highlighting the catalytic activity of biomass char blending on coal combustion reactivity. The catalytic effect increases dramatically with increasing proportions of biomass char in the blends.

6. The catalytic effects were found to be considerably more pronounced in CO_2-rich or oxy-fuel conditions, with the coal and biomass char blends being able to burn off almost up to twice faster than the unblended coal chars.

7. Under oxy-fuel conditions, the CO_2/char gasification reactions appear to be preferentially catalysed with biomass blending. This may lead to increased char surface areas and enhanced transformation and mobilisation of biomass-contained catalytically active mineral matters, which may together account for the particularly improved char burnout performance of the char blends in oxy-fuel conditions.

8. The removal of alkali and alkaline- metals from biomass via a well-defined acid leaching process resulted in the nearly complete loss of the catalytic activity of biomass char, confirming that they were responsible for the catalytic activity observed from co-firing biomass in high percentages.

9. Although combustion modelling was not involved in this experimental study, it is envisaged that the fundamentally important results obtained in this investigation can effectively be used to aid the combustion

modelling of biomass co-firing particularly in high percentages in both oxy-fuel and air-firing conditions. Co-firing biomass at high ratios has received huge interest over recent years as an effective means to reduce CO2 emissions from coal-fired power generation sector.

12.3 SUGGESTIONS FOR FURTHER WORK

This study has demonstrated that co-firing biomass at high ratios in both air and oxy-fuel conditions can give rise to significantly improved combustion performances, particularly in oxy-fuel conditions. In order to aid the ongoing development of oxy-fuel firing technology and/or to optimise the biomass co-firing operation at high ratios in power plants, the following areas of further investigation are of interest:

1 In oxy-coal firing, it has been reported that O_2 concentrations in the range of 30-40% are required to produce temperature profiles matching those of conventional air firing condition. However, given the significantly improved char burnout performances due to the synergistic catalytic effect of biomass co-firing, it may worth to investigate whether biomass co-firing particularly in high percentages can lead to lower O_2 concentrations needed for stable oxy-coal/biomass combustion, compared to oxy-coal combustion.

2 The catalytic effect of biomass-contained alkali and alkaline metals on coal combustion is potentially important as complete coal char burnout becomes increasingly more difficult nowadays to achieve, because of a combination of the increasing amount of unreactive inertinite in internationally traded coals and the use of low NO_x burners. It will be of

importance to investigate how biomass co-firing can potential affect the ignition behaviours of coal/biomass fuel feedstock as a whole.

3 Due to the limitations of the DTF at present, the shortest residence time achieved for DTF devolatilisation and char burnout tests in this study was 200 ms, which may not be short enough to obtain the fundamentally important kinetic parameters at very early stages of devolatilisation/char burnout. Therefore, the devolatilisation and char burnout behaviours of biomass and coal at very short residence times (e.g 25 to 100 ms) may need to examined in order to better related combustion modelling.

4 In this study, only wood-derived biomass samples were investigated, and these biomass materials are usually treated as the quality biomass feedstock. However, in an increasingly carbon-restrained world, firing and co-firing of difficult biomass fuels (e.g. biomass with difficult physical properties, wet biomass fuels and fuels with difficult ashes) is set to receive increasing interest. Oxy-fuel combustion may provide a sound combustion environment for these difficult biomass fuels, and this needs to be investigated.

REFERENCES

ABOULKAS, A., EL HARFI, K. E., NADIFIYINE, M. & EL BOUADILI, A. 2008. Investigation on pyrolysis of Moroccan oil shale/plastic mixtures by thermogravometric analysis. *Fuel Processing Technology,* 89, 1000-1006.

ADAMS, R. G., ALIN, J., BIEDE, O., BOOTH, N. J., DEMONTIGNY, D., DREW, R., IDEM, R., LAURSEN, M., PERALTA-SOLORIO, D., SANPASERTPARNICH, T. & TRUNKFIELD, A. 2009. CAPRICE project—Engineering study on the integration of post combustion capture technology into the power plant gas path and heat cycle. *Energy Procedia,* 1, 3801-3808.

ADANEZ, J., DE DIEGO, L. F., GARCIA-LABIANO, F., ABAD, A. & ABANADES, J. C. 2001. Determination of Biomass Char Combustion Reactivities for FBC Applications by a Combined Method. *Industrial & Engineering Chemistry Research,* 40, 4317-4323.

AMBALAE, A., MAHINPEY, N. & FREITAG, N. 2006. Thermogravimetric Studies on Pyrolysis and Combustion Behavior of a Heavy Oil and Its Asphaltenes.

AMUTIO, M., LOPEZ, G., AGUADO, R., ARTETXE, M., BILBAO, J. & OLAZAR, M. 2011a. Kinetic study of lignocellulosic biomass oxidative pyrolysis. *Fuel.*

ANNAMALAI, K., THIEN, B. & SWEETEN, J. 2003. Co-firing of coal and cattle feedlot biomass (FB) fuels. Part II. Performance results from 30 kWt (100,000) BTU/h laboratory scale boiler burner[small star, filled]. *Fuel,* 82, 1183-1193.

ARENILLAS, A., RUBIERA, F., PARRA, J. B. & PIS, J. J. 2002b. Influence of char structure on reactivity and nitric oxide emissions. *Fuel Processing Technology,* 77-78, 103-109.

ARIAS, B., PEVIDA, C., RUBIERA, F. & PIS, J. J. 2008. Effect of biomass blending on coal ignition and burnout during oxy-fuel combustion. *Fuel,* 87, 2753-2759.

ASADULLAH, M., ZHANG, S., MIN, Z., YIMSIRI, P. & LI, C.-Z. 2009. Importance of Biomass Particle Size in Structural Evolution and Reactivity of Char in Steam Gasification. *Industrial & Engineering Chemistry Research,* 48, 9858-9863.

ASADULLAH, M., ZHANG, S., MIN, Z., YIMSIRI, P. & LI, C.-Z. 2010b. Effects of biomass char structure on its gasification reactivity. *Bioresource Technology,* 101, 7935-7943.

BACKREEDY, R. I., HABIB, R., JONES, J. M., POURKASHANIAN, M. & WILLIAMS, A. 1999. An extended coal combustion model. *Fuel,* 78, 1745-1754.

BACKREEDY, R. I., JONES, J. M., POURKASHANIAN, M. & WILLIAMS, A. 2003. Burn-out of pulverised coal and biomass chars[small star, filled]. *Fuel,* 82, 2097-2105.

BAILEY, J. G., TATE, A., DIESSEL, C. F. K. & WALL, T. F. 1990. A char morphology system with applications to coal combustion. *Fuel,* 69, 225-239.

BAIN, R. L., OVEREND, R. P. & CRAIG, K. R. 1998. Biomass-fired power generation. *Fuel Processing Technology,* 54, 1-16.

BALLANTYNE, T. R., ASHMAN, P. J. & MULLINGER, P. J. 2005. A new method for determining the conversion of low-ash coals using synthetic ash as a tracer. *Fuel,* 84, 1980-1985.

BARRANCO, R. 2001. *The characterization and combustion of South American coals, PhD Thesis.* PhD Thesis, University of Nottingham.

BASU, P., BUTLER, J. & LEON, M. A. 2011. Biomass co-firing options on the emission reduction and electricity generation costs in coal-fired power plants. *Renewable Energy,* 36, 282-288.

BAXTER, L. 2005. Biomass-coal co-combustion: opportunity for affordable renewable energy. *Fuel,* 84, 1295-1302.

BECHER, V., BOHN, J.-P., GOANTA, A. & SPLIETHOFF, H. 2011. A combustion concept for oxyfuel processes with low recirculation rate - Experimental validation. *Combustion and Flame,* 158, 1542-1552.

BERGGREN, M. R., LJUNGGREN, E. & JOHNSSON, F. 2008. Biomass co-firing potentials for electricity generation in Polandâ€"Matching supply and co-firing opportunities. *Biomass and Bioenergy,* 32, 865-879.

BERKOWITZ, N. 1994. *An introduction to coal technology* Academic press Inc. .

BIAGINI, E., BARONTINI, F. & TOGNOTTI, L. 2006. Devolatilization of Biomass fuels and Biomass components studied by TG/FTIR technique. *Industrial & Engineering Chemistry Research,* 45, 4486-4493.

BIAGINI, E., FANTEI, A. & TOGNOTTI, L. 2008b. Effect of the heating rate on the devolatilization of biomass residues. *Thermochimica Acta,* 472, 55-63.

BIAGINI, E., LIPPI, F., PETARCA, L. & TOGNOTTI, L. 2002a. Devolatilization rate of biomasses and coal-biomass blends: an experimental investigation. *Fuel,* 81, 1041-1050.

BIAGINI, E., NARDUCCI, P. & TOGNOTTI, L. 2008a. Size and structural characterization of lignin-cellulosic fuels after the rapid devolatilization. *Fuel,* 87, 177-186.

BIAGINI, E., SIMONE, M. & TOGNOTTI, L. 2009. Characterization of high heating rate chars of biomass fuels. *Proceedings of the Combustion Institute,* 32, 2043-2050.

BISWAS, S., CHOUDHURY, N., SARKAR, P., MUKHERJEE, A., SAHU, S. G., BORAL, P. & CHOUDHURY, A. 2006. Studies on the combustion behaviour of blends of Indian coals by TGA and Drop Tube Furnace. *Fuel Processing Technology,* 87, 191-199.

BLESA, M. J., MIRANDA, J. L., MOLINER, R., IZQUIERDO, M. T. & PALACIOS, J. M. 2003. Low-temperature co-pyrolysis of a low-rank coal and biomass to prepare smokeless fuel briquettes. *Journal of Analytical and Applied Pyrolysis,* 70, 665-677.

BORREGO, A. G. & ALVAREZ, D. 2007. Comparison of Chars Obtained under Oxy-Fuel and Conventional Pulverized Coal Combustion Atmospheres. *Energy Fuels,* 21, 3171-3179.

BORREGO, A. G., GARAVAGLIA, L. & KALKREUTH, W. D. 2009. Characteristics of high heating rate biomass chars prepared under N2 and CO2 atmospheres. *International Journal of Coal Geology,* 77, 409-415.

BOYLAN, D., BUSH, V. & BRANSBY, D. I. 2000. Switchgrass cofiring: pilot scale and field evaluation. *Biomass and Bioenergy,* 19, 411-417.

BP. June 2012. BP Statistical Review of World Energy, bp.com/statisticalreview.

BROWN, R. C., LIU, Q. & NORTON, G. 2000. Catalytic effects observed during the co-gasification of coal and switchgrass. *Biomass and Bioenergy,* 18, 499-506.

BUHRE, B. J. P., ELLIOTT, L. K., SHENG, C. D., GUPTA, R. P. & WALL, T. F. 2005. Oxy-fuel combustion technology for coal-fired power generation. *Progress in Energy and Combustion Science,* 31, 283-307.

CAI, H. Y., GÜELL, A. J., CHATZAKIS, I. N., LIM, J. Y., DUGWELL, D. R. & KANDIYOTI, R. 1996. Combustion reactivity and morphological change in coal chars: Effect of pyrolysis temperature, heating rate and pressure. *Fuel,* 75, 15-24.

CAI, J., WANG, Y., ZHOU, L. & HUANG, Q. 2008. Thermogravimetric analysis and kinetics of coal/plastic blends during co-pyrolysis in nitrogen atmosphere. *Fuel Processing Technology,* 89, 21-27.

CAO, H., SUN, S., LIU, Y. & WALL, T. F. 2010. Computational Fluid Dynamics Modeling of NOx Reduction Mechanism in Oxy-Fuel Combustionâ€ *Energy & Fuels,* 24, 131-135.

CARBO, M. C., JANSEN, D., BOON, J., DIJKSTRA, J. W., VAN DEN BRINK, R. W. & VERKOOIJEN, A. H. M. 2009. Staged water-gas shift configuration: Key to efficiency penalty reduction during pre-combustion decarbonisation in IGCC. *Energy Procedia,* 1, 661-668.

CARRONI, R., SCHMIDT, V. & GRIFFIN, T. 2002. Catalytic combustion for power generation. *Catalysis Today,* 75, 287-295.

CCC 2009. Decarbonising the GB power sector: evaluating investment pathways, generation patterns and emissions through to 2030. The Committee on Climate Change, September 2009 Working Draft Report_v1.doc. .

CETIN, E., GUPTA, R. & MOGHTADERI, B. 2005. Effect of pyrolysis pressure and heating rate on radiata pine char structure and apparent gasification reactivity. *Fuel,* 84, 1328-1334.

CETIN, E., MOGHTADERI, B., GUPTA, R. & WALL, T. F. 2004. Influence of pyrolysis conditions on the structure and gasification reactivity of biomass chars. *Fuel,* 83, 2139-2150.

CETINKAYA, S. & YU¨RU¨M, Y. 2000. Oxidative pyrolysis of Turkish lignites in air up to 500Â°C. *Fuel Processing Technology,* 67, 177-189.

CHAO, C. Y. H., KWONG, P. C. W., WANG, J. H., CHEUNG, C. W. & KENDALL, G. 2008. Co-firing coal with rice husk and bamboo and the impact on particulate matters and associated polycyclic aromatic hydrocarbon emissions. *Bioresource Technology,* 99, 83-93.

CHIARAMONTI, D., OASMAA, A. & SOLANTAUSTA, Y. 2007. Power generation using fast pyrolysis liquids from biomass. *Renewable and Sustainable Energy Reviews,* 11, 1056-1086.

CHOU, C.-L. 2001. *ORIGINS AND EVOLUTION OF SULFUR IN COALS, GSA Annual Meeting, November 5-8,*

Boston, Massachusetts, https://gsa.confex.com/gsa/2001AM/finalprogram/abstract_20186.htm [Online].

CHOUDHURY, N., BISWAS, S., SARKAR, P., KUMAR, M., GHOSAL, S., MITRA, T., MUKHERJEE, A. & CHOUDHURY, A. 2008. Influence of rank and macerals on the burnout behaviour of pulverized Indian coal. *International Journal of Coal Geology,* 74, 145-153.

CHUI, E. H., DOUGLAS, M. A. & TAN, Y. 2003. Modeling of oxy-fuel combustion for a western Canadian sub-bituminous coal[small star, filled]. *Fuel,* 82, 1201-1210.

CLOKE, M., LESTER, E. & GIBB, W. 1997. Characterization of coal with respect to carbon burnout in p.f.-fired boilers. *Fuel,* 76, 1257-1267.

CLOKE, M., WU, T., BARRANCO, R. & LESTER, E. 2003. Char characterisation and its application in a coal burnout model[small star, filled]. *Fuel,* 82, 1989-2000.

CONESA, J. A., MARCILLA, A., CABALLERO, J. A. & FONT, R. 2001. Comments on the validity and utility of the different methods for kinetic analysis of thermogravimetric data. *Journal of Analytical and Applied Pyrolysis,* 58-59, 617-633.

CORDERO, T., RODRÍGUEZ-MAROTO, J. M., GARCÍA, F. & RODRÍGUEZ, J. J. 1991. Thermal decomposition of wood in oxidizing atmosphere. A kinetic study from non-isothermal TG experiments. *Thermochimica Acta,* 191, 161-178.

CORDERO, T., RODRÍGUEZ-MAROTO, J. M., RODRÍGUEZ-MIRASOL, J. & RODRÍGUEZ, J. J. 1990. On the kinetics of thermal decomposition of wood and wood components. *Thermochimica Acta,* 164, 135-144.

CROISET, E. & THAMBIMUTHU, K. V. 2001. NOx and SO2 emissions from O2/CO2 recycle coal combustion. *Fuel,* 80, 2117-2121.

DAMARTZIS, T., KOSTOGLOU, M. & ZABANIOTOU, A. 2009. Simulation of the Agro-Biomass(Olive Kernel) Fast Pyrolysis in a Wire Mesh Reactor Considering Intra-particle Radial and temporal Distribution of Products. *INTERNATIONAL JOURNAL OF CHEMICAL REACTOR ENGINEERING,* 7, 1-31.

DARE, P., GIFFORD, J., HOOPER, R. J., CLEMENS, A. H., DAMIANO, L. F., GONG, D. & MATHESON, T. W. 2001. Combustion performance of biomass residue and purpose grown species. *Biomass and Bioenergy,* 21, 277-287.

DAVIDSON, R. M. & SANTOS, S. O. 2010. Oxyfuel combustion of pulverised coal, IEA Report, CCC/168 (ISBN: 978-92-9029-488-7).

DECC. 2012a. Renewable Heat Incentive: Providing certainty, improving performance, Department of Energy and Climate Change.

DECC 2012b. Government response to the consultation on proposals for the levels of banded support under the Renewables Obligation for the period 2013-17 and the Renewables Obligation order 2012, HM Government.

DEMIRBAS, A. 2003. Sustainable cofiring of biomass with coal. *Energy Conversion and Management,* 44, 1465-1479.

DEMIRBAS, A. 2004. Combustion characteristics of different biomass fuels. *Progress in Energy and Combustion Science,* 30, 219-230.

DEMIRBAS, A. 2005. Potential applications of renewable energy sources, biomass combustion problems in boiler power systems and combustion related environmental issues. *Progress in Energy and Combustion Science,* 31, 171-192.

DI BLASI, C. 2009. Combustion and gasification rates of lignocellulosic chars. *Progress in Energy and Combustion Science,* 35, 121-140.

DI BLASI, C. & BRANCA, C. 2001. Kinetics of Primary Product Formation from Wood Pyrolysis. *Industrial & Engineering Chemistry Research,* 40, 5547-5556.

DI BLASI, C., BUONANNO, F. & BRANCA, C. 1999a. Reactivities of some biomass chars in air. *Carbon,* 37, 1227-1238.

DI NOLA, G., DE JONG, W. & SPLIETHOFF, H. 2010. TG-FTIR characterization of coal and biomass single fuels and blends under slow heating rate conditions: Partitioning of the fuel-bound nitrogen. *Fuel Processing Technology,* 91, 103-115.

DOMENICHINI, R., GASPARINI, F., COTONE, P. & SANTOS, S. 2011. Techno-economic evaluation of biomass fired or co-fired power plants with post combustion CO2 capture. *Energy Procedia,* 4, 1851-1860.

DONG, C., YANG, Y., YANG, R. & ZHANG, J. 2010a. Numerical modeling of the gasification based biomass co-firing in a 600 MW pulverized coal boiler. *Applied Energy,* 87, 2834-2838.

DONG, L., GAO, S. & XU, G. 2010b. NO Reduction over Biomass Char in the Combustion Process. *Energy & Fuels,* 24, 446-450.

DRAGE, T. C., SMITH, K. M., ARENILLAS, A. & SNAPE, C. E. 2009. Developing strategies for the regeneration of polyethylenimine based CO2 adsorbents. *Energy Procedia,* 1, 875-880.

DUKES. 2012. Digest of UK Energy Statistics 2012, London, TSO.

EDGE, P., GHAREBAGHI, M., IRONS, R., PORTER, R., PORTER, R. T. J., POURKASHANIAN, M., SMITH, D., STEPHENSON, P. & WILLIAMS, A. 2011. Combustion modelling opportunities and challenges for oxy-coal carbon capture technology. *Chemical Engineering Research and Design,* 89, 1470-1493.

EKINS, P. 2004. Step changes for decarbonising the energy system: research needs for renewables, energy efficiency and nuclear power. *Energy Policy,* 32, 1891-1904.

ENCINAR, J. M., GONZÁLEZ, J. F. & GONZÁLEZ, J. 2000. Fixed-bed pyrolysis of Cynara cardunculus L. Product yields and compositions. *Fuel Processing Technology,* 68, 209-222.

EREC 2010. European Renewable Energy Council.

EREC 2011. *European Renewable Energy Council.*

EVANS, A., STREZOV, V. & EVANS, T. J. 2010. Sustainability considerations for electricity generation from biomass. *Renewable and Sustainable Energy Reviews,* 14, 1419-1427.

EVERSON, R. C., NEOMAGUS, H. W. J. P., KASAINI, H. & NJAPHA, D. 2006. reaction Kinetics of pulverized coal-chars derived from inertinite-rich coal discard: Characterisation and combustion. *Fuel,* 85, 1067-1075.

FANG, H., HAIBIN, L. & ZENGLI, Z. 2009. Advancements in Development of Chemical-Looping Combustion: A Review. *International Journal of Chemical Engineering*.

FENG, B. & BHATIA, S. K. 2002. On the validity of thermogravimetric determination of carbon gasification kinetics. *Chemical Engineering Science,* 57, 2907-2920.

FERMOSO, J., GIL, M. V., PEVIDA, C., PIS, J. J. & RUBIERA, F. 2010b. Kinetic models comparison for non-isothermal steam gasification of coal-biomass blend chars. *Chemical Engineering Journal,* 161, 276-284.

FERNANDO, R. 2012. Co-firing High Ratios of Biomass with Coal; IEA Report, CCC/194 (ISBN: 978-92-9029-514-3).

FOLGUERAS, M. B., DAIAZ, R. M. & XIBERTA, I. P. 2003. Thermogravimetric analysis of the co-combustion of coal and sewage sludge. *Fuel,* 82, 2051-2055.

FUSHIMI, C., ARAKI, K., YAMAGUCHI, Y. & TSUTSUMI, A. 2003. Effect of Heating Rate on Steam Gasification of Biomass. 1. Reactivity of Char. *Industrial & Engineering Chemistry Research,* 42, 3922-3928.

GANI, A., MORISHITA, K., NISHIKAWA, K. & NARUSE, I. 2005a. Characteristics of co-combustion of low-rank coal with biomass. *Energy & Fuels,* 19, 1652-1659.

GANI, A. & NARUSE, I. 2007. Effect of cellulose and lignin content on pyrolysis and combustion characteristics for several types of biomass. *Renewable Energy,* 32, 649-661.

GHAREBAGHI, M., IRONS, R., POURKASHANIAN, M. & WILLIAMS, A. 2011. An investigation into a carbon burnout kinetic model for oxy-coal combustion. *fuel Processing Technology,* 92, 2455-2464.

GHAREBAGHI, M., IRONS, R. M., POURKASHANIAN, M. & WILLIAMS, A. 2011a. An investigation into a carbon burnout kinetic model for oxy-coal combustion. *Fuel Processing Technology,* 92, 2455-2464.

GIL, M. V., CASAL, D., PEVIDA, C., PIS, J. J. & RUBIERA, F. 2010. Thermal behaviour and kinetics of coal/biomass blends during co-combustion. *Bioresource Technology,* 101, 5601-5608.

GIL, M. V., RIAZA, J., ÁLVAREZ, L., PEVIDA, C., PIS, J. J. & RUBIERA, F. 2012. Oxy-fuel combustion kinetics and morphology of coal chars obtained in N2 and CO2 atmospheres in an entrained flow reactor. *Applied Energy,* 91, 67-74.

GLARBORG, P., JENSEN, A. D. & JOHNSSON, J. E. 2003. Fuel nitrogen conversion in solid fuel fired systems. *Progress in Energy and Combustion Science,* 29, 89-113.

GONG, X., GUO, Z. & WANG, Z. 2010. Reactivity of pulverized coals during combustion catalyzed by CeO2 and Fe2O3. *Combustion and Flame,* 157, 351-356.

GONZÁLEZ, J. F., ENCINAR, J. M., CANITO, J. L., SABIO, E. & CHACÓN, M. 2003. Pyrolysis of cherry stones: energy uses of the different fractions and kinetic study. *Journal of Analytical and Applied Pyrolysis,* 67, 165-190.

GONZÁLEZ, J. F., ROMÁN, S., ENCINAR, J. M. & MARTÍNEZ, G. 2009. Pyrolysis of various biomass residues and char utilization for the production of activated carbons. *Journal of Analytical and Applied Pyrolysis,* 85, 134-141.

GRONLI, M. G., VARHEGYI, G. & DI BLASI, C. 2002. Thermogravimetric Analysis and Devolatilization Kinetics of Wood. *Industrial & Engineering Chemistry Research,* 41, 4201-4208.

GUERRERO, M., RUIZ, M. P., ALZUETA, M. U., BILBAO, R. & MILLERA, A. 2005. Pyrolysis of eucalyptus at different heating rates: studies of char characterization and oxidative reactivity. *Journal of Analytical and Applied Pyrolysis,* 74, 307-314.

GUO, J. & LUA, A. C. 2001. Kinetic study on pyrolytic process of oil-palm solid waste using two-step consecutive reaction model. *Biomass and Bioenergy,* 20, 223-233.

HAHN, W., PARK, C. S., KIM, S. O. & CHOI, S. I. 2003. Characteristics of NOx reduction in pulverized coals combustion using drop tube furnace. *Journal of Industrial and Engineering Chemistry,* 9, 275-280.

HASAN KHAN TUSHAR, M. S., MAHINPEY, N., KHAN, A., IBRAHIM, H., KUMAR, P. & IDEM, R. 2012. Production, characterization and reactivity studies of chars produced by the isothermal pyrolysis of flax straw. *Biomass and Bioenergy,* 37, 97-105.

HAYKIRI-ACMA, H., TURAN, A. Z., YAMAN, S. & KUCUKBAYRAK, S. 2010a. Controlling the excess heat from oxy-combustion of coal by blending with biomass. *Fuel Processing Technology,* In Press, Corrected Proof.

HAYKIRI-ACMA, H., TURAN, A. Z., YAMAN, S. & KUCUKBAYRAK, S. 2010b. Controlling the excess heat from oxy-combustion of coal by blending with biomass. *Fuel Processing Technology,* 91, 1569-1575.

HAYKIRI-ACMA, H. & YAMAN, S. 2007. Synergy in devolatilization characteristics of lignite and hazelnut shell during co-pyrolysis. *Fuel,* 86, 373-380.

HAYKIRI-ACMA, H. & YAMAN, S. 2008a. Effect of co-combustion on the burnout of lignite/biomass blends: A Turkish case study. *Waste Management,* 28, 2077-2084.

HAYKIRI-ACMA, H. & YAMAN, S. 2009. Effect of biomass on burnouts of Turkish lignites during co-firing. *Energy Conversion and Management,* 50, 2422-2427.

HAYKIRI-ACMA, H. & YAMAN, S. 2010. Interaction between biomass and different rank coals during co-pyrolysis. *Renewable Energy,* 35, 288-292.

HECHT, E. S., SHADDIX, C. R., GEIER, M., MOLINA, A. & HAYNES, B. S. 2012. Effect of CO2 and steam gasification reactions on the oxy-combustion of pulverized coal char. *Combustion and Flame.*

HJÄRTSTAM, S., ANDERSSON, K., JOHNSSON, F. & LECKNER, B. 2009. Combustion characteristics of lignite-fired oxy-fuel flames. *Fuel,* 88, 2216-2224.

HOLTMEYER, M. L., KUMFER, B. M. & AXELBAUM, R. L. 2012. Effects of biomass particle size during cofiring under air-fired and oxyfuel conditions. *Applied Energy*.

HU, S., XIANG, J., SUN, L., XU, M., QIU, J. & FU, P. 2008. Characterization of char from rapid pyrolysis of rice husk. *Fuel Processing Technology*, 89, 1096-1105.

HU, Y., NAITO, S., KOBAYASHI, N. & HASATANI, M. 2000. CO2, NOx and SO2 emissions from the combustion of coal with high oxygen concentration gases. *Fuel*, 79, 1925-1932.

HU, Y. & YAN, J. 2012. Characterization of flue gas in oxy-coal combustion processes for CO2 capture. *Applied Energy*, 90, 113-121.

HUANG, Y., MCILVEEN-WRIGHT, D., REZVANI, S., WANG, Y. D., HEWITT, N. & WILLIAMS, B. C. 2006. Biomass co-firing in a pressurized fluidized bed combustion (PFBC) combined cycle power plant: A techno-environmental assessment based on computational simulations. *Fuel Processing Technology*, 87, 927-934.

HUGHES, E. E. & TILLMAN, D. A. 1998. Biomass cofiring: status and prospects 1996. *Fuel Processing Technology*, 54, 127-142.

HURT, R., SUN, J.-K. & LUNDEN, M. 1998. A Kinetic Model of Carbon Burnout in Pulverized Coal Combustion. *Combustion and Flame*, 113, 181-197.

HURT, R. H. & CALO, J. M. 2001. Semi-global intrinsic kinetics for char combustion modeling. *Combustion and Flame*, 125, 1138-1149.

IDRIS, S. S., RAHMAN, N. A., ISMAIL, K., ALIAS, A. B., RASHID, Z. A. & ARIS, M. J. 2010. Investigation on thermochemical behaviour of low rank Malaysian coal, oil palm biomass and their blends during pyrolysis via thermogravimetric analysis (TGA). *Bioresource Technology*, 101, 4584-4592.

IEA 2011. The Development of the 500MW Co-firing facility atDrax Power Station, workshop on co-firing biomass with coal, Copenhegan, Denmark, 25-26 January 2011.

IEA & REPORT: Trends in NOx emissions from coal utilisation, CCC/02 ISBN: 92-9029-302-0.

IEO 2011. *US Information Administration.*

IKEDA, M., TOPOROV, D., CHRIST, D., STADLER, H., FÖRSTER, M. & KNEER, R. 2012. Trends in NOx Emissions during Pulverized Fuel Oxy-fuel Combustion. *Energy & Fuels,* 26, 3141-3149.

IPCC 2005. *Intergovernmental Panel on Climate Change, Special Report on Carbon Dioxide Capture and Storage, Cambridge University press, Cambridge, UK.*

IPCC 2007. *Intergovernmental Panel on Climate Change; Fourth Assessment Report: Climate Change.*

JESS, A. & ANDRESEN, A.-K. 2010. Influence of mass transfer on thermogravimetric analysis of combustion and gasification reactivity of coke. *Fuel,* 89, 1541-1548.

JONES, J. M., DARVELL, L. I., BRIDGEMAN, T. G., POURKASHANIAN, M. & WILLIAMS, A. 2007. An investigation of the thermal and catalytic behaviour of potassium in biomass combustion. *Proceedings of the Combustion Institute,* 31, 1955-1963.

JONES, J. M., POURKASHANIAN, M., WILLIAMS, A. & HAINSWORTH, D. 2000. A comprehensive biomass combustion model. *Renewable Energy,* 19, 229-234.

JOSEPH, T. J., FISHER, B. R. & MASIN, A. C. 1991. Coal Maceral Chemistry. 1. Liquefaction Behaviour. *Eergy and Fuel,* 724-729.

JOYCE, J., DIXON, T. & DINIZ DA COSTA, J. C. 2006. Characterization of Sugar Cane Waste Biomass Derived Chars from Pressurized Gasification. *Process Safety and Environmental Protection,* 84, 429-439.

JR, J. J. B., HUGHES, E. E. & TILLMAN, D. A. 2000. Biomass cofiring at Seward Station. *Biomass and Bioenergy,* 19, 419-427.

KAKARAS, E. & VOURLIOTIS, P. 1998. Coal combustion with simulated gas turbine exhaust gas and catalytic oxidation of the unburnt fuel. *Fuel,* 77, 1357-1365.

KASTANAKI, E. & VAMVUKA, D. 2006. A comparative reactivity and kinetic study on the combustion of coal - biomass char blends. *Fuel,* 85, 1186-1193.

KASTANAKI, E., VAMVUKA, D., GRAMMELIS, P. & KAKARAS, E. 2002. Thermogravimetric studies of the behavior of lignite-biomass blends during devolatilization. *Fuel Processing Technology,* 77-78, 159-166.

KAZANC, F., KHATAMI, R., MANOEL CRNKOVIC, P. & LEVENDIS, Y. A. 2011. Emissions of NOx and SO2 from Coals of Various Ranks, Bagasse, and Coal-Bagasse Blends Burning in O2/N2 and O2/CO2 Environments. *Energy & Fuels,* 25, 2850-2861.

KIDENA, K., MATSUMOTO, K., KATSUYAMA, M., MURATA, S. & NOMURA, M. 2004. Development of aromatic ring size in bituminous coals during heat treatment in the plastic temperature range. *Fuel Processing Technology,* 85, 827-835.

KIM, J. K. & LEE, H. D. 2010. Investigation on the combustion possibility of dry sewage sludge as a pulverized fuel of thermal power plant. *Journal of Industrial and Engineering Chemistry,* 16, 510-516.

KOORNNEEF, J., RAMIREZ, A., VAN HARMELEN, T., VAN HORSSEN, A., TURKENBURG, W. & FAAIJ, A. 2010. The impact of CO2 capture in the power and heat sector on the emission of SO2, NOx, particulate matter, volatile organic compounds and NH3 in the European Union. *Atmospheric Environment,* 44, 1369-1385.

KRUSE, A. & GAWLIK, A. 2003. Biomass Conversion in Water at 330â^'410 Â°C and 30â^'50 MPa. Identification of Key Compounds for Indicating Different Chemical Reaction Pathways. *Industrial & Engineering Chemistry Research,* 42, 267-279.

KÜLAOTS, I., HSU, A. & SUUBERG, E. M. 2007. The role of porosity in char combustion. *Proceedings of the Combustion Institute,* 31, 1897-1903.

KUTNE, P., KAPADIA, B. K., MEIER, W. & AIGNER, M. 2011. Experimental analysis of the combustion behaviour of oxyfuel flames in a gas turbine model combustor. *Proceedings of the Combustion Institute,* 33, 3383-3390.

LE MANQUAIS, K. 2011a. *Combustion Enhancing Additives for Coal Firing, PhD Thesis.* University of Nottingham.

LE MANQUAIS, K., SNAPE, C., BARKER, J. & MCROBBIE, I. 2012. TGA and Drop Tube Furnace Investigation of Alkali and Alkaline Earth Metal Compounds as Coal Combustion Additives. *Energy & Fuels.*

LE MANQUAIS, K., SNAPE, C., MCROBBIE, I., BARKER, J. & PELLEGRINI, V. 2009. Comparison of the Combustion Reactivity of TGA and Drop Tube Furnace Chars from a Bituminous Coal. *Energy & Fuels,* 23, 4269-4277.

LE MANQUAIS, K., SNAPE, C. E., MCROBBIE, I. & BARKER, J. 2011b. Evaluating the Combustion Reactivity of Drop Tube Furnace and Thermogravimetric Analysis Coal Chars with a Selection of Metal Additives. *Energy & Fuels,* 25, 981-989.

LECI, C. L. 1996. Financial implications on power generation costs resulting from the parasitic effect of CO2 capture using liquid scrubbing technology from power station flue gases. *Energy Conversion and Management,* 37, 915-921.

LESTER, E. 1994. *The characterisation of coal for combustion, PhD Thesis.* University of Nottingham.

LEVENSPIEL, O. 1999. *Chemical Reaction Engineering,* New York, John Wiley & Sons.

LEVINE, D. G., SCHLOSBERG, R. H. & SILBERNAGEL, B. G. 1982. Understanding the chemistry and physics of coal structure (A Review). *Proceedings of the national academy of science,* 79, 3365-3370.

LI, X. G., MA, B. G., XU, L., LUO, Z. T. & WANG, K. 2007. Catalytic Effect of Metallic Oxides on Combustion Behavior of High Ash Coal. *Energy & Fuels,* 21, 2669-2672.

LIU, H., YUAN, Y., YAO, H., DONG, S., ANDO, T. & OKAZAKI, K. 2011. Factors Affecting NO Reduction during O2/CO2 Combustion. *Energy & Fuels,* 25, 2487-2492.

LIU, H., ZAILANI, R. & GIBBS, B. M. 2005a. Comparisons of pulverized coal combustion in air and in mixtures of O2/CO2. *Fuel,* 84, 833-840.

LIU, H., ZAILANI, R. & GIBBS, B. M. 2005b. Pulverized coal combustion in air and in O2/CO2 mixtures with NOx recycle. *Fuel,* 84, 2109-2115.

LIU, Y., GUPTA, R., SHARMA, A., WALL, T., BUTCHER, A., MILLER, G., GOTTLIEB, P. & FRENCH, D. 2005. Mineral matter-organic matter association characterisation by QEMSCAN and applications in coal utilisation. *Fuel,* 84, 1259-1267.

LOISON, R., FOCH, P. & BOYER, A. 1989. Coke: Quality and Production, London & Boston, Butterworths.

LORENZ, H., CARREA, E., TAMURA, M. & HAAS, J. 2000. The role of char surface structure development in pulverized fuel combustion. *Fuel,* 79, 1161-1172.

LU, L., KONG, C., SAHAJWALLA, V. & HARRIS, D. 2002. Char structural ordering during pyrolysis and combustion and its influence on char reactivity. *Fuel,* 81, 1215-1225.

MA, B.-G., LI, X.-G., XU, L., WANG, K. & WANG, X.-G. 2006. Investigation on catalyzed combustion of high ash coal by thermogravimetric analysis. *Thermochimica Acta,* 445, 19-22.

MA, L., GHAREBAGHI, M., PORTER, R., POURKASHANIAN, M., JONES, J. M. & WILLIAMS, A. 2009. Modelling methods for co-fired pulverised fuel furnaces. *Fuel,* 88, 2448-2454.

MAN, C. K. & GIBBINS, J. R. 2011. Factors affecting coal particle ignition under oxyfuel combustion atmospheres. *Fuel,* 90, 294-304.

MANYA, J. J., VELO, E. & PUIGJANER, L. 2003. Kinetics of Biomass Pyrolysis: a Reformulated Three-Parallel-Reactions Model.

MCILVEEN-WRIGHT, D. R., HUANG, Y., REZVANI, S., MONDOL, J. D., REDPATH, D., ANDERSON, M., HEWITT, N. J. & WILLIAMS, B. C. 2011. A Techno-economic assessment of the reduction of carbon dioxide emissions through the use of biomass co-combustion. *Fuel,* 90, 11-18.

MEESRI, C. & MOGHTADERI, B. 2002. Lack of synergetic effects in the pyrolytic characteristics of woody biomass/coal blends under low and high heating rate regimes. *Biomass and Bioenergy,* 23, 55-66.

MEESRI, C. & MOGHTADERI, B. 2003. Experimental and Numerical Analysis of Sawdust-Char Combustion Reactivity in a Drop Tube Reactor. *Combustion Science and Technology,* 175, 793-823.

MENGHINI, D., MARRA, F. S., ALLOUIS, C. & BERETTA, F. 2008. Effect of excess air on the optimization of heating appliances for biomass combustion. *Experimental Thermal and Fluid Science,* 32, 1371-1380.

MESSENBÖCK, R. C., DUGWELL, D. R. & KANDIYOTI, R. 1999. CO2 and steam-gasification in a high-pressure wire-mesh reactor: the reactivity of Daw Mill coal and combustion reactivity of its chars. *Fuel,* 78, 781-793.

MIRANDA, T., ESTEBAN, A., ROJAS, S., MONTERO, I. & RUIZ, A. 2008. combustion Analysis of Different Olive Residues. *International Journal of Molecular Sciences,* 9, 512-525.

MOGHTADERI, B., MEESRI, C. & WALL, T. F. 2004. Pyrolytic characteristics of blended coal and woody biomass. *Fuel,* 83, 745-750.

MOLCAN, P., LU, G., BRIS, T. L., YAN, Y., TAUPIN, B. T. & CAILLAT, S. B. 2009. Characterisation of biomass and coal co-firing on a 3 MWth Combustion Test Facility using flame imaging and gas/ash sampling techniques. *Fuel,* 88, 2328-2334.

MOLINA, A. & SHADDIX, C. R. 2007. Ignition and devolatilization of pulverized bituminous coal particles during oxygen/carbon dioxide coal combustion. *Proceedings of the Combustion Institute,* 31, 1905-1912.

MOON, J.-H., LEE, J.-W. & LEE, U.-D. 2011. Economic analysis of biomass power generation schemes under renewable energy initiative with Renewable

Portfolio Standards (RPS) in Korea. *Bioresource Technology,* 102, 9550-9557.

MUNIR, S., DAOOD, S. S., NIMMO, W., CUNCLIFFE, A. M. & GIBBS, B. M. 2009. Thermal analysis and devolatilization kinetics of cotton stalk, sugar cane baggasse and shea meal under nitrogen and air atmosphere. *Bioresource Technology,* 100, 1413-1418.

NAREDI, P. & PISUPATI, S. 2011a. Effect of CO2 during Coal Pyrolysis and Char Burnout in Oxy-Coal Combustion. *Energy & Fuels,* 25, 2452-2459.

NAREDI, P. & PISUPATI, S. V. 2008. Interpretation of Char Reactivity Profiles Obtained Using a Thermogravimetric Analyzer.

NAREDI, P., YEBOAH, Y. D. & PISUPATI, S. V. 2011b. Effect of Furnace Purging on Kinetic Rate Parameter Determination Using Isothermal Thermogravimetric Analysis. *Energy & Fuels,* 25, 4937-4943.

NARODOSLAWSKY, M. & OBERNBERGER, I. 1996. From waste to raw materialâ€"the route from biomass to wood ash for cadmium and other heavy metals. *Journal of Hazardous Materials,* 50, 157-168.

NIMMO, W., DAOOD, S. S. & GIBBS, B. M. 2010. The effect of O2 enrichment on NOx formation in biomass co-fired pulverised coal combustion. *Fuel,* 89, 2945-2952.

NORMANN, F., THUNMAN, H. & JOHNSSON, F. 2009. Process analysis of an oxygen lean oxy-fuel power plant with co-production of synthesis gas. *Energy Conversion and Management,* 50, 279-286.

NOWAK, B., KARLSTRO, O., BACKMAN, P., ZEVENHOVEN, M., VOGLSAM, S., WINTER, F. & HUPA, M. 2013. Mass transfer limitation in thermogravimetry of biomass gasification. *J Therm Anal Calorim,* 111, 183-192.

ORFÃO, J. J. M., ANTUNES, F. J. A. & FIGUEIREDO, J. L. 1999. Pyrolysis kinetics of lignocellulosic materials--three independent reactions model. *Fuel,* 78, 349-358.

OTERO, M., CALVO, L. F., GIL, M. V., GARCIA, A. I. & MORGAN, A. 2008. Co-combustion of different sewage sludge and coal: A non-isothermal thermogravimetric kinetic analysis. *Bioresource Technology,* 99, 6311-6319.

PARK, D. K., KIM, S. D., LEE, S. H. & LEE, J. G. 2010. Co-pyrolysis characteristics of sawdust and coal blend in TGA and a fixed bed reactor. *Bioresource Technology,* 101, 6151-6156.

PARK, Y.-M., KIM, S.-S. & PARK, Y.-K. 2009. Pyrolysis characteristics and kinetics of oak trees using thermogravimetric analyzer and micro-tubing reactor. *Bioresource Technology,* 100, 400-405.

PIHL, E., HEYNE, S., THUNMAN, H. & JOHNSSON, F. 2010. Highly efficient electricity generation from biomass by integration and hybridization with combined cycle gas turbine (CCGT) plants for natural gas. *Energy,* 35, 4042-4052.

POSTNOTE. 2008. The Transition to a Low Carbon Economy, Parliamentary office of Science and technology, www.parliament.uk/document/post/postn318.

PRONOBIS, M. 2006. The influence of biomass co-combustion on boiler fouling and efficiency. *Fuel,* 85, 474-480.

RATHNAM, R. K., ELLIOTT, L. K., WALL, T. F., LIU, Y. & MOGHTADERI, B. 2009. Differences in reactivity of pulverised coal in air (O2/N2) and oxy-fuel (O2/CO2) conditions. *Fuel Processing Technology,* 90, 797-802.

REHFELDT, S., KUHR, C., SCHIFFER, F.-P., WECKES, P. & BERGINS, C. 2011. First test results of Oxyfuel combustion with Hitachi's DST-burner at Vattenfall's 30 MWth Pilot Plant at Schwarze Pumpe. *Energy Procedia,* 4, 1002-1009.

REN, H., ZHANG, Y., FANG, Y. & WANG, Y. 2011. Co-gasification behavior of meat and bone meal char and coal char. *Fuel Processing Technology,* 92, 298-307.

RIAZA, J., ÃLVAREZ, L., GIL, M. V., PEVIDA, C., PIS, J. J. & RUBIERA, F. 2011. Effect of oxy-fuel combustion with steam addition on coal ignition and burnout in an entrained flow reactor. *Energy,* 36, 5314-5319.

ROBINSON, A. L., JUNKER, H. & BAXTER, L. L. 2002. Pilot-Scale Investigation of the Influence of Coal-Biomass Cofiring on Ash Deposition. *Energy Fuels,* 16, 343-355.

RYU, C., YANG, Y. B., KHOR, A., YATES, N. E., SHARIFI, V. N. & SWITHENBANK, J. 2006. Effect of fuel properties on biomass combustion: Part I. Experiments--fuel type, equivalence ratio and particle size. *Fuel,* 85, 1039-1046.

SADDAWI, A., JONES, J. M., WILLIAMS, A. & WOÌJTOWICZ, M. A. 2010. Kinetics of the Thermal Decomposition of Biomass. *Energy & Fuels,* 24, 1274-1282.

SADHUKHAN, A. K., GUPTA, P., GOYAL, T. & SAHA, R. K. 2008. Modelling of pyrolysis of coal-biomass blends using thermogravimetric analysis. *Bioresource Technology,* 99, 8022-8026.

SAHU, S. G., SARKAR, P., CHAKRABORTY, N. & ADAK, A. K. 2010. Thermogravimetric assessment of combustion characteristics of blends of a coal with different biomass chars. *Fuel Processing Technology,* 91, 369-378.

SAMI, M., ANNAMALAI, K. & WOOLDRIDGE, M. 2001. Co-firing of coal and biomass fuel blends. *Progress in Energy and Combustion Science,* 27, 171-214.

SCHEFFKNECHT, G., AL-MAKHADMEH, L., SCHNELL, U. & MAIER, J. 2011. Oxy-fuel coal combustion—A review of the current state-of-the-art. *International Journal of Greenhouse Gas Control,* 5, Supplement 1, S16-S35.

SENNECA, O. 2008. Characterisation of meat and bone mill for coal co-firing. *Fuel,* 87, 3262-3270.

SENNECA, O., CHIRONE, R. & SALATINO, P. 2004a. Oxidative pyrolysis of solid fuels. *Journal of Analytical and Applied Pyrolysis,* 71, 959-970.

SENNECA, O. & SALATINO, P. 2011. A semi-detailed kinetic model of char combustion with consideration of thermal annealing. *Proceedings of the Combustion Institute,* 33, 1763-1770.

SENNECA, O., SALATINO, P. & MASI, S. 2004b. Heat treatment-induced loss of combustion reactivity of a coal char: the effect of exposure to oxygen. *Experimental Thermal and Fluid Science,* 28, 735-741.

SENNECA, O., SALATINO, P. & MASI, S. 2005. The influence of char surface oxidation on thermal annealing and loss of combustion reactivity. *Proceedings of the Combustion Institute,* 30, 2223-2230.

SENNECA, O., SALATINO, P. & MENGHINI, D. 2007b. The influence of thermal annealing on oxygen uptake and combustion rates of a bituminous coal char. *Proceedings of the Combustion Institute,* 31, 1889-1895.

SHADDIX, C. R. & MOLINA, A. 2009. Particle imaging of ignition and devolatilization of pulverized coal during oxy-fuel combustion. *Proceedings of the Combustion Institute,* 32, 2091-2098.

SHARMA, R. K., WOOTEN, J. B., BALIGA, V. L. & HAJALIGOL, M. R. 2001. Characterization of chars from biomass-derived materials: pectin chars. *Fuel,* 80, 1825-1836.

SHARMA, R. K., WOOTEN, J. B., BALIGA, V. L., LIN, X., GEOFFREY CHAN, W. & HAJALIGOL, M. R. 2004. Characterization of chars from pyrolysis of lignin. *Fuel,* 83, 1469-1482.

SHARYPOV, V. I., BEREGOVTSOVA, N. G., KUZNETSOV, B. N., CEBOLLA, V. L., COLLURA, S., FINQUENEISEL, G., ZIMNY, T. & WEBER, J. V. 2007. Influence of reaction parameters on brown coal-polyolefinic plastic co-pyrolysis behavior. *Journal of Analytical and Applied Pyrolysis,* 78, 257-264.

SHEN, D. K., GU, S., LUO, K. H., BRIDGWATER, A. V. & FANG, M. X. 2009. Kinetic study on thermal decomposition of woods in oxidative environment. *Fuel,* 88, 1024-1030.

SHENG, C. 2007. Char structure characterised by Raman spectroscopy and its correlations with combustion reactivity. *Fuel,* 86, 2316-2324.

SHUANGNING, X., ZHIHE, L., BAOMING, L., WEIMING, Y. & XUEYUAN, B. 2006. Devolatilization characteristics of biomass at flash heating rate. *Fuel,* 85, 664-670.

SIMA-ELLA, E., YUAN, G. & MAYS, T. 2005b. A simple kinetic analysis to determine the intrinsic reactivity of coal char. *Fuel* 84, 1920-1925.

SIMONE, M., BIAGINI, E., GALLETTI, C. & TOGNOTTI, L. 2009. Evaluation of global biomass devolatilization kinetics in a drop tube reactor with CFD aided experiments. *Fuel,* 88, 1818-1827.

SJÖSTRÖM, K., CHEN, G., YU, Q., BRAGE, C. & ROSÉN, C. 1999. Promoted reactivity of char in co-gasification of biomass and coal: synergies in the thermochemical process. *Fuel,* 78, 1189-1194.

SKODRAS, G., GRAMMELIS, P., BASINAS, P., KAKARAS, E. & SAKELLAROPOULOS, G. 2006. Pyrolysis and Combustion Characteristics of Biomass and Waste-Derived Feedstock.

SMART, J. P., O'NIONS, P. & RILEY, G. S. 2010a. Radiation and convective heat transfer, and burnout in oxy-coal combustion. *Fuel,* 89, 2468-2476.

SMART, J. P., PATEL, R. & RILEY, G. S. 2010b. Oxy-fuel combustion of coal and biomass, the effect on radiative and convective heat transfer and burnout. *Combustion and Flame,* 157, 2230-2240.

SMITH, I. W. THE COMBUSTION RATES OF COAL CHARS: A REVIEW. Nineteenth Symposium (International) on Combustion/The Combustion Institute, 1982 North Ryde, NSW 2113, Australia. 1045-1065.

SONOBE, T., WORASUWANNARAK, N. & PIPATMANOMAI, S. 2008. Synergies in co-pyrolysis of Thai lignite and corncob. *Fuel Processing Technology,* 89, 1371-1378.

SØRENSEN, H. S., ROSENBERG, P., PETERSEN, H. I. & SØRENSEN, L. H. 2000. Char porosity characterisation by scanning electron microscopy and image analysis. *Fuel,* 79, 1379-1388.

SPLIETHOFF, H. & HEIN, K. R. G. 1998. Effect of co-combustion of biomass on emissions in pulverized fuel furnaces. *Fuel Processing Technology,* 54, 189-205.

SRICHAROENCHAIKUL, V., HICKS, A. L. & FREDERICK, W. J. 2001. Carbon and char residue yields from rapid pyrolysis of kraft black liquor. *Bioresource Technology,* 77, 131-138.

STRAKA, P., NÁHUNKOVÁ, J. & BROZOVÁ, Z. 2004. Kinetics of copyrolysis of coal with polyamide 6. *Journal of Analytical and Applied Pyrolysis,* 71, 213-221.

STURGEON, D. W., CAMERON, E. D. & FITZGERALD, F. D. 2009. Demonstration of an oxyfuel combustion system. *Energy Procedia,* 1, 471-478.

STURGEON, D. W., CAMERON, E. D., FITZGERALD, F. D. & MCGHIE, C. 2011. Demonstration of the Doosan Power Systems 40MWt OxyCoal(TM) combustion system. *Energy Procedia,* 4, 933-940.

SUN, C. & SNAPE, C., E. 2009. Characteristics of Coal Devolatilisation, Char Combustion and Nitrogen Partitioning Under Oxy-fuel Firing Conditions. *International Conference on Coal Science & Technology (ICCS&T).* Cape Town, South Africa.

SUN, S., CAO, H., CHEN, H., WANG, X., QIAN, J. & WALL, T. 2011. Experimental study of influence of temperature on fuel-N conversion and recycle NO reduction in oxyfuel combustion. *Proceedings of the Combustion Institute,* 33, 1731-1738.

SUTCU, H. 2007. Pyrolysis by thermogravimetric analysis of blends of peat with coals of different characteristics and biomass. *Journal of the Chinese Institute of Chemical Engineers,* 38, 245-249.

SUUBERG, E. M. & AARNA, I. 2009. Kinetics of tire derived fuel (TDF) char oxidation and accompanying changes in surface area. *Fuel,* 88, 179-186.

SYED, A. U., SIMMS, N. J. & OAKEY, J. E. 2011. Fireside corrosion of superheaters: Effects of air and oxy-firing of coal and biomass. *Fuel*.

SZEKELY, J., EVANS, J. W. & SOHN, H. Y. 1976. *Gas-Solid Reactions*, New York, Academic Press.

TAN, Y., CROISET, E., DOUGLAS, M. A. & THAMBIMUTHU, K. V. 2006. Combustion characteristics of coal in a mixture of oxygen and recycled flue gas. *Fuel*, 85, 507-512.

TANIGUCHI, M., YAMAMOTO, K., KOBAYASHI, H. & KIYAMA, K. 2002. A reduced NOx reaction model for pulverized coal combustion under fuel-rich conditions. *Fuel*, 81, 363-371.

TARELHO, L. A. C., NEVES, D. S. F. & MATOS, M. A. A. 2011. Forest biomass waste combustion in a pilot-scale bubbling fluidised bed combustor. *Biomass and Bioenergy*, 35, 1511-1523.

TEIXEIRA, P., LOPES, H., GULYURTLU, I. & LAPA, N. 2011. Use of chemical fractionation to understand partitioning of biomass ash constituents during co-firing in fluidized bed combustion. *Fuel*.

TILLMAN, D. A. 2000. Biomass cofiring: the technology, the experience, the combustion consequences. *Biomass and Bioenergy*, 19, 365-384.

TING, F. T. C. 1982. Introduction-origin of coal and coal macerals. *In:* MEYER, R. A. (ed.) *Coal structure*. Academic press inc. London.

TOMECZEK, J. & PALUGNIOK, H. 2002. Kinetics of mineral matter transformation during coal combustion. *Fuel*, 81, 1251-1258.

TOUS, M., PAVLAS, M., STEHLÃK, P. & POPELA, P. 2011. Effective biomass integration into existing combustion plant. *Energy*, 36, 4654-4662.

TREMEL, A. & SPLIETHOFF, H. 2013. Gasification kinetics during entrained flow gasification – Part I; Devolatilisation and char deactivation. *Fuel*, 103, 663-671.

VAMVUKA, D., KAKARAS, E., KASTANAKI, E. & GRAMMELIS, P. 2003a. Pyrolysis characteristics and kinetics of biomass residuals mixtures with lignite[small star, filled]. *Fuel*, 82, 1949-1960.

VAMVUKA, D., PASADAKIS, N., KASTANAKI, E., GRAMMELIS, P. & KAKARAS, E. 2003b. Kinetic Modeling of Coal/Agricultural By-Product Blends. *Energy Fuels,* 17, 549-558.

VAN DEN BROEK, R., FAAIJ, A. & VAN WIJK, A. 1996. Biomass combustion for power generation. *Biomass and Bioenergy,* 11, 271-281.

VAN LOO, S. & KOPPEJAN, J. 2008. *The handbook of Biomass Combustion and Co-firing, Bioenergy Task 32, editors: Loo, S.V., Koppejan, J. Earthscan, USA and UK*

VÁRHEGYI, G., ANTAL, M. J., JAKAB, E. & SZABÓ, P. 1997. Kinetic modeling of biomass pyrolysis. *Journal of Analytical and Applied Pyrolysis,* 42, 73-87.

VAROL, M., ATIMTAY, A. T., BAY, B. & OLGUN, H. 2010. Investigation of co-combustion characteristics of low quality lignite coals and biomass with thermogravimetric analysis. *Thermochimica Acta,* 510, 195-201.

VASSILEV, S. V., BAXTER, D., ANDERSEN, L. K. & VASSILEVA, C. G. 2010. An overview of the chemical composition of biomass. *Fuel,* 89, 913-933.

VASSILEV, S. V., KITANO, K., TAKEDA, S. & TSURUE, T. 1995. Influence of mineral and chemical composition of coal ashes on their fusibility. *Fuel Processing Technology,* 45, 27-51.

VUTHALURU, H. B. 2004. Investigations into the pyrolytic behaviour of coal/biomass blends using thermogravimetric analysis. *Bioresource Technology,* 92, 187-195.

WAGENAAR, B. M. & VAN DEN HEUVEL, E. J. M. T. 1997. Co-combustion of Miscanthus in a pulverised coal combustor: Experiments in a droptube furnace. *Biomass and Bioenergy,* 12, 185-197.

WALL, T. 2005. Fundamental of Oxy-fuel Combustion. *IEAGHG Inaugural Workshop on Oxy-fuel Combustion.* Cottbus, Germany, November.

WALL, T., LIU, Y., SPERO, C., ELLIOTT, L., KHARE, S., RATHNAM, R., ZEENATHAL, F., MOGHTADERI, B., BUHRE, B., SHENG, C., GUPTA, R., YAMADA, T., MAKINO, K. & YU, J. 2009. An overview on oxyfuel coal

combustion--State of the art research and technology development. *Chemical Engineering Research and Design,* 87, 1003-1016.

WALL, T., STANGER, R. & LIU, Y. 2011. Gas cleaning challenges for coal-fired oxy-fuel technology with carbon capture and storage. *Fuel,* In Press, Corrected Proof.

WALL, T. F. 2007. Combustion processes for carbon capture. *Proceedings of the Combustion Institute,* 31, 31-47.

WANG, C., WANG, F., YANG, Q. & LIANG, R. 2009. Thermogravimetric studies of the behavior of wheat straw with added coal during combustion. *Biomass and Bioenergy,* 33, 50-56.

WANG, L., WELLER, C. L., JONES, D. D. & HANNA, M. A. 2008. Contemporary issues in thermal gasification of biomass and its application to electricity and fuel production. *Biomass and Bioenergy,* 32, 573-581.

WANG, Q., YAO, H., YU, D., DAI, L. & XU, M. 2007a. Emission Behavior of Particulate Matter during Co-combustion of Coal and Biomass in a Drop Tube Furnace. *Energy Fuels,* 21, 513-516.

WANG, S. & BAXTER, L. 2007. Comprehensive study of biomass fly ash in concrete: Strength, microscopy, kinetics and durability. *Fuel Processing Technology,* 88, 1165-1170.

WCA 2011. World Coal Association. *Coal and Electricity,* http://www.worldcoal.org/coal/uses-of-coal/coal-electricity.

WERTHER, J., SAENGER, M., HARTGE, E. U., OGADA, T. & SIAGI, Z. 2000. Combustion of agricultural residues. *Progress in Energy and Combustion Science,* 26, 1-27.

WHITE, J. E., CATALLO, W. J. & LEGENDRE, B. L. 2011. Biomass pyrolysis kinetics: A comparative critical review with relevant agricultural residue case studies. *Journal of Analytical and Applied Pyrolysis,* 91, 1-33.

WILLIAMS, A., POURKASHANIAN, M. & JONES, J. M. 2001. Combustion of pulverised coal and biomass. *Progress in Energy and Combustion Science,* 27, 587-610.

WORNAT, M. J., HURT, R. H., DAVIS, K. A. & YANG, N. Y. C. 1996. Single-Particle Combustion of Two Biomass Chars. *Twenty-sixth Symposium (International) on Combustion/ The Combustion Institute*

WU, Z., XU, L., WANG, Z. & ZHANG, Z. 1998. Catalytic effects on the ignition temperature of coal. *Fuel,* 77, 891-893.

XIONG, J., ZHAO, H., ZHENG, C., LIU, Z., ZENG, L., LIU, H. & QIU, J. 2009. An economic feasibility study of O2/CO2 recycle combustion technology based on existing coal-fired power plants in China. *Fuel,* 88, 1135-1142.

YANG, Y. B., RYU, C., KHOR, A., YATES, N. E., SHARIFI, V. N. & SWITHENBANK, J. 2005. Effect of fuel properties on biomass combustion. Part II. Modelling approach--identification of the controlling factors. *Fuel,* 84, 2116-2130.

YU, D., XU, M., SUI, J., LIU, X., YU, Y. & CAO, Q. 2005. Effect of coal particle size on the proximate composition and combustion properties. *Thermochimica Acta,* 439, 103-109.

YU, J., LUCAS, J. A. & WALL, T. F. 2007. Formation of the structure of chars during devolatilization of pulverized coal and its thermoproperties: A review. *Progress in Energy and Combustion Science,* 33, 135-170.

YU, J., STREZOV, V., LUCAS, J. & WALL, T. 2003. Swelling behaviour of individual coal particles in the single particle reactor. *Fuel,* 82, 1977-1987.

YUZBASI, N. S. & SELÇUK, N. 2011. Air and oxy-fuel combustion characteristics of biomass/lignite blends in TGA-FTIR. *Fuel Processing Technology,* 92, 1101-1108.

ZHANG, L.-M., TAN, Z.-C., WANG, S.-D. & WU, D.-Y. 1997. Combustion calorimetric and thermogravimetric studies of graphite and coals doped with a coal-burning additive. *Thermochimica Acta,* 299, 13-17.

ZHANG, L., XU, S., ZHAO, W. & LIU, S. 2007. Co-pyrolysis of biomass and coal in a free fall reactor. *Fuel,* 86, 353-359.

ZHANG, X., YANG, W. & BLASIAK, W. 2011. Modeling Study of Woody Biomass: Interactions of Cellulose, Hemicellulose, and Lignin. *Energy & Fuels,* 25, 4786-4795.

ZHOU, C. Q., NEAL, L. G., BOLI, R., HASLBECK, J. & CHANG, A. 1996. Control of NOx emissions by NOx recycle approach. *Symposium (International) on Combustion,* 26, 2091-2097.

ZHU, W., SONG, W. & LIN, W. 2008. Catalytic gasification of char from co-pyrolysis of coal and biomass. *Fuel Processing Technology,* 89, 890-896.

ZOLIN, A., JENSEN, A. & DAM-JOHANSEN, K. 2001a. Coupling thermal deactivation with oxidation for predicting the combustion of a solid fuel. *Combustion and Flame,* 125, 1341-1360.

ZOLIN, A., JENSEN, A. D., JENSEN, P. A. & DAM-JOHNSEN, K. 2002. Experimental study of char deactivation. *Fuel,* 81, 1065-1075.